DOCTOR OF PHILOSOPHY

Multimodal characterisation of sensorimotor oscillations

Kim Ronnqvist

2013

Aston University

MULTIMODAL CHARACTERISATION OF SENSORIMOTOR OSCILLATIONS

Kim Christine Rönnqvist

Doctor of Philosophy

Aston University, UK

December 2012

Aston University

Multimodal characterisation of sensorimotor oscillations

Kim Christine Rönnqvist

Doctor of Philosophy
2012

Thesis summary

The studies in this project have investigated the ongoing neuronal network oscillatory activity found in the sensorimotor cortex using two modalities; magnetoencephalography (MEG) and *in vitro* slice recordings. The results have established that ongoing sensorimotor oscillations span the mu and beta frequency region both *in vitro* and in MEG recordings, with distinct frequency profiles for each recorded laminae *in vitro*, while MI and SI show less difference in humans. In addition, these studies show that connections between MI and SI modulate the ongoing neuronal network activity in these areas.

The stimulation studies indicate that specific frequencies of stimulation affect the ongoing activity in the sensorimotor cortex. The continuous theta burst stimulation (cTBS) study demonstrates that cTBS predominantly enhances the power of the local ongoing activity. The stimulation studies in this project show limited comparison between modalities, which is informative of the role of connectivity in these effects. However, independently these studies provide novel information on the mechanisms on sensorimotor oscillatory interaction.

The pharmacological studies reveal that GABAergic modulation with zolpidem changes the neuronal oscillatory network activity in both healthy and pathological MI. Zolpidem enhances the power of ongoing oscillatory activity in both sensorimotor laminae and in healthy subjects. In contrast, zolpidem attenuates the "abnormal" beta oscillatory activity in the affected hemisphere in Parkinsonian patients, while restoring the hemispheric beta power ratio and frequency variability and thereby improving motor symptomatology.

Finally we show that independent signals from MI laminae can be integrated *in silico* to resemble the aggregate MEG MI oscillatory signals. This highlights the usefulness of combining these two methods when elucidating neuronal network oscillations in the sensorimotor cortex and any interventions.

Keywords: Networks, Parkinson's, zolpidem, stimulation, variability

Acknowledgements

Contents

Figures

Tables

Abbreviations

5-HT	5-hydroxytryptamine
6-OHDA	6-hydroxydopamine
aCSF	articifical cerebrospinal fluid
AMPA	α-amino-3-hydroxy-5-methyl-4-isoxazolepropionic acid
AMT	Active motor threshold
BDNF	Brain-derived neurotrophic factor
CCh	Carbachol
cTBS	Continuous theta burst stimulation
DBS	Deep brain stimulation
DMN	Default mode network
EcoG	Electrocorticography
EEG	Electroencephalography
EMG	Electromyographic
EPSC	Excitatory postsynaptic current
EPSP	Excitatory postsynaptic potential
ERD	Event-related desynchronisation
ERS	Event-related synchronisation
FDI	First dorsal interosseos
FFT	Fast Fourier Transform
fMRI	Functional magnetic resonance imaging
FS	Fast spiking
FWHM	Full-width half-maximum
GABA	Gamma-aminobutyric acid
IPSC	Inhibitory postsynaptic current
IPSP	Inhibitory postsynaptic potential
KA	Kainic acid
LTD	Long term depression
LFP	Local field potential
LTP	Long term potentiation
MEG	Magnetoencephalography
MEP	Motor evoked potential

MI LIII	Superficial layers of primary motor cortex
MI LV	Deeper layers of primary motor cortex
MI	Primary motor cortex
MNS	Median nerve stimulation
MPTP	1-methyl-4-phenyl-1, 2, 3, 6-tetrahydropyridine
MRI	Magnetic resonance imaging
NMDA	N-methyl-D-aspartate
PD	Parkinson's disease
PMBR	Post-movement beta rebound
PSD	Power spectral density
RM	Repeated measures
RS	Regular spiking
RSN	Resting state network
rTMS	repetitive transcranial magnetic stimulation
SAM	Synthetic aperture magnetometry
SMC	Sensorimotor cortex
SI LIV	Middle layers of primary somatosensory cortex
SI	Primary somatosensory cortex
STN	Subthalamic nucleus
TMS	Transcranial magnetic stimulation
UPDRS	Unified Parkinson's Disease Rating Scale
VE	Virtual electrode

Chapter 1. Introduction

1.1. The mammalian brain

1.1.1. Structure of the cerebral cortex

The evolution of the mammalian brain can be traced back 200 million years. The cerebral cortex is the area which shows the most dramatic development through evolution (Deacon 1990; Rowe *et al.*, 2011). The brain exerts its centralised control on the rest of the physiological system in an individual and is ultimately responsible for function and, in humans at least, the existence of the mind (Kanwisher 2010). The average male human brain is reported to contain 86 billion neurons, and the average size of a neuronal cell, the neuron, is assumed to be 0.03-0.05 mm (Azevedo *et al.*, 2009), with an average connectivity of 7000 synapses per neuronal cell (Drachman, 2005). These small neurons connect together and create large networks and areas, usually with specific functions, for example the sub-areas of the cerebral cortex. The mammalian cortex comprises the outer layer of the brain and is responsible for a myriad of functions; cognition, movement, sensation, perception and vision are a few examples. It covers the cerebrum and cerebellum, but here we focus on the cerebral cortex only. The cerebral cortex is a structure that typically has six layers or 'laminae' (I-VI). Efferent cortico-cortical connections arise primarily from layers II/III, whereas the subcortical connectivity mainly is found in layer V/VI (Mountcastle, 1997). The work of Mountcastle was based on studies in the primary somatosensory cortex (SI). In the primary motor cortex (MI) layer IV is almost non-existent, perhaps due to this layer receiving primarily sensory input, and as motor cortex controls movement it is likely that its prominent role is that of an output station. Motor cortex also has a thinner layer III (Donoghue & Wise 1982; Shipp, 2005). The laminar organization is maintained, with the above exception, in different cortical areas and also to some extent between species. Canonical neocortical hierarchy indicates the primary input from other cortical areas to arrive to layers I, IV and V. Thalamic input arrives in layer IV (Shipp, 2007). Layer I is believed to integrate information from other cortical and subcortical areas, especially since this layer also is the main target for feedback connections (Chu *et al.*, 2003; Douglas & Martin 2004; 2007b; Shipp, 2007; Thomson & Lamy 2007). Layer II/III cells extend axons laterally and also extend axons horizontally into layer V. Pyramidal cells with somata in layer III extend straight to layer V (Douglas & Martin 2004; 2007a). Layer IV, of which the motor cortex has none, receives sensory input from the thalamus, and to some extent also from layer VI. Projections from layer IV mainly end in layer III. Layer V receives cortico-cortical inputs, and the pyramidal cells with somata in layer V commonly project to subcortical structures, but some cortico-cortical connectivity has also been found, primarily to the superficial layers. Layer V pyramidal cells are interconnected to some extent, but most layer V pyramidal cells

connect outside of this layer, likewise for layer VI (Douglas & Martin 2004; Thomson & Lamy 2007). Layer V of motor cortex, for example, contains the large Betz cells which are responsible for motor output from the cortex (Rivara *et al.*, 2003). Layer VI pyramidal cells are primarily responsible for the cortico-thalamic connections, but also show some cortico-cortical reciprocal connectivity in between deeper layers of sensory and motor cortices (Douglas & Martin 2004; 2007a; Thomson & Lamy 2007).

1.1.2. Neuronal microcircuits

Connections between layers or functional areas are called microcircuits, or pathways. Microcircuits in the brain here refer to synaptic connections between different types of neuronal cells, predominantly pyramidal cells and local interneurons. Cortico-cortical connections can be found in all layers to different extents and involve primarily pyramidal cells. Pyramidal cells are particularly suitable for connectivity over areas further apart due to their canonical anatomy with one long axon and smaller dendrites. Interneuronal connectivity is usually short-range and local since their axonal length is often much shorter (Markram *et al.*, 2004; Shipp, 2005; Thomson & Lamy 2007). Different connections and interactions between neurons in the same cortical region have been found to be consistent and in many cases the intrinsic connectivity in smaller areas of a region outnumbers the connections over the larger areas (Capaday *et al.*, 2009). The canonical microcircuit connecting layer IV upwards with II/III, and then down to layer V, is called the ascending or feedforward pathway, and its main purpose has been theorized to be processing rather than relaying (Shipp, 2007). The descending or feedback pathway starts with input from layers II/III to V, or VI. Pyramidal cells in these deeper layers then project up to layer I resulting in the characteristic feedback loop suggested for neocortical microcircuitry (Shipp, 2007). In the cortical circuit loop suggested by Gilbert & Wiesel in 1989, there was also a small loop in overall pathway from layer VI back to layer IV. An overview of the layer connectivity can be seen figure 1.1 further down.

In a recent study of layers in rodent somatosensory cortex, Adesnik & Scanzani (2010) found layer II/III pyramidal cells to project both vertically and horizontally, but the overall effect (feedforward or feedback) was intricately determined on the ratio of inhibitory and excitatory signals. The ratio of inhibitory to excitatory cell distribution in the cortex is approximately 1:5 to 1:9 depending on area and laminae, and although there is less inhibitory neurons in relation to the pyramidal cells the first group has proven to be far more diverse in its characteristic properties (Somogyi & Klausberger 2005; Shipp, 2007; Thomson & Lamy 2007; Meyer *et al.*, 2011). Adesnik & Scanzani (2010) concluded that

layer II/III pyramidal cells were efficient in driving pyramidal cells in layer V by horizontal connections: feedforward excitation, and at the same time suppress the neighbouring pyramidal cells within the same layer: lateral suppression. The inhibition of the next-door pyramidal cells results in subsequent non-activation of those horizontally linked pyramidal cells in layer V. These results also add to the underlying concept of networks as dynamic entities with spatial constraints in the form of possible cellular connections, rather than simply static constructs solely determined by anatomical connectivity.
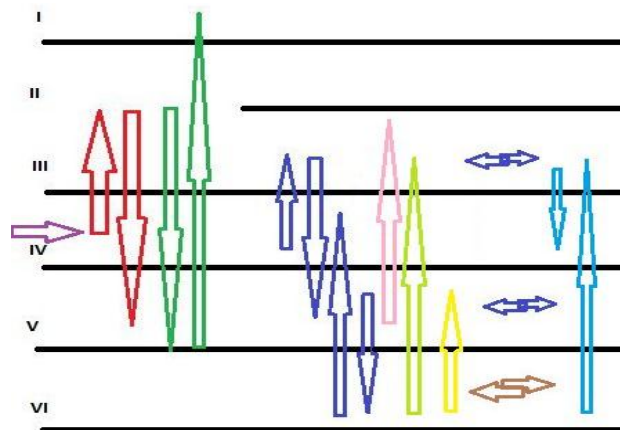
Figure 1. 1. Generalized overview of interlaminar connectivity in the sensory neocortex. The purple arrow represents thalamic sensory input. Red and green arrows are the canonical feed forward and feedback pathways described in Shipp (2007). Blue and teal arrows show a summarised view of Gilbert & Wiesel's cortical circuitry (1989), blue arrows are connections within one area, and teal represent connections found between areas. Pink, lime green, yellow and brown arrows are additional to Gilbert & Wiesel's circuit (by Lund, 1979, Martin & Whitteridge 1984, Hirsch *et al.,* 1998, Zhang & Deschenes 1997, Katz 1987, respectively). The diagram is summarised from above authors, as well as Douglas & Martin (2004).

1.1.3. The sensorimotor cortex

The primary motor and somatosensory areas take up the cortical region anterior and posterior to central sulcus, referred to as the sensorimotor cortex (SMC). The research on the cardinal somatotopic arrangements of the primary sensorimotor cortex dates back to the 19th century and is a well-established phenomenon (Hluštík et al, 2001; Scheiber, 2001). The motor cortex plays a critical role in the ability to perform movement and in order to do this, information is required from the surroundings. The primary motor cortex exercises control over muscles in a functionally integrated manner, which requires sensory feedback (Devanne *et al.*, 2002; Capaday *et al.*, 2004; d'Avella *et al.*, 2006; Ting & McKay 2007). The finer the movement, the greater is the demand for information from the exterior environment to carefully calibrate the movement (Neuper & Pfurtscheller 2001; Tsujimoto *et al.,* 2009). The interactions between sensory and motor areas, and their laminae, are thus of great importance in executing and maintaining motor function.

Countless studies have proven that there are structural connections, functional interactions and dynamic connectivity (see review by Neuper & Pfurtscheller 2001), although specific details, especially in humans, are lacking. Figure 1.2 below provides an example of the vast complexity in the structural connectivity in sensorimotor areas.
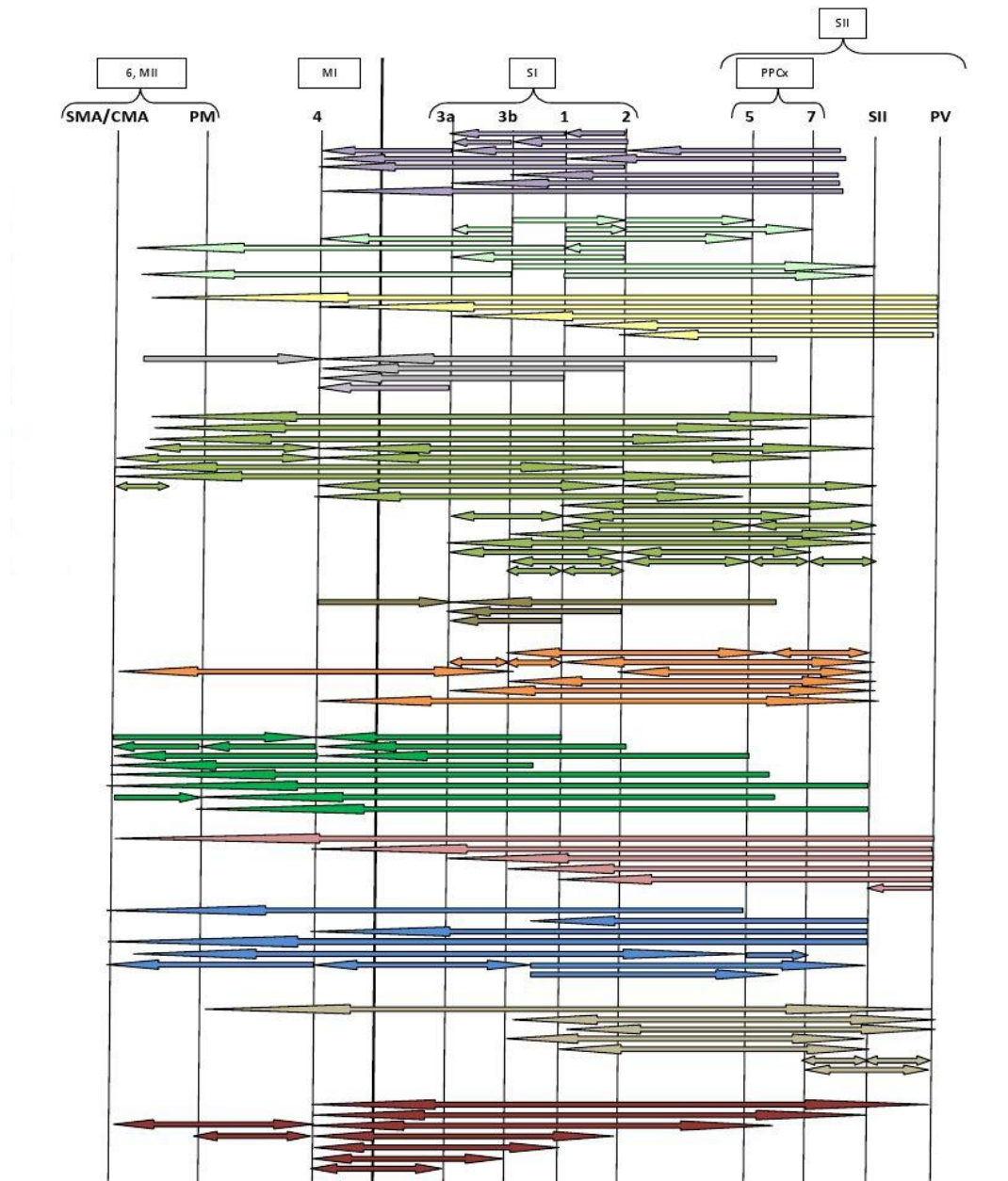
Figure 1. 2. Connectivity between areas of the sensorimotor cortex. The different colours represent different research references. Different authors use different connotations for certain areas, these have been summarised at the top of the figure. Adapted from Jones & Powell 1970; Vogt & Pandya 1978; Jones & Wise 1979; Ghosh *et al.* 1987; Krubizer & Kaas 1990; Felleman & van Essen 1991; Stepniewska *et al.*1993; Geyer *et al.* 2000; Lewis & van Essen 2000; Huffman & Krubitzer 2001; Qi *et al.* 2002; Disbrow *et al.* 2003.

There is a multifaceted system of interconnectivity between the areas of the sensorimotor cortex. Dependent on species, the connectivity has distinct features, although there is a basic mammalian connectivity plan, which has further evolved in simians (Krubitzer &

Kaas 1990). In between different subclasses of apes and monkeys there are additional connectivity distinctions; evolutionary development has depended on what sensorimotor functions were required to survive in the concurrent surrounding (Kaas, 2007; 2008). In some cortical areas, processing of information has changed during evolution (Pons *et al.*, 1992). The size of functionally defined cortical fields has been suggested to change with the genotype of the mammal (Larsen & Krubitzer 2008). The brain of primates has during evolution increased its amount of neurons, from apes to humans, requiring an altered architecture. Organisation between the non-human mammals, primates and humans include modifications in cortical areas with increased number, or altered types, of functional groups in some areas (Herculano-Houzel *et al.*, 2008; Kaas 2008).

The most prominent local circuits found in the primary somatosensory cortex have been mapped as connections between layer II/III to layer V and from layer IV to III (Hooks *et al.*, 2011). In contrast to the primary somatosensory cortex, the motor cortex lacks layer IV, hence the question of how the connectivity is organised in this area is well-posed. The feedforward and feedback pathways observed in sensory cortical areas lose their validity in a cortical area which lacks the major thalamic input layer, e.g. layer IV. In addition, layer III is also thinner. Due to this, the ascending/feedforward pathway, which consists of layer IV projecting to layer III and then down to layer V is absent in the agranular, e.g. motor, cortex and thalamic input is instead directed mainly to layer III (Donoghue & Wise 1982; Shipp, 2005). The circuitry in the agranular cortex, e.g. primary motor cortex, has been summarised as a descending synaptic circuit from layer II/III to layer V and a weak ascending circuit from layer V to layer II/III (Weiler *et al.*, 2008; Shepherd, 2009; Anderson *et al.*, 2010; Hooks *et al.*, 2011). In a recent study, Anderson *et al.* (2010) also concluded that there are parallel pathways for the layer II/III to V projections, depending on the projection target after layer V. In addition to the altered interlaminar route, there appear to be differences in the hierarchical processing in the motor cortex compared to the sensory processing, as suggested by Shipp (2005). Additionally, in the motor cortical region the association areas, premotor and supplementary areas, are more involved in the integrating and modulating of information compared to sensory areas (Shipp, 2005).

1.1.4. Neuronal activity

A typical neuron has a resting membrane potential of -60 to -70 mV. There is a constant flow of ions and molecules over the neuronal membrane, which at cellular rest results in the *resting membrane potential*. Changes to the flow of ions can either depolarise (the intracellular compartment becomes more positive), or hyperpolarise (the intracellular

compartment becomes more negative) the neuron. Ion transport over the membrane can be specific and actively facilitated by transport proteins, or it can be passive along the electrochemical gradient. The active or passive flows of ions over the neuronal membrane are also considered currents; contributions to hyperpolarisation are considered as inhibitory postsynaptic potentials/currents (IPSP/IPSC) and contributions to depolarisation are considered excitatory postsynaptic potentials/currents (EPSP/EPSC). If the overall depolarisation of the neuron, resulting from the summed ion currents, reaches the action potential threshold the neuron fires an action potential. The time it takes for the membrane potential to return to its resting potential from hyper- or depolarisation, e.g. the absolute and relative refractory periods, and any further IPSPs and/or ESPSs, dictate how often a neuron can fire. When an action potential is fired, vesicles with chemical signalling messengers are released at the axonal synaptic terminals of the neuron.

1.1.5. Neurotransmitters

The signalling molecules disperse throughout the 20-40 nM gap between cells, e.g. the synaptic cleft, and bind to specific receptors either on the postsynaptic or, in some cases, on the pre-synaptic cell. Ramon y Cajal, Lorente de No and Otto Loewi established early in the 19th century the important existence of neuronal circuits, synaptic transmission and signalling agents. Today, there are over one hundred different substances that are considered signalling agents, e.g. neurotransmitters such as glutamate, gamma-amino-butyric acid (GABA), serotonin (5-HT, 5-hydroxytryptamine), norepinephrine, acetylcholine and dopamine. These all bind to distinct receptors with several subtypes. Neurotransmitters are responsible for synaptic signalling in the nervous system and bind to receptors on the postsynaptic and presynaptic cell. The cellular response depends on the effect of the receptor activation, so the use of the terminology *excitatory* and *inhibitory* neurotransmitters is only relevant to the two most common substances: glutamate and GABA, respectively. Other transmitters, for example the first neurotransmitter to be identified – acetylcholine, can exert both these mechanisms (Picciotto *et al.*, 2012). Here we consider glutamate as an example of how neurotransmitters can work and what excitation is. Glutamate is the most abundant excitatory neurotransmitter and upon binding to its receptor causes depolarisation/excitation of the target neuronal cell. The excitation is achieved by two different mechanisms initiated when glutamate binds to its receptor, and which of these mechanisms is dependent on the type of receptor. Binding can lead to opening of a cation channel in the transmembrane compartment of the receptor allowing for influx of sodium and calcium ions. This mechanism is typical for *ionotropic* glutamate receptors which are responsible for fast synaptic transmission.

Alternatively, glutamate binding can initiate a slow postsynaptic intracellular signalling cascade, as with the *metabotropic* glutamate receptors. The binding here indirectly leads to depolarisation of the postsynaptic cell through opening of cellular membrane channels. There are three groups of ionotropic glutamate receptors: N-methyl-D-aspartate (NMDA), α-amino-3-hydroxy-5-methyl-4-isoxazolepropionic acid (AMPA) and the kainate receptors. There are eight sub-types of the metabotrophic glutamate receptor, GluR1-R8. Ionotropic and metabotropic receptors co-exist predominantly in synaptic cleft, although kainate receptors also found outside the synapse on the presynaptic cell (Meldrum 2000; Niswender & Conn 2010; Granger *et al.*, 2011; Jackson & Nicoll 2011). Glutamate is released by pyramidal cells, e.g. *excitatory* pyramidal cells. Pyramidal cells generally display the classical neuron structure with one long axon propagating the output through the synaptic terminals while many small dendrites receive input. Pyramidal cells are known for their capacity to connect to more distant areas than within a cortical area or local microcircuits (Brown & Hestrin 2009), for example the large Betz cells discussed earlier (Rivara *et al.*, 2003).

1.1.6. GABA and GABA-receptors

Although two types of inhibitory substances exist in the nervous system, glycine and GABA, here we will pay particular attention to the GABAergic transmission since this is the primary modulation target in our pharmacological intervention. GABA is considered the primary inhibitory neurotransmitter since it hyperpolarises/inhibits the activity of the target cell. Similarly to the example above with glutamate, the effect, e.g. hyperpolarisation/inhibition, is achieved by different mechanisms depending on which type of GABA-receptor GABA binds to (Johnston 1996). There are ionotropic $GABA_A$, or metabotropic $GABA_B$, -receptors. Additionally, the ligand-gated $GABA_C$-receptors, or GABA-Rho receptors are found in the visual system and were for a while considered being a sub-type of the $GABA_A$-receptors since they are also ionotropic (Sedelnikova *et al.*, 2005). Here we predominantly consider $GABA_A$-receptors, which are pentameric proteins of pronounced structural heterogeneity and comprise a transmembrane chloride channel. This channel allows for increased influx of chloride ions when GABA binds to the receptor (Johnston 1996; Sieghart & Sperk 2002; Möhler 2007). $GABA_A$-receptor subunits are classified into 7 sub-families; α, β, γ, θ, δ, ε and ρ. The most predominant receptor in the human brain has an arrangement of two $α_1$, two $β_2$, and one $γ_2$. GABA binds in the interface of the $α_1$- and $β_2$-subunits, which results in two GABA molecules bound per receptor. Deficits in the structure of $GABA_A$-receptors have been linked to a variety of

neurological conditions; anxiety, epilepsy, schizophrenia and insomnia, to name a few (Wong & Snead 2001; Möhler 2006).

Inhibition is mediated predominantly through synaptic transmission. IPSP kinetics depends on the composition of subunits in the $GABA_A$-receptor (Farrant & Nusser 205; Wang & Buzsaki 2012). Neurons releasing GABA are often smaller and connect more locally compared to pyramidal cells, and often interconnect groups of pyramidal cells. These neurons are thus termed GABAergic or inhibitory interneurons. An abundance of different GABAergic interneurons with varying electrophysiological characteristics have been found and there has been several strong attempts to classify interneurons based on varying inherent molecular, anatomical and physiological features of the individual interneurons. To date, the Petilla terminology project offers the most comprehensive overview of the different categories and features of interneurons (Markram *et al.*, 2004; Somogyi & Klausberger 2005; Ascoli *et al.*, 2008).

Intrinsic inhibitory and excitatory circuits in the sensorimotor cortex are predominantly based on GABA and glutamate synaptic transmission between neuronal cells (Keller 1993; Markram *et al.*, 2004; Somogyi & Klausberger 2005). The type of inhibitory cell and synapse determines effects of inhibition (Gupta *et al.*, 2000). Fast-spiking (FS) inhibitory neurons, late-spiking and regular spiking non-pyramidal cells are all found in the rodent frontal cortex, e.g. in the motor areas (Kawaguchi 1993; 1995; Kawaguchi & Kubota 1997). Three main groups of neurons are involved in the synchronous activity in rodent somatosensory cortex (Chagnac-Amitai and Connors 1989). Intrinsically bursting pyramidal cells were found in layers IV or V, FS inhibitory neurons were found in all layers, and regular spiking (RS) pyramidal cells were found in layers II to VI. The IB and FS cells were found to be consistently excited with each synchronous event, whereas the RS cells were inhibited. RS cells and IB cells are found in abundance in layer V of the sensorimotor cortex in rats (Franceschetti *et al.*, 1995; Guatteo *et al.,* 1996). In particular FS interneurons are important for the synchronous activity in the cortex (Hausenstaub *et al.*, 2005; Cardin *et al.*, 2009; Tiesinga & Sejnowski 2009; Wang 2010; Buzsaki & Wang 2012), which will be discussed further in the next section.

1.1.7. GABAergic modulation of neuronal activity

The neuronal output ultimately depends on the balance of excitation and inhibition (Wang 2010; Zhu *et al.*, 2011; Wang & Buzsaki 2012). The modulation of neural activity and essentially physiological functionality, by administration of barbiturates and benzodiazepines, described and used as anxiolytics, hypnotics, anticonvulsants and

myorelaxants has been well-documented and reviewed (Tan *et al.*, 2011; Rudolph & Knophlach 2012), see figure 1.3a-c below. These substances act on the pentameric $GABA_A$-receptors and enhance the inhibitory effects of GABA binding to its receptor. Binding of benzodiazepines requires one of the subunit $\alpha_{1-3,5}$. Benzodiazepines bind in the 'classic' benzodiazepine pocket, located between the α_1 and γ_2-subunits, and increase the frequency of chloride channel opening (Johnston 1996; Priker *et al.* 2002; Mohler 2007).

A   B   C
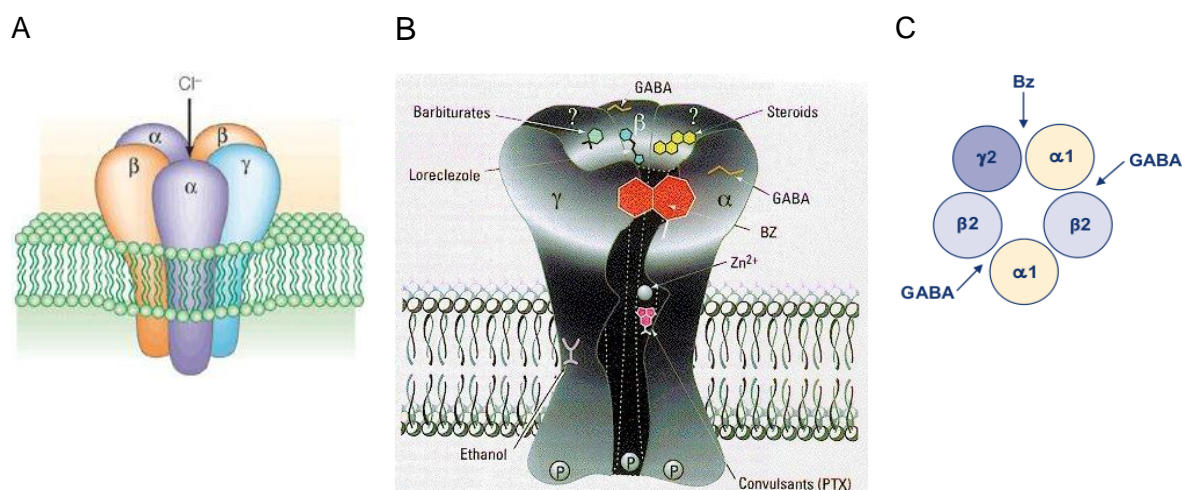
Figure 1. 3a-c. $GABA_A$-receptors have a pentameric arrangement with a chloride channel in the center (a, left). Different substances have different binding sites (b, middle). Benzodiazepines bind specifically between the γ2 and α1 subunit (c, right). A: modified from Belelli & Lambert (2005), B: McKernan & Whiting (1996), C: Martin & Dunn (2002).

Non-benzodiazepines are substances with similar effects to benzodiazepines but significantly different molecular structures; see figure 1.4a-b, below. In particular one of these substances is of interest here; the imidazopyridine zolpidem, prescribed for insomnia for decades (Nicholson & Pascoe 1989).

A   B
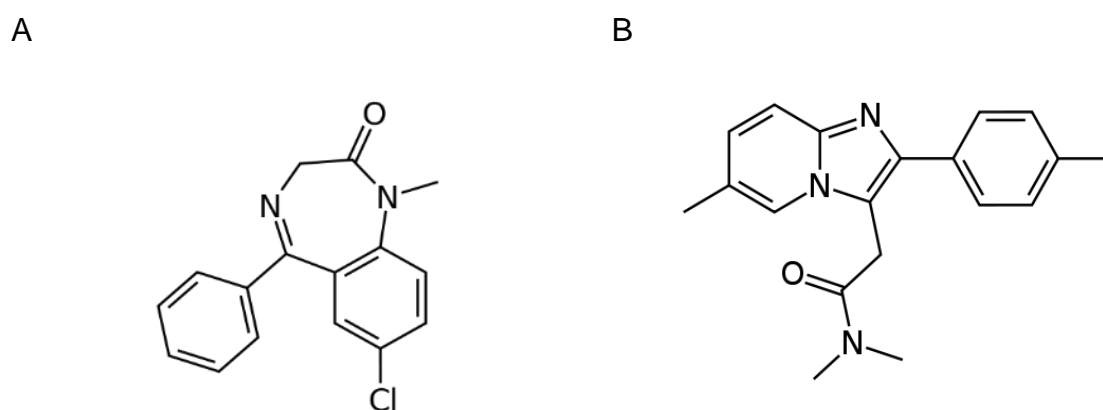
Figure 1. 4a-b. Benzodiazepines, such as diazepam (a, left), and non-benzodiazepines, such as zolpidem (b, right), both bind to the benzodiazepine pocket but have very different structures. Structures modified from PubChem Compound, National Center for Biotechnology Information (2012).

Zolpidem is a GABA$_A$-receptor benzodiazepine site agonist, also known under the registered trademark names Ambien, Stilnox and Lorex. Modelling studies have recently confirmed previous research that zolpidem indeed binds to the benzodiazepine binding site in GABA$_A$-receptor (Sancar *et al.*, 2007; Richter *et al.*, 2012). Zolpidem is less efficient as a myorelaxant and anticonvulsive, as well as at maintaining sleep performance, and more efficient at simply initiating sleep (Depoortere *et al.*, 1986; Rosenberg 2006). However, more than a decade of research on zolpidem has also suggested its beneficial effects in comatose, stroke and Parkinson's disease patients; which are suggested to be due to the effects on the GABAergic transmission in the brain (Daniele *et al.*, 1997; Clauss *et al.*, 2001; Hall *et al.*, 2010). As with other GABAergic drugs there is a risk of abuse (Hsu & Chiu 2012). Further details on the action of zolpidem and its relevance in PD are discussed in chapters 5 and 8.

1.2. Neuronal network activity

1.2.1. Historical perspective on neuronal activity

The first recordings of brain rhythms in humans are often ascribed to Hans Berger in 1924 and were published in the article *Über das Elektrenkephalogramm des Menschen,* in 1929. However, previous to this, recordings of oscillations had been done in dogs by Pravdich-Neminsky, in 1912 and Berger himself based his theories and experiments on the work done by Richard Caton in the 1870's. Caton's work described changes in the baseline currents, measured over the human scalp, relating to sleep and phenomena that could not be attributed to respiratory and cardiac functions. The findings by Caton and Berger were not initially well received by the neuroscience community. Not until Berger's findings of alpha and beta oscillations measured over the scalp, and their attenuation with eye opening and limb movements, had been replicated by the famous electrophysiologist Lord Adrian at Cambridge in 1934 were they recognized as important (Swartz & Goldberg 1998; Millet, 2002; Haas, 2003).

1.2.2. Neuronal network oscillations

The flow of ions over the neuronal membrane results in changes to the membrane potential, e.g. depolarisation or hyperpolarisation. An oscillation is the periodic variation in amplitude around a central value. Neuronal network oscillations are the summed activity of many thousands of neurons. When neurons fire simultaneously (i.e. within a short time window), these cells are said to be firing in synchrony. The summed activity of these neuronal ensembles produces a large enough exchange of current for it to be measured using a range of electrophysiological methods (see chapter 2 for methods of measurement used in this project). Whether the neuronal network activity is measured using *in vitro* electrode recordings or non-invasive human measurements, the observation is a periodic fluctuation in amplitude reflecting current exchange over time; the neuronal network oscillation or 'brain rhythm'. See figure 1.5 for examples of brain rhythms.

The requirement for the activity of individual components of the population to be summed into the average ongoing oscillation is that the events take place within *the time window of synchrony* (Buzaki & Draguhn 2004; Schnitzler & Gross 2005). The time window of synchrony is defined as the time in which two inputs can be added or subtracted before one or both inputs have decayed, which is also dependent on the participating neurons distance from each other. Any event taking place outside of this time window does not contribute to the synchronised activity, since it simply does not interact with the already occurring response. Instead it detracts from the overall synchrony by reducing the signal-

to-noise ratio (Buzsáki, 2006). Higher frequency oscillations (>30 Hz) are believed to have a smaller participating neuronal pool, compared to slower oscillations (<30 Hz), since the time window of synchrony is greater for slower oscillations and more neurons, at larger distances, can theoretically participate. Further distances between reciprocal connections also create a time lag which contributes to slower oscillations (Kopell *et al.*, 2000; Buzsaki & Draguhn 2004; Schnitzler & Gross 2005).
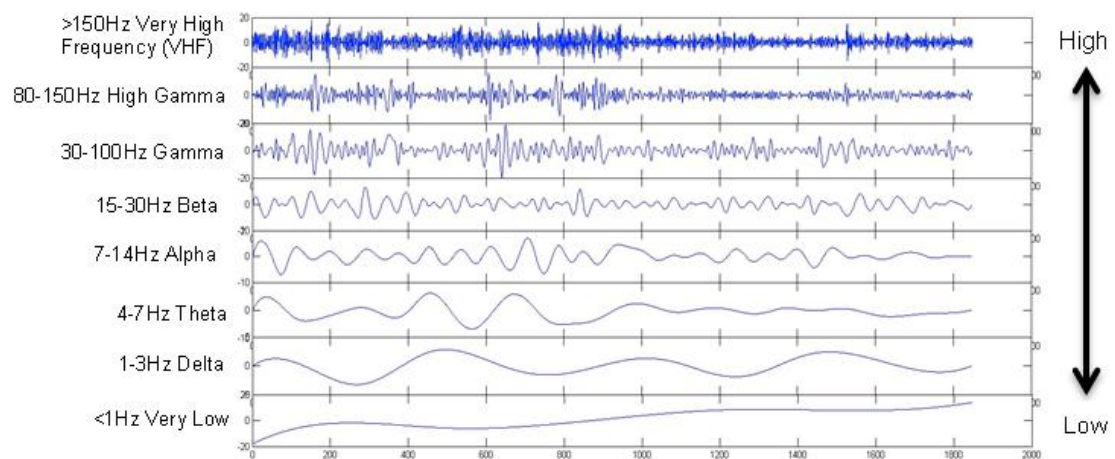
Figure 1. 5. Brain rhythms are amplitude oscillations in the underlying neuronal populations. This figure shows how oscillations at different frequencies appear as fluctuations in amplitude in the recorded signals. The oscillations are often classified according to their frequency, seen to the left. Frequency classes are discussed further in section 1.2.5. Figure is courtesy of Dr SD Hall.

1.2.3. Mechanisms of neuronal synchrony

Due to the fact that brain rhythms are the integrated activity of many thousands of neurons, there are a number of possible bases for their emergence. There can be a common input from a local or remotely located cell, or it can be the neuronal population itself that generates the synchronous activity (Whittington *et al.*, 2000; Wang 2010).

In computer models neuronal network oscillatory activity depends on the dynamic nature of the IPSPs and EPSPs, in the participating neurons, and their connectivity (Whittington *et al.*, 2000; Buzsáki, 2006; Wang, 2010). However, perisomatic IPSPs were early on shown to be more efficient at synchronisation than dendritic EPSPs (Lytton & Sejnowski 1991). This realisation, that the inhibitory activity was better at synchronisation of local neuronal network oscillations, resulted in the originating idea of GABAergically mediated synchronisation and the role of inhibitory interneurons in neuronal network oscillations, such as beta and gamma (Buzsaki & Wang 2012). The original computer models based the rhythmogenesis on inhibitory interneuronal networks (interneuron-based gamma, ING), featuring inter-connected inhibitory interneurons only. These paced each other by

generating synchronous IPSPs and temporally aligned the spike probability in the connected interneurons to when the $GABA_A$-receptor mediated hyperpolarisation had decayed, allowing the interneuron to fire again.

The field of *in vitro* electrophysiology has also contributed greatly to our understanding of some of the physiological mechanisms by which familiar oscillations such as beta (15-30Hz) and gamma (30-100Hz) arise. The frequency of the gamma oscillations generated from the ING model depends on IPSP kinetics and excitation of the interneurons, as shown by both modelling, and *in vitro* experiments in neocortex and hippocampus where the excitatory drive was abolished (Whittington *et al.*, 1995, Wang & Buzsaki 1996). *In vitro* experiments also showed that interneurons and their networks entrain pyramidal cells and pace neuronal network oscillations (Cobb *et al.*, 1995), and pharmacological blocking of the $GABA_A$-receptor abolished oscillations (Whittington *et al.*, 1995).

While ING is a neat model which highlights the simplicity of creating such a complex phenomenon as neuronal network oscillations, it is less relevant in a physiological setting where pyramidal cells are certain to exert effects on the interneurons present, e.g. feedback. Subsequently, when taking pyramidal cells into account the pyramidal-interneuron based gamma (PING) model arose (Whittington *et al.*, 2000; Tiesinga & Sejnowski 2009; Wang & Buszaki 2012). The central difference is which cell class effectively excites the interneurons, the interneurons pacing each other, or pyramidal cells exciting interneurons which then pace the network activity (Whittington *et al.*, 2000). Recently the PING mechanism of oscillatory neuronal network activity was confirmed in the cat visual cortex. Additionally, the PING mechanism model derived from these experiments was extended with computer modelling to encompass the intrinsic membrane resonance, e.g. the natural frequency preference of the interneurons, in the participating interneurons. The resulting model was termed resonance induced gamma (RING) (Moca *et al.*, 2012).

Whether ING, PING or RING is the most relevant mechanism, the core components are interneurons, and in the latter two, also pyramidal cells. Interneurons always pace the network in one fashion or the other (Cobb *et al.*, 1995, Whittington *et al.*, 2000; Wang & Buszaki 2012). In particular, FS interneurons play a role in the rhythmogenesis in neocortex and show strong phase coherence with the ongoing gamma oscillation (Bacci *et al.* 2003, Hasenstaub *et al.*, 2005), see figure 1.6.

Increasing GABAergic drive with, for example, the application of benzodiazepines, infers increased interneuron mediated recruitment to the oscillation, with an increase in the time

that the channel remains open. The effect is a well-characterised reduction in frequency of the net oscillation (Whittington *et al.* 1995, Johnston, 1996; Traub *et al.* 1996a).
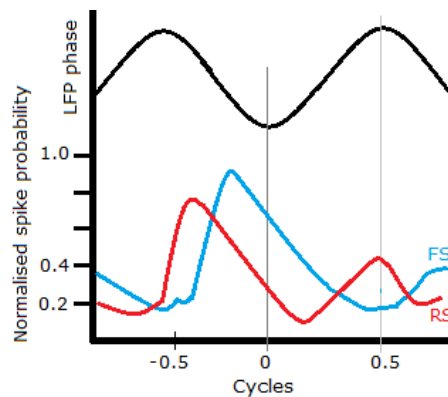
Figure 1. 6. Fast-spiking interneurons and regular spiking pyramidal cells fire at different points of the gamma oscillatory cycle. Adapted from Hasenstaub *et al.* (2005).

Inhibitory modulation, and subsequently oscillatory frequency, is to a great extent dependent on IPSC kinetics; the GABAergic decay and chloride currents (Traub *et al.*, 1996; Uhlhaas *et al.*, 2009). However, electrical gap junctions are also of importance. Apart from providing tonic currents, these have, in combination with synaptic interactions in dendrites, been found to pace action potential generation in the somata (Fukuda & Kosaka 2000; Szabadics *et al.*, 2001; Mann & Paulsen 2007). The combination of electrical gap junctions and proximal GABAergic synaptic interactions will rapidly synchronise the network in the gamma frequency range (30-70 Hz) in the rat somatosensory cortex, whereas alone neither of these could create synchrony between pre- and postsynaptic activity (Tamás *et al.* 2000). Gap junctions promote synchrony, primarily by decreasing the difference in membrane potential between connected neurons. Simulations and pharmacological *in vitro* studies, where gap-junctions were blocked, abolished oscillations; supporting the theory of collaboration between electrical and synaptic signalling (Tamas *et al.*, 2000; Kopell & Ermentrout 2004; Roopun *et al.*, 2006; Yamawaki *et al.*, 2008).

1.2.4. Measuring population activity on different scales

Regardless of the method used to record brain rhythms, whether it is an invasive animal or non-invasive human approach, the recorded activity is the sum product of the synchronous current exchange of tens of thousands of neurons. Measurement of direct electrical activity with small *in vitro* glass electrode as is done in this thesis, the local field

potential (LFP) results from the current variation in the immediate electrode surroundings, estimated at approximately 500-3000 µm around the electrode tip (Mitzdorf, 1987; Logothetis, 2003). LFPs are thus considered an average of the somato-dendritic input signals: inhibitory and excitatory postsynaptic potentials. As a result they indirectly take action potentials into account (Logothetis, 2003; Buzsaki & Draguhn 2004; Schnitzler & Gross 2005).

Measurement of neuronal interaction in living subjects is more complex. This increased complexity is due to the recorded signals from additional areas present both in the source surrounding and in the preparation itself, e.g. compare an isolated sagittal *in vitro* brain slice preparation to the sensorimotor cortex in an intact brain. The additional areas and networks present in and around the source have independent activity patterns. In combination with more connections that are not present in an *in vitro* preparation, these factors contribute to the increased complexity in recorded source signals from non-invasive neuroimaging methods, see figure 1.7 below. Observing neuronal activity on a larger scale, such as in neuroimaging, the summed activity of many neurons in a population, as well as between populations, can be visualized as the oscillatory electrical currents in electroencephalography (EEG), and their corresponding magnetic fields in magnetoencephalography (MEG) (Hämäläinen *et al.*, 1993; Gray, 1994; Buzsaki & Draguhn 2004)*.*
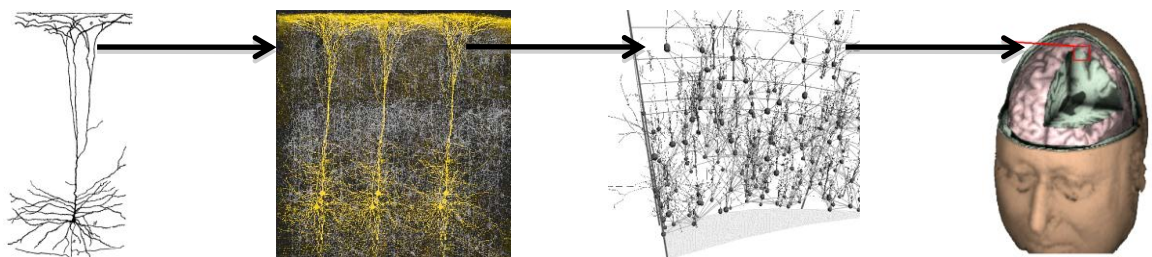
Figure 1. 7. Scaling up through the source sizes of recordings. Going from left to right, the individual neurons can be seen in isolation, in the cortical laminae and finally in the intact brain. This gives an indication about the complexity in a whole brain as measured with non-invasive techniques such as MEG and EEG. Figure is courtesy of Dr SD Hall.

By using non-invasive methods like EEG/MEG, or more invasive methods like electrocorticography (EcoG), the neuronal oscillations in a complex setting can be characterised. The estimated source size of activity seen in neuroimaging recordings depend on the technique used. Functional MRI (fMRI) has a spatial resolution >1-5mm^3 at best, but poor temporal resolution (Olman & Yacoub 2011). EEG recordings have better temporal resolution, but poorer spatial resolution due to the conduction of current through distorting biological tissues. These techniques are therefore often combined in recent

studies (Mantini *et al.*, 2010). Likewise, MEG recordings depend on the signal-to-noise ratio, but also the orientation of cells (see *Methods* for details*)*. The spatial resolution is suggested to be >2 mm of cortical tissue (Hillebrand & Barnes 2003; 2005; 2011; Papadelis *et al.*, 2009). A more precise mathematical assessment of the minimum number of neurons that can be picked up by a MEG signal was proposed by Murakami & Okada (2006) to be 10000-50000; this is also discussed in the methods chapter.

1.2.5. Classification of brain rhythms

Historically, oscillatory activity is classified into different frequency ranges, based on findings from the classic EEG literature (Berger 1929; Adrian & Yamagiwa 1935; Gastaut & Bert 1954). An example of the frequency ranges was seen in figure 1.5, but can also be seen in table 1.1. In reality, EEG was not initially aimed at distinguishing frequencies. Rhythmicity and periodicity were difficult to determine from paper traces, although even Berger attempted this (figure 1.8).
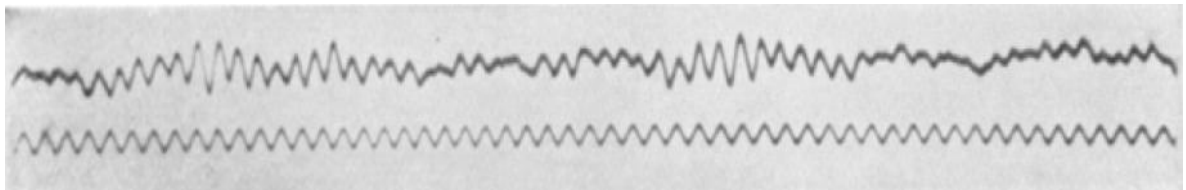
Figure 1. 8. The top trace shows a recording of Berger's original findings of alpha activity over the scalp. The bottom trace shows an artificial 10 Hz pace added externally. Modified from Berger's paper in 1929.

Rather, the focus was often on the shape of the trace, as exemplified by the mu rhythm reported by Gastaut & Bert in 1954, which was named after the Greek letter with the similar shape. The traditional frequency bins developed in different and often clinical, laboratory settings. There was a focus on determining normality in behaviour, and characterisation was initially based on the appearance, while the approximate frequency band and the location that was currently investigated in the particular research laboratory were noted as additions. For example, the mu rhythm was originally characterised as indicative of restlessness and general dysfunction (Gastaut & Bert 1954). Different researchers have used different classifications, thus we consider 'frequency bins' approximate and loosely associated with different functions, see table 1.1.

Sorting oscillations into approximate frequency bins, and their designations, is accepted practise in neuroscience. Some researchers put both beta and gamma oscillations in the same group (Pfurtscheller & Lopes da Silva 1999; Steriade, 2006), while other emphasise

strong distinctions between different small frequency bands and argue that there are clear differences between the rhythms. Reduced computer models of network oscillations show that beta oscillations rapidly can transform into gamma frequency oscillations after further membrane depolarisation and additional recruitment of pyramidal cells to an ongoing interneuron network oscillation (Kopell *et al.*, 2000). While the contributions to network oscillations in computer models are clear, the exact neuronal composition and participation in any biological preparation is less clear. This makes it difficult to extrapolate computer models to neuronal network oscillations in more physiological and complex situation, for example in neuroimaging settings.

Table1. 1. Different frequency classes of oscillations

1-4 Hz	Delta	Associated with slow wave sleep.
4-8 Hz	Theta	Drowsiness. Prominent over hippocampal structures during orienting, conditioning and memory encoding/ retrieving.
8-12 Hz	Alpha	Relaxed state. Most prominent over occipital lobe when eyes are closed.
	Mu (~10 Hz)	Found over somatosensory cortex, related to and attenuates with actual and imagined movement, as well as somatosensory stimulation in normal subjects. Also linked to attention and cognitive functions within the sensorimotor system.
	Tau (~10 Hz)	Found in the auditory system, responsive to auditory stimuli.
12-35 Hz	Beta	Found over motor cortex and basal ganglia, related to and attenuates with actual and imagined movement, as well as somatosensory stimulation in normal subjects. Also linked to attention and sensorimotor processing.
35-100 Hz	Gamma	Suggested to play a role in attention and higher cognitive processes.

(Adapted from Ward, 2003; Steriade, 2006b; Ritter *et al.,* 2008).

1.2.6. Functional significance and relevance of neuronal oscillations

Different frequencies are, as mentioned, traditionally classified into different bins. As the development of EEG recording techniques progressed and researchers were reporting oscillations of particular frequencies, certain frequency bands became associated with specific functions. Table 1.1 presented an overview of common functions associated with particular frequency bands. The idea of functional significance of oscillations dates back to Berger's experiments in 1929, where the ongoing alpha activity recorded over the subjects scalp was attenuated by the subject (in this case Berger's own son) opening his eyes. For this reason the alpha oscillations gained the alternative name *Berger's rhythm.* Later research established that alpha activity (8-12 Hz) was particularly evident over the occipital areas of the scalp, overlying the visual cortex when the subject's eyes were closed. Additionally, alpha oscillations also appear to have further functions since they are enhanced during internal processing such as calculation and visual imagery (Palva &

Palva 2007). Berger also reported on ongoing beta (13-30 Hz) oscillations and since then this rhythm has been primarily associated with motor performance and movement (Neuper & Pfurtscheller 2001). Another rhythm that can be found over the sensorimotor cortex is the ongoing mu rhythm (~10 Hz), which is functionally linked to action and perception (Hari, 2006). Gamma activity (30-100 Hz) is currently also linked to both motor and visual function and stimulus presentation (Gray & McCormick 1996; Tallon-Baudry & Bertrand 1999; Muthukumaswaramy 2010). A century of research highlights the importance of oscillations for cognitive function and the need for further understanding of neuronal network activity in the cortex (Başar *et al.*, 2001).

An attractive rationale for the existence of oscillations, as opposed to a binary system, is the capacity for energy conservation and information encoding (Buzsáki, 2006). The relevance of oscillations to information encoding is particularly well illustrated by the *binding hypothesis*; rhythms such as beta and gamma in visual areas serve to temporally align the neuronal substrates responsible for the relevant input/output and subsequent information processing and integration (Crick & Koch 1990, Gray & Singer 1995; Tallon-Baudry & Bertrand 1999; Ward 2003; Womelsdorf *et al.*, 2006; Fries 2009).

1.2.7. Sensorimotor network activity

The focus of this thesis is the neuronal network activity that arises in the SMC. In the SMC, as reflected in the original work by Berger in 1929 and Gastaut & Bert in 1954, the prominent feature of electrophysiological recordings from the sensorimotor areas in the human brain are beta (15-30Hz), and mu (~10Hz) rhythms. The established peak of the mu rhythm in human studies is peculiarly shaped, featuring a double peak; albeit not harmonics (Tiihonen *et al.*, 1989; Hari 2006). The mu rhythm is reported to be found over the somatosensory cortex, while the beta rhythm is observed over the motor cortex. The somatotopic organisation of the sensorimotor cortex, and the homunculus, were established by Penfield and colleagues in the 1930's and 40's, and oscillations are also observed to have a somatotopic arrangement (Salmelin & Hari 1994; Salmelin *et al.*, 1995; Pfurtscheller & Lopes da Silva 1999; Salenius & Hari 2003).

1.2.8. Functional relevance of sensorimotor mu and beta oscillations

Ongoing beta and mu oscillations decrease and increase in amplitude during different phases of motor and somatosensory events. The amplitude decrease is termed event-related desynchronisation (ERD), while the amplitude increase is called event-related synchronisation (ERS) (Pfurtscheller & Aranibar 1977; Pfurtscheller & Lopes da Silva 1999, Neuper & Pfurtsceller 2001; Neuper *et al.*, 2009). Synchronisation of oscillatory activity in an area is suggested by some researchers to represent deactivation of that area, e.g. increased inhibition, not needed for the task. In contrast, desynchronisation represents activation, e.g. increased excitation, of an area relevant to the task (Pfurtscheller & Lopes da Silva 1999; Pfurtscheller & Neuper 2001).

1.2.8.1. Event-related desynchronisation – before the event

The attenuation of the mu and beta rhythms with movement first reported by Berger, in 1929, are now referred to as mu and beta ERD (Pfurtscheller & Aranibar 1977; Pfurtscheller & Lopes da Silva 1999, Neuper *et al.*, 2009), or movement related beta desynchronisation (MRBD) (Defebvre *et al.*, 1996; Hall *et al.*, 2011). Beta ERD is, however, also seen prior to somatosensory stimulation; attenuation of the ongoing beta oscillations in the sensorimotor cortex during stimulation was reported already in Jasper & Andrew's experiments in the 1930's, and confirmed by Pfurtscheller in 1981.The beta ERD prior to voluntary movement has been reported to start in the contralateral hemisphere up to 2 seconds before movement onset (Stancák & Pfurtscheller 1995; 1996; Alegre *et al,.* 2004). The mu ERD starts approximately 1 second later. The beta ERD spreads to a bilateral pattern just prior to and during execution of the movement itself, although the contralateral beta ERD remains stronger (Stancák & Pfurtscheller 1995). In early experiments by Jasper & Penfield (1949), the ERD was sustained during successive voluntary movements, but short-lasting around a single self-paced movement execution. The beta ERD prior to voluntary movement is argued to modulate change in muscle tone and general activation of motor cortex (Stancák & Pfurtscheller 1995; 1996), and the later part of the beta ERD is proposed to relate to afferent inputs (Alegre *et al.*, 2002). Beta ERD is suggested to be an effect of input and activation in contralateral sensorimotor areas. Different activation patterns in the beta and mu frequency ranges for cued/externally paced and internally/self-paced movements were found by Gerloff *et al.* (1998). Essentially, small, but distinct, differences in activation pattern and functional coupling between beta and mu ERD indicate that these rhythms contain different aspects

of information processing relevant for optimising and preparing the motor task, potentially within the same sensorimotor network (Pfurtscheller 1992; Gerloff *et al.* 1998).

1.2.8.2. Event-related synchronisation – after the event

The beta ERS after movement/stimulation offset generally reaches higher power than before the initial baseline period, and is therefore called post-movement/post-stimulation beta-rebound (PMBR). The mu rhythm shows event-related synchronisation, but does not display rebound activity (Pfurtscheller 1992; Stancák & Pfurtscheller 1995; Neuper *et al.*, 2006). Subjects imagining or watching a movement display both beta ERS (and ERD) (Pfurtscheller & Neuper 1997; Schnitzler *et al.* 1997). The PMBR occurs within 0.5s of movement offset and the motor cortex shows reduced excitability during this time period (Chen *et al.*, 1998; Tokimura *et al.*, 2000). The beta rebound usually occurs while the mu rhythm is still in its ERD state (Salmelin *et al.*, 1995; Neuper & Pfurtscheller 2001). There are also reports of a significantly greater beta ERS for hand movements, compared to finger movements. This is suggested to be due to the size difference in the neuronal population responsible for the movement, more neurons are responsible for the movement of two fingers than for one finger (Pfurtscheller *et al.*, 1998).

1.2.9. Cognitive relevance of sensorimotor mu and beta oscillations

The similarity in beta oscillatory activity patterns and underlying effects on the sensorimotor cortex with movement and stimulation has been substantially verified in the last decade, and research has indeed shown that effects of stimulation and movements involve parts of the same sensorimotor network; exemplified by the suppression of rebound activity from actual and imagined movement (Schnitzler *et al.* 1997; Neuper *et al.* 2006).

The beta rebound activity is believed to reflect the "task-complete" state and represents the inactivated or "idling" state of the motor cortex (Pfurtscheller 1992; Chen *et al.*, 1998; Alegre *et al.*, 2004). However, some researchers argue that this is not the complete picture; the beta rebound activity also reflects the somatosensory feedback after a movement. The hypothesis of rebound activity as an indicator of *feedback* is based on experiments where stimulation-induced rebound activity in the motor cortex is reduced by actual or imagined movement (Schnitzler *et al.* 1997; Neuper *et al.* 2006). Additionally, movements performed under ischaemic nerve block have been shown to result in a lack of PMBR (Cassim *et al.* 2001), although another similar study reported that there was no difference in the rebound activity (Schnitzler *et al.* 1997). The feedback theory has also

been supported by studies showing a reduction in PMBR after forced termination of movement (Alegre *et al.,* 2008) and earlier occurrence of PMBR in no-go movement trials (Leocani *et al.*, 2001). These results suggest that the rebound activity in MI is a feedback mechanism; potentially encompassing other areas than simply the somatosensory cortices. Closely related to the feedback theory is the hypothesis of beta ERS as a resetting mechanism of involved [sensorimotor] networks (Pfurtscheller *et al.* 2005; Pfurtscheller & Solis-Escalante 2009), where the short-lasting synchronisation prepares and retunes the networks to the default, input-accepting, state.

1.2.10. Rhythmogenesis in sensorimotor cortex

1.2.10.1. Beta rhythm

A substantial body of *in vitro* and *in vivo* animal research over the last decades has aimed to reveal information about the mechanisms underlying rhythmogenesis in the sensorimotor cortex (Whittington *et al.*, 1995; Murthy & Fetz 1996; Buhl *et al.*, 1998; Cunningham *et al.*, 2004; Roopun *et al.*, 2006; Yamawaki *et al.*, 2008). Consistent with computational models (Traub *et al.,* 2000), additional studies have shown that beta oscillations in rodent MI *in vitro* show dependency upon $GABA_A$-receptor activation (Yamawaki *et al.*, 2008). These observations are in agreement with human MEG studies, in which the motor cortex beta rhythm is augmented following the introduction of GABAergic modulators such as benzodiazepines (Jensen *et al.*, 2005; Hall *et al.*, 2010). Recordings from discrete laminae of rodent MI *in vitro* reveal beta oscillations in layers II/III and V; layer V appears to drive the superficial layers (Yamawaki *et al.*, 2008). Yamawaki and colleagues showed that FS cell firing at beta frequency is strongly coherent with the LFP activity with a constant phase relationship, see figure 1.9a-f.
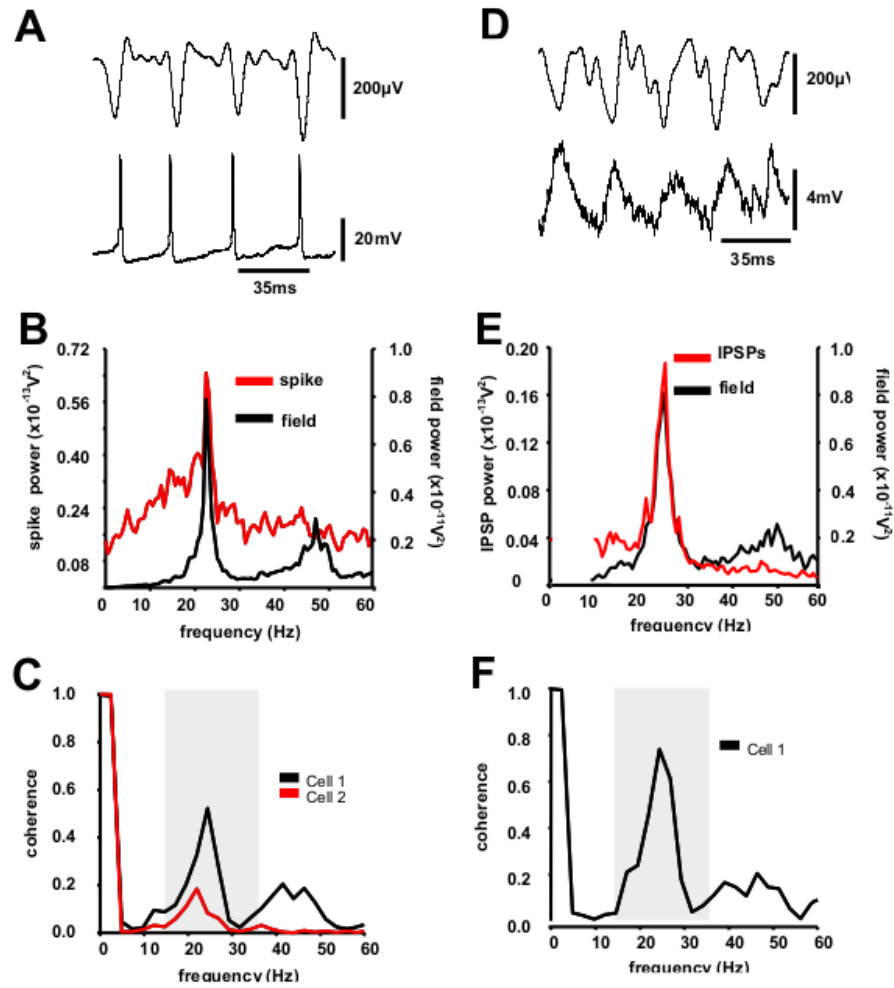
Figure 1. 9a-f. Relationship between beta frequency LFP oscillations and action potentials and IPSPs of FS cells. Example traces of simultaneously recorded beta field activity (top) and APs (bottom), is seen in **A**. In **B** the averaged power spectrum from two recordings of field activity (black) and APs (red) can be seen. Coherence analysis of field and APs from each recording is shown in **C**. Example traces of simultaneously recorded beta field activity (top) and reversed IPSPs (bottom, cell held at -90mV), is seen in **D**. In **E** the power spectrum of field and IPSPs received by FS cells is seen. Coherence analysis of field activity and IPSPs received by FS cell is shown in **F**. Grey shadow indicates beta band of 15-35 Hz. Modified from Yamawaki (2008: PhD thesis).

1.2.10.2. Mu rhythm

Apart from the beta rhythm, other sensorimotor oscillations are less well characterised in the *in vitro* literature. The mu rhythm, e.g. 8-12 Hz, is typically not a feature of the power spectrum seen for MI *in vitro*. It is unclear whether this scarcity is the result of methodological limitations, whereby the absence of extensive cortico-cortical or other connections precludes their observation. Mu rhythms seen in human EEG/MEG studies appear to be particularly influenced by cognitive and attention factors (Zhang & Ding 2010; Anderson & Ding 2011; van Ede *et al.*, 2011), and simulation studies have indicated

that oscillations in the 8-12 Hz range can be produced and modulated by feed forward and backwards connections (Jones *et al.*, 2009). The mu rhythm will be discussed in further detail in chapter 3.

1.2.10.3. Gamma rhythm

In contrast to the abundance of research literature supporting the existence of sensorimotor mu and beta oscillations, spontaneous activity in the gamma frequency region is not regularly reported in human EEG/MEG studies. However, increasing GABAergic drive with benzodiazipines does elicit an increase in power in the gamma frequency range, limited to SI in MEG (Hall *et al.,* 2010). This finding is consistent with recordings from sensory areas *in vitro*, in which gamma oscillations are GABAergically mediated (Roopun *et al.,* 2006; 2010).

1.2.11. Spontaneous oscillations and resting state networks

There is a great deal of current interest in attempting to characterise and understand the intrinsic activity of the human brain between functional states. Comparable to the observation that global oscillatory changes occur across the brain during the various phases of sleep and waking, the idea that the brain possesses an intrinsic 'resting' or 'default' state is one that carries favour at the time of writing. These networks comprise a series of interconnected loci across the brain that exhibit a baseline communication state, from which functional commands can be initiated. This network, initially termed the default mode network (DMN), has been extensively studied with functional magnetic resonance imaging (Raichle, 2001). The underlying concept of a task-negative state as a criterion for the DMN has come under questioning since there are many cognitive processes which do not necessarily result in a task being performed, but still requires activation of particular areas of the brain. One relevant sensorimotor example is the difference between imagined and actual movements; they both change the network activity, but only one of these is actually a task-positive state (Deco *et al.* 2011). Enter the idea of resting-state networks (RSN). The activity during resting is used as a description of network dynamics, rather than tasks-negative states. Functional connectivity in a resting-state network involving the motor system was described by Biswel *et al.* (1995), and other research has since described several resting states networks using fMRI (Damoiseaux *et al.* 2006, Deco *et al.* 2011). In an attempt to find the electrophysiological basis for RSNs, Mantini *et al.* (2007) combined EEG with fMRI. They identified 6 RSNs, one of which was similar to the previously proposed principal DMN; responsible for internal processing. Interestingly, one of the RSNs identified was related to sensorimotor activities and comprised the precentral,

postcentral and medial frontal gyri, primary sensory and motor cortices as well as the supplementary motor area. See figure 1.10 below, for the somato-motor RSN that was suggested by Mantini *et al.*.
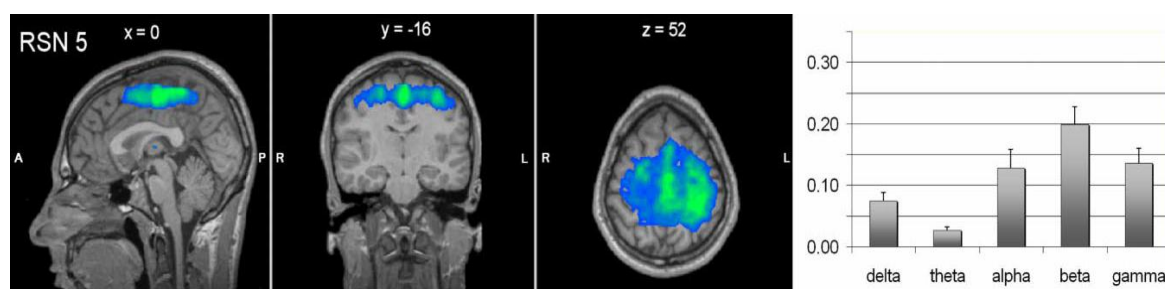
Figure 1. 10. Mantini *et al.* (2007) identified a somato-motor resting state network which they correlated to alpha, e.g. mu, and beta activity in the sensorimotor cortex. Adapted from Mantini *et al.* (2007). Y-axis is correlation.

This *somato-motor* RSN was associated with beta rhythms and to some extent alpha and gamma; although Mantini *et al.* (2007) do point out that it would be an oversimplification to assume that the complex dynamic networks interacting in the areas covered in the RSNs would display one or two rhythms only.

Network theory from other areas of science has generated several models of how the information flows in the sensorimotor areas. Brovelli *et al.* (2004) demonstrated, using a Granger causality model, that during motor behaviour the synchronized beta oscillations bind several sensorimotor areas into one single large-scale network. This network is a functioning sensorimotor loop with a unidirectional pattern in the activity of the different subareas of the sensorimotor cortex. The results indicated that the information from the periphery gives rise to an activity pattern starting in the somatosensory and inferior posterior parietal cortex, and subsequently ending in the motor cortex. Detailed results from directional modelling, or the precise nature of RSNs, intrinsic activity or dynamics, are less than straight-forward. Although the complexity of neural networks and their dynamics prevent exact definitions and mapping of cognitive processes, there is still the actuality of what is known about resting-state and intrinsic network activity and dynamics in healthy subjects; these indeed appear disturbed in many of the neurological disorders and conditions that affect humans and other mammals. One of these is Parkinson's disease (PD). The synchronisation patterns in the beta frequency band are altered in PD, which is coupled to the severity of clinical symptoms. This implies that neural synchrony is a physiological mechanism for coordination of brain areas required for particular functions (Uhlhaas & Singer 2006; Hammond *et al.*, 2007Uhlhaas *et al.*, 2009).

1.3. Parkinson's disease

1.3.1. The shaking palsy

An Essay on the Shaking Palsy was written nearly two hundred years ago, in 1817, by the English physician James Parkinson, and contained the first description of two of the clinical symptoms today associated with the disease: resting tremor and akinesia (or *palsy* in historical terminology). Today the symptoms of PD also include bradykinesia and rigidity, as well as atypical posture and gait (Rivlin-Etzion *et al.*, 2006). PD has a prevalence of 1%, rising higher after age 65, thus age is the most important risk factor for PD. As the elderly population grows, so will the number of PD patients, creating a demand for better understanding and treatments of PD (Davie, 2008).

1.3.2. The role of the cerebral cortex in PD

In PD the symptomatic motor problems can be associated with changes in the oscillatory activity in the brain. Cortical and subcortical areas have been found to display abnormally synchronized beta frequency outputs in PD patients (Brown, 2007; Kühn *et al.*, 2009, Vardy *et al.*, 2011). To date the cortical activity alterations in PD patients and the central role of cortex in functional connectivity, are implicit, but poorly understood. The effect of the altered activity in the basal ganglia affects the cortical processing and characteristic brain-state activity and one study suggested that the afferents to STN from motor cortex, in the hyperdirect pathway, played an important, but unknown, role in the pathological beta activity that can be seen in PD (Gradinaru *et al.*, 2009).

The dynamics of the beta frequency activity in the motor cortex, in PD patients, has been found to differ to those in healthy subjects (Labyt *et al.*, 2005; Brown, 2007), again suggesting an undetermined role of the cerebral cortex in generating and/or maintaining the abnormal rhythm. The post-movement synchronisation of beta frequency activity, in the motor cortex is decreased in PD subjects (Degardin *et al.*, 2009). This has been suggested to indicate that somatosensory processing and somaesthetics are changed in PD (Tamburin *et al.*, 2003), since beta ERS is believed to reflect not only the motor offset command, but also inhibition from the somatosensory areas (Cassim *et al.*, 2001; Pfurtscheller *et al.*, 2005). Sailer *et al.* (2003) further concluded that the sensorimotor integration is altered in PD patients. Cortical excitability has been found to be changed in PD (Ridding *et al.*, 1995; Lefaucheur, 2005) and MacKinnon *et al.* (2005) also suggested that there is a change in facilitation and inhibition in the intracortical pathways in PD patients.

1.3.3. Network activity and connectivity in PD

The notion of PD induced altered cortical excitability and activity fits well with the suggestions of transformed network activity and layout, followed by changes in synchrony found in PD as well as other neuropathies (Uhlhaas & Singer 2006; Brown, 2007; Hammond *et al.*, 2007). In particular, the findings of increased cortico-cortical functional connectivity in early-stage PD patients, as well as a slowing of oscillatory activity as a marker of non-demented PD patients, with changes in theta, alpha, beta and gamma bands, are interesting when considering sensorimotor integration (Stoffers *et al.*, 2007; 2008). The cortico-cortical coherence in the upper and lower beta band was found to correlate with the severity of the Parkinsonian symptoms by Silberstein *et al.* (2005), as well as a subsequent reduction in correlation and clinical status when levodopa or STN-stimulation was administrated. Bidirectional communication between the cortex and the basal ganglia was found during movement in PD patients (Lalo *et al.*, 2008) and these findings, taken together, indicates that there several levels of bidirectional network activity to take into account when considering the altered cortical network activity and responses in PD.

Since reaction time depends on the processing and interaction of information from the periphery with the motor system, this has been a focus of studies in PD patients. Evarts *et al.* (1981) found only minor deficit in reaction time in patients, and later investigations are equally ambiguous. Results from response tasks where PD patients show decreased response inhibition and response initiation, have often been interpreted as failure of the basal ganglia to correctly modulate the cortical output to movement (Cooper *et al.*, 1994; Gauggel *et al.*, 2004). Bradykinesia, i.e. slowing of movement, could potentially confuse the results of reaction time and response experiments, and is a more severe problem for patients than simply the possible slowing of reactions (Hammond *et al.*, 2007). However, reaction time is still an interesting point of investigation in PD patients; this would yield information about the sensorimotor processing mechanisms in PD compared to healthy subjects.

Resting state, e.g. ongoing, oscillations in primary motor cortex in the alpha, beta and gamma frequency range, have been found to be decreased frequency-wise in PD patients (Bosboom *et al.,* 2006; Moazami *et al.,* 2008), with a further reduction in PD patients with dementia (Bosboom *et al.,* 2006). This reduction in frequency during rest was shown by Vardy *et al.* (2011) to correspond to disease severity, measured by UPDRS scores, and specifically pertaining to the cognitive sub-scores.

1.4. General aims of this thesis

In this thesis the aim was to explore the comparable nature of SMC oscillations recorded *in vitro* and with MEG. Integration and comparisons of these approaches were performed and interpreted in context of generation of oscillations in the SMC. The scale of the observed neuronal network activities were also studied, as well as the relevance and dependence of connectivity within and between sensorimotor areas. Additionally, the effects on sensorimotor oscillations from pharmacological modulation in healthy and PD subjects were determined. Finally the effects on ongoing sensorimotor oscillations from stimulation interventions with frequency specific stimulation protocols were assessed.

Chapter 2. Material & methods

2.1. Neuroimaging

2.1.1 Magnetoencephalography

MEG is a non-invasive method, which allows for measuring brain activity through the magnetic fields created when current flows through neurons in the cortex. Magnetic fields can be mathematically described according to Maxwell's equations, and are perpendicular to the electrical current flow.

2.1.1.1. MEG technology

MEG was first introduced by David Cohen in 1968 and is based on the detection of the magnetic activity in the femtoTesla range (fT, 10^{-15} Tesla), the typical MEG signal is 50-500fT. This is made possible by an array of superconducting quantum interference devices (SQUIDs). Superconducting devices contain metals with no conduction resistance and need to be cryogenically maintained to function optimally, usually in a vacuum container with liquid helium (Dewar). SQUID sensors are connected to flux transformers; consisting of a pickup coil and connections to the SQUID. The pickup-coil is positioned closest to the participant's scalp and converts the magnetic fields generated by the cortex into current. In order to reduce the external (non-biological) noise, and thus distinguish the weak biomagnetic signals from other magnetic signals and electric devices in the surround, the MEG participant is placed in a closed and magnetically shielded room (Zimmerman, 1970, Hämäläinen *et al.*, 1993). The basic (dc)SQUID sensor consists of superconducting rings, allowing electrical current to pass without resistance, and Josephson junctions, singling out the electrons through the tunnelling effect as they pass through the junctions. The pickup coils in the flux transformers work as magnetometers; efficient at spatial filtering. Magnetic noise signals from the surrounding will be further reduced than signals close to the flux transformer itself, due to the inherent decay constant of the dipolar magnetic signal (Hämäläinen *et al.*, 1993; Vrba & Robinson 2001; 2002). Aston University's CTF MEG system employed third order gradiometers and had 275 channels. Flux transformer function relies on electromagnetic induction and magnetometers; the magnetic fields emanating from the brain induce a current in the electrical superconducting wire in the magnetometer/gradiometer. The simplest is the magnetometer. In a third order gradiometer the wire is looped several times; these loops have distinct distances from each other, allowing the decay in the magnetic field, and subsequent induced electrical current, to be calculated in relation to these distances (Vrba & Robinson 2001). See figure 2.1a-c.

Figure 2. 1a-c. The dewar with arrangement is shown in a (top left). A schematic of a magnetometer and third-order gradiometer is shown in b (top right). The layout of the dcSQUID sensor is seen in c (bottom). Pictures from Vrba & Robinson 2001; 2002.

2.1.1.2. Neuronal basis of the MEG signal

The main contributors to the magnetic fields are the dendritic postsynaptic currents due to their dipolar shape, as opposed to the quadrupolar-shaped axonal current. The difference between these fields is the different decay times; the field around the axonal current falls of more rapidly compared to the dendritic field dipole. This characteristic of magnetic fields, in combination with the overwhelmingly larger amount of dendrites compared to axons indicates the postsynaptic currents as contributors to the magnetic fields measured with MEG (Hämäläinen *et al.*, 1993). Additionally, due to the decay of the magnetic field, MEG is also not suitable for deep structures (Hämäläinen *et al.*, 1993), but essentially MEG is able to detect most cortical signals, apart from <2 mm of the gyri crest (Hillebrand & Barnes 2002).

Since the dendritic currents are the major contributors to magnetic fields, the distribution of cortical cell dendrites is relevant for the biomagnetic activity. Cells with a symmetrical dendrite organisation, such as stellate cells in layer IV, will contribute less to the overall magnetic field because the fields cancel out overall. In an asymmetrically organised cell, for example the pyramidal cells mainly found in layer V and II/III, the magnetic fields generated around the somato-dendritic currents will not cancel out and can therefore be picked up by the SQUIDs (Murakami & Okada 2006).

Several studies have investigated the underlying source size of, and orientation, in the MEG signal using a variety of methods, often combined with mathematical models. Recording magnetic field activity from a hippocampal excised tissue, Murakami *et al.* (2002) showed that the sensitivity of a dcSQUID is capable of detecting population activity from an area as small as 100-400 μm. However, recording of this activity was not only done in optimal conditions with stimulation-induced activity, but also in a small piece of tissue. In essence, the MEG equipment used in whole head MEG is capable of detecting magnetic tangential field activity from 10000-50000 synchronised pyramidal cells in layer II/III and layer V (Vrba & Robinson 2001; Murakami & Okada 2006).

2.1.1.3. Source localisation of the MEG signal

For each magnetic field there is an underlying current dipole. Empirical data, from measuring the change in magnetic fields, need to be attributed to their electrical origin. This is an example of an inverse and ill-posed problem, where the empirical data exists, but the underlying actual source is one of an infinite number of possibilities (Hauk, 2004; Barnes *et al.*, 2006). Since the changes in oscillatory frequency and power between two time points, or states, were the focus of this project, this allowed circumvention of the inverse problem by using a non-linear beamformer method called synthetic aperture magnetometry (SAM). This method is based on defining constraints for the output (e.g. time windows and frequency bands) and then weighting all output from the 275 sensors to give a picture of the activity in the predefined MRI space, which is divided into 5 mm^3 cubic voxels, see figure 2.2.

Figure 2. 2. SAM uses a spatially weighted summation of the outputs of the SQUID sensor array to focus on one target voxel and minimise the received power from other regions. Picture from Vrba & Robinson 2002.

Two SAM time windows are defined: the pre-functional (or passive) and the functional (or active). The computed difference in oscillatory power in a predefined frequency band,

between the specified time periods, are given as t-scores over the voxels; effectively a 3-dimensional map of oscillatory power change. Usually 10-30 events results in a good signal-to-noise ratio and SAM produces a t-statistic for each voxel (van Veen, 1997; Vrba & Robinson 2002; Hillebrand & Barnes 2003). This 'standard' SAM approach foregoes temporal resolution, in exchange for a fairly low number of trials needed. However, some functional effects occur over a very short period of time and can be hard to detect with this SAM approach. Event-related SAM (ERSAM) is a related approach, where the focus is on the time- and phase-locked responses to an event, rather than the induced oscillatory changes. This method requires more trials but allows for higher temporal resolution. Here, in the human MEG recordings, we used these two SAM-based approaches to localise MI and SI. The PMBR was used as the active period for localisation of MI, by using the standard SAM beamformer technique. ERSAM and somatosensory evoked potentials were used to localise SI (Cheyne *et al.* 2006; Jurkiewicz *et al.*, 2006), see section 2.1.1.5. and chapter 3 (methods), for further details.

The source location of the underlying cellular currents, giving rise to the magnetic fields is pinpointed in several steps. The MRI of the subject's brain (see section 2.1.2 for details on MRI methodology), is linked by spatial reference points on the subject's head before the actual experiment. The spatial reference points are recorded by a Polhemus Isotrak digitisation system (Kaiser Aerospace Inc. U.S.A), these points also assist in tracking any movement in relation to the SQUIDs during the experiment. The polhemus digitisation process consists of first attaching electrodes to the nasion and to the left and right preauriculars, the position of these are monitored continuously during the experiment. This is followed by digitisation of the position of these electrodes and scalp surface. The digitised scalp surface coordinates are co-registered with the scalp surface of the MRI image, i.e. the two images are digitally fitted to each other (Adjamian *et al.*, 2004). The t-scores from the SAM analysis will then correspond in spatial localisation to anatomical sites determined from the subject's co-registered MRI (Hillebrand & Barnes 2003).

2.1.1.4. Virtual electrodes

The location of interest, detected by the SAM beamformer analysis and anatomically identified in the subject-specific MRI, can be used to position a virtual electrode (VE). A VE is a spatially precise implementation of the SAM algorithm which allows for recreating of the neuronal activity underlying the signal in the precise voxels of interest (Hillebrand & Barnes 2003; Hillebrand *et al.*, 2005). The approximate source size for detection of neuronal activity with a SAM-based VE is >2mm, and mainly depends on the signal-to-

noise ratio and orientation (Hillebrand & Barnes 2002,; 2003; Hillebrand *et al.*, 2005). See section 2.4 for details of offline analyses applied to MEG data in this project.

2.1.1.5. SAM and VE analysis of sensorimotor cortex

In this project VEs were put in MI, identified using the PMBR (Jurkiewicz *et al.*, 2006), see figure 2.3a-b. The change in oscillatory power in the beta frequency band approximately 0.5 to 1.5s after a voluntary or cued movement, compared to a passive pre-movement period 2 to 1s before the cue or movement onset was used as the parameters for the SAM beamformer method described above. VEs were also reconstructed in SI. This area was identified using ERSAM (Cheyne *et al.*, 2006), by averaging >90 0.5s trials with a single pulse electrical median nerve stimulation. The stimulation elicited evoked potentials, which when they were averaged, could be distinguished in the bundled central channels. The time point for the largest deflection was used to set the constraint for evoked response SAM analysis. Once individual coordinates of MI and SI had been acquired, these were used to focus the output data from MI and SI into VE-channels. The data from the VE were then exported to Matlab (The Mathworks, USA).
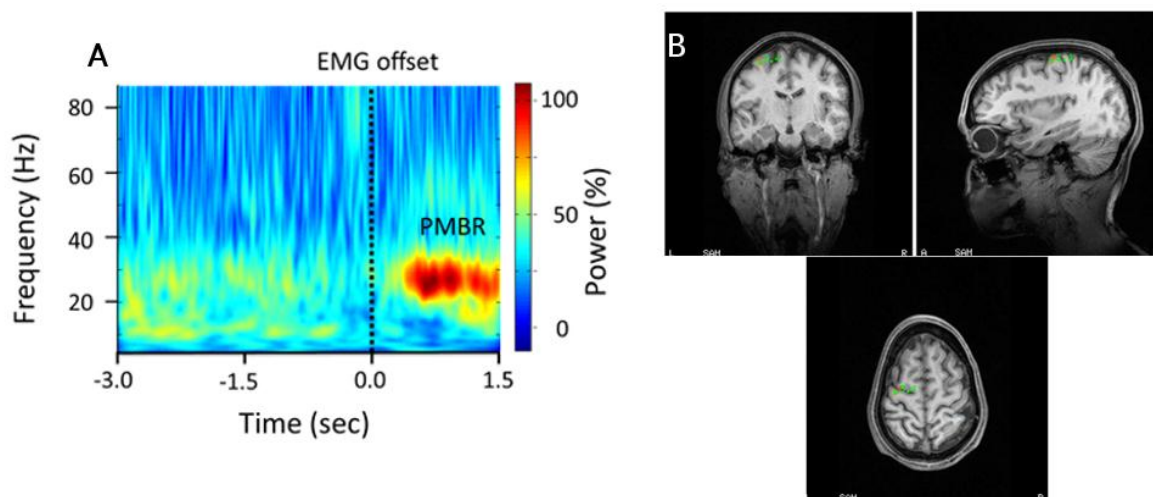
Figure 2. 3a-b. The contralateral MI was localised using the post-movement increase in beta power, e.g. PMBR, seen in A (left). The SAM pseudo-T value is superimposed on the subjects MRI, seen in B (right).

2.1.2. Magnetic resonance imaging

Magnetic resonance imaging (MRI) is based on the principle of exciting hydrogen protons in the body; subsequently measuring their relaxation properties. The Siemens Magnetom

Trio MRI scanner at Aston University has an external magnetic field of 3 tesla (3T) (Siemens, Erlangen). The subjects who participated in the MEG experiments all underwent MRI at Aston University to allow for co-registration of the neuronal network activity onto their MRI. An MPRAGE structural MRI image was acquired for each participant using an 8-channel head coil. Scans of 1mm resolution, were collected as a 256 x 256 x 256 matrix, TR = 8.3 ms, TR = 3.9 ms, TI = 960 ms, shot interval = 3 s, FA = 8°, and mSENSE factor = 3. Images were an averaged image integration of two repetitions, with a full scan time of approximately 17 minutes.

2.1.3. Transcranial magnetic stimulation

2.1.3.1. Brain stimulation

Transcranial magnetic stimulation (TMS) is a brain stimulation method which exerts its effect by electromagnetic induction, i.e. the induction of electrical current by addition of a changing magnetic field. This is achieved by passing an electrical current through a copper coil (inside the TMS coil) which creates a focused magnetic field perpendicular to the electrical current in the coil. The magnetic field from the coil can be aimed at a specific scalp location, overlying the desired cortical location, to induce a local electrical current.

2.1.3.2. Effects of TMS

Although the exact cell-specific details of transcranial stimulation still remain unknown, the more general effects on cortical cells are clear; TMS pulses depolarise neurons and if this depolarisation reaches the firing threshold of the membrane potential it results in the firing of action potentials (Siebner *et al.,* 2010). TMS is a minimally invasive and spatially distinctive neuroimaging method; it is possible to evoke a motor potential in distinct muscles (Ilmonemi *et al.,* 1997; Hallett, 2000; O'Shea & Walsh 2007). The magnetic field and spatial spread of a TMS pulse diminishes over a short space, further contributing to spatial accuracy. The diffusion of the magnetic field is dependent on the coil type and orientation, as well as the stimulus intensity (Siebner *et al.,* 2010, Fleming *et al.,* 2012).

2.1.3.3. TMS purposes

TMS has become both a clinical and widely used research tool to study cortical excitability, connectivity, as well as virtual lesioning. Inducing an electrical current at a specified location with a single pulse TMS generates an action potential. This can be used

to determine cortical motor and corticomuscular excitability by measuring the motor evoked potential after application of TMS over MI (Chen *et al.*, 1998).

Apart from single pulse TMS; there is a variety of different TMS protocols. There are different forms of distributing the TMS pulses with varying effects (notably reviewed by Hoogendam *et al.*, 2010; Funke & Benali 2011). The repetition of pulses, e.g. repetitive TMS (rTMS), has different effects on function depending on the pattern of repetition. High frequency rTMS (>1 or 5 Hz) increases cortex excitability and low frequency rTMS (<1 Hz) decreases it (Pascual-Leone *et al.*, 1994; Chen *et al.*, 1997; Muellbacher *et al.,* 2000) and the effect duration is variable and according to some researchers depends on the duration of the stimulation (Hoogendam *et al.*, 2010). Repetitive TMS of suitable frequency, pattern and intensity can be used to create a 'virtual lesion' in the underlying neuronal substrate, with obvious benefits in studying dysfunction, but in healthy subjects (Pascual-Leone *et al.*, 1999; 2000). Continuous theta burst stimulation (cTBS) is a form of repetitive TMS shown to have a long-lasting effect on motor cortical excitability of <45 min (Huang *et al.*, 2005). Additionally, several groups have combined TMS with other recording techniques, such as MEG and EEG (Thut & Miniussi 2009). Parkinson's disease has been investigated with TMS over the last decade and high-frequency rTMS has been shown to have a beneficial effect on some of the symptoms in PD, for example bradykinesia (Siebner *et al.,* 2000; Elahi *et al.,* 2008).

2.1.3.4. TMS in this project

In this project we used single pulse TMS and cTBS, applied with a 70 mm figure-of-eight stimulating coil, which was placed over the motor area. The hand motor area was localised by locating the vertex on the scalp, and then marking 4 cm lateral and 1 cm anterior to the vertex. For the rTMS protocols a Magstim Super Rapid was chosen, and for the single TMS pulse the Magstim 200 was used (both from The Magstim Company Ltd, UK). The motor evoked potentials elicited by the TMS pulses were recorded by placing an electromyelographic (EMG) electrode over the first dorsal intraosseous muscle. This electrode was connected to a 2-channel EMG kit (Delsys, US) and a computer with the software Signal (CED Ltd, UK), which displayed the shape and size of the MEP online.

2.1.4. Electrical median nerve/digit stimulation

Several decades of research has validated the findings of evoked potentials in the somatosensory cortex areas as a response to peripheral stimulation of, for example, the

digits and/or the median nerve and detected with EEG or MEG (Hari *et al.*, 1983; Kawamura *et al.,* 1996; Vanni *et al.,* 1996; Wikstrom *et al.,* 1999; Huttonen & Lauronen 2012; Lim *et al.,* 2012). The median nerve innervates the palmar side of the hand; the thumb and index finger. Stimulation above muscle activation threshold of the median nerve causes the thumb to twitch, while stimulation under activation can still result in sensation depending on stimulation intensity, but does not result in a twitch. This distinction allows for probing of the relationship between MI and SI, since muscle activation will evoke activity in MI (evoked potential), while under active threshold somatosensory stimulation should not evoke a potential in MI (Hari *et al.*, 1983; 1994; Hari & Kaukoranta 1985).

In this project electrical median nerve stimulation (MNS) or digit stimulation was performed by delivering electrical pulses from a constant current stimulator (Digitimer Ltd). For MNS, two electrodes were placed on the right wrist of each participant over the median nerve. The intensity was set to 50-70% of the thumb twitch reflex. If the subject found a test train stimulation of 60 Hz painful, the lower intensity was used. No participant reported the single or train stimulation as painful. The pulse width was 200 µs at all frequencies. The same principle was used for digit stimulation, but here the intensity was set at 1.5x sensation threshold. The stimulator was externally controlled by Presentation software (Neurobehavioral systems, UK).

2.2. *In vitro* techniques

2.2.1. *In vitro* preparation and recording procedures

By placing small glass electrodes, with a resistance of 1-3 MΩ, in a cortical brain slice, the aggregate extracellular neuronal activity in the area approximately 500-3000 μm around the tip can be measured as local field potentials (Mitzdorf, 1987, Juergens *et al.*, 1999, Logothetis *et al.*, 2001).

2.2.1.1. Preparation of brain slices

The *in vitro* experiments in this project used two different protocols for the preparation of sagittal sensorimotor cortex slices from rats. It is not in the scope of this thesis to discuss the intricate details that arise from differences in the two protocols. Instead, when interpreting the results from the *in vitro* experiments performed in this project, the *a priori* assumption has been made that the resulting oscillatory activity in the sensorimotor cortex is comparable in power and frequency characteristics, between the before and after conditions. The primary difference between the protocols is the improvement in slice viability, due to fine-tuning of concentrations and adding extra neuroprotectants, as established by Prokic *et al.* (under review). A summary of the two protocols can be found in table 2.1. The rats used in the *in vitro* experiments were treated in accordance with the Animal Scientific Procedures Act 1984 (Home Office, UK). Male Wistar rats were anaesthetised with isoflurane until the heart had stopped for protocol 1; these rats were then decapitated and the brains were quickly excised and put in ice-cold preparatory artificial cerebrospinal fluid (aCSF) saturated with 95% O_2 and 5% CO_2. In protocol 2 the rats were transcardially perfused with the preparatory aCSF instead of decapitation, before extraction of the brains. The brains were dissected and sagittal sensorimotor cortical slices, 450 μm thick, were cut with a microslicer at 4 °C, regardless of the initial extraction procedure. The slices were stored in an interface chamber (Scientific System Design Inc, Canada) with standard aCSF, also specific for the protocol type, for >60 minutes in room temperature before being transferred to the recording chamber (Scientific System Design Inc, Canada). The recording chamber was perfused with oxygenated standard aCSF at a flow rate of 1.3 mL/min, and maintained a temperature of 33-34°C. After 10 minutes in the recording chamber, KA and CCh were added to the aCSF to induce oscillatory activity. The oscillatory activity was stabile after 45-60 minutes at which point interventions were initiated.

Table 2. 1. The two *in vitro* preparation protocol

	Protocol 1	Protocol 2
Method of termination	Anaesthetic overdose and decapitation	Anaesthetic overdose and transcardial perfusion
Preparatory aCSF (mM)	206 sucrose 126 NaCl 2 KCl 1.6 MgSO4 26 NaHCO3 1.25 NaH2PO4 10 glucose 2 CaCl2 0.045 indomethacin 0.4 uric acid	171 sucrose 2.5 KCl 10 MgCl2 25 NaHCO3 1.25 NaH2PO4 10 glucose 2 NAC 1 taurine 20 pyruvate 0.5 CaCl2 1 ascorbic acid 0.045 indomethacin 0.4 uric acid 0.2 aminoguanidine
Standard aCSF (mM)	126 NaCl 2 KCl 1.6 MgSO4 26 NaHCO3 1.25 NaH2PO4 10 glucose 2 CaCl2	126 NaCl 3 KCl 1 MgCl2 26 NaHCO3 1.25 NaH2PO4 10 glucose 2 CaCl2 0.2 ascorbic acid
Oscillatory agent	50 µM CCh 400 nM KA	5-10 µM CCh 20-50 nM KA

2.2.1.2. Recording from brain slices

The excised brain tissue is held in specific conditions to prolong its viability, and as far as possible, resemble physiological conditions, both in the storage chamber and the recording chamber. The main difference between these chambers is the temperature, e.g. the slices are stored at room temperature but while recording the slices are in a heated environment in the recording chamber. The recording chamber is connected to polystyrene and silicone tubes and receives a continuous flow of artificial cerebrospinal fluid (aCSF), see figure 2.4a-b. The temperature in the recording chamber is controlled by a thermostat. Pharmacological substances are then applied to the aCSF, or locally to the tissue; these methods are used to study the pharmacological effects on the tissue. Here we applied all drugs used to the aCSF. The electrodes used for the LFP recordings *in vitro* were chlorided silver wire inserted into a borosilicate glass electrode filled with standard aCSF; resistance 1-3 MΩ. Using a stereotaxic anatomical rat atlas (Paxino & Watson, 1997) and a dissecting microscope, the glass electrodes were inserted in deep and superficial layers of the primary motor cortex, as well as the middle layers of the

somatosensory cortex (figure 2.5). The LFP signals were filtered to 1-500 Hz and amplified 1000x, with an applied notch filter at 50 Hz (EXT 10-2F, npi electronic GmbH, Germany), then converted and digitized at 10kHz by an analog to digital converter (CED 1401, CED Ltd, UK). Observation and saving of the signal was done with Spike2 v6.08 (CED Ltd, UK). The signal was then downsampled to 1kHz and exported to MatLab (Mathworks, Inc.) for further analysis.
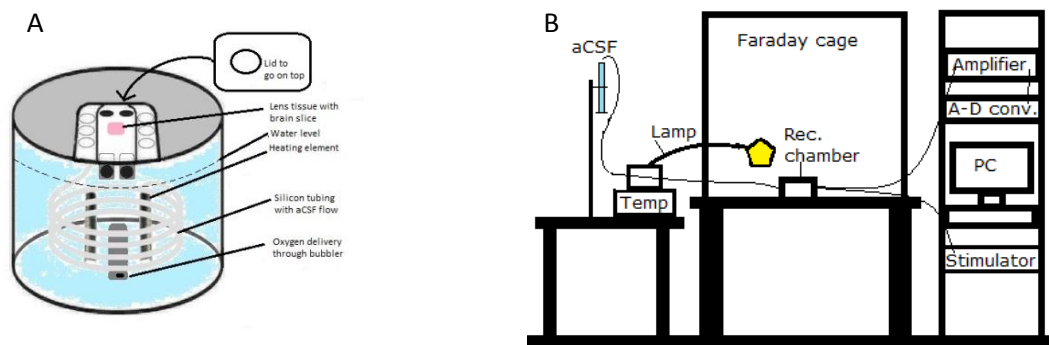
Figure 2. 4a-b. Drawn schematic of the recording chamber, seen in a (left), used in the *in vitro* experiments. Summarised schematic over the *in vitro* recording equipment can be seen in b (right). The temperature in the chamber is maintained at 32-33°C through submerged heating rods inside the chamber, which are connected to the external thermostat. Artificial cerebrospinal fluid flows from a cylinder outside of the Faraday cage, into the recording chamber and is heated. The continuous heated aCSF flow is delivered through submerged silicon tubing. The slice is placed in the interface of the aCSF on top of a lens tissue piece; the area is then covered with a small plastic lid. The aCSF flows over the interface and keeps the slice and surrounding at optimal humidity before draining out through two wells at the front of the chamber. Oxygen is delivered from a gas tank (not shown) and maintains the humidity in the recording chamber.
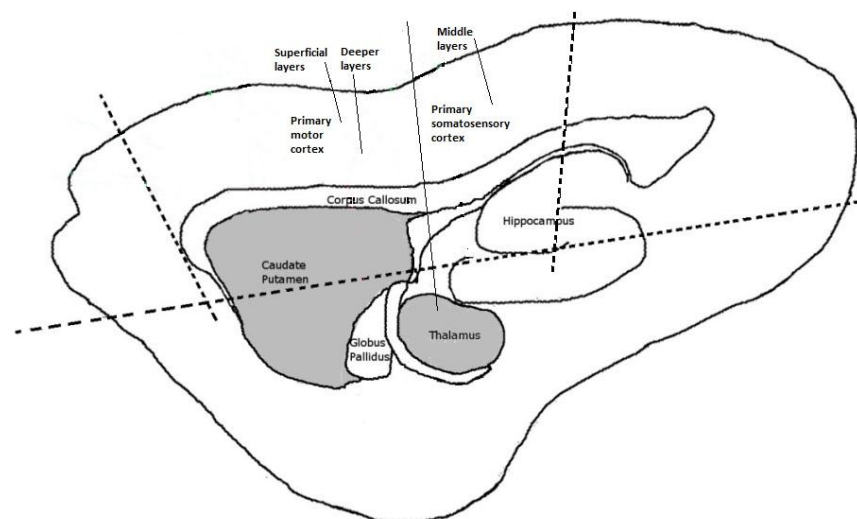
Figure 2. 5. Schematic of sagittal slices used in the *in vitro* recordings. The dashed lines indicate where cuts were placed to excise the sensorimotor cortex. The thin line indicates the border between sensory and motor cortex, which varies horizontally depending on lateral location.

2.2.1.3. Oscillations in brain slices

Several studies have investigated the pharmacological conditions required to induce cortical oscillatory activity, as well as modulate it, in specific *in vitro* preparations. Kainate (KA), is an agonist at the non-NMDA, non-AMPA, glutamate receptors named after this agonist (see review by Contractor *et al.*, 2003). Carbachol (CCh) is a cholinergic agonist that binds to the muscarinic acethylcholine receptors and results in glutamate release from both GABAergic interneurons and pyramidal cells. Acetylcholine is well-researched as one of the main neurotransmitters and has been shown to modulate cortical network activity (Lucas-Meunier *et al.*, 2003). KA and CCh have been used in different *in vitro* preparations of motor (Yamawaki *et al.* 2008) and somatosensory cortex (Buhl *et al.*, 1998), sensory and auditory cortex (Cunningham *et al.*, 2004; Rooopun *et al.*, 2006; 2008), hippocampus (Fishahn *et al.*, 1998) and entorhinal cortex (Cunningham *et al.*, 2003), to elicit oscillatory activity in the conventionally defined beta and gamma ranges. In essence, kainate and carbachol have been found to both be necessary to induce oscillations in the sensorimotor cortex *in vitro* (Buhl *et al.*, 1998; Yamawaki *et al.*, 2008, Prokic *et al.*, 2012).

2.2.2 Electrical stimulation *in vitro*

Using electrical stimulation *in vitro* has previously shown to affect ongoing activity in the slice (Yamawaki *et al.* 2008). Here, electrical stimulation to slices was performed by using a custom-made bipolar wire electrode, in surface contact with the slice at the desired area of interest. Using a similar protocol to Yamawaki *et al.* (2008), the intensity of the constant current stimulator was set at 1.5mA with a pulse width of 100 μs (Digitimer, Ltd). Stimulation was delivered in trains with specific frequencies. The stimulator was externally controlled by Spike2 (CED Ltd, UK).

The concern of overall temporal effect of applying several stimulation events in a slice was addressed on two levels. Firstly, by investigating at the changes to ongoing beta oscillations from the first to the last stimulation event, where no trends or changes could be attributable to specific frequencies, increased time or number of stimulations. Secondly, by using time periods of 30s before and after when analysing the effects on the ongoing oscillations, this concern was further abolished.

2.3. Multimodal approach

2.3.1. Advantages and limitations to techniques used in this project

The primary advantage with neuroimaging methods is their non-invasive nature. Recording magnetic fields in the scalp surroundings, as is done in MEG, is a passive process, although there is a small risk of contact with cryogenics. MEG results generally display excellent temporal resolution and combined with SAM analysis, good spatial resolution. However, this requires an MRI, which does present the participant with risks as strong magnetic fields are used, in addition to exposure to loud noise and cryogenics. There is also a chance of developing claustrophobia as the MRI scanner itself presents a small and constricted compartment. The final neuroimaging method used here is TMS. There have been reports of induced seizures using this technique, but in most cases these were found to be the result of ignoring safety guidelines and TMS threshold recommendations. The loud clicking noise from the coil, minor discomfort during stimulation and cognitive changes, as well as headaches have been suggested as adverse effects, but have yet to be scientifically evaluated and validated. The recent years have seen the emergence of global safety and practise guidelines based on published data, emphasising that TMS is a minimally invasive technique (Rossi *et al.,* 2009).

Essentially, the invasive nature of the *in vitro* animal studies makes it unsuitable for human research, but this is also what makes it advantageous. These methods provide us with fundamental understanding of the cellular and biological mechanisms that underlie function and activity in the brain. These techniques assist in elucidating the effects of exogenous and endogenous substances, and in the long run contribute to a more complete picture of the human brain. One difficulty when recording LFPs is noise elimination. Noise, in the *in vitro* electrophysiology setup, comes in different forms. Vibration noise is environmental, for example ground vibration or acoustics. A vibration isolation table is therefore used while recording. Electrical noise is also external, and is reduced by shielding the recording equipment, e.g. chamber with slice and electrodes, with a Faraday cage connected to a common ground. Additionally, the electrical noise at 50 and 60 Hz can be reduced by using hardware and/or software notch filters in the amplifiers and recording programs, or noise elimination devices.

2.3.2. Rationale for using a parallel approach

Further to the limitations and advantages discussed above there are three main arguments to why a parallel approach of *in vitro* and MEG recordings was appropriate in this project. Firstly, there is the concern of scale. With neuroimaging techniques it is not possible to record from specific laminae using MEG, which is easily achieved from *in vitro* recordings in cortical slices. Secondly, there are constraints in human MEG recordings with regards to invasive intervention protocols; we cannot administer some pharmaceutical substances or stimulation protocols as this would be unethical and harmful for the participant. In contrast, the final point concerns the functions and connectivity of neuronal networks. While a spatially focused recording of oscillations is possible and freedom of intervention application is vast *in vitro*; this is still a reduced model since the neuronal networks recorded from are neither connected to the rest of the brain, nor able to display functionally relevant and related activity. In order to address these limitations we have used both approaches when trying to disentangle beta oscillations in the sensorimotor cortex. The differences in experimental approaches also encompassed the analysis, making it difficult to optimally compare the results from these methods used in parallel. This led us to develop a different analysis approach.

2.4. Analysis

2.4.1. Characterisation of sensorimotor beta oscillations

2.4.1.1. Methodological differences in oscillations

Beta oscillations studied in an *in vitro* preparation typically appear different to those studied in neuroimaging. In *in vitro* experiments, beta oscillations in MI typically have a narrow peak at approximately 27 Hz with an obvious amplitude difference from the baseline (Yamawaki *et al.*, 2008). In MEG experiments, beta oscillations recorded over the motor cortex are typically broad in frequency (15-30Hz) and sometimes appear co-existent with mu (~10 Hz) (Hall *et al.*, 2011).
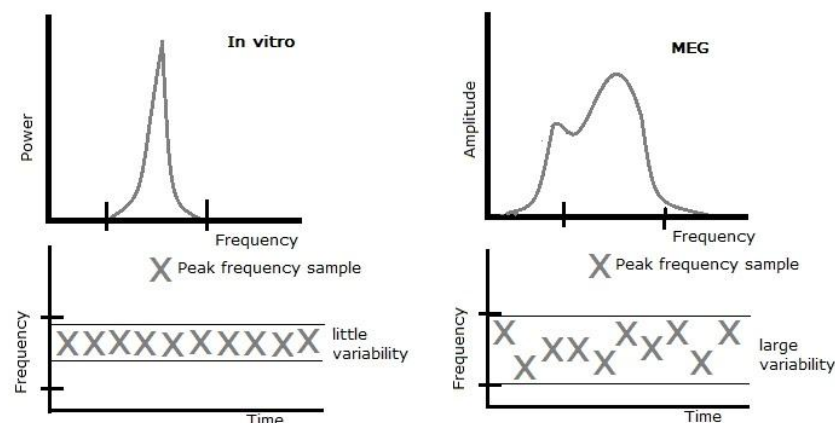
Figure 2. 6. Schematic showing the shape of the oscillatory peak and its relation to the underlying variation in frequency. There are obvious visual differences between oscillatory peaks seen in MEG and *in vitro* experiments.

The difference in appearance between the oscillatory signals recorded in the two modalities (figure 2.6), as well as conventional analysis between MEG and *in vitro* research, point to the need for different analysis approaches. This is especially important since the continuous *a priori* assumption is made that the elicited oscillations seen in the *in vitro* experiments are physiologically and functionally comparable to those observed in neuroimaging studies, and that they will respond in a similar way to any intervention as would the intact brain in a living subject. Conversely, with MEG the assumption is that oscillations observed in humans are a direct reflection of the underlying neuronal networks. As previously discussed, the limitations imposed by reduced connectivity in the *in vitro* preparation and limitation to macroscopic measurement in MEG, leaves a gap in our understanding of the extent to which these approaches are comparable. In order to approach these questions, it is important that analytical processes are comparable between methods.

2.4.1.2. Limitations of typical analysis approaches

Analysis is often based on pre-defined frequency bands from the EEG literature, such as the beta band (15-30Hz). *In vitro* experiments typically make comparisons of power and frequency at the peak of the oscillation within that range. In comparison, MEG and EEG experiments typically make comparisons based upon the peak frequency within that range and the power within the entire band. This poses obvious difficulties in comparing between the two approaches, which need to be addressed. Furthermore, oscillatory frequency varies over time within and between measurements. Consequently, measurements from the peak of an averaged PSD computation may be misrepresentative in terms of frequency, see figure 2.7 below.
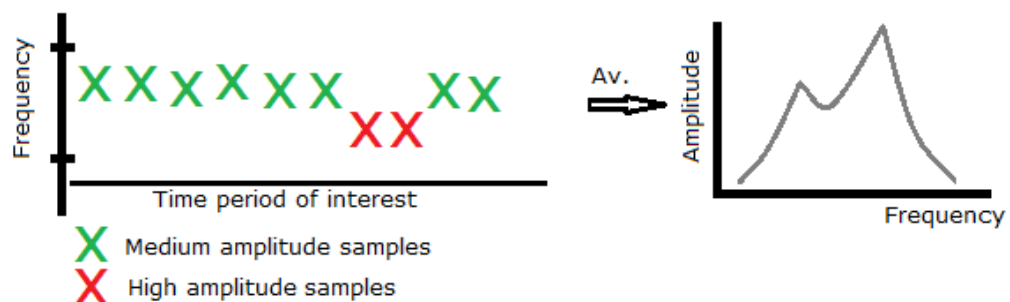
Figure 2. 7. A few samples with high amplitude information can skew an averaged PSD, as seen in this schematic. The average of all samples is a broad and bimodal peak.

Additionally, measurement of a fixed frequency band does not take into account either a mean frequency shift or change in the distribution of an oscillatory peak, or change between conditions. For example following pharmacological manipulation (Hall *et al.*, 2010), power in the frequency band may be misrepresentative of the actual change, see figure 2.8 below.
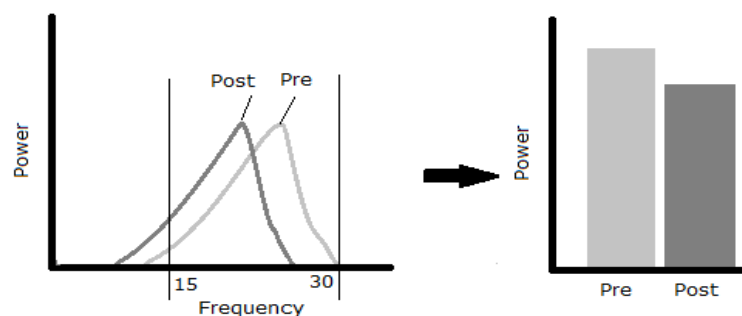
Figure 2. 8. Oscillatory power is often measured within a pre-defined band, as illustrated in this schematic, for example the 15-30 Hz 'beta band'. The beta peak in the pre-intervention condition is well within the 'beta band'. However, when looking at the power within the 'beta band' after intervention, there is a decrease. Calculating the average power within this band in an average PSD plot leads to misinterpretations of results and principally reveals nothing about the oscillation.

In both *in vitro* and MEG recordings, the signal arises from different neuronal populations, for example in MEG different laminae (layers II/III and IV) contribute to the signal (Murakami & Okada 2006). The composition of an oscillatory signal will inevitably contribute to the variability seen in frequency and power, which highlights the importance of understanding the variation and distribution of the signals.

2.4.2. Comparative analysis of neuronal network oscillations

With the differences between beta oscillations seen in the different modalities, this project required the development of analysis software capable of disentangling information about the underlying neuronal networks generating the oscillations. The analysis also required ability to compare the similarities in responses to the manipulations presented to beta oscillations in the sensorimotor cortex recorded from different conditions. The analysis approaches presented here were therefore developed with these key points, and concerns from above, in mind.

The recorded signals from MEG and *in vitro* experiments were analysed with custom-made MatLab scripts. The initial step was to process 30s Morelet-Wavelet spectrograms, 1-100 Hz. Morelet-wavelet spectrograms display the change in frequency and power over time. The time is found on the x-axis and the frequency on the y-axis. The power is displayed as colour changes, usually on the RGB colour spectrum, e.g. red colours indicate high power and blue less power. Morelet-wavelet spectrograms and associated PSDs were calculated for each sample (for a recording period of 30s the number of samples in an epoch will be related to the sampling rate; *in vitro*: 1000kHz, e.g. 30000 samples; MEG: 600 Hz, e.g. 36000 samples) in each time-period for each subject or recording, using a sliding window approach. For specific details of the outputs from the custom-made MatLab scripts, see section 2.4.2.6.

2.4.2.1. Oscillatory frequency analysis

Measurements of oscillatory frequency usually assume that the frequency is constant throughout the measurement period. As a consequence, the frequency measurement is dependent upon the frequency variability and power at each frequency over the measurement window. To circumvent this, frequency is here determined from a sliding window PSD measurement from each sample in the time period and, independent of power, the mean frequency is derived from this. An example of the differences in peak frequency result between approaches can be seen in figure 2.9 below.
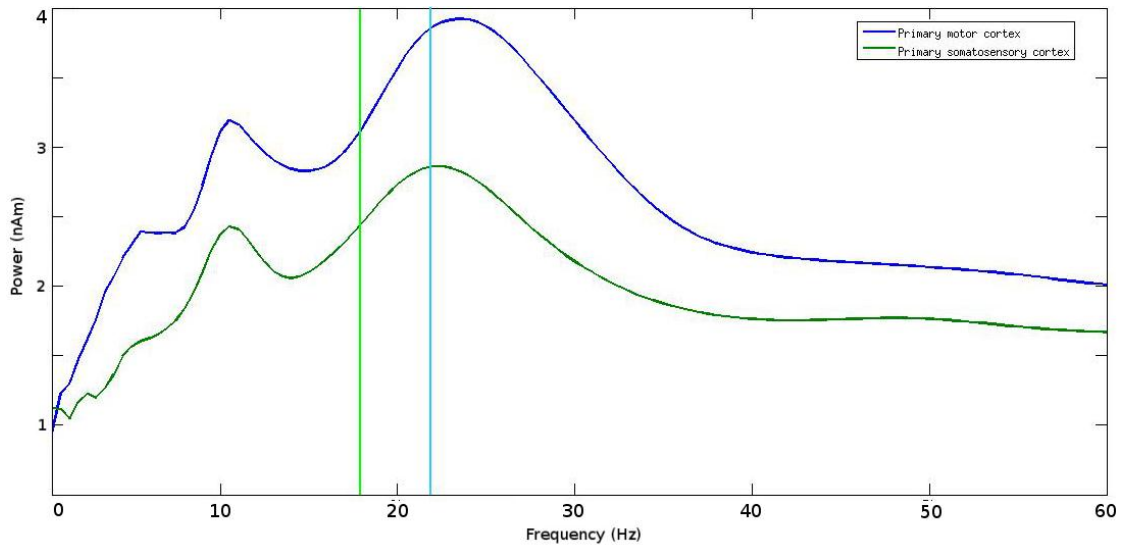
Figure 2. 9. The averaged PSD plot of the spontaneous oscillatory activity from MI and SI. The peak values for the beta range in this plot are 24.5 Hz for MI and 22 Hz for SI. The mean peak frequency using the sliding window approach were 22.2 Hz for MI, illustrated by the blue vertical line, and 18 Hz for SI, illustrated by the light green vertical line.

2.4.2.2. Oscillatory power

Similar to the observation of frequency, power at the peak is dependent upon the variability of the frequency over time and the power at each peak frequency. Here, oscillatory power is analysed by taking a measurement of power at the peak frequency at each sample throughout the time period of interest. This provides a measurement of power at the frequency peak, these individual measurements of power at the peak frequencies are averaged to provide the mean peak power for the whole epoch. The current analysis approach will provide a more accurate representation of the oscillatory power during the epoch. In the example provided in the figure 2.9, above, the beta peak power in MI was 3.9 nAm and 2.6 nAm in SI. Using the different analysis approach we developed for this project, the mean peak power was 4.44±1.53 nAm in MI, and 3.06±1.09 nAm in SI.

2.4.2.3. Frequency distribution

As discussed above, the measurement of power in a pre-defined frequency band is dependent upon changes in frequency and also the morphology of the frequency peak. As a result, these approaches are insensitive to frequency variability, condition-dependent shifts and changes in frequency distribution. The distribution of the oscillatory peak, which is indicative of frequency composition and distribution networks involved in the measured neuronal oscillation, is addressed by using the objective measure of *full-width half-maximum* measurement (FWHM), see figure 2.10 below.

61
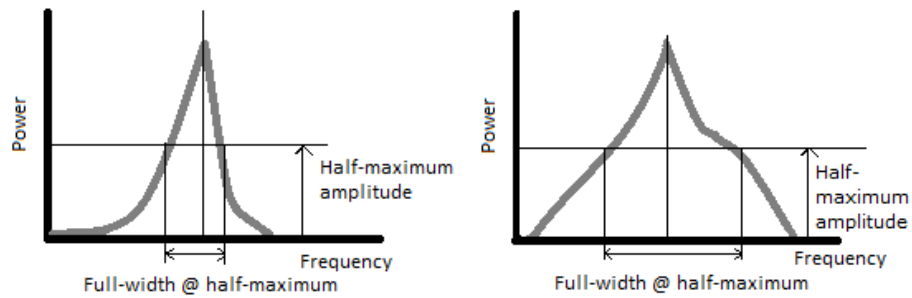
Figure 2. 10. Schematics showing full-width at half-maximum amplitude (FWHM). Difficulties in determining the frequency width of an oscillatory peak in a PSD, due to baseline fluctuations, are circumvented by using the FWHM measure. Right peak has wider FWHM.

FWHM output provides an objective measure of variability and network distribution through its peak sharpness and frequency width. The FWHM width is combined with the mean frequency peak to provide a shape measurement of the oscillatory peak for each individual recording. The peak shape indicates the presence of underlying oscillatory signals, see figure 2.11 below. If one network is responsible for an oscillation, e.g. driven by a single oscillator it should have an even distribution around the mean frequency. If this is not the case it suggests that additional oscillators are contributing to the activity.
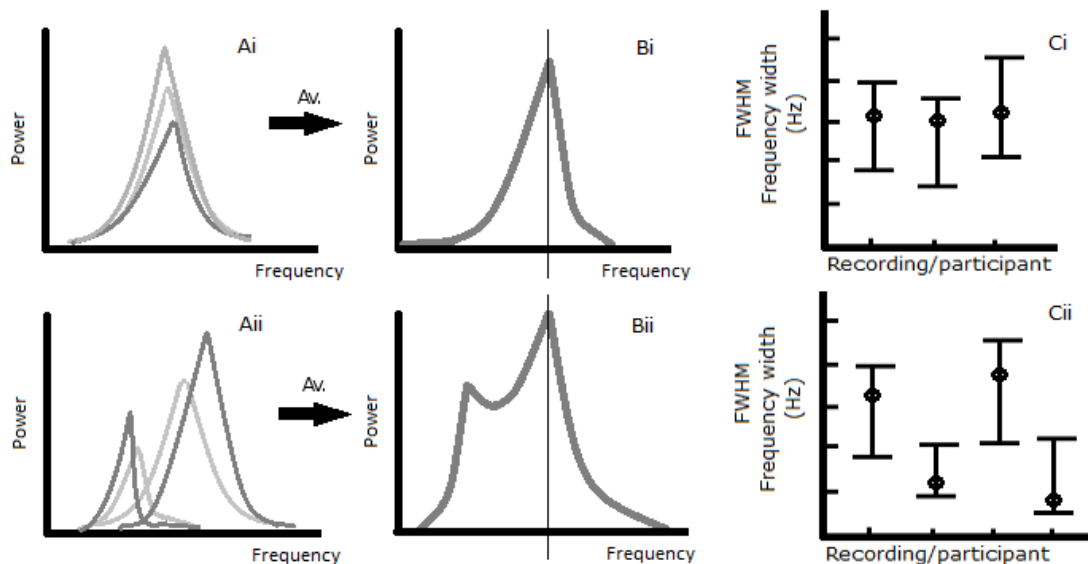
Figure 2. 11. Ai-Cii. Schematic pictures showing the oscillatory PSDs and FWHM. In Ai and Aii (left top and bottom), the individual PSD profiles can be seen, these are averaged as seen in Bi and Bii (middle top and bottom). The existence and characteristics of more than one network oscillator and its frequency can be determined by looking at the shape of the peak in conjunction with the mean frequency of the peak. The average PSD on the bottom row (Bii) is broader and most likely contains frequency contributions from more than one oscillation frequency. The FWHM plots, seen in Ci and Cii (right top and bottom), show the individual frequency ranges and the mean frequency peak, which in Cii indeed shows contribution from more than one oscillation.

For each recording one FWHM value is produced, see figure 2.12a-b for examples of this. These can then be averaged over the group to provide the mean FWHM, giving a representation of the frequency range of the network responsible for the ongoing oscillations in the area/condition of interest, see figure 2.12c below for an example of this.
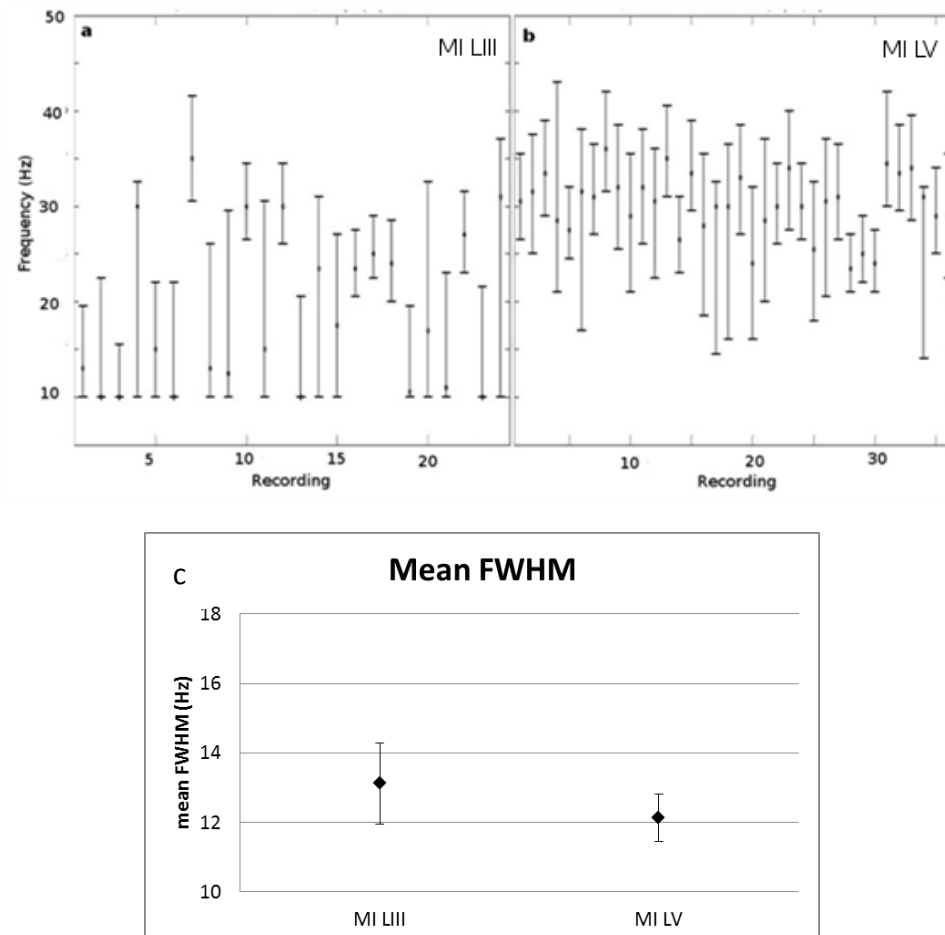
Figure 2. 12a-c. FWHM measurements in individual recordings from motor cortex superficial and deeper layers (MI LIII and LV) is seen in a and b, respectively in left and right top. FWHM values are averaged across the recording groups to provide the mean FWHM for the group in the area/condition of interest, shown in c (bottom).

2.4.2.4. Frequency variability and stationarity

As discussed previously, the mean frequency, amplitude and distribution are subject to the variability of the oscillation over time. In order to further disentangle the composition of the oscillatory signals the *peak frequency distribution* was quantified. This provides an understanding of how the peak frequency varies over the measurement epoch. We used a histogram approach, whereby the peak frequency is computed for each sample in the measurement epoch and assigned to the appropriate frequency bin (1Hz bin widths were used). The frequency distribution is thus presented as a power-independent representation frequency and indicates the contribution of frequency variability or Stationarity to the oscillatory profile and mean peak frequency. See figure 2.13a for an

example of the power-independent frequency distribution histogram. Additionally, the power in each frequency bin can be computed to provide a normalised power/sample distribution for each frequency. This provides a method of determining the proportional contribution of each frequency to the PSD, see figure 2.13b below for an example of the frequency distribution when power per sample is taken into account. This is useful to indicate changes in power for a specific peak frequency.
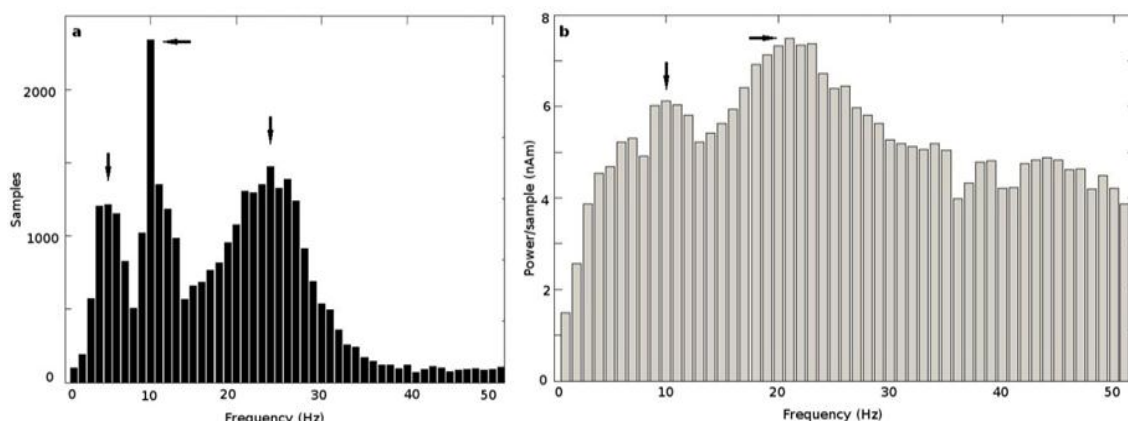
Figure 2. 13a-b. The peak frequency distribution in MI can be plotted independent of amplitude to provide information about the non-stationarity in peak frequency, seen in a (left). The power per sampled peak frequency can also be taken into account to establish if there are any changes in power for a specific peak frequency, seen in b (right). The black arrows indicate where most of the peak frequency measurements from all samples were found, e.g. the frequency distribution peaks.

2.4.2.5. Oscillatory power and state change

Oscillatory measurements, whether made from E/MEG or *in vitro* recordings, show a large degree of non-uniformity in the power of the signal. For example, measurements of the beta band in motor cortex shows periodic bursts of power, particularly in Parkinson's disease patients. However, although these phenomena have the capacity to impact strongly upon the observed changes in power, there is rarely any consideration made for the power composition or intrinsic variability. When determining the impact of a change in conditions it is important to understand the nature of that change. Here, to disentangle this, an objective measurement of the power in the signal was used by sorting the power data from each sample in terms of amplitude. This distribution was then ranked in order of amplitude, converted to a zero-mean signal and cumulative summation applied. The effect of this is an objective sorting of power into low and high *power states* defined as above or below a minimum change point, e.g. the point of difference between the states. Samples were then determined as high or low power and the contribution of this determined before and after intervention. This addresses the question of the contribution of so called 'oscillatory bursting', see figure 2.14 below for an example. The mean power in the upstate, e.g. the state above the change point, and the downstate, e.g. below the change

point, can be calculated to provide a quantitative determination of the variability of power. These can then be averaged over the group and compared between conditions and areas. Changes in power states after an intervention indicate a change in the pattern of activity.
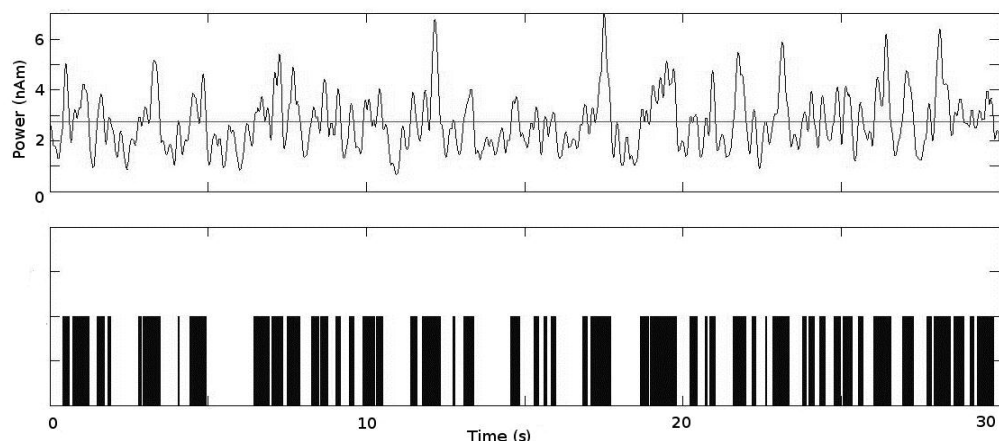
Figure 2. 14. Oscillatory power state analysis of MI oscillations in one participant. The oscillatory power peaks in the beta band (15-35 Hz) are plotted over time per recording. The top box illustrates the peak power values, while the bottom box illustrates which samples were above the change point.

2.4.2.6. MatLab scripts

Custom-made MatLab scripts were designed to extract these oscillatory frequency and power characteristics. These scripts used the data from the sliding window Morelet-Wavelet spectrograms/PSDs and provided the following specific outputs: mean peak frequency ± standard deviation, mean power at the frequency peak ± standard deviation, mean full width half-maximum ± standard deviation, mean % of samples at peak frequency ± standard deviation, mean % samples at peak frequency ±5Hz ± standard deviation, mean % samples at peak frequency ±10Hz ± standard deviation, % up-and downstate, mean power in up- and downstate. There custom-made MatLab scripts which tested the results with t-tests and the statistical outputs were t-statistics and p-values. We tested between 'before' and 'after' time periods in the same participants and slices, and between oscillatory signals within the same participants or slices. Furthermore, the integration of *in vitro* signals for a designated location into an *in silico* aggregation was done by averaging the Morelet-wavelet spectrograms into one dataset. These integrated datasets were then analysed in the same way as the *in vitro* and MEG data.

Chapter 3. Spontaneous oscillations in the sensorimotor cortex

3.1. Introduction

3.1.1. Background

The presence of beta frequency (15-30Hz) and mu frequency (~10Hz) oscillations in the sensorimotor cortex has been the subject of both research and debate over several decades. Although the full relevance of these rhythms still eludes researchers, they are nonetheless an integral part of the activity in the sensorimotor cortex. In the absence of movement or somatosensory stimulation, the sensorimotor cortex display ongoing and regular beta oscillatory activity. A number of animal *in vivo* and human neuroimaging studies have reported on beta oscillations in primary motor cortex (MI) (Pfurtscheller, 1981; Murthy & Fetz 1992; Sanes & Donoghue 1993; Salmelin & Hari 1994; Murthy & Fetz 1996; Baker *et al.* 1997; 1999). In addition, mu oscillations are reported in human neuroimaging studies and are believed to be generated the primary somatosensory cortex (SI) (Salmelin & Hari 1994; Salmenlin *et al.*, 1995). The mu and beta rhythms have been established to not be harmonics of each other (Tiihonen *et al.*, 1989), and are individually modulated (Nagamine *et al.*, 1996). Both rhythms display patterns related to function. The mu rhythm has in animal *in vivo* experiments been reported as the sensorimotor rhythm (SMR, 10-14 Hz) (Kaplan 1979; Rougeul *et al.* 1979), and was recently confirmed to spatially correspond to the functional mu rhythm, in addition to similar features such as the classic wicket shape of the oscillation itself (Marini *et al.* 2008; Tort *et al.*, 2010; Sobolewski *et al.*, 2011). Both beta and mu rhythms attenuate prior to onset of motor events and resynchronises after the offset with different spatiotemporal characteristics, as evidenced by several neuroimaging studies the last decades (Pfurtscheller, 1981; Salmelin & Hari 1994; Jensen *et al.*, 2005; Gaetz & Cheyne 2006; Jurkiewicz *et al.*, 2006, Neuper *et al.*, 2006; Avanzini *et al.*, 2012).

Although MEG and EEG have provided the spatiotemporal identification for the functional modulation of beta oscillations in humans, these methods are macroscopic and reveal little about the underlying mechanism of spontaneous rhythmogenesis or intrinsic characteristics of the beta rhythm itself. Conversely, *in vitro* brain slice protocols have been used for decades to study underlying neuronal mechanisms of observed brain activity (Yamamoto & McIlwain 1966; Andersen *et al.*, 1972). The synchronised activity in and around cells has been correlated to their intrinsic distinct electrophysiological properties (Chagnac-Amitai & Connors 1989; Fransceschetti *et al.*; 1995, Flint & Connors 1996), which is further supported by observations of co-existing rhythms in sub-areas (Flint & Connors 1996; Roopun *et al.*, 2006). There is a large collection of research describing the potential mechanisms for rhythmogenesis and oscillations, in different

areas of the rodent brain; in hippocampus (Whittington *et al.*; 1995; Traub *et al.*, 1996), entorhinal cortex (Cunningham *et al.*, 2003), somatosensory cortex (Buhl *et al.*, 1998), secondary somatosensory and auditory cortex (Cunningham *et al.*, 2004; Roopun *et al.*, 2006), primary motor cortex (Yamawaki *et al.,* 2008). Buhl *et al.* (1998) reported on the existence of gamma oscillations in the somatosensory cortex, although it is unclear if this was the primary or secondary areas. Research in MI reports that beta oscillations originate in layer V of the primary motor cortex in slice preparations (Yamawaki *et al.*, 2008). There is a lack of current research reporting on the existence and characteristics of beta or mu oscillations in other specific layers of the primary sensorimotor cortex in rats.

The MEG signal has an optimally resolved source size of approximately $5mm^{3}$, or 10000-50000 synchronised pyramidal cells, primarily located in layer II/III and V of the cortical area of interest (Vrba & Robinson 2001; Hillebrand & Barnes 2002; Murakami & Okada 2006). This area of recording is considerably larger than that of *in vitro* glass microelectrode LFP recordings, which comprise an average measurement from approximately 500-3000 μm around the electrode tip (Mitzdorf, 1987, Juergens *et al.*, 1999, Logothetis *et al.*, 2001). These differences in source size consequently infer that the MEG signal is a spatial aggregate that is more complex with regards to neuronal network composition. There is currently a lack of research aimed at establishing the differences and similarities between these oscillatory signals, although many MEG and *in vitro* research reports draw on conclusions used in one modality to rationalise and interpret their own experiments and results in the other modality. If these recording methods are going to be used in comparison and inferences are to be made between them, it is essential that comparative features of the oscillatory signals are elucidated.

The current conventional analysis approaches in M/EEG and *in vitro* literature differ to some extent from each other. The limitations in the conventional approaches were discussed in detail in the methods chapter and limitations concern the variability of frequency and power. Understanding the variability in oscillatory signals is particularly important when looking at spontaneous ongoing oscillations and using these as baselines for any intervention or functional modulation. Variability in frequency and power is indicative of the underlying neuronal network activity and communication. Recently the beta band stationarity was found to correlate to rigidity and bradykinesia in PD patients (Little *et al.*, 2012), indicating that the importance of variability in analysis of oscillatory signals has yet to be fully realised.

3.1.2. Aims and research objectives

Previously mentioned studies have recorded MI and SI oscillations *in vitro* and with MEG, but it is unclear to what extent the neuronal network activity of MI and SI is comparable. Here, we aim to address the questions:

What are the oscillatory profiles of MI and SI recordings *in vitro* and MEG?

- o Which oscillations arise from each area?

- o How do these oscillations compare in power between areas?

- o How do these oscillations compare in frequency between areas?

Previous studies have characterised oscillatory activity using band or peak analysis approaches, but it is unclear whether these time averaged measurements are true representations of the network signals from which they arise. Here we aim to address the questions:

What are the similarities and differences in oscillation between laminae *in vitro*?

- o What oscillations occur in each layer of MI?

- o How do oscillations vary in distribution between layers?

- o What is the variance in frequency and power between layers?

Previous studies suggest that *in vitro* LFP and MEG signals are comparable, but there is a scarcity of empirical data supporting this. It is unclear to what extent the oscillatory signals can be compared between modalities. Here, we use a signal integration approach to address the questions:

To what extent are integrated oscillatory signals from MI *in vitro* comparable with MI oscillatory signal from MEG?

- o Does integration of layer III and V better reflect MEG MI signals?

3.2. Methods

3.2.1. *In vitro*

Brain slices were prepared using a similar protocol to Yamawaki *et al.* (2008), as described in chapter 2. All animal experiments were performed in accordance with the Aston University ethical review board regulations, as well as the Animals Scientific Procedures Act 1986; European Communities Directive (86/609/EEC). Brains from p18-p22 (50-60g) male Wistar rats were extracted and prepared according to *in vitro* protocol 2. 450 µm thick sagittal sensorimotor slices were stored in a tissue interface chamber at room temperature for >1h. The slices were then transferred to a recording chamber with a temperature of 33-34°C and a continuous flow rate of 2 ml/min aCSF with added KA and CCh; concentrations and preparations according to protocol 2. Recordings of LFPs from superficial layers (II/III) and deeper layers (V) of MI and middle layer (IV) of SI (figure 2.6) were made. The electrodes were placed in relevant layers, identified by using a dissecting microscope and the Rat Brain Atlas (Paxinos & Watson 1986) as reference. LFP recording started after the KA- and CCh-induced oscillatory activity had stabilised, >1h in the recording chamber with KA and CCh in the aCSF flow, and lasted for >3h.

Recording of *in vitro* data was performed with Spike2 v.6.02 (CED Ltd.) Online analysis was performed with fast-Fourier transform (FFT) with the size of 16384, applying a Hamming window and a finite resolution of 0.61104. This was only done to identify oscillatory activity in laminae of interest and to distinguish and select representative LFP recordings. After recording, the data was down-sampled at 1kHz and exported in spreadsheet format (.txt) to MatLab (The Mathworks, Inc.) for offline analysis. From these converted datasets, 30s Morelet-wavelet spectrograms were processed before applying the custom-made analysis described previously (see Chapter 2, but also briefly in 3.2.3). The number of recordings from the different *in vitro* locations was: superficial layers of primary motor cortex (MI LIII), n=24; deeper layers of primary motor cortex (MI LV), n=36; middle layers of primary somatosensory cortex (SI LIV), n=37.

Integration of *in vitro* recordings from superficial and deeper layers of MI was done through MatLab: n=20. To summarise, the two corresponding signals from the two locations (MI LIII and LV) in each slice were used to create an averaged epoch of data. This was then analysed in the same manner as other *in vitro* recordings, described below.

3.2.2. MEG

Magnetic field activity from 13 healthy participants (7 M), mean age 29-46 years, was recorded while the subjects were sitting at rest in the 275-channel MEG scanner (CTF, Canada). The study was performed in accordance with the Declaration of Helsinki, and approved by the Ethics Committee of the School of Life and Health Sciences at Aston University. Written informed consent was obtained from all participants. The participants received visual instructions from a computer screen, in addition to audio instructions from the experiementer.

Primary motor cortex was localised with a SAM beamformer approach based on the PMBR seen after voluntary finger movements (Jurkiewicz *et al.*, 2006). The PMBR was identified by an increase in the 15-30 Hz frequency band 0.5 to 1.5 seconds following movement offset compared to and -2.0 to -1.0 seconds before movement. EMG electrodes were placed on the FDI muscle to determine the onset and offset of finger movements. Primary somatosensory cortex was localised in 8 participants with ERSAM (Cheyne *et al.*, 2006), using the stimulation events in a 2 Hz electrical stimulation train delivered through two electrodes (Digitimer Ltd.) to the median nerve at 50% of the thumb-twitch threshold. We focused the ERSAM on gamma (30-100Hz) activity around the evoked potential latency. Trials containing artefacts were discarded and the data was filtered to 1-200 Hz, with additional notch filters at 50 and 60 Hz. Virtual electrode data from MI and SI loci, during 30 second rest periods, were processed in MatLab (The Mathworks, Inc.) as Morelet-wavelet spectrograms. These data were then analysed using the same process as used for *in vitro* analysis.

3.2.3. Analysis approach

The mean peak frequency and peak power was determined for each sample with a sliding window approach, in which the frequency of the oscillatory peak and the power of that peak was determined for each sample in each 30s epoch. The frequency distribution of the oscillations was determined using FWHM. The frequency variability was computed using the amplitude-independent peak frequency distribution, where the peak frequency of each sample was sorted into frequency bins of 1 Hz. Variability in oscillatory power was determined using an amplitude sorting measurement to determine the time and amplitude changes of oscillatory up and down states. We used student's T-tests to statistically test for differences. Further details regarding this analysis approach can be found in chapter 2.

3.3. Results

3.3.1. Oscillatory neuronal network activity in MI and SI

3.3.1.1. Oscillatory peak frequency and power in MI and SI in MEG recordings

The group-averaged Morelet-wavelet spectrograms from the different locations show distinct oscillations in mu and beta bands, in both MI (n=13) and SI (n=8). The amplitude and persistence of the beta frequency appeared greatest in MI (figure 3.1a-b.).
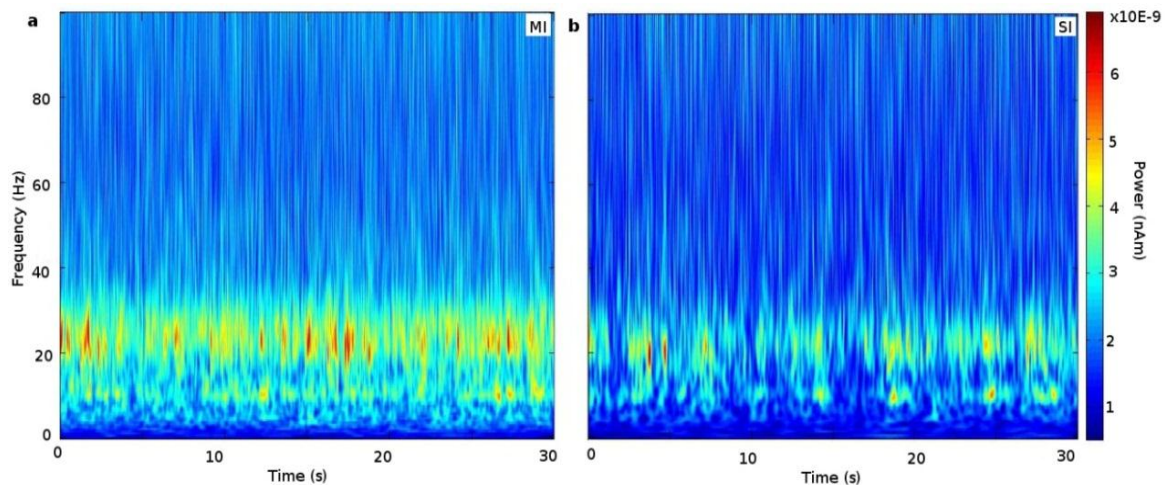
Figure 3. 1a-b. Group-averaged Morelet-wavelet spectrograms of MI (n=13) and SI (n=8) showing variation over time in the oscillatory activity recorded with MEG. The oscillatory beta frequency activity appears less dominant in SI (b, right), than in MI (a, left).

Group average PSDs from MI and SI showed little distinction in oscillatory profiles, with regard to frequency and peak shapes, between the two areas (figure 3.2)
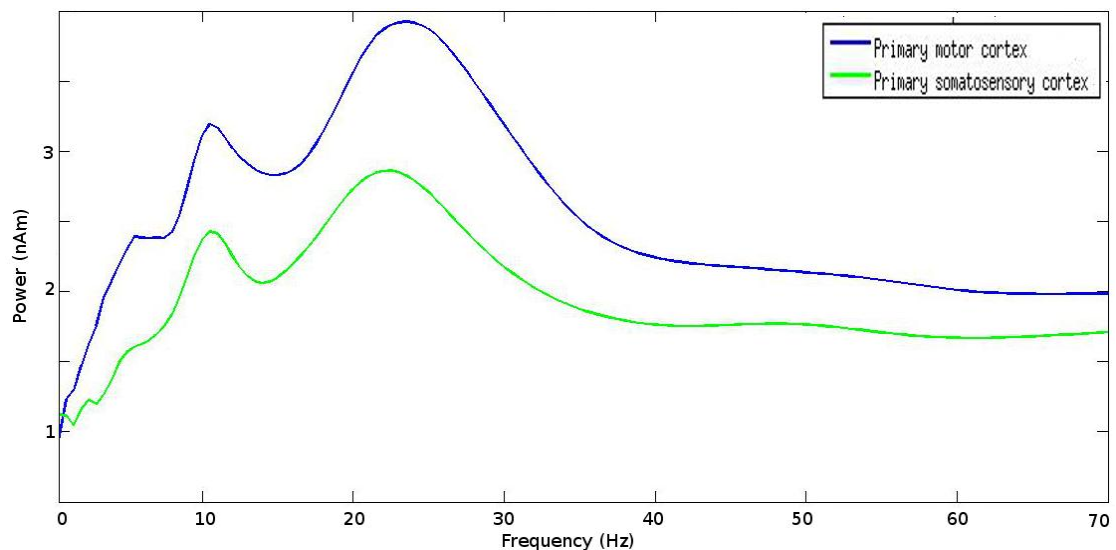
Figure 3. 2. Group- and time-averaged PSD from primary motor and somatosensory cortex (MI and SI) in MEG experiments. The blue and green lines indicate MI (n=13 and SI (n=8), respectively. There was a significant difference in peak power, but not frequency, see figure 3.3a-b.

The mean peak frequency in MI was 22.23±6.07 Hz and mean peak amplitude 4.44±1.53 nAm. The mean peak frequency in SI was 18.79±5.33 Hz and mean peak amplitude 3.06±1.09 nAm. The difference in power between MI and SI was significant, $t_{[7]}=4.0114$, $p=0.0051$. The difference in frequency was non-significant $t_{[7]}=2.1689$, $p=0.0667$ (figure 3.3a-b).
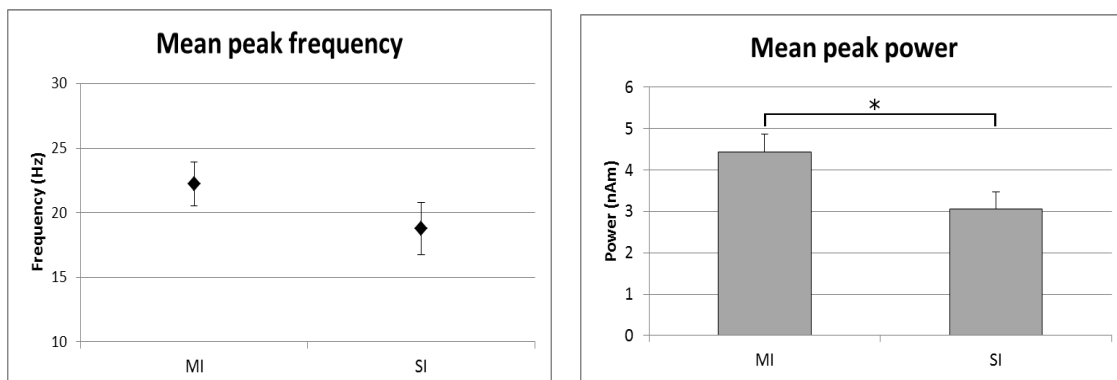
Figure 3. 3a-b. Mean peak frequency, seen in a (left), and power, seen in b (right), in MI (n=13) and SI (n=8) in MEG recordings from humans. The difference in mean peak power was significant, p<0.05, marked with *. Error bars represent SEMs.

3.3.1.2. Oscillatory frequency and power in MI and SI *in vitro*

Group- and time-averaged PSDs from the three different recordings locations showed distinct oscillatory profiles (figure 3.4), with regards to frequency and peak shape. Broad ongoing activity in mu and beta frequency ranges was seen in superficial layers of MI (MI LIII, n=24) throughout the time period. Constant and narrow beta oscillations were seen in deeper layers of MI (MI LV, n=36), whereas middle layers of SI (SI LIV, n=37) showed broad oscillatory activity with stronger power in the beta range (figure 3.5a-c).
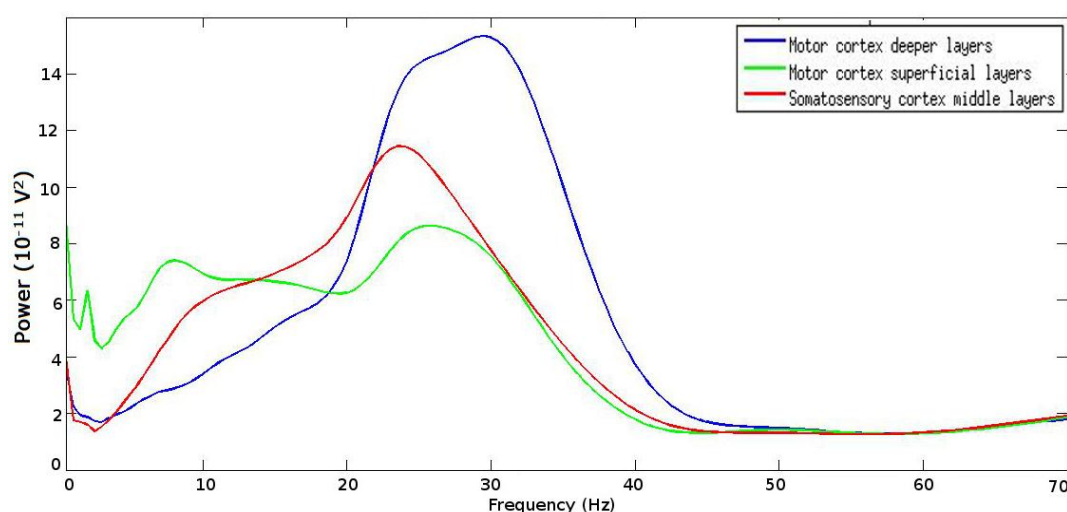
Figure 3. 4. Group- and time-averaged PSDs from the three different locations *in vitro*. The blue and green lines indicate deeper and superficial layers of MI (MI LV, n=36 and MI LIII, n=24), respectively. The red line indicates the recordings from the middle layers of SI (SI LIV, n=37). Each location has a distinct oscillatory profile.
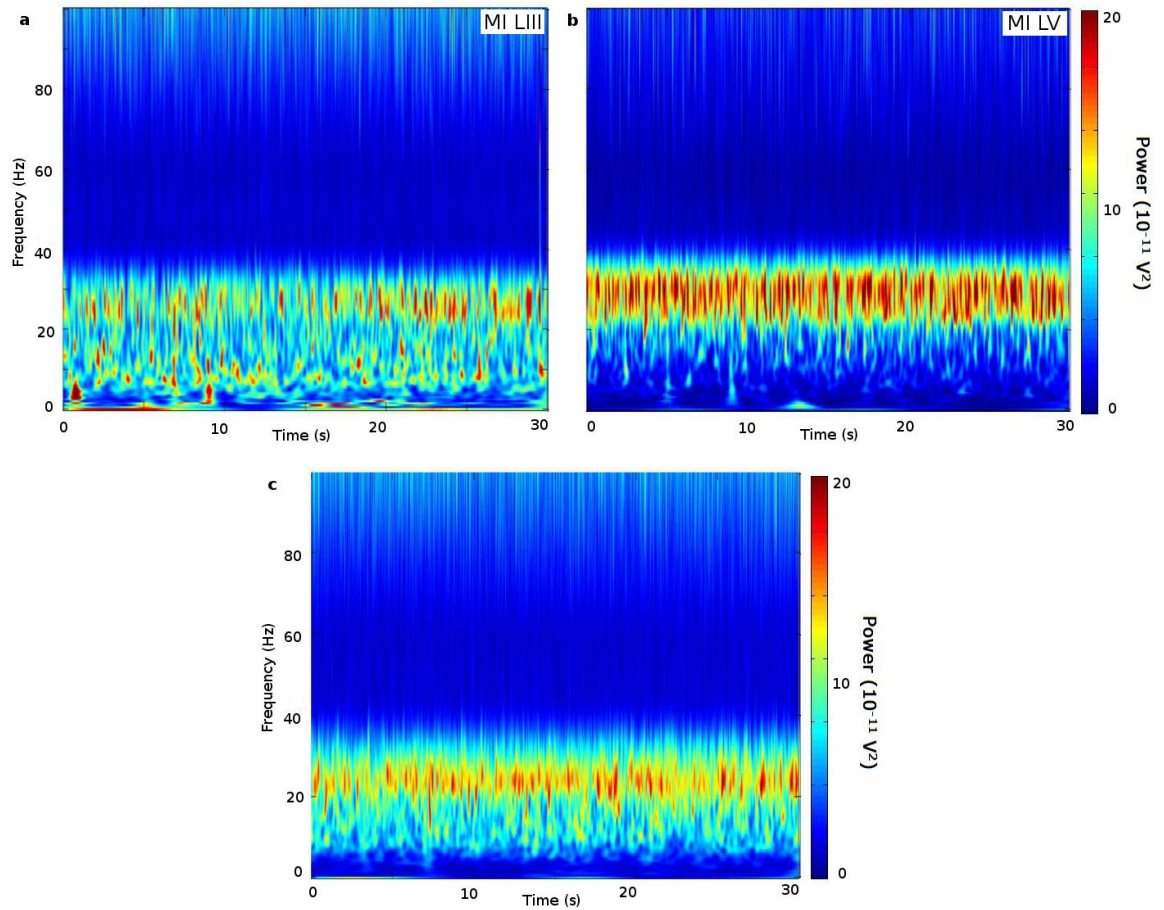
Figure 3. 5a-c. Group-averaged Morelet-wavelet spectrograms of the ongoing activity in different layers of the primary sensorimotor cortex *in vitro* show variation in power and frequency over time. In MI LIII (n=24), sporadic activity throughout the time period can be seen to span over a broader frequency range (a, top left). MI LV (n=36), show a frequency-wise narrow beta oscillatory activity (b, top right). In SI LIV (n=37) more power in the beta range is seen, but also mu (c, bottom).

The mean peak frequency in MI LV was 30.18±3.22 Hz, and mean peak amplitude was 20.75±27.92 x10^{-11}V^2. In MI LIII the mean peak frequency was 18.89±6.07 Hz and mean peak amplitude 13.38±18.17 x10^{-11}V^2. The mean peak frequency in SI LIV was 12.38±6.76 Hz, and mean peak amplitude was 14.61±14.37 x10^{-11}V^2 (figure 3.6a-b). The differences in amplitude were non-significant; between MI LIII and MI LV: $t_{[23]}$=-1.5993, p=0.1234; between MI LIII and SI LIV: $t_{[23]}$=-0.4001, p=0.6928; between MI LV and SI LIV: $t_{[23]}$=-1.4035, p=0.1738. The difference in mean peak frequency between MI LIII and MI LV was highly significant, $t_{[23]}$=-5.4872, p<0.001; between SI LIV and MI LV significant, $t_{[23]}$=-3.1961, p=0.004; and between MI LIII and SI LIV significant, $t_{[23]}$=-3.2607, p=0.0034.
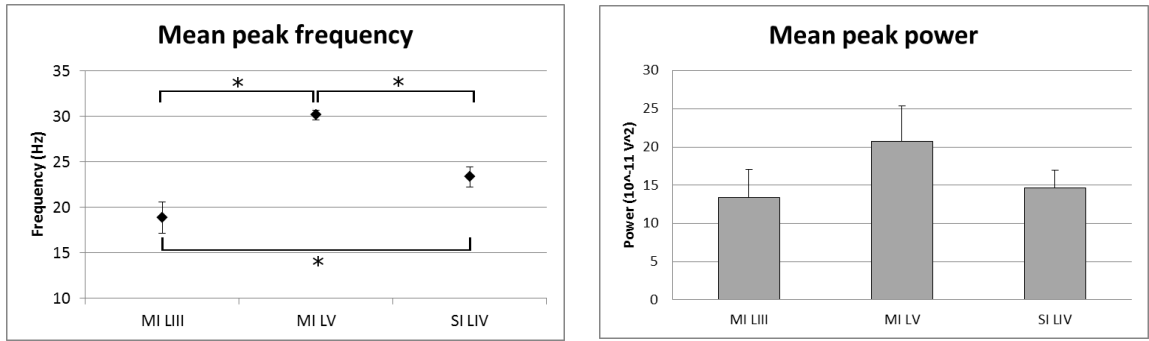
Figure 3. 6a-b. The mean peak frequency, seen in a (left), and power, seen in b (right), in MI LIII (n=24), MI LV (n=36) and SI LIV (n=37) *in vitro*. The mean peak frequency differed significantly between all locations, p<0.05, marked with *. There were no significant power differences. SEMs are indicated as errorbars.

3.3.2. Oscillatory distribution and variability in sensorimotor cortex

3.3.2.1. Oscillatory distribution in MI and SI in MEG

The mean FWHM in MI was 24.58±11.22 Hz. The mean FWHM in SI was 25.64±10.68 Hz (figure 3.7). There were no statistical differences between mean FWHM in MI and SI, $t_{[7]}$=-0.257, p=0.8046.
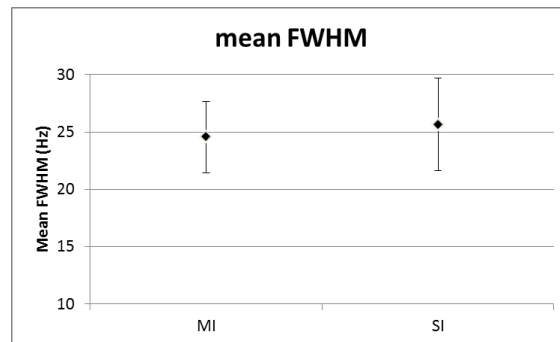
Figure 3. 7. Mean FWHM in MI (n=13) and SI (n=8) in humans. There are no significant difference in frequency between the locations. Error bars represent SEMs.

3.3.2.2. Frequency Distribution in MI and SI *in vitro*

The mean FWHM in MI LIII recordings was 13.13±5.72 Hz. In MI LV the mean FWHM was 12.13±4.09 Hz. In SI LIV the mean FWHM 16.14±6.6 Hz (figure 3.8). The difference between the mean FWHM in MI LV and SI LIV was highly significant, $t_{[23]}$=4.5018, p= 0.00016116. Statistical comparison between other locations showed no significant differences; between MI LIII and SI LIV: $t_{[23]}$=-1.653, p=0.1119; between MI LIII and MI LV: $t_{[23]}$=-1.781, p=0.0881.
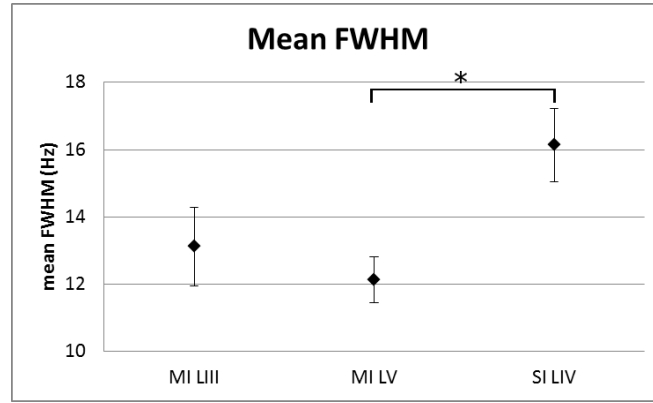
Figure 3. 8. Mean FWHM in MI LIII (n=24), MI LV (n=36) and SI LIV (n=37) from *in vitro* recordings. The difference in mean FWHM between MI LV and SI LIV was highly significant, p<0.001, marked with *. Error bars represent SEMs.

3.3.2.3. Frequency Variability in MI and SI in MEG

In MI two peaks in the frequency variability were found at 10 and 25 Hz. The power-normalised distribution showed peaks at 10 and 21 Hz, with 6.1 and 7.5 nAm in power (figure 3.9a-b). The percentage of samples found at the beta peak frequency was 6.86±4.12%, at peak frequency ±5Hz: 45.60±15.19% and at peak frequency ±10Hz: 55.32±17.71%.

The frequency distribution in SI contained two peaks at 11 and 22 Hz. The normalised power per sample distribution showed peaks at 10 and 18 Hz, with 5.1 and 5.7 nAm in amplitude respectively (figure 3.10a-b and 3.11). The percentage of samples found at the beta peak frequency was 6.41±2.55%, at peak frequency ±5Hz: 40.66±8.27% and at peak frequency ±10Hz: 49.71±8.52%. There was no statistically significant difference between the frequency distribution in MI and SI, $t_{[7]}=0.0071$, p=0.9945.
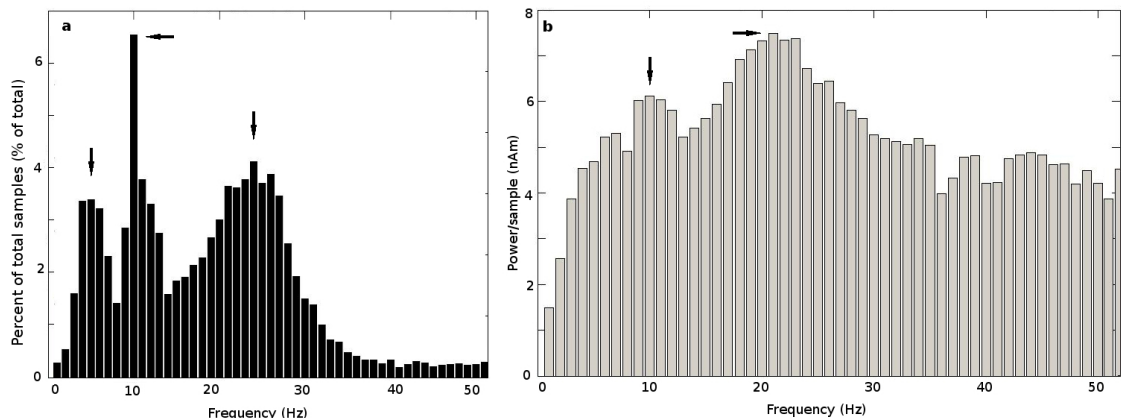
Figure 3. 9a-b. Group-average peak frequency distribution and its related power distribution in MI (n=13) in humans. The frequency distribution, seen in a (left) shows the highest count of samples with frequency peaks were found at 10 and 25 Hz, indicated by black arrows. The normalised power to sample distribution, seen in b (right), shows two peaks: one at 10 Hz with less power than the one at 21 Hz, also indicated by black arrows.

Figure 3. 10a-b. Group-average peak frequency distribution and its related power distribution in SI (n=8) in humans. The frequency distribution, seen in a (left), shows frequency peaks at 11 and 22 Hz (black arrows). The normalised power-to-sample distribution, seen in b (right), shows two peaks at 10 and 18 Hz (black arrows).
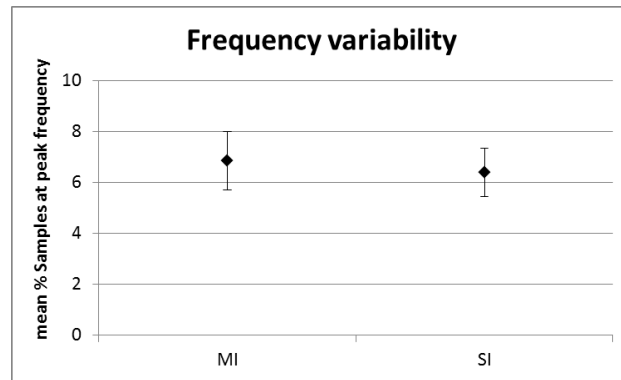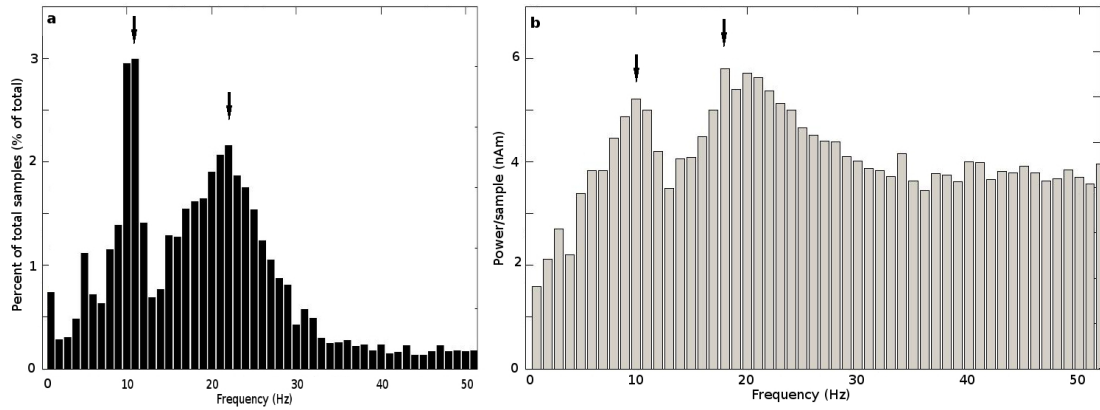
Figure 3. 11. Mean peak frequency distribution in MI (n=13) and SI (n=8) from MEG recordings. There were no significant differences between MI and SI. Error bars represent SEMs.

3.3.2.4. Frequency Variability in MI and SI *in vitro*

In MI LIII, most peak frequency samples were <10Hz, with two additional peaks at 24 and 30 Hz. In the power-normalised distribution show two flat and broad peaks at 12 and 23 Hz, 23.5 and 23.1 x10^{-11} V^2, respectively (figure 3.12a-b). The percentage of samples found at the beta peak frequency in MI LIII was 7.39±6.77 %, at peak frequency ±5Hz: 45.98±23.66 % and at peak frequency ±10Hz: 59.25±24.19 %.

The frequency distribution in MI LV displayed two peaks at 23 and 30 Hz. The normalised power per sample distribution showed a broad peak at 29 Hz, 28.8 x10^{-11} V^2 (figure 3.13.a-b). The percentage of samples found at the beta peak frequency in MI LV was 13.33±8.50 %, at peak frequency ±5Hz: 61.98±19.04 % and at peak frequency ±10Hz: 67.80±17.68 %.

The frequency distribution in SI LIV showed two frequency peaks at 9 and 23 Hz. The highest peak was found at 22 Hz in the power normalised distribution, 24.8x10^{-11} V^2 (figure 3.14a-b). The percentage of samples found at the beta peak frequency was 10.02±8.50 %, at peak frequency ±5Hz: 54.71±18.85 % and at peak frequency ±10Hz: 65.70±16.15 %. There was no significant difference in variability between MI LIII and SI LIV, $t_{[23]}$=-1.0693, p=0.269; The difference in variability was significant between MI LIII and MI LV, $t_{[23]}$=-3.446, p=0.0022; and between SI LIV and MI LV, $t_{[23]}$=-2.3381, p=0.0284 (figure 3.15).
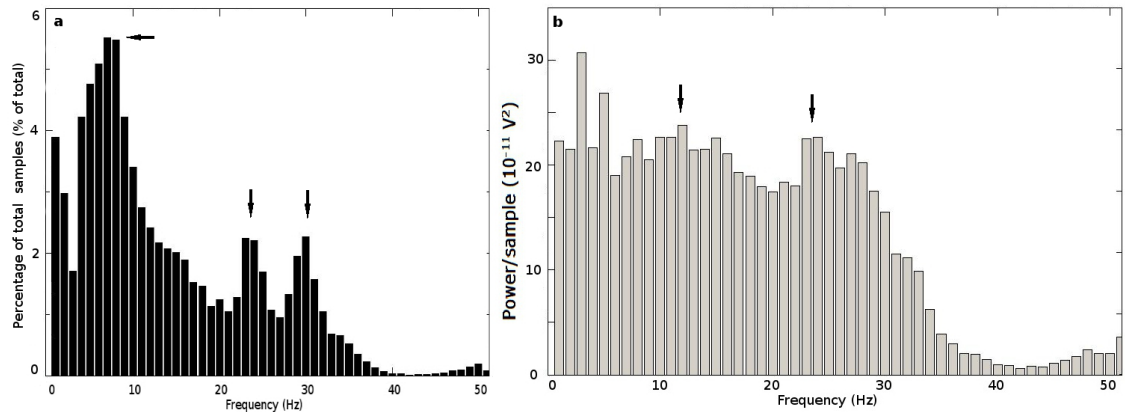
Figure 3. 12a-b. Group-average peak frequency distribution, a (left), and its related power distribution, b (right), in MI LIII (n=24) *in vitro*. The frequency distribution shows an abundance of frequency peaks <10 Hz, with accumulation of peak frequencies at 24 and 30 Hz, indicated by black arrows. The normalised power to sample distribution shows a flat distribution with distinguishable peaks at 12 and 24 Hz, indicated by black arrows.
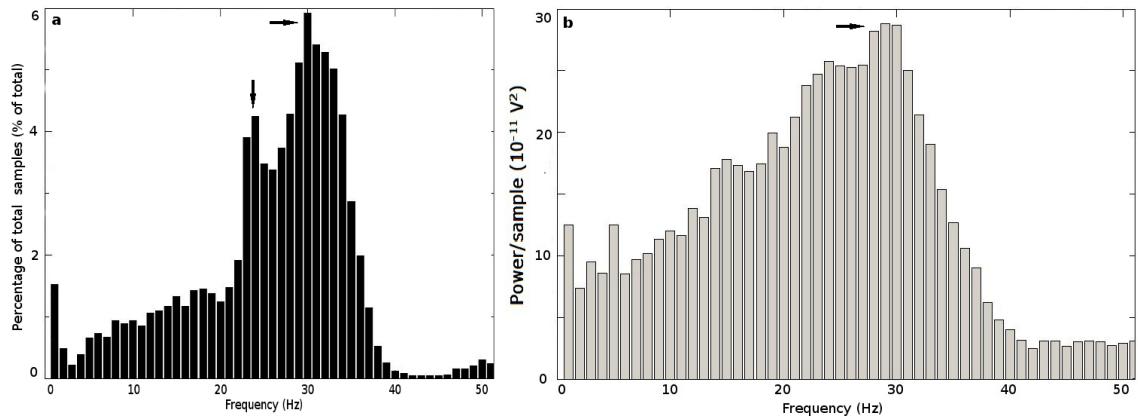
Figure 3. 13a-b. Group-average peak frequency distribution and its related power distribution in MI LV (n=36) *in vitro*. The frequency distribution, seen in a (left), shows frequency peaks at 23 and30 Hz, indicated by arrows. The normalised power to sample distribution, seen in b (right), showed a peak at 29 Hz, indicated with arrow.
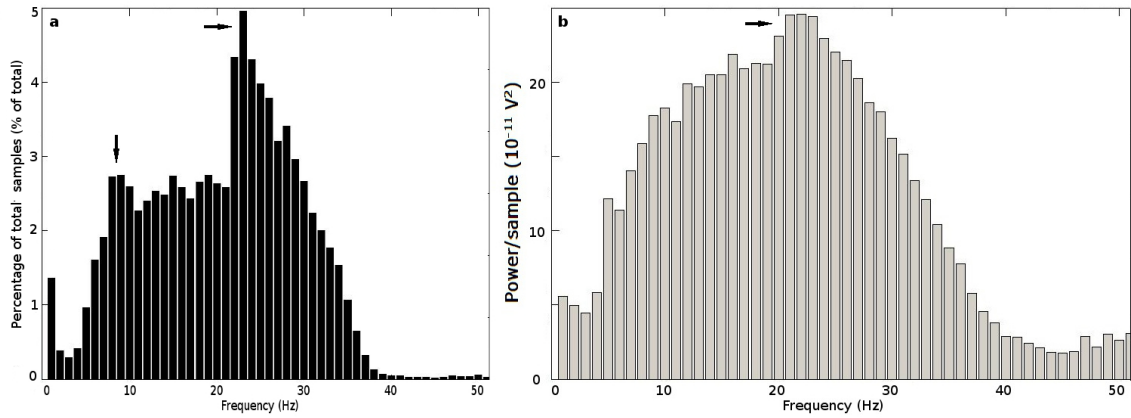
Figure 3. 14a-b. Group-average peak frequency distribution and its related power distribution in SI LIV (n=37) *in vitro*. The frequency distribution, seen in a (left), shows frequency peaks around 9 and 23 Hz, indicated with arrows. The normalised power to sample distribution, seen in b (right), showed a peak at 22Hz, indicated with arrow.
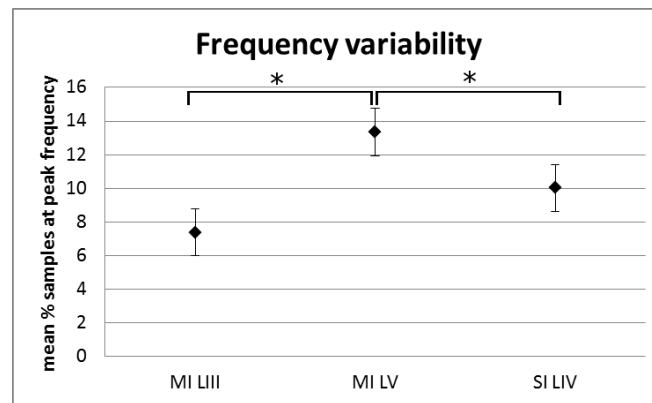
Figure 3. 15. Mean beta peak distribution in MI LIII (n=24), MI LV (n=36) and SI LIV (n=37). There were significant differences in variance between MI LV and MI LIII, and MI LV and SI LIV, p<0.05, marked with *.

3.3.2.5. Oscillatory Power State analysis in MI and SI in MEG

In MI, the percentage of samples found in the upstate was 43.28 %, with a mean upstate power of 3.66 nAm and a mean downstate power was 2.67 nAm (figure 3.16). In SI, the percentage of samples found in the upstate was 42.39 %., with a mean upstate power of 2.64 nAm and a mean downstate power was 1.92 nAm (figure 3.17). Figure 3.18a-b presents an overview of the oscillatory state analysis results. The difference in percentage of samples found in the upstate between MI and SI was non-significant, $t_{[7]}=0.4525$, p=0.6646. The difference in oscillatory state power between MI and SI was highly significant for the upstate difference, $t_{[7]}=5.7314$, p<0.001, and significant for the downstate difference, $t_{[7]}=5.0179$, p=0.0015.
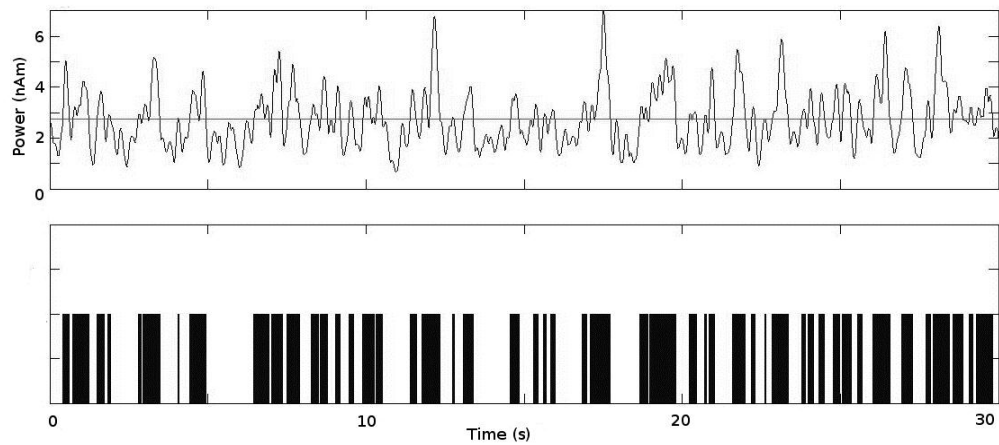
Figure 3. 16. Example of oscillatory power analysis of signal recorded from MI in one human participant. Sporadic increases in power with varying length and power can be seen in the top plot. The thin line represents the change point between states.The bottom box indicates where the samples have surpassed the change point.
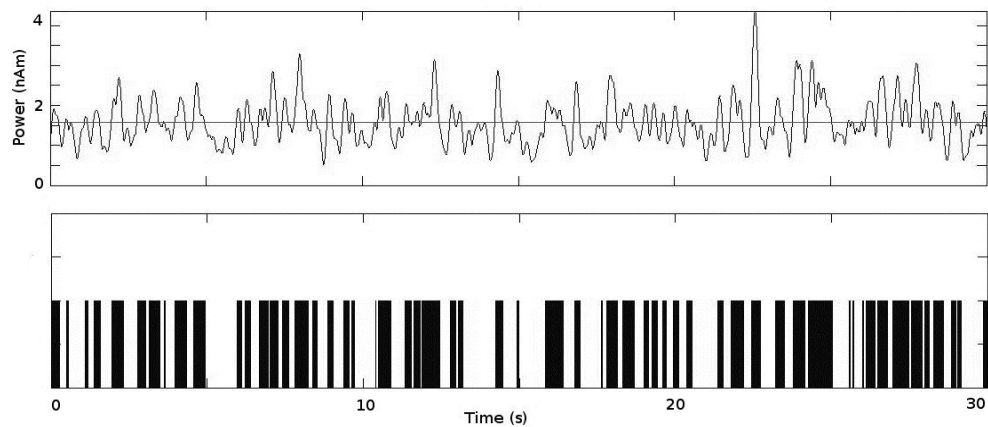
Figure 3. 17. Example of oscillatory power analysis of signal recorded from SI in one human participant. Sporadic increases in power with varying length and power can be seen in the top plot.
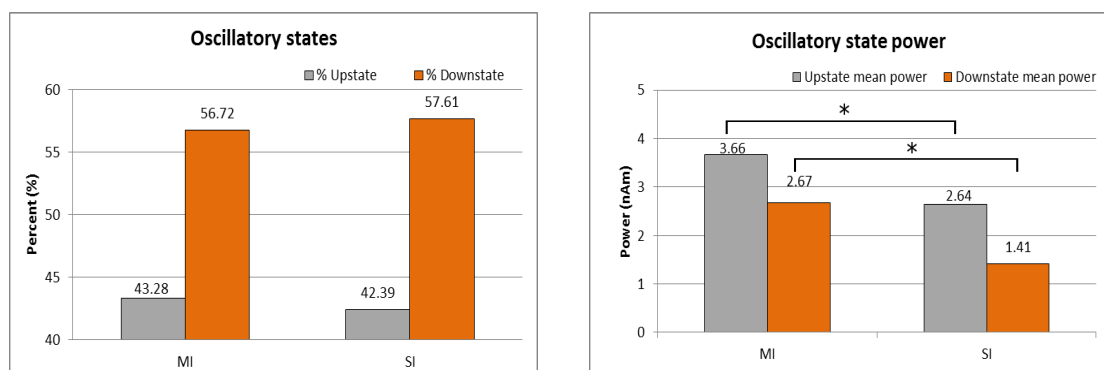
Figure 3. 18a-b. Group-averages of percentages of samples found in the oscillatory up- (grey) and downstate (orange), seen in a (left), and their mean power, seen in b (right). Oscillatory activity show no significant differences in states between MI (n=13) and SI (n=8). The mean power in the up- and downstates differ significantly between MI and SI, p<0.05, marked with *.

3.3.2.6. Oscillatory Power State analysis in MI and SI *in vitro*

In MI LIII, the percentage of samples found in the upstate was 39.69 %, the mean upstate power was 10.09 $\times 10^{-11} V^2$, and the mean downstate power was 3.85 $\times 10^{-11} V^2$ (figure 3.19). In MI LV, percentage of samples found in the upstate was 37.89 %, the mean upstate power was 8.79 $\times 10^{-11} V^2$ and the mean downstate power was 2.59 $\times 10^{-11} V^2$ (figure 3.20). In SI LIV, percentage of samples found in the upstate was 38.84 %, the mean upstate power was 9.21 $\times 10^{-11} V^2$ and the mean downstate power was 3.22 $\times 10^{-11} V^2$ (figure 3.21). The percentage upstate difference between MI LIII and MI LV was significant, $t_{[23]}$=2.6357, p=0.0148, but not between MI LIII and SI LIV: $t_{[23]}$=0.7852, p=0.4403 or MI LV and SI LIV: $t_{[23]}$=2.0291, p=0.0542 .There was no significant difference between power in the upstates in MI LIII and MI LV: $t_{[23]}$=0.4315, p=0.6701, or MI LIII and SI LIV: $t_{[23]}$=0.0334, p=0.9736, or MI LV and SI LIV: $t_{[23]}$=0.378, p=0.7089. There was no significant difference between power in the downstates in MI LIII and MI LV: $t_{[23]}$=0.3189, p=0.2002, or MI LIII and SI LIV: $t_{[23]}$=0.4041, p=0.6899, or MI LV and SI LIV: $t_{[23]}$=0.8341, p=0.4128 (figure 3.22a-b).
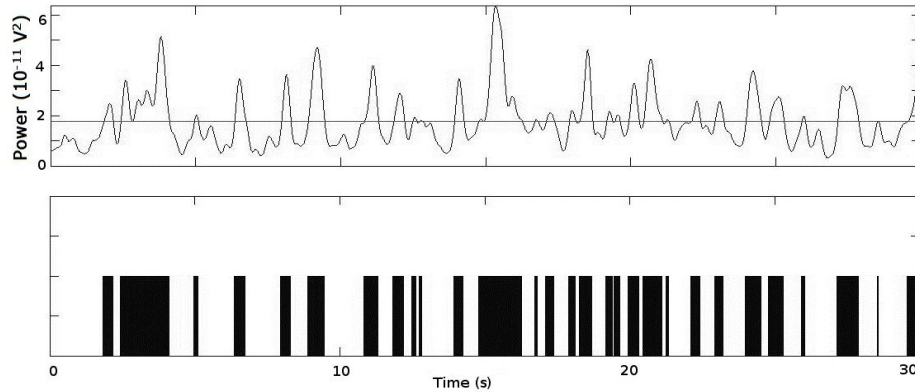
Figure 3. 19. Example of oscillatory power activity in the beta frequency band in one recording from MI LIII *in vitro,* which shows a sporadic pattern, as seen in the top plot. The thin line indicate the change point power value and the bottom box the samples in either state.
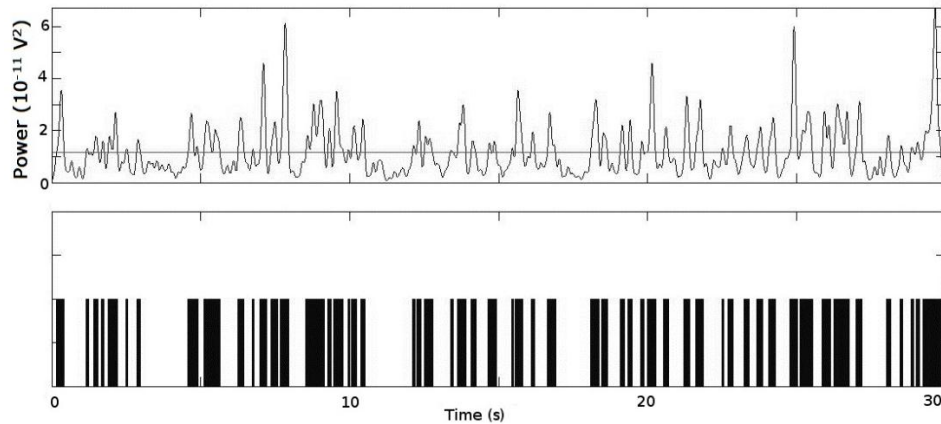
Figure 3. 20. Example of oscillatory power activity in the beta frequency band in one recording from MI LV *in vitro*, which shows a sporadic pattern, as seen in the top plot.
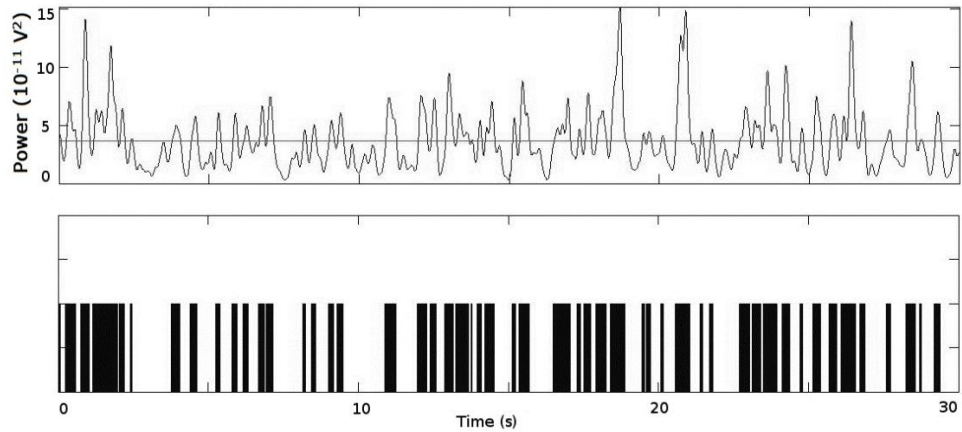
Figure 3. 21. Example of oscillatory power activity in the beta frequency band in one recording from SI LIV *in vitro,* which also shows a sporadic pattern.
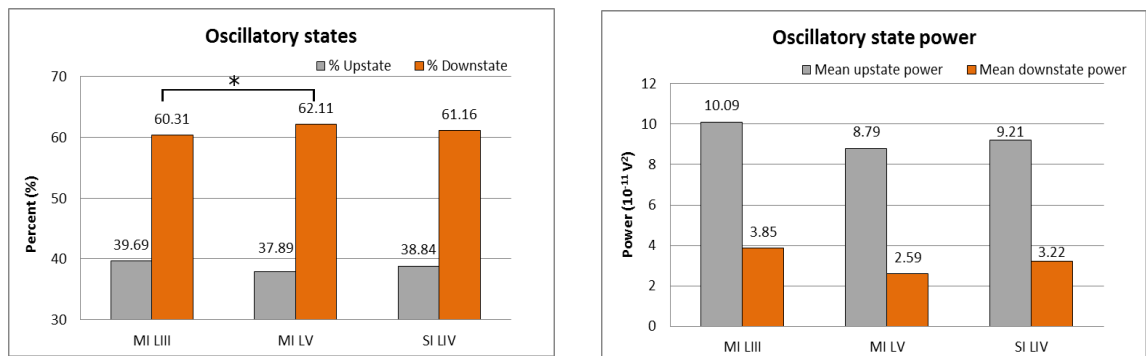
Figure 3. 22a-b. Group-averages of percentages of samples found in the oscillatory states and their mean power *in vitro* (MI LIII: n=24, MI LV: n=36, SI LIV: n=37). Percentage of samples in the upstate (grey) was significant between MI LIII and MI LV, p<0.05, seen in a (left), and marked with *. There were no differences of power in the up- and downstates, seen in b (right). Downstate is indicated by the colour orange.

3.3.3. Integration of oscillatory signals from MI *in vitro* versus MI in MEG recordings

Overall, oscillatory activity with similar frequency range appears in superficial and deeper layers of MI *in vitro* as in MEG MI recordings. However, as can be seen above, there are some differences. The frequency distribution, e.g. the mean FWHM, is narrower for MI *in vitro* recordings when compared to MI MEG recordings, the frequencies and variability also vary slightly. We theorised that these differences are due to the differences in spatial nature of the signals; MEG is an aggregate signal from layers II/III and V, while the *in vitro* signal is spatially precise to the laminae. Hence, we hypothesised that the combined signals from MI laminae would be a better representative of MEG than individual laminae signals.

3.3.3.1. Oscillatory power and frequency analysis

The integrated oscillatory signals from MI LV (n=20) and MI LIII (n=20) from the same slices: MI_{int} (n=20), were investigated with the previously described analysis approach. The oscillatory profiles in MI LIII and MI LV differed in appearance, as can be seen in the group- and time averaged oscillatory PSD profiles in figure 3.23. Integrating the recordings from these layers resulted in an oscillatory profile that showed more resemblance with the MEG MI oscillatory signal than the signal from the individual layers alone.
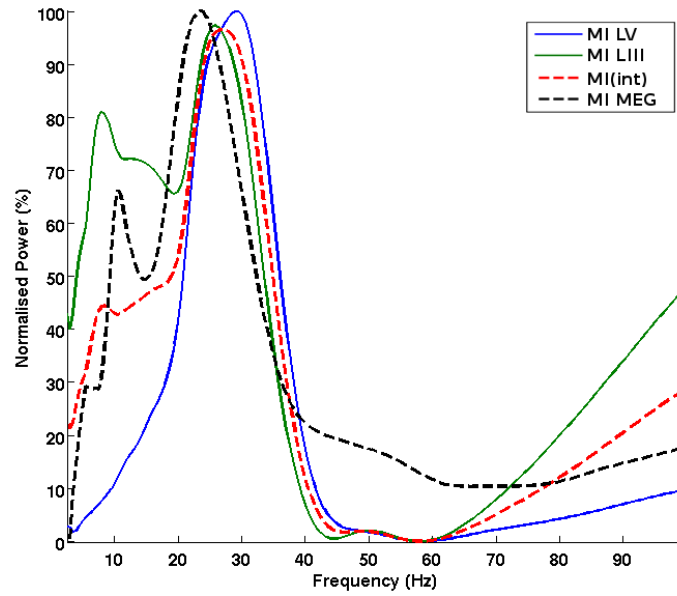
Figure 3. 23. Group-average PSD showing the oscillation profiles from the individual locations MI LV (n=20) and MI LIII (n=20) *in vitro* in blue and green, MI_{int} (=20) in red, and MI (n=13) from MEG recordings in black.

The mean peak frequency in MI_{int} (n=20) recordings was 25.93±7.4 Hz. There was no significant difference in mean peak frequency between MI_{int} and MEG MI recordings: $t_{[12]}$=-1.2316, p=0.2417, or between MI LIII and MEG MI: $t_{[12]}$=1.496, p=0.1605 (figure 3.24). The mean peak frequency in MI LV was significantly higher than in MEG MI recordings, $t_{[12]}$=-4.9751, p=0.00032249, while MI LV was not significantly different in peak frequency to MI_{int}: $t_{[19]}$=2.01, p=0.0588.
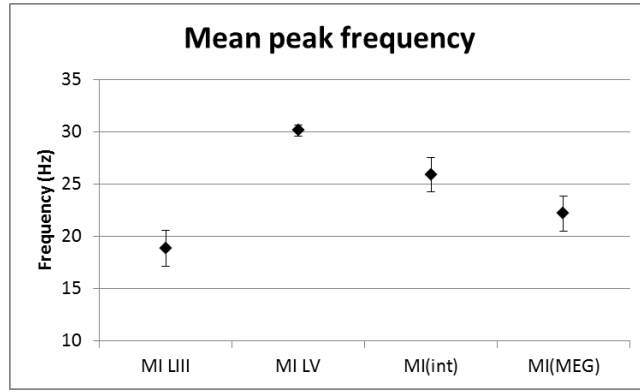
Figure 3. 24. Mean peak frequency in the individual MI (MI LIII: n=20, MI LV: n=20) and integrated MI (n=20), as well as MEG MI (n=13), recordings. There was a highly significant difference between MI LV and MI MEG recordings, p<0.001, marked with *. Error bars are SEMs.

3.3.3.2. Frequency distribution

The mean FWHM for MI_{int} recordings was 14.60±7.89 Hz (figure 3.25). There was no significant difference between MI_{int} and MEG MI recordings: $t_{[12]}$=1.3681, p=0.1964. MI LV showed a significant difference to MEG MI: $t_{[12]}$=4.4216, p=0.00083319; as did MI LV compared to MI_{int} recordings $t_{[19]}$=-2.8326, p=0.0106.
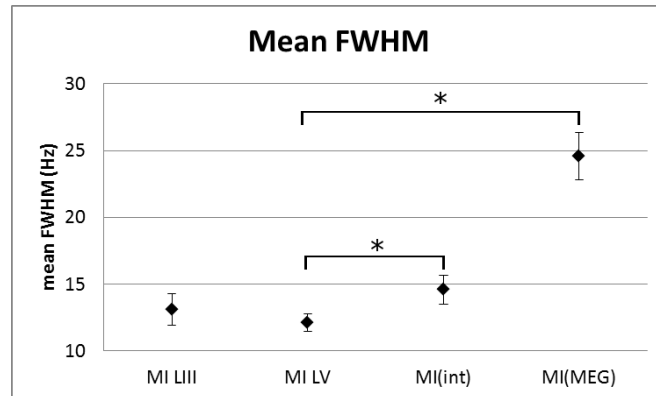
Figure 3. 25. Mean FWHM shows a narrow FWHM in MI LV (n=20), compared to MI from MEG (n=13) recordings. There were no significant differences between MEG MI recordings and MI_{int} (n=20). There were significant differences between MEG MI and MI LV, and between MI LV and MI_{int}, p<0.05, marked with *. Errorbars are SEMs.

3.3.3.3. Frequency variability

The sample count at the frequency distribution peak in MI_{int} was 13.4±10.98 %. There were no significant differences between MI_{int}, and MEG MI recordings: $t_{[12]}$=-0.9136, p=0.3789, or between MI LIII and MEG MI recordings: $t_{[12]}$=1.2772, p=0.2257 (figure 3.26-27). There no significant difference in frequency variability between MI LV and MI_{int}: $t_{[12]}$=1.6986, p=0.1057. There was a significant difference between MI LV and MEG MI; $t_{[12]}$=-3.6257, p=0.0035.
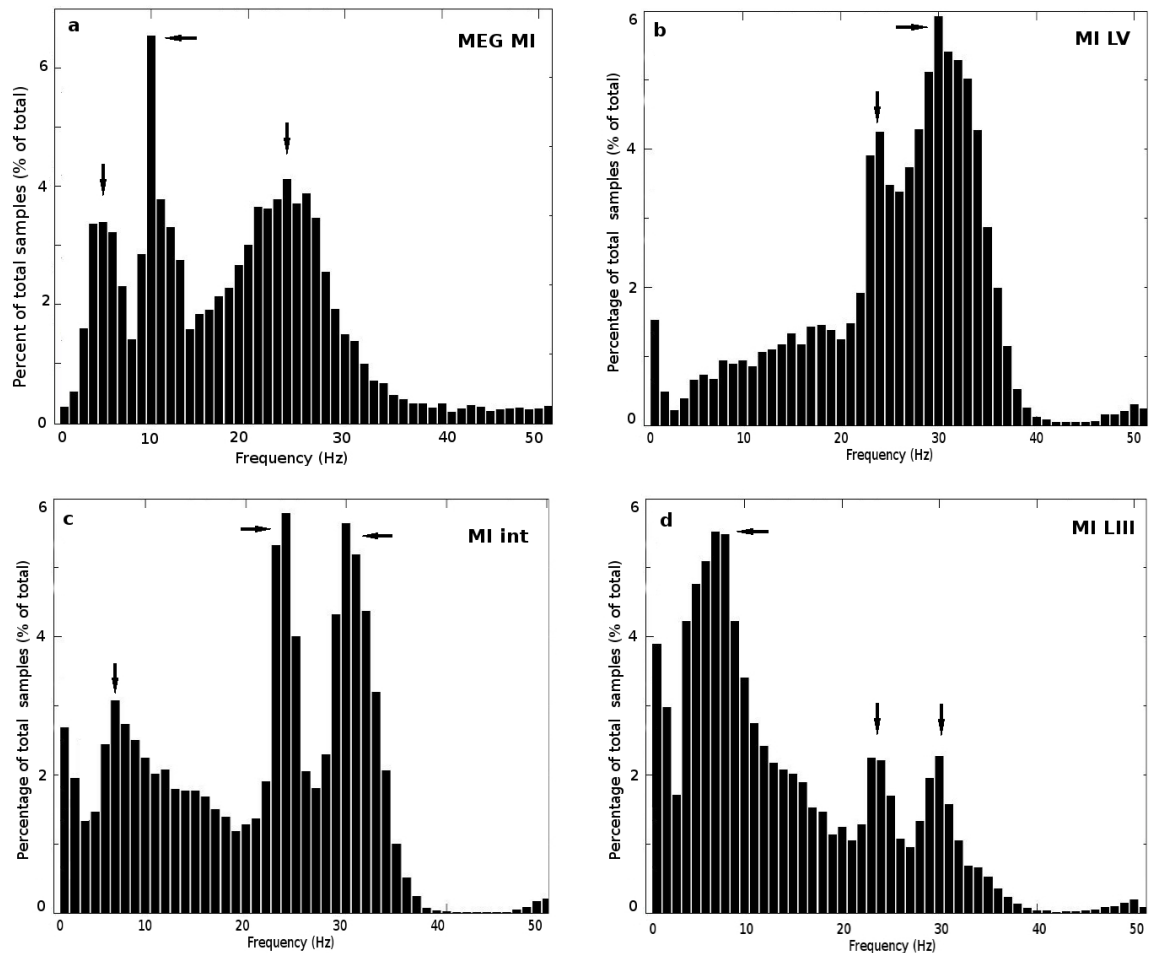
Figure 3. 26a-d. Mean peak frequency variability distribution in MEG MI (a), MI LV (b), MI$_{int}$ (c) and MI LIII (d), recordings. The left column show that in both MEG MI and MI$_{int}$ recordings there are beta and mu oscillations, while the individual laminae recordings in the right column show beta in MI LV and mu and beta in MI LIII. The black arrows indicate the frequency distribution peaks: in a these are found at 5, 10 and 25 Hz, in b at 24 and 30 Hz, in c at 6, 24, 30 Hz, and in d at 8, 23 and 30 Hz. MI LIII: n=20, MI LV: n=20, MEG MI: n=13, MI$_{int}$: n=20.
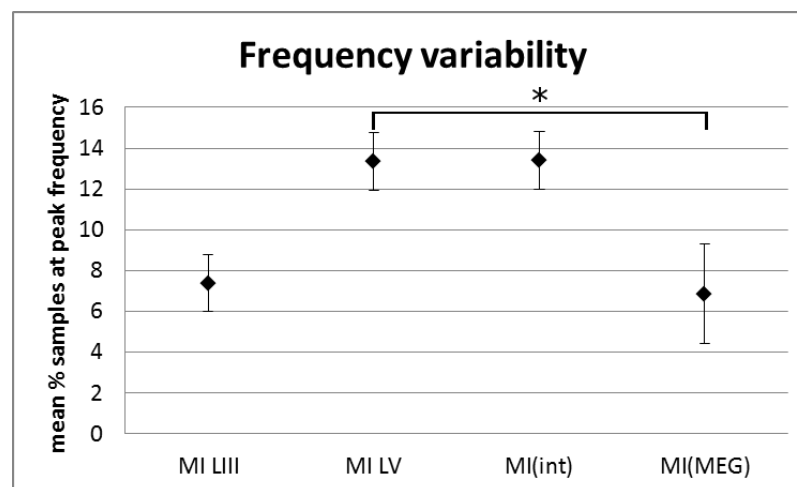
Figure 3. 27. Mean peak frequency variability distribution in MI LIII (n=20), MI LV (n=20), MI$_{int}$ (n=20) and MEG MI (n=13) recordings. The mean % of samples at the peak frequency is significantly different between MI LV and MEG MI, p<0.05, marked with *. Errorbars are SEMs.

3.4. Discussion

3.4.1. Summary

This study has investigated the oscillatory signals from sensorimotor areas recorded with MEG and *in vitro*, and differences between them. We found distinct oscillatory profiles in different areas *in vitro* and MEG, confirmed by significant differences between the mean peak power in MI and SI in MEG recordings and significant differences in mean peak frequency between all areas recorded. The *in vitro* experiments also revealed oscillatory mu in a sensorimotor sagittal brain slice, which has not been widely reported before. There were clear differences in network distribution and variability of oscillatory frequency and power. There was a significant difference in the mean FWHM between SI LIV and MI LV. The peak frequency distribution differed significantly between MI LIII and MI LV, as well as SI LIV and MI LV. There was a significant difference in the percentage of samples found in the upstate between MI LIII and MI LV. Finally, we have showed that integrating signals from MI LIII and MI LV provides an oscillatory signal that profile that resembles the MEG signal more than MI LV alone.

3.4.2. Spatial localisation of generators of sensorimotor cortex oscillations

Animal *in vivo* and neuroimaging literature describe the presence of beta and mu oscillations to great extents (Jasper & Penfield 1949; Gastaut & Bert 1954; Rougeul *et al.* 1979; Pfurtscheller 1981; Bouyer *et al.* 1987; Murthy & Fetz 1992; Sanes & Donoghue 1993; Salmelin & Hari 1994; Salmelin *et al.* 1995; Murthy & Fetz 1996; Pfurtscheller *et al.*, 1997; Crone *et al.*, 1998; Baker *et al.* 1999; McFarland *et al.*, 2000; Marini *et al.* 2008; Tort *et al.*, 2010; Sobolewski *et al.*, 2011). Induced oscillatory activity in different cortical and sub-cortical areas *in vitro* has been described by several research groups (Llinas *et al.*, 1991; Whittington *et al.*; 1995; Traub *et al.*, 1996; Buhl *et al.*, 1998; Cunningham *et al.*, 2003; 2004; Roopun *et al.*, 2006; Yamawaki *et al.,* 2008). The beta and mu oscillations are also reported as network activity in the mammalian primary sensorimotor cortex *in vitro*; mu and beta/gamma oscillations have been induced in middle laminae of the rodent somatosensory cortex (Flint & Connors 1996; Buhl *et al.*, 1998). Beta oscillations have been reported in the deeper layers of MI, which can also be seen in the superficial layers (Yamawaki *et al.*, 2008). However, overall there are few reports specifically detailing oscillatory beta and mu activity in the individual layers of primary somatosensory and motor cortex *in vitro*.

The *in vitro* experiments in this project revealed oscillatory mu activity in MI LIII and SI LIV, resulting in distinct oscillatory profiles from that of MI LV. Previously, it has been proposed that the mu rhythm is indicative of long-range neuronal communication, for example thalamocortical communication and the functional changes in the mu rhythm are reflective of thalamocortical activity and modulation (Lopes da Silva *et al.*, 1980; Suffczynski *et al.*, 2001). However, there are researchers who argue that there are multiple generators of the alpha rhythm with distinct origins (Jones *et al.*, 2009; Kopell *et al.*, 2010; Tort *et al.*, 2010). Furthermore, different frequencies of brain oscillations have been proposed to reflect distinctions in network sizes and range of communication between neuronal assemblies. Lower frequencies encompass larger areas, alternatively longer distances. The higher frequencies would synchronise local assemblies and integrate information and processing (Kopell *et al.*, 2000, Steriade 2001; Varela *et al.*, 2001; Csicsvari *et al.*, 2003; Sirota *et al.*, 2003). As the sensorimotor slice is isolated from other areas, our finding of mu *in vitro* supports the concept of multiple generators of mu. Our results do not support the mu rhythm as only a thalamocortical feature.

The finding of co-existing and simultaneous mu and beta oscillations in the MI LIII and SI LIV support the notion that laminae and sub-areas are distinct in their electrophysiological make-up and that neuronal network activity and ongoing oscillations reflect these distinctions (Chagnac-Amitai & Connors 1989; Franschetti *et al.*; 1995, Flint & Connors 1996; Cunningham *et al.*, 2004; Roopun *et al.*, 2006; Rosanova *et al.*, 2009). These differences in neuronal network activity were evidenced by significant differences in mean peak frequencies between all areas recorded.

In addition, the findings of mu in these *in vitro* experiments queries the simplified view that the mu rhythm is purely a consequence of long-range communication alone, and brings question to the functional and cognitive relevance of the mu rhythm. The relevance of mu oscillations has been reviewed heavily during the last decades with respect to mirror neurons (Cochin *et al.*, 1998; Francuz & Zapala 2011), attention and cognition (Moore *et al.*, 2008; van Dijk *et al.*, 2008; Jones *et al.*, 2010; Anderson & Ding 2011; van Ede *et al.*, 2011; Freyer *et al.*, 2012) and sensory and motor responses (Salmelin *et al.*, 1995; Pfurtscheller *et al.*, 1997; Neuper *et al.* 2001a; also see Pineda, 2005, for a review on the mu rhythm). The brain slice preparation does not allow for cognitive or functional probing, but the finding of mu in this preparation indicates that the mu rhythm does exist in isolated neuronal networks, similarly to beta and gamma rhythms, and is not a direct consequence of cognition or function.

It is interesting that the beta rhythm is found in solitude in layer V of MI, which is considered the output station (Rivara *et al.*, 2003). This stands in contrast to the co-existence of mu and beta oscillations in superficial layers of MI. The superficial laminae are believed to be the input laminae from other areas (Douglas & Martin 2004; Thomson & Lamy 2007), including SI. Layer IV of SI is reported to contain the barrel cortex in rodents and also be the major input station from primarily thalamus (Douglas & Martin 2004; Shipp 2007; Thomson & Lamy 2007). The findings in this study suggests that it is likely the mu neuronal network activity is both a reflection of large-scale communication, as well as a feature of oscillatory activity in small-scale networks, e.g. *in vitro*, primed to sustain this activity and receive/transmit information relevant for the long-range communication. The co-existence with beta in MI LIII and SI LIV further supports this as beta, in particular higher frequencies, is considered a local rhythm.

The MEG experiments showed a significant difference in mean peak power between MI and SI in the MEG recordings, but not in mean peak frequency. Early research reports implicitly suggested exclusivity in the distinction between mu oscillations representing the somatosensory rhythm, and beta as the motor rhythm (Salmelin & Hari 1994; Salmelin *et al.*, 1995); a view that is also upheld in recent research of mu and beta ERD and ERS (McFarland *et al.*, 2000; Gaetz & Cheyne 2006; Jurkiewicz *et al.*, 2006; Koelewijn *et al.*, 2008; van Ede *et al.*, 2011). However, there are also recent reports that suggest that beta and mu oscillations co-exist in the sensorimotor network and that these rhythms are not exclusive to either area (Kopell *et al.*, 2000; Pinto *et al.*, 2003; Szurhaj *et al.*, 2003; Brovelli *et al.*, 2004; Gaetz & Cheyne 2006; Jones *et al.*, 2009). If there was a distinction in spatial localisation of mu and beta oscillations, a significant difference in the mean peak frequency and oscillatory profiles of the ongoing activity from these two areas would be expected. The empirical findings from the MEG experiments performed in this chapter instead support the view that ongoing beta and mu oscillations co-exist simultaneously in both MI and SI. These rhythms are inter-dependent in the sensorimotor network to varying degrees in any individual and contribute to differences in event-related changes to the ongoing beta and mu oscillations surrounding movement and stimulation (Szurhaj *et al.*, 2003, Jones *et al.*, 2009). The *in vitro* findings of mu oscillations in MI LIII further confirm simultaneous co-existence of mu and beta in MI and SI.

3.4.3. The characteristics of neuronal network oscillations in sensorimotor cortex

Beta and mu oscillations are implicit network phenomena in the sensorimotor cortex. The relationship of task performance and pre-stimulus, e.g. ongoing, sensorimotor oscillatory network activity is currently a popular research topic (Linkenkaer-Hansen *et al.*, 2004; Koelewijn *et al.*, 2008; Haegens *et al.*, 2011; van Ede *et al.*, 2011). These networks are supposedly altered in neurological pathologies such as PD (Uhlhaas & Singer 2006), giving rise to different and abnormal functional features (Hall *et al.*, under review) and dynamics (Sailer *et al.*, 2003). Research of sensorimotor beta and mu oscillations are predominantly aimed at the functional changes seen in these rhythms surrounding motor and somatosensory sensory events (Jasper & Penfield 1949; Gastaut & Bert 1954; Pfurtscheller 1981; Salmelin & Hari 1994; Salmelin *et al.* 1995; Pfurtscheller *et al.*, 1997; Crone *et al.*, 1998; McFarland *et al.*, 2000; Cheyne *et al.*, 2003; Jensen *et al.*, 2005; Jurkiewicz *et al.*, 2006; Koelewijn *et al.*, 2008; Zhang *et al.*, 2008; Gaetz *et al.*, 2010; van Ede *et al.*, 2010; 2011). There is little detailed research on the characteristics of the spontaneous ongoing mu and beta oscillations in the human sensorimotor cortex during rest. This is somewhat surprising since insight into the features of the ongoing oscillations during rest would be valuable when using this activity as a baseline for comparisons with functional changes, interventions and pathological states, e.g. PD. The MEG experiments in this study therefore aimed to provide further details on the characteristics of the beta oscillatory activity found in the sensorimotor cortex in humans.

In addition, conventional approaches to peak measurements display average representations of the oscillatory neuronal network activity. Group- and/or time-averages lack distribution and variability information regarding the oscillatory activity, hence very little about the intrinsic distribution and variability of oscillatory frequency and power in the sensorimotor cortex is known. We investigated the variability and distribution of the ongoing beta and mu activity we found in the different sensorimotor areas discussed above. The mean FWHM show the average width of the frequency distribution of the oscillatory activity in an area. By using the amplitude-independent distribution histogram we investigated the distribution and variability of the peak frequency; depicting how the peak frequencies from all of the samples in the epoch are distributed over the frequency range. In addition, we assessed the mean percentage of samples in found in the upstate in the beta band and their mean power. This indicates differences in activity patterns, commonly referred to as "oscillatory bursting".

The lack of significant differences in mean FWHM and peak distribution of the oscillatory frequencies further supports the similarities of the broad ongoing mu and beta activity at rest in MI and SI. Individual variability and ratio in peak power of beta and mu oscillations

in the sensorimotor cortex contributes to the significant difference between the peak power in MI and SI, also emphasised by the significant difference in the mean power of oscillatory states. The presence of dissimilar neuronal network activity in the different sensorimotor laminae underlying the recorded oscillatory activity was demonstrated by the significant difference in the mean FWHM between SI LIV and MI LV. In addition, the frequency distribution differed significantly between MI LIII and MI LV, as well as SI LIV and MI LV, but not MI LIII and SI LIV. The lack of non-significant differences between SI LIV and MI LIII are not surprising as both displayed co-existence of mu and beta rhythms to varying degrees. There was no significant difference in mean peak power or mean state power *in vitro*; however there was a significant difference in the percentage of samples found in the upstate between MI LIII and MI LV. This indicates a difference in the oscillatory activity pattern between these two areas; this can also be seen to some extent in the averaged Morelet-Wavelet spectrogram as well and could be one possible source of frequency variability. We are only aware of a few studies that have begun to report frequency variability as important. Little *et al.* (2012) found that the beta band stationarity correlated to rigidity-bradykinesia in PD patients. Although this study did not use the same approach to assessing frequency variability, they too highlight the emerging importance of understanding frequency non-stationarity. The lack of previously reported results of variability in beta and mu oscillations in the sensorimotor areas is most likely due to differences in recording technology and analysis approaches.

3.4.4. Comparing oscillatory signals from MI *in vitro* and MI in MEG recordings

Investigation into the differences and similarities of oscillatory signals recorded from the human sensorimotor cortex with MEG, and the oscillatory signals recorded from the sensorimotor cortex in a rodent *in vitro* preparation is essential as researchers continue to make inferences and interpretations between these two recording modalities (Fingelkurtz *et al.*, 2004; Gaetz *et al.*, 2010; Hall *et al.*, 2010; 2011). *In silico* approaches are often used as a comparative approach when investigating and interpreting the results from recording oscillatory activity in the sensorimotor cortex (Destexhe, 2000; Kopell *et al.*, 2000; Brovelli *et al.*, 2004; Jensen *et al.*, 2005; Jones *et al.*, 2009). These modelling approaches conventionally compare the neuronal network composition and resulting output, rather than a direct comparison of empirical data. We investigated the differences and similarities of the empirical sensorimotor MEG and LFP oscillatory signals during rest, with a particular aim towards mu and beta oscillations. Due to substantial inherent differences in the modalities, some features of the oscillatory signals, e.g. amplitude, cannot reliably be compared between techniques. Thus we have focused on frequency.

The source size of oscillations recorded *in vitro* is 500-3000 μm around the electrode tip (Mitzdorf, 1987, Juergens *et al.*, 1999, Logothetis *et al.*, 2001). The source size in MEG is substantially larger with a source size of >5mm^3, or >10000-50000 cells, in layer II/III and V of the sensorimotor cortex (Vrba & Robinson 2001; Hillebrand & Barnes 2002; Murakami & Okada 2006). The MEG signal is therefore considered an aggregate signal with an inherently larger underlying substrate; the number of neuronal networks in the MEG signal is greater than in the LFP recordings. The prediction from this difference is a greater mean FWHMs in MEG recordings. This was confirmed in comparing the MEG and *in vitro* results in this chapter. Differences in the source size and number of contributing networks are also visible in the appearance of the frequency variability between the two modalities.

Previous *in silico* approaches have been used to investigate the network composition in relation to the oscillatory input/output (Whittington *et al.*, 1995; Traub *et al.*, 1996a; Wang & Buszaki 1996; Wang, 1999; Destexhe 2000; Kopell *et al.*, 2000; Brovelli *et al.*, 2004; Jensen *et al.*, 2005; Jones *et al.*, 2009; Moran & Bar-Gad 2010; Yang & Guo 2011). However, using empirical data to create a large-scale representation of the resulting output from local areas is arguably a more realistic recreation of a complex signal than a large network model.

The large-scale integrated motor cortex oscillatory signal presents with more similarity to an aggregate signal like MEG than the oscillatory signals from individual laminae in the motor cortex. The individual laminae display distinct and significantly different oscillatory profiles; the oscillatory activity in MI LV displays a sharp peak in the higher beta frequency range and the oscillatory activity in MI LIII spans over a broad frequency range encompassing both mu and beta regions. The oscillatory signal from MI in MEG displays two peaks in mu and higher beta frequency regions. Integrating the signals from MI LIII and MI LV did indeed create an oscillatory profile that further resembled the complex MEG MI profile seen in these neuroimaging experiments. However, there were also some obvious differences in the profiles, primarily in the lower beta and mu frequency regions. Hypothesising that this was partly due to the difference in proximity of MI LIII and MI LV to the SQUIDS in the MEG, weighting of the integrated signal was performed. The signals from the superficial and deeper lamiae were weighted in different ratios. This procedure created oscillatory profiles that further resembled the aggregate MEG signal, see figure 3.28 below.

There are still differences between the weighted integrated MI oscillatory profile and the MEG MI profile. These differences could be due to inherent physiological distinctions in the areas and species recorded, or further unknown effects of the recording methods, or an effect of large-scale communications. More research in the individual methodologies is needed to establish the cause of the remaining differences. In addition, further examination of the comparisons between MEG and *in vitro* is warranted for the same reasons. One route would be beneficially aimed at investigation into what degree the *in vitro* recordings could be further amalgamated *in silico* to represent an aggregate signals like the one seen in MEG recordings.
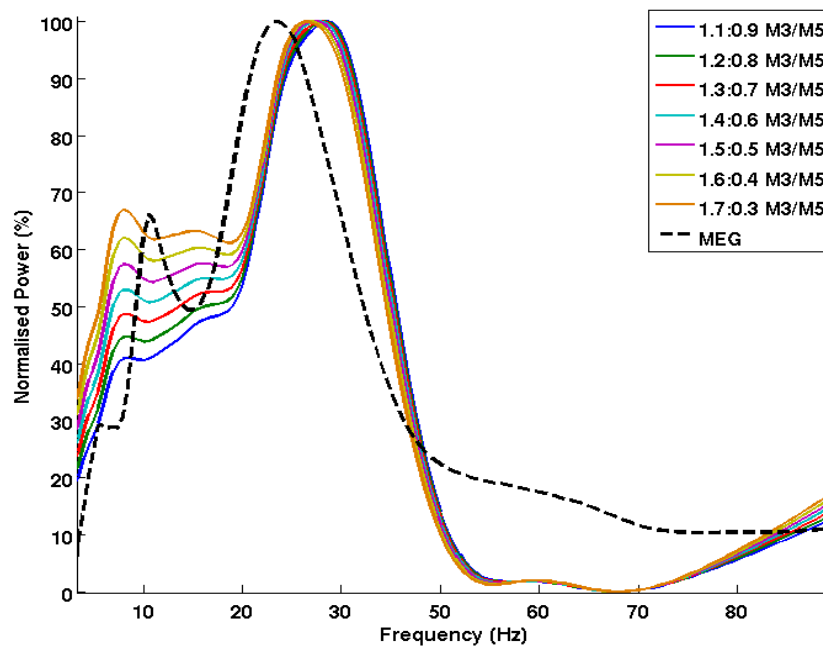
Figure 3. 28. Different weighting of the contribution from different laminae *in vitro* when integrating the oscillatory signals in the motor cortex creates oscillatory profiles that resemble the MEG MI profile. M3= MI LIII, M5= MI LV.

3.5. Conclusion

We conclude that the spontaneous *ongoing* oscillatory network activity in MI and SI show significant differences in mean peak amplitude between MI and SI, but there were no significant differences in mean peak frequency. Furthermore, we revealed oscillatory network activity in the mu frequency range in MI LIII and SI LIV *in vitro*, co-existing with the ongoing beta activity. This has implications for the debate of functional relevance and origins of the mu rhythm. Finally, we conclude that integrated signals from MI *in vitro* results in oscillatory activity resembling the ongoing oscillatory network activity in human MI. These findings contribute strong arguments to why using *both* methods in combination, when studying and elucidating the role of beta oscillations in the sensorimotor cortex, was optimal. As much as differences are obstacles to comparison, they also point to the importance of the very same distinctions.

Chapter 4. The influence of cortical connectivity on sensorimotor beta oscillations

4.1. Introduction

4.1.1. Background

Beta and mu oscillations are well-reported phenomena in the sensorimotor cortices. In the previous chapter we showed that the spatial distinction between *ongoing* beta oscillations in MI and *ongoing* mu oscillations in SI (Salmelin & Hari 1994; Salenius *et al.*, 1995; Gaetz & Cheyne 2006; Cheyne 2012) is not clear cut in MEG recordings in humans. In addition, we confirmed that beta oscillations exist *in vitro* in deeper layers of motor cortex (Yamawaki *et al.*, 2008), and we also revealed that beta and mu oscillations co-exist in superficial layers, as well as the middle layers of SI. However, it is unclear to what extent the beta and mu oscillations we see in sensorimotor areas depend on intrinsic connections between these areas.

A wealth of research literature during the last half century has found that cortical areas and laminae are heavily interconnected (Jones & Powell 1970; Vogt & Pandya 1978; Zarzecki *et al.*, 1978; Krubizer & Kaas 1990; Jones & Wise 1997; Lewis & van Essen 2000; Disbrow *et al.* 2003; Shipp 2005; Douglas & Martin 2004; 2007a; 2007b; Shipp 2007; Thomson & Lamy 2007; Weiler *et al.*, 2008). Figure 1.2 in chapter 1 illustrated the complex connectivity between regions in the sensorimotor areas. Modelling approaches have been used to assign direction and also suggest complex connectivity as a feature of the oscillatory activity in the sensorimotor cortex (Brovelli *et al.*, 2004; Tsujimoto *et al.*, 2009). This intricacy of sensorimotor connections is also evident in the oscillatory dynamics surrounding motor and somatosensory processing, which are believed to be dependent on sensorimotor connectivity (Cassim *et al.*, 2001; Alegre *et al.,* 2002). The functional relevance of the beta and mu rhythms in the sensorimotor cortex is a topic of debate. Functional modulation of the beta rhythm is widely reported as event-related changes, suggested to involve both primary motor and somatosensory areas (Pfurtscheller, 1981; Salmelin & Hari 1994; Jensen *et al.*, 2005; Gaetz & Cheyne 2006; Jurkiewicz *et al.*, 2006, Neuper *et al.*, 2006; Avanzini *et al.*, 2012). Recently sensorimotor beta oscillations have also been suggested to reflect more cognitive functions such as somatosensory decision-making (Haegens *et al.*, 2011a). The functional dynamics of the beta rhythm is not solely dependent on the connectivity to somatosensory areas. There is also an important influence of association areas, evidenced by differences in beta ERD patterns and cortico-spinal excitability between internally and externally paced movements. Internally, e.g. self-paced, movements display an earlier increase in cortico-spinal excitability, and an earlier beta ERD, although these two are necessarily not linked (Chen *et al.*, 1998; Gerloff *et al.*, 1998). Earlier electrophysiological recordings in monkeys

have reported that the two different types of movement cue correlate to activation of the supplementary motor area for the self-paced movement, and the premotor area for the externally paced (Wessel *et al.*, 1997; Jenkins *et al.*, 2000; Haslinger 2001). Functional brain imaging studies in humans have confirmed this localisation to some degree, but also argue that there are more complex interactions and motor programs in humans (Cunnington *et al.*, 2002). Functional modulation of the mu rhythm has been linked to attention and cognitive functions (Moore *et al.*, 2008; van Dijk *et al.*, 2008; Anderson & Ding 2011; Haegens *et al.*, 2011b; 2011c; van Ede *et al.*, 2011; Freyer *et al.*, 2012), sensory and motor responses (Salmelin *et al.*, 1995; Pfurtscheller *et al.*, 1997; Neuper *et al.* 2001; Pineda, 2005) and modulation of thalamocortical activity (Lopes da Silva *et al.*, 1980; Suffczynski *et al.*, 2001).

Apart from the examples mentioned above regarding functional relevance for each rhythm, the independency of these rhythms is conventionally discussed with regards to distinct experimental modulation of one, but not the other, rhythm in varying degrees. One example of this is the differences in ERD and ERS of beta and mu oscillations during a movement task. Both the beta and mu oscillatory activity desynchronise prior to movement onset approximately at the same time. However, the beta activity resynchronises more rapidly, usually with a temporary increase in power before returning to baseline power e.g. PMBR. This is not the mu activity pattern, which instead desynchronises approximately 1 second later than the beta ERD and also returns to baseline over a longer time period, without any rebound activity (Stancák & Pfurtscheller 1995; 1996; Pfurtscheller & Lopes da Silva 1999; Alegre *et al,.* 2004).

The beta and mu oscillations and their functional dynamics exemplify the existence of a sensorimotor network and its intrinsic functional changes. Furthermore, there is a multitude of neuroimaging studies and reviews discussing resting state network activity and functional connectivity in sensorimotor areas (Biswel *et al.*, 1995; Damoiseaux *et al.*, 2006; Mantini *et al.*, 2007; Deco *et al.*, 2011), and with regards to changes in pathological states, e.g. PD (Uhlhaas & Singer 2006; Hammond *et al.*, 2007, Stam, 2010). One recent study applying a novel analysis approach on MEG data determined a strong source of beta power in the region corresponding to the sensorimotor resting-state network (Hillebrand *et al.*, 2012), corresponding to the idea of natural frequencies where beta oscillations are linked to motor cortex and mu oscillation are found over the parietal cortex (Rosanova *et al.*, 2009). One recent review suggested that sensorimotor beta oscillations are reflective of large-scale interactions between sensorimotor areas and other regions, as well as the periphery (Kilavik *et al.*, 2012). However, to date there are no clear

suggestions of the extent to which MI and SI areas affect the ongoing oscillatory activity in their neighbouring areas.

Mechanistically, we know from *in vitro* experiments that beta oscillations can be observed in deeper layers of MI (Yamawaki *et al.*, 2008), and in sensory areas (Buhl *et al.*, 1998; Cunningham *et al.*, 2004; Roopun *et al.*, 2006). Previous experiments have also shown that rhythms can co-exist in laminae of areas (Flint & Connors 1996; Roopun *et al.*, 2006). However, it is unclear to what degree the connectivity between sensorimotor areas affects the ongoing oscillations; if and to what degree mu and beta oscillations co-exist in isolation.

4.1.2. Aims and research objectives

Previous research has investigated beta and mu oscillations in MI and SI, but it is unclear to what extent these rhythms exist in solitude from other areas. Furthermore, it is unclear what effect the connections within MI have on the oscillations it exhibits. Here we aim to determine whether the oscillations that exist in the intact MI LV are dependent on laminar connections. We address the following questions:

- o Which oscillations arise from MI LIII and LV in microslices, e.g. physically isolated MI?
- o How do oscillations MI LIII and LV compare in frequency and power between intact sensorimotor slices and microslices of MI?
- o How do the oscillations in MI LIII and LV compare in variability and distribution between intact sensorimotor slices and microslices of MI?

Furthermore, and perhaps more importantly with regards to macroscopic observations such as MEG, it is unclear to what extent connectivity between MI and SI influences oscillations in these areas. We address the following questions:
- o What effect does severing the connection between MI and SI have on frequency and power in these areas?
- o What effect does severing the connection between MI and SI have on frequency distribution and variability in these areas?

4.2. Methods

In vitro preparation of sagittal brain slices was performed according to protocol 1 and 2, described in chapter 2. Microslices were excised during microtome slicing by identifying MI from the Rat Brain Atlas (Paxinos & Watson 1986) and physically removing all areas except MI from the slice. See figure 2.6 in the Methods chapter for a schematic image of a sagittal sensorimotor slice and where incisions were placed. The microslices were stored in the same manner as intact slices, described in chapter 3. Here we focused on microslices of MI and recorded from LV: n=14, and LIII: n=5.

In the incision, e.g. cutting, experiments an incision was placed at the approximate border between SI and MI, identified with the Rat Brain Atlas (Paxinos & Watson 1986), using a custom-made device. This held a ceramic blade attached to a plastic rod, which was very gently lowered by a manual manipulator fastened on a magnetic stand, through the slice over a period of approximately 1 minute, to avoid disturbing the ongoing recording or positions of the inserted electrodes. LFPs were recorded continuously from MI LIII (n=1), MI LV (n=12) and SI LIV (n=5) in these intact slices. 30 second epochs before and after incision were used in the offline analysis to determine peak frequency and power, frequency distribution and variability as well as state information.

In vitro data were analysed as described in chapters 2 and 3. Briefly, LFP recordings from all laminae of interest were exported to MatLab (MathWorks, Inc.). Morelet-wavelet spectrograms were derived for each sample in all 30 second epochs, and these were used in further analysis of mean peak frequency and power, FWHM, frequency and power distribution and variability. Student's t-test was used to test for statistical difference between two conditions: before and after incision, or intact vs. microslices.

4.3. Results

4.3.1. Sensorimotor neuronal network activity and MI-SI connectivity

We have shown so far that there are differences in the ongoing oscillatory activity in MI and SI of intact slices. Next, we determined whether these differences seen in the ongoing oscillatory activity in MI and SI depended on the direct connectivity between MI and SI. We did this by placing an incision between the MI and SI border while recording LFPs from MI LIII (n=1), MI LV (n=12) and SI LIV (n=5) (figure 4.1-4.3).
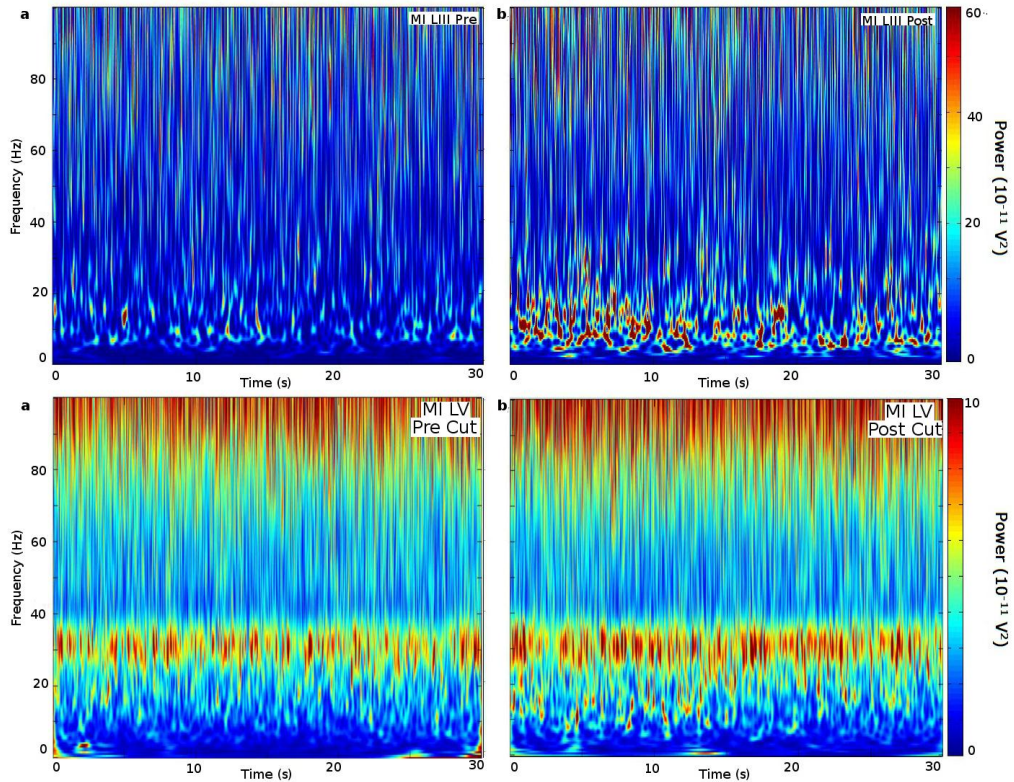
Figure 4. 1. Group-average Morelet-wavelet spectrograms showing effects on oscillatory activity in MI LIII (n=1), seen in a and b (top row), and MI LV (n=12), seen in c and d (bottom row) from severing connections between MI and SI *in vitro*.
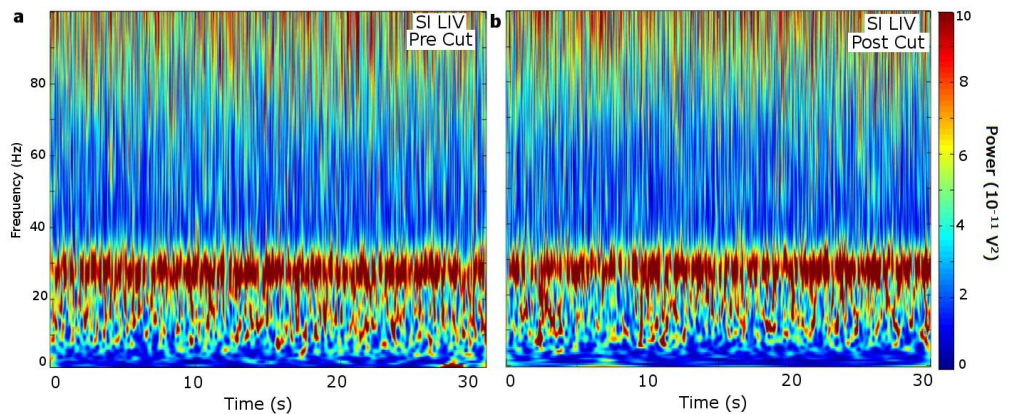
Figure 4. 2. Group-average Morelet-wavelet spectrograms showing effects on oscillatory activity in SI LIV (n=5) before (a, left) and after (b, right) incision between MI and SI *in vitro*.
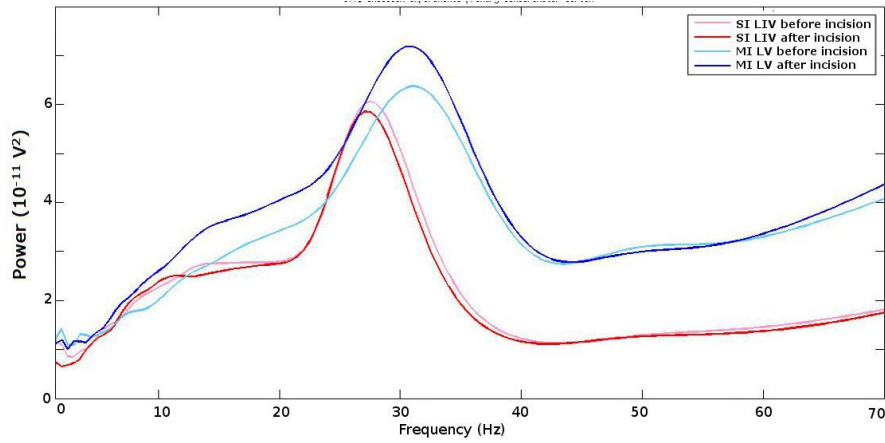
Figure 4. 3 Group- and time-average PSD showing oscillatory profiles of ongoing activity in MI LV (n=12, blue) and SI LIV (n=5, red) before and after severing connections between MI and SI *in vitro*. MI LIII is not shown due to low n number (n=1) and large power difference in the recordings. There is little change in profiles after incision.

4.3.1.1. Frequency and power

The mean peak frequency in MI LIII was 15.50±0 Hz before incision, compared to 11.00±0 Hz after. The mean peak power was 7.24±0 $\times 10^{-11}$ V^2 before, compared to 19.33±0 $\times 10^{-11}$ V^2 after. In MI LV the mean peak frequency before was 26.08±6.12 Hz, compared to 25.04±5.81 Hz, after incision. The mean peak power was 7.68±6.50 $\times 10^{-11}$ V^2, compared to 8.89±8.92 $\times 10^{-11}$ V^2 after incision. The mean peak frequency in SI LIV before incision was 24.70±5.13 Hz, compared to 22.00±7.50 Hz after. The mean peak power was 6.46±4.37 $\times 10^{-11}$ V^2, compared to 6.53±6.31 $\times 10^{-11}$ V^2 (figure 4.4-5). Significance between before and after was tested with Student's t-test. There were no significant differences. For MI LV and peak frequency: $t_{[11]}$=0.8576, p=0.4094; for peak power: $t_{[11]}$=-1.1984, p=0.2559. For SI LIV and peak frequency: $t_{[4]}$=0.8089, p=0.4639; for peak power: $t_{[4]}$=-0.1418, p=0.8941
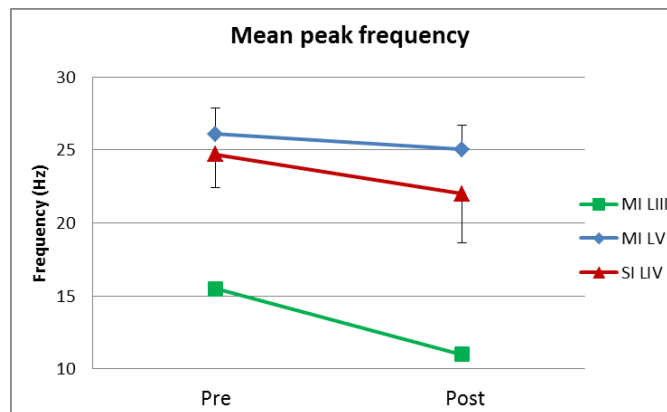
Figure 4. 4. Mean peak frequency in MI LIII (n=1, green), MI LV (n=12, blue) and SI LIV (n=5, red) before and after incision between MI and SI *in vitro*. There were no significant differences. Errorbars are SEM.
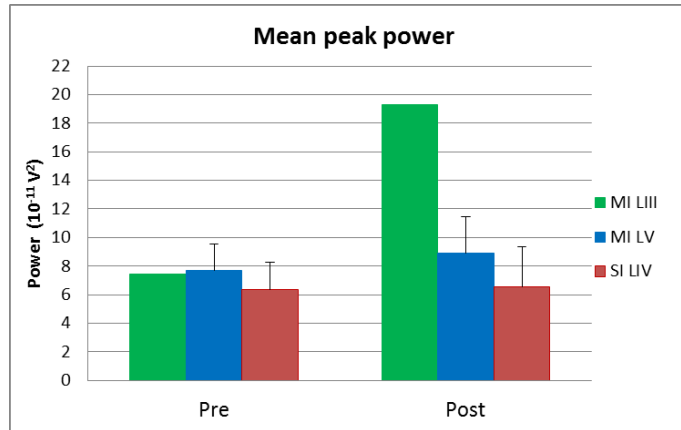
Figure 4. 5. Mean peak power in MI LIII (n=1, green), MI LV (n=12, blue) and SI LIV (n=5, red) before and after incision between MI and SI *in vitro*. There were no significant differences. SEMs are displayed as error bars.

4.3.1.2 Sensorimotor frequency distribution and variability and MI-SI connectivity

There were no significant differences in the distribution of network activity in the different locations after incision, as measured by mean FWHM. The mean FWHM in MI LIII before incision was 40.5±0 Hz, compared to 14.50±0 Hz after. In MI LV the mean FWHM before incision was 21.54±9.43 Hz, compared to 20.33±9.71 Hz after. SI LIV the mean FWHM before incision was 18.40±7.73 Hz, compared to 19.4±7.03 (figure 4.6). There were no significant changes; MI LV: $t_{[11]}$=0.8595, p=0.4053; and SI LIV: $t_{[4]}$=-0.9428, p=0.3992.
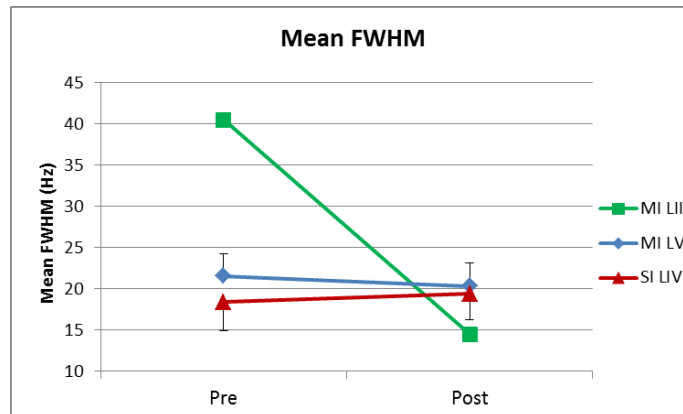
Figure 4. 6. Mean FWHM and frequency distribution in MI LIII (n=1, green), MI LV (n=12, blue) and SI LIV (n=5, red), before and after incision between MI and SI *in vitro*. There were no significant differeces. SEMs are indicated as error-bars.

We found that the peak frequency variability significantly decreased: 8.84±9.27 to 7.67±8.94 %, $t_{[4]}$=6.1841, p=0.0035, in SI LIV after incision. The mean percentage of samples at the peak frequency in MI LIII was 1.31±0 before incision, compared to 5.24±0 % after. In MI LV the mean percentage was 5.84±4.85 before incision, compared to 5.75±9.71 % after (figure 4.7-8); this was non-significant: $t_{[11]}$=0.1545, p=0.88.

101
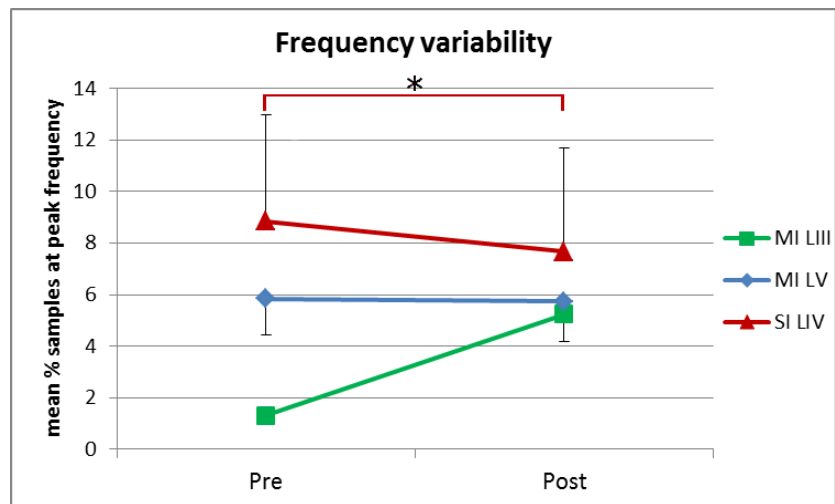
Figure 4. 7. Mean frequency peak distribution in MI LIII :(n=1, green), MI LV (n=12, blue) and SI LIV (n=5, red), before and after incision between MI and SI *in vitro*. The mean % of samples found at the peak frequency in SI LIV decreased significantly after incision, p<0.05, marked with *. SEMs are indicated as error-bars.
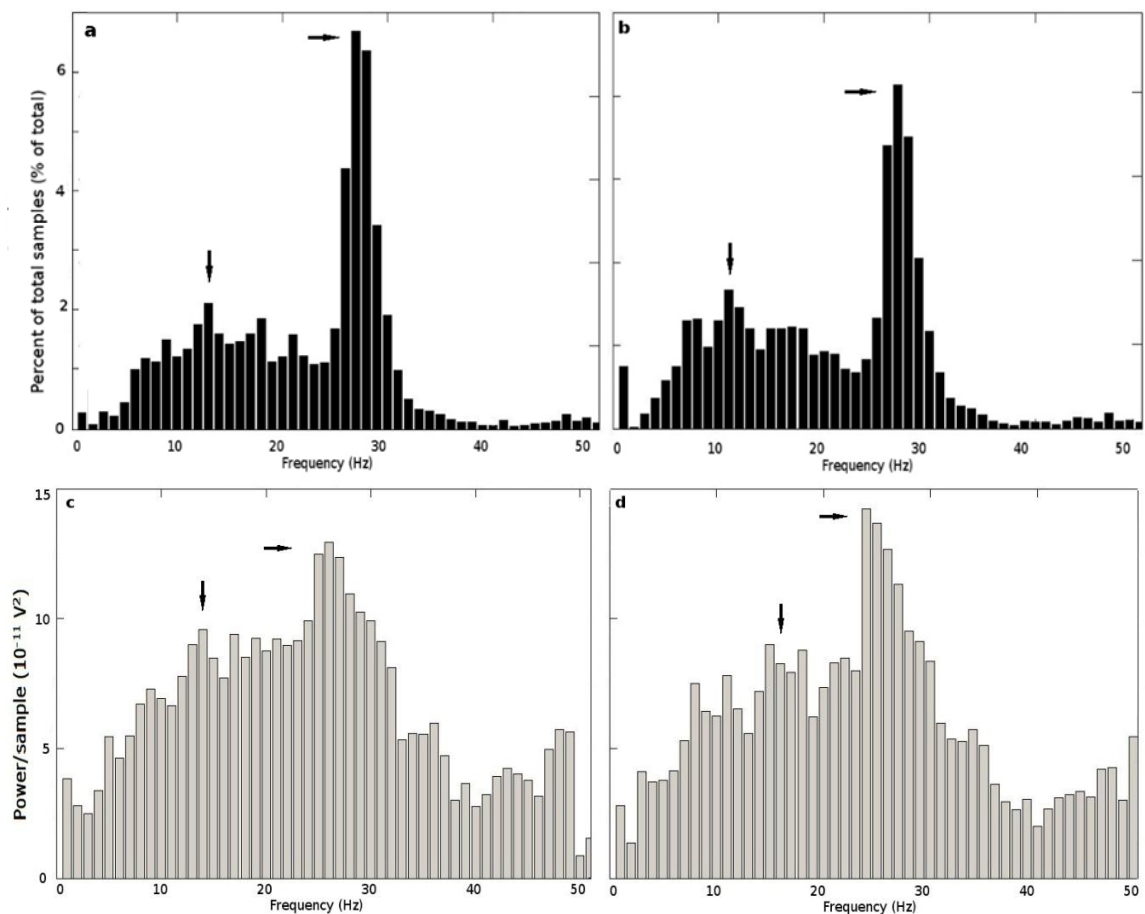
Figure 4. 8a-d. Group-average peak frequency distribution in SI LIV (n=5), seen in a and b (top row) and normalised power frequency distribution, seen in c and d (bottom row), before and after incision (left vs. right column) between MI and SI *in vitro*. Physically separating MI and SI *in vitro* in a sensorimotor slice significantly decreased the variability in SI LIV, p<0.05.

4.3.1.3. Sensorimotor power state and MI-SI connectivity

The oscillatory power states and associated mean power showed no significant differences after severing connections between MI and SI. In MI LIII the percentage of samples found in the upstate was 38.26 % before and 40.59 % after incision. The mean power in the upstate was 8.93 x10^{-11} V^2 before and 20.03 x10^{-11} V^2 after incision. The mean power in the downstate was 3.72 x10^{-11} V^2 before and 9.62 x10^{-11} V^2 after incision.

In MI LV the percentage of samples found in the upstate was 38.62 % and 38.15 % after. The mean power in the upstate was 4.00 x10^{-11} V^2 before and 4.95 x10^{-11} V^2 after incision. The mean power in the downstate was 1.37 x10^{-11} V^2 before and 1.63 x10^{-11} V^2 after incision. There were no significant difference in upstate percentage: $t_{[11]}$=0.6842, p=0.508; in upstate power: $t_{[11]}$=-1.0789, p=0.3037; or in downstate power: $t_{[11]}$=-1.2383, p=0.2414.

In SI LIV the percentage of samples found in the upstate was 38.59 % and 37.16 % after. The mean power in the upstate was 3.96 x10^{-11} V^2 before and 3.29 x10^{-11} V^2 after incision. The mean power in the downstate was 1.46 x10^{-11} V^2 before and 1.17 x10^{-11} V^2 after incision (figure 4.9-10). There were no significant difference in upstate percentage: $t_{[4]}$=1.0455, p=0.2548; in upstate power: $t_{[4]}$=1.0397, p=0.3572; or in downstate power: $t_{[4]}$=1.0213, p=0.3648.
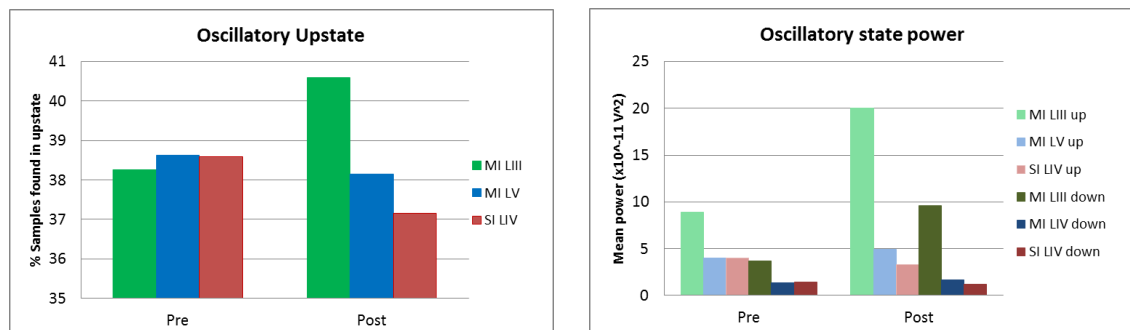
Figure 4. 9a-b. Group-averages of the percentages of samples found in the oscillatory upstate in MI LIII (n=1, green), MI LV (n=12, blue) and SI LIV (n=5, red) before and after severing connections between MI and SI *in vitro*, can be seen in a (left). Figure b shows group-averages of the mean power of the samples found the oscillatory up- and downstate in MI LIII (n=1, greens), MI LV (n=12, blues) and SI LIV (n=5, reds) before (Pre) and after (Post) severing connections between MI and SI *in vitro*. There were no significant differencesThere were no significant differences.

4.3.2. The role of inter-laminar connectivity in MI oscillations

We wanted to determine the extent to which the connections within MI, e.g. intra-laminar connections, affect the ongoing oscillations in MI LV. We did this by comparing ongoing oscillatory activity in MI LV (n=36) from intact sensorimotor slices and microslices (n=14) (figure 4.11-12). MI LIII was not compared due to low n-numbers.
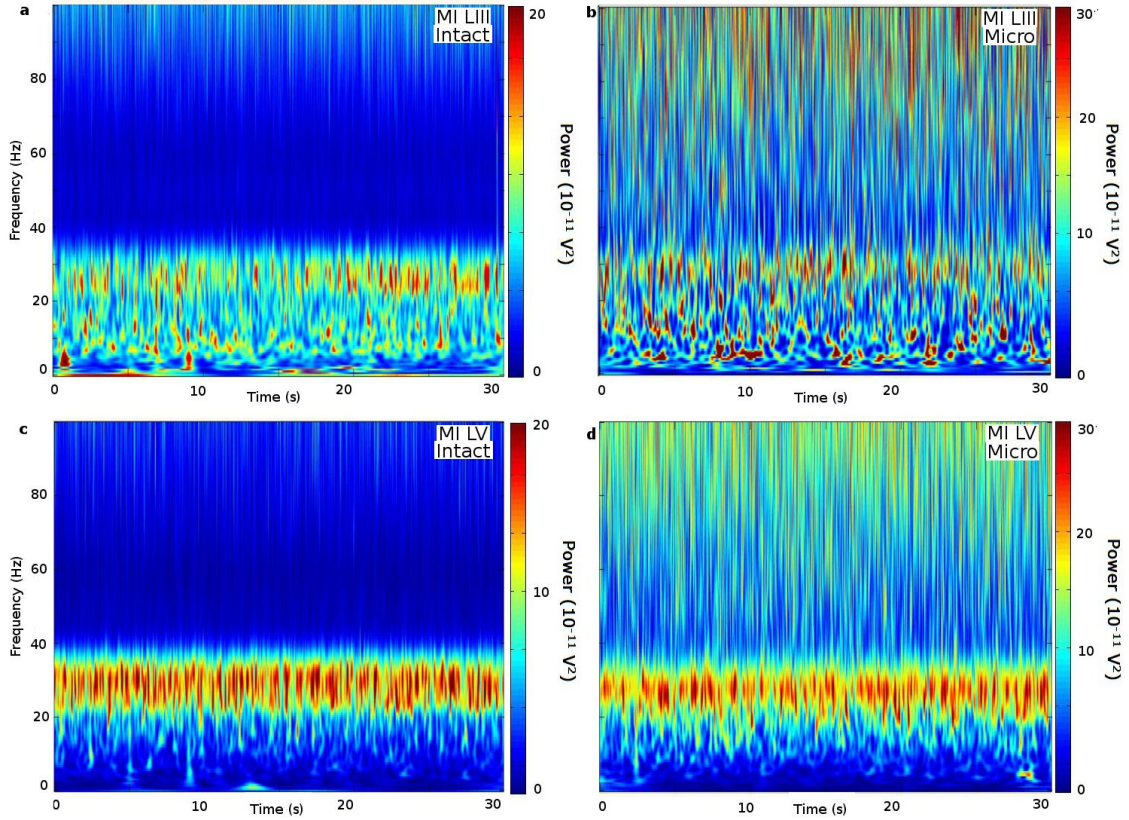
Figure 4. 10a-d. Group-average Morelet-wavelet spectrograms of recordings from MI LIII (a&b, top) and MI LV (c&d, bottom) in intact slices (left) and microslices (right). Observe the difference in power between the intact preparation and microslices. MI LIII from intact slices: n=24, MI LIII from microslices: n=5, MI LV from intact slices: n=36, MI LV from microslices: n=14.
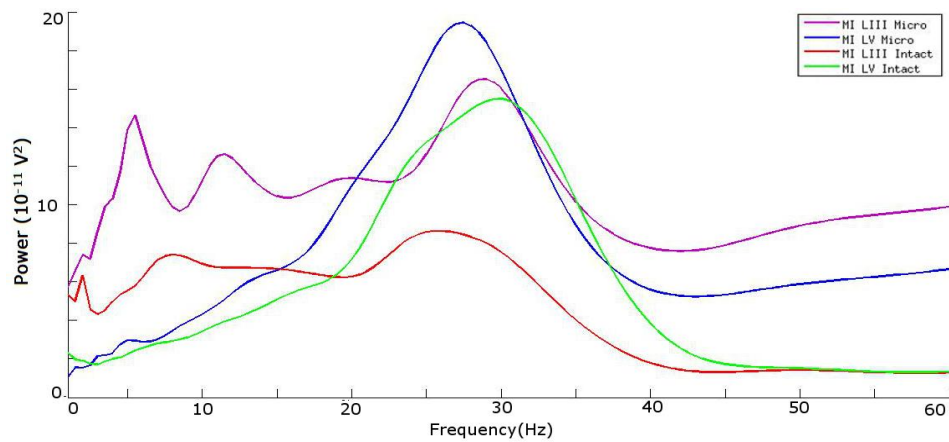
Figure 4. 11. Group- and time averaged PSD plots of oscillatory activity recorded from MI LIII and LV in intact slices and microslices. MI LIII in intact slices: n=24 (red), MI LIII in microslices (purple): n=5, MI LV in intact slices (green): n=36, MI LV in microslices: n=14 (blue).

4.3.2.1. MI frequency and power and laminar connectivity

In MI LIII in microslices mean peak frequency was 17.77±7.6 Hz, and mean peak amplitude was 21.11±21.90 x10^{-11} V^2. In intact slices mean peak frequency was 18.89±6.07 Hz and mean peak amplitude 13.38±18.17 x10^{-11}V^2. In MI LV in microslices mean peak frequency was 26.46±3.70 Hz. Mean peak amplitude was 23.87±23.53 x10^{-11} V^2. In intact slices frequency was 30.18±3.22 Hz, and mean peak amplitude was 20.75±27.92 x10^{-11}V^2. We were primarily interested in differences in the activity in MI LV between the two conditions: Student's t-test was used to test for significance. There was no significant difference in mean peak power between recordings from MI LV in microslices and intact slices: $t_{[13]}$= 1.8611, p=0.0855, but the difference in mean peak frequency between MI LV in the microslices and in the intact slices was significant, $t_{[13]}$= -3.2529, p=0.0063 (figure 4.13-14).
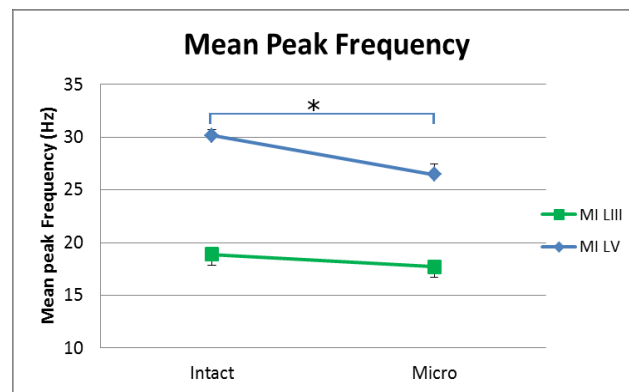
Figure 4. 12. Mean peak frequency in the two locations in the two different slice preparations. The difference in mean peak frequency in MI LV in intact slices (n=36) compared to microslices (n=14) was significant (blue), p<0.05, marked with *. MI LIII from intact slices: n=24, MI LIII from microslices: n=5 (green). Error bars represent SEMs.
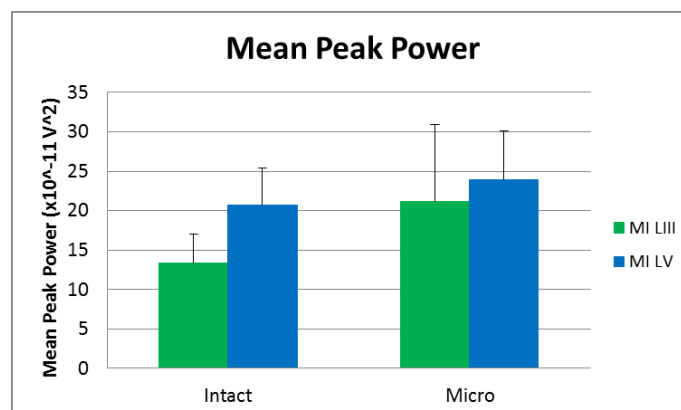
Figure 4. 13. Mean peak power in the *in vitro* intact and microslice preparation. There were no significant differences in MI LV between intact and microslices. MI LIII from intact slices: n=24, MI LIII from microslices: n=5, MI LV from intact slices: n=36, MI LV from microslices: n=14. Error bars represent SEMs.

4.3.2.2. MI frequency distribution and variability and laminar connectivity

The mean FWHM in MI LIII in microslices was 21.40±12.1 Hz. The mean FWHM in MI LIII intact slices was 13.13±5.72 Hz. The mean FWHM in MI LV in microslices was 13.43±5.71 Hz. In MI LV the mean FWHM in the intact slices was 12.13±4.09 Hz. There was no significant difference between MI LV oscillatory activity in the micro and intact slices (figure 4.15): $t_{[13]}$= 0.4922, p=0.626.
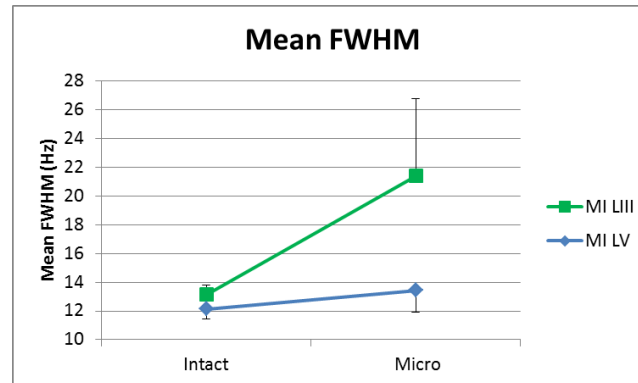
Figure 4. 14. Mean FWHM in the *in vitro* intact and microslice preparations. There were no significant differences in the mean FWHM in MI LV between micro (n=14) and intact slices (n=36) (blue). MI LIII from intact slices: n=24, MI LIII from microslices: n=5. Error bars represent SEMs.

The sample count at the peak frequency in MI LIII in microslices was 5.19±4.97 %. The percentage of samples found at the beta peak frequency in MI LIII in intact slices was 7.39±6.77 %. The sample count at the peak in MI LV in microslices was 10.42±5.72 %. The percentage of samples found at the beta peak frequency in MI LV in intact slices was 13.33±8.50 %. There was no significant difference in frequency variability in MI LV between intact and microslices: $t_{[13]}$= -0.6403, p=0.5331 (figure 4.16).
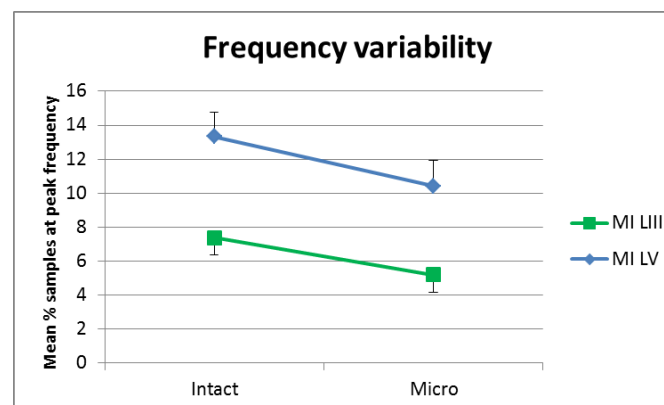
Figure 4. 15. Mean peak frequency variability in MI LIII and MI LV in the *in vitro* intact and microslice preparations. There were no significant differences in mean peak frequency variability in MI LV between micro (n=14) and intact slices (n=36). MI LIII from intact slices: n=24, MI LIII from microslices: n=5. Error bars represent SEMs.

4.3.2.3. MI oscillatory power state and laminar connectivity

To determine if there were any particular characteristics of the pattern of oscillatory activity with regards to power in microslices, we investigated the oscillatory state and state mean power in MI LIII and MI LV. We also made statistically comparisions for MI LV between micro and intact slices.

In MI LIII in microslices the mean percentage of samples found in the upstate was 38.58 %. The mean upstate power for MI LIII in microslices was 17.67 $\times10^{-11}$ V^2, compared to the mean downstate power which was 7.16 $\times10^{-11}$ V^2. In MI LIII in intact slices, the percentage of samples found in the upstate was 39.69 %, the mean upstate power was 10.09 $\times10^{-11}V^2$, and the mean downstate power was 3.85 $\times10^{-11}V^2$.

In MI LV in microslices the mean percentage of samples found in the upstate was 38.95 %. The mean upstate power for MI LV was 9.48 $\times10^{-11}$ V^2, compared to the mean downstate power which was 3.19 $\times10^{-11}$ V^2. In MI LV in intact slices, the percentage of samples found in the upstate was 37.89 %, the mean upstate power was 8.79 $\times10^{-11}V^2$ and the mean downstate power was 2.59 $\times10^{-11}V^2$.

There was no significant differences in percentage of samples in the oscillatory upstate in MI LV: $t_{[13]}=0.9728$, p=0.3484 (figure 4.17). There was a significant difference in the MI LV oscillatory mean power in the upstate between the two types of slices, $t_{[13]}=-2.7846$, p=0.0155. The difference in the oscillatory mean power in the downstate was also significant, $t_{[13]}=-2.9817$, p=0.0106 (figure 4.18).
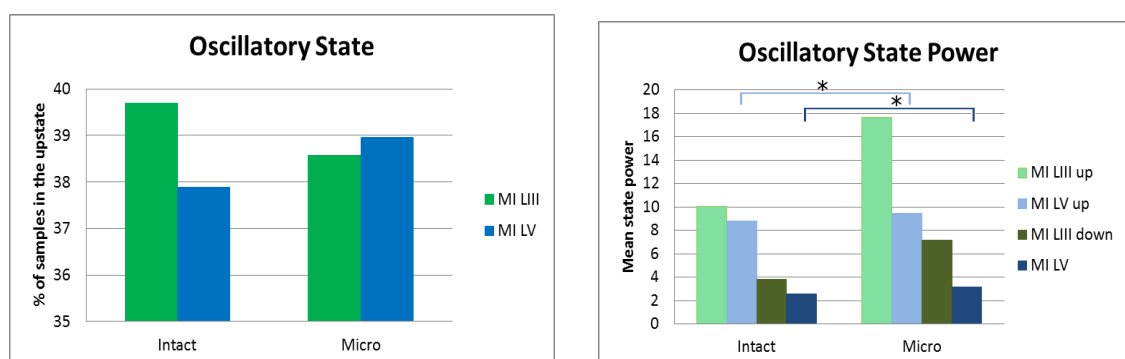
Figure 4. 16a-b. Figure a shows group-averages of the percentage of samples in the oscillatory upstate in MI LIII (green) and MI LV (blue) in the *in vitro* intact and microslice preparations. There were no significant differences between MI LV in the two preparations. Figure b shows group-averages of the mean power in the oscillatory up- and downstates in intact and microslice MI LIII and MI LV recordings. There were significant differences in mean state power in MI LV between intact and microslices, p<0.05, marked with *. MI LIII from intact slices: n=24, MI LIII from microslices: n=5, MI LV from intact slices: n=36, MI LV from microslices: n=14.

4.4. Discussion

4.4.1. Summary

The effect of connectivity between MI and SI, as well as the effects of the intra-laminar MI connections, on the ongoing oscillations observed in the sensorimotor cortex *in vitro* were investigated in these experiments. There is an effect on the oscillatory activity in MI and SI of MI-SI connectivity. The incision experiments resulted in a significant decrease in peak frequency distribution in SI LIV after incision. The oscillatory activity observed in microslices was compared to intact slices to determine the intra-laminar relevance on MI oscillations. There were significant differences between MI LV in microslices and intact slices in mean peak frequency and oscillatory mean power in the up- and downstate.

4.4.2. Severing connections between MI and SI decreases the frequency variability in SI

Most sensorimotor research reports do not consider the effects of connectivity between areas as a factor of contribution on oscillatory characteristics. The effect of connectivity have, however, been considered in studies aiming to characterise anatomical and functional connectivity. Recently research reports have integrated the functional connectivity measurements with oscillatory measurements (Stam 2010; Hillebrand *et al.*, 2012; Stam & Straaten 2012). Oscillatory activity in 'microslices' in the sensorimotor have been reported previously (Roopun *et al.*, 2006; Yamawaki *et al.*, 2008). However, we are not aware of any reports that have performed a physical separation between MI from SI, with the aim of characterising the effects on oscillatory activity in the same areas. The incision experiments showed a significant decrease in peak frequency variance in SI LIV after the incision, while no significant changes were seen in MI LV. Regardless of specific oscillatory frequency within the beta band in MI LV this rhythm appears isolated in our slice experiments. A horizontal incision, separating along middle layers within an MI microslice showed no effect on MI LV beta oscillations, but abolished beta oscillatory activity in MI LIII (Yamawaki *et al.*, 2008). In agreement with this, we confirm that the beta rhythm in MI LV is generated by local networks within the deeper layers of MI. Furthermore, we suggest that this rhythm have little dependency on generators, modulators and networks in areas and laminae further away.

Interestingly, physically separating a microslice along middle layers of secondary sensory areas did not abolish beta oscillations in deeper layers either (Roopun *et al.*, 2006),

suggesting local attributes of this rhythm in secondary sensory areas as well. We did not perform a horizontal incision, nor did we use secondary somatosensory areas. However, our results do not completely agree with oscillatory activity in somatosensory areas being local phenomena. Although oscillatory activity in SI LIV in our experiments was not abolished by a vertical incision between MI and SI, we found a significant decrease in the frequency variability. This suggests some aspects of connectivity between MI and SI, indicating that activity in SI LIV is not simply a local phenomenon. A multitude of recent research and reviews have highlighted the information integration and processing relevance of beta and mu oscillations, which in light of these findings become particularly interesting (Brovelli *et al.*, 2004; Bardouille *et al.*, 2010; Haegens *et al.*, 2011; van Ede *et al.*, 2011; Cheyne 2012; Kilavik *et al.*, 2012) as integration and information processing requires connectivity.

In the analysis that was undertaken for this chapter we were only able to extract the data from one slice for MI LIII. However, subsequent stringent filtering and additional analysis allowed us to increase the n-number of MI LIII to 4 and perform preliminary tests of the effects on peak power before and after incision (figure 4.19a-c). This revealed that the mean power in the mu frequency band in MI LIII significantly increased after severing the connections between MI and SI (156%, t=6.84, p=0.006). The small increase in the mean beta power in LV was non-significant (10%, t=1.19, p=0.26). These results confirm connectivity between superficial layers of MI and SI (Shipp 2005; Hook *et al.*, 2011). This result also contradicts the idea of SI as the sole generator of the sensorimotor mu rhythm, further emphasising the novel finding of mu in MI LIII in this project.
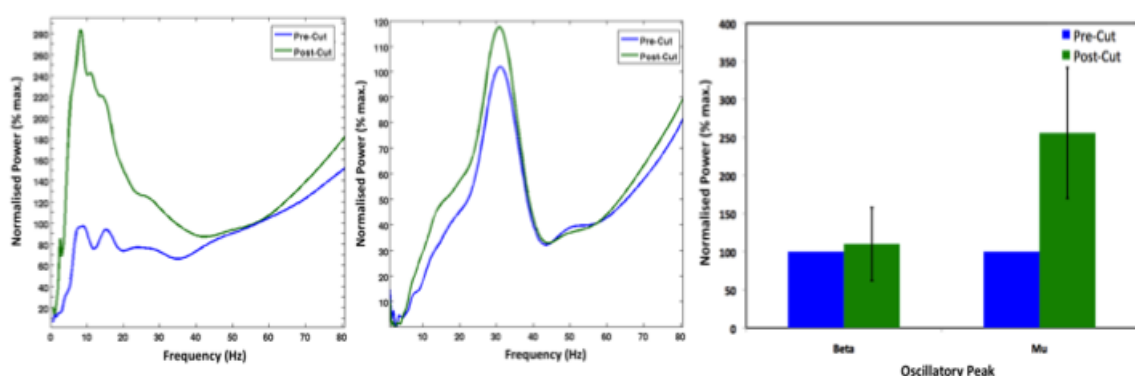
Figure 4. 17a-c. The effects of severing MI-SI connectivity on oscillatory activity in MI LIII, a (left), MI LV, b (middle). The bar graph in c, right, shows the comparison between power before and after cut in the different frequency bands of beta and mu. The increase in mean power in the mu frequency range in MI LIII was significant, p<0.05.

4.4.3. Oscillations in MI are different between micro and intact slices

Although there are suggestions of differences in network activity from changing variables such as slice orientation (Trudel & Bourque 2003), there are no studies focusing directly on the connectivity between MI and SI and therefore it is unclear if there is a difference in sensorimotor oscillatory network activity with regards to MI-SI connectivity. This complex connectivity is reportedly both direct and indirect between MI and SI (Zarzecki *et al.*, 1978; Krubizer & Kaas 1990; Lewis & van Essen 2000; Shipp 2005; 2007; Douglas & Martin 2004; 2007a; 2007b; Thomson & Lamy 2007; Weiler *et al.*, 2008). In this chapter we determined the oscillatory profiles in MI LIII and MI LV in microslices and compared these to intact slices. We observed oscillations in the higher beta frequency region, in agreement with Yamawaki *et al.* (2008), who also used microslices. The higher beta frequency oscillations in MI LV have also been observed in intact slices (Prokic *et al.*, under review), and in chapter 3. Additionally, one of our primary findings from chapter 3, mu and beta range oscillatory activity, was observed in MI LIII in microslices as well. This is in agreement with the prior research evidence pointing to the co-existence of different rhythms in superficial and deeper layers of somatosensory areas (Flint & Connors 1996; Roopun *et al.*, 2006), although there are no specific reports on mu or beta co-existing in MI *in vitro*. This was discussed in detail in chapter 3.

We assessed the effects of intra-laminar connectivity on the ongoing oscillatory activity in MI by comparing the network activity in MI LIII and LV in intact slices to microslices. Although there were no observable differences in the oscillatory profiles for MI LV, the oscillatory activity in MI LV in microslices showed a significantly lower mean peak frequency compared to intact slices, as well as a significantly higher mean power in the oscillatory power states. Several studies over the last decades have suggested that cortical areas have specific intrinsic resonant frequencies (Chagnac-Amitai & Connors 1982; Flint & Connors 1996; Paus *et al.*, 2001; Rosanova *et al.*, 2009; Zaehle *et al.*, 2010; Thut *et al.*, 2011b). The mean peak frequency differences can reflect changed preference for resonance, e.g. differences in network arrangement resulted in alteration of electrophysiological characteristics and constraints, and therefore changed the mean peak frequency of the ongoing oscillations, without significantly changing the distribution of the frequency or mean peak power of the ongoing activity. The neuronal networks responsible for the MI LV oscillations in both intact slices and microslices appear highly localised and less dependent on generators outside of the physical slice size. This theory of local network activity in MI LV in a slice preparation, with little effective connective modulation from other laterally located areas, is further strengthened by the lack of significant effects after incision.

4.5. Conclusions

We conclude that there are effects on the ongoing sensorimotor oscillations of MI-SI connectivity. There is a significant difference in mean peak frequency between the ongoing beta oscillations in MI LV in an isolated microslice compared to those in an intact slice. It is unclear to what degree the differences are due to limitation of the laminar connections. The neuronal network activity in MI LV in both types of slice preparations is localised and show little dependency on generators/modulators outside the direct proximity of the recording sphere. In contrast, the neuronal network activity, specifically the peak frequency distribution of the ongoing oscillations, in SI LIV shows dependence on connectivity to MI at evidenced by the incision experiments. Additionally the mu rhythm, but not the beta rhythm in MI LIII appears modulated by the SI connectivity. This study has aimed at determining aspects of the complex connectivity between MI and SI relevant to the continuous sensorimotor oscillations. We have discussed consequences of severing this connectivity, with regards to the ongoing neuronal network activity in MI and SI laminae.

Chapter 5. Pharmacological modulation of ongoing oscillations in the sensorimotor cortex

5.1 Introduction

We have so far discussed characteristics of spontaneous oscillatory activity in the sensorimotor cortex *in vitro* and in MEG, and respective effects of intra-cortical and cortico-cortical connectivity. We have also shown in previous chapters that ongoing oscillatory activity *in vitro* and in MEG are comparable. In this chapter, we draw upon our understanding of the role of GABAergic interneuron systems, as discussed in chapter 1, and focus on the effects of pharmacological intervention with the GABAergic modulator zolpidem on the established neuronal network characteristic described in chapters 3 and 4.

5.1.1. Background

Beta oscillations in the sensorimotor cortex are GABA-dependent and representative of neuronal network activity. GABAergic modulators, such as benzodiazepines, were initially used to describe the beta oscillatory power increase seen after drug administration as the "beta buzz" (Domino *et al.* 1989; Glaze, 1990). This increase in beta oscillatory power in motor cortex after diazepam administration has been further investigated in the last decade (Baker & Baker 2003; Jensen *et al.*, 2005; Hall *et al.,* 2011). The role of GABA in the sensorimotor cortex has also been approached using magnetic resonance spectroscopy to detect levels of GABA. The link between beta oscillations and GABA concentration in the motor cortex was investigated by Gaetz *et al.* (2011), who showed a linear relation between GABA-concentration and power in the PMBR, in addition to age-dependent differences in GABA-levels.

The imidazopyridine zolpidem, a $GABA_A$-R modulator with unique specificity at the α1 subunit, is a sedative hypnotic (Nicholson & Pascoe 1989). Recent observations have garnered increasing interest in this drug as therapeutic benefits have been demonstrated in disorders such as persistent vegetative state (Clauss *et al.*, 2000), stroke (Hall *et al.*, 2010; Nyakale *et al.*, 2010) and Parkinson's disease (Daniele *et al.*, 1997; Hall *et al.*, in review). The improvement in symptom severity after administration of sub-sedative doses of zolpidem has been suggested to be due to the decrease in of abnormal oscillatory activity. This is particularly evidenced by the reduction of abnormal beta oscillatory activity in a stroke patient with sensorimotor lesions (Hall *et al.*, 2010). Although there is research portraying the effects of benzodiazepines on sensorimotor beta oscillatory activity in healthy subjects, there are, to date, few studies exploring the detailed effects of zolpidem administration on sensorimotor beta oscillations and their characteristics in healthy subjects.

In vitro, the application of 30 and 100 nM zolpidem increases the power, as well as decreased the frequency, of the KA- and CCh-induced beta oscillations found in MI LV (Yamawaki *et al.,* 2008; Prokic *et al.*, 2012). The effects of zolpidem administration on oscillatory characteristics in other laminae of the sensorimotor cortex have not yet been reported. The finding of zolpidem-increased beta power in MI appear paradoxical with the research showing that zolpidem in sub-sedative doses decrease the pathological sensorimotor oscillatory activity seen in stroke patients (Hall *et al.*, 2010). Recent *in vitro* research shows that the desynchronising effects of zolpidem are dose-dependent and occur only at 10 nM zolpidem. The mechanism for this decrease in the power appears to be related to α1 subunit mediated tonic changes in interneuron drive (Prokic *et al.*, 2012).

The underlying cellular mechanisms of modulating beta oscillations are predominantly studied in animal models, supported by work from computer modelling, due to the invasive nature of the research itself. Zolpidem binds to the benzodiazepine binding site, located at the interface of the α- and γ-subunits, on the $GABA_A$-receptors, as confirmed by recent modelling (Sancar *et al.*, 2007; Richter *et al.*, 2012). Both sub-unit types are essential for modulation, but in particular the α1 subunit appears important (Rudolph *et al.*, 1999; Crestani *et al.,* 2000). Modulation with the benzodiazepine diazepam increase in beta power arises primarily from increased IPSCs on interneurons, rather than from IPSCs on pyramidal cells (Baker & Baker 2003; Jensen *et al.*, 2005). In the studies by Baker & Baker (2003) and Jensen *et al.* (2005), modelling provided insights into the rhythmogenesis of sensorimotor beta oscillations, confirming earlier modelling and *in vitro* results in the hippocampus; interneurons are responsible for synchronising the activity of pyramidal cells into local cell population oscillations and as such, GABA receptors and phasic synaptic activity are of particular importance for the oscillations (Cobb *et al.*, 1995; Whittington *et al.*, 1995; Traub *et al.,* 1996a; 1996b; Fisahn *et al.*, 1998; see Somogyi & Klausberger 2005 for a review of interneurons and GABA).

In neurological pathologies, like PD, functional connectivity and network activity is altered. Subsequently synchronisation is perturbed with differences in oscillatory activity (Uhlhaas & Singer 2006; Hammond *et al.*, 2007; Stoffers *et al.*, 2008; Bosboom *et al.*, 2009; Wu *et al.*, 2009; Stam, 2010). Here, to understand the extent to which $GABA_A$-R α1 modulation is comparable between *in vitro* and MEG experiments, we compared the effects of zolpidem in these two approaches in parallel.

5.1.2. Aims and research objectives

Previous studies have investigated the effects of GABAergic modulation on oscillatory dynamics in the sensorimotor cortex, with a focus on either *in vitro* or human approaches. Here we aim to describe the effects of GABA$_A$-receptor α-1 modulation on oscillatory characteristics in the sensorimotor cortex using parallel *in vitro* and MEG experiments. We address the following questions:

- o How do the changes in mean peak power and frequency in MI after zolpidem administration compare between MEG and *in vitro*?
- o How do the changes in distribution and variability of frequency and power in MI after zolpidem administration compare between MEG and *in vitro*?

Previous studies have looked at GABA modulation in MI or SI, but a comparison of the effects on oscillatory characteristics in these areas has not been done. Here we aim to compare the differences in MI and SI in oscillatory responses to GABAergic modulation. We address the questions:

- o How do the changes in mean peak frequency and power in MI compare to the changes seen in SI?
- o How do the changes in distribution and variability of frequency and power in MI compare to the changes seen in SI?

5.2 Methods

5.2.1 MEG

8 participants took part in this experiment (2F), age 29-45 years. The same protocol was run before and 50 min after administration of a sub-sedative oral dose of zolpidem (0.05mg/Kg). Subjects were seated in an upright position in the 275-channel MEG scanner (CTF, Canada). The study was performed in accordance with the Declaration of Helsinki, and approved by the Ethics Committee of the School of Life and Health Sciences at Aston University. Written informed consent was obtained from all participants. The participants received visual instructions from a monitor positioned outside the shielded room, which was visible through a small window, and informing the subjects about when to perform self-paced finger movements and when they should remain seated and rest. The self-paced finger movements were performed with an interval of approximately 5 seconds and for 2-3 minutes. The visual instruction and stimulation events were delivered through the software Presentation (Neurobehavioural Systems Inc., US). Primary motor cortex was localised with a SAM beamformer approach based on the PMBR seen after voluntary finger movements (Jurkiewicz *et al.*, 2006). The PMBR was identified by an increase in the 15-30 Hz frequency band 0.5 to 1.5 seconds following movement offset compared to and -2.0 to -1.0 seconds before movement. EMG electrodes were placed on the FDI muscle to determine the onset and offset of finger movements. Trials containing artefacts were discarded and the data was filtered to 1-200 Hz, with additional notch filters at 50 and 60 Hz. Virtual electrode data from MI loci, during 30 second rest periods, were processed in MatLab (The Mathworks, Inc.) as Morelet-wavelet spectrograms. These data were then analysed using the same process as used for *in vitro* analysis, described below.

5.2.2 *In vitro*

This study used protocol 1 for preparation of sensorimotor brain slices, similar to the study of spontaneous oscillations in chapters 3 and 4, also described in chapter 2. Briefly, brain slices were prepared from p18-p22 (50-60g) male Wistar rats. 450 μm thick sagittal slices were stored in a tissue interface chamber in room temperature for 1h. The slices were transferred to a recording chamber, temperature 33°C and continuous flow rate of 2 ml/min aCSF with added KA and CCh (protocol 1). LFP recordings from MI and SI laminae were made; in intact slices: MI LIII: n=10, MI LV: n=17. In microslices: MI LIII: n=2, MI LV: n=9, SI LIV: n=5. The correct areas were identified by using a dissecting microscope and the Rat Brain Atlas (Paxinos & Watson 1986) as reference. Zolpidem (100 nM) was applied through aCSF perfusion of the bath, during continuous recording

after >45 minutes in the interface recording chamber. Online analysis during recording was done with Spike2. After recording was finished the data was exported to MatLab and periods of 30s immediately before and <60 minutes after zolpidem application, were used to create Morelet-wavelet spectrograms, which were used for further analysed by the custom-made MatLab scripts described below.

5.2.3. Analysis approach

The mean peak frequency and peak power was determined for each sample in the 30s epoch (30000 samples for *in vitro* and 36000 samples for MEG data) with a sliding window approach applied to the Morelet-wavelet spectrograms. The frequency distribution of the oscillations was determined using FWHM. The frequency variability was computed using the amplitude-independent peak frequency distribution, where the peak frequency of each sample was sorted into frequency bins of 1 Hz. Variability in oscillatory power was determined using an amplitude sorting measurement to determine the time and amplitude changes of oscillatory up and down states. We used student's T-tests to statistically test for differences between before and after zolpidem conditions. Further details regarding this analysis approach can be found in chapter 2.

5.3 Results

5.3.1. GABA$_A$-R α1 subunit modulation and MI oscillatory activity

We found an overall increase in ongoing activity in the broad beta and mu range after zolpidem administration, which is summarised in overviews in figure 5.1-4 below. There were no specific effects of zolpidem relating to any particular frequency range in the ongoing oscillatory activity in MI in MEG or *in vitro*.
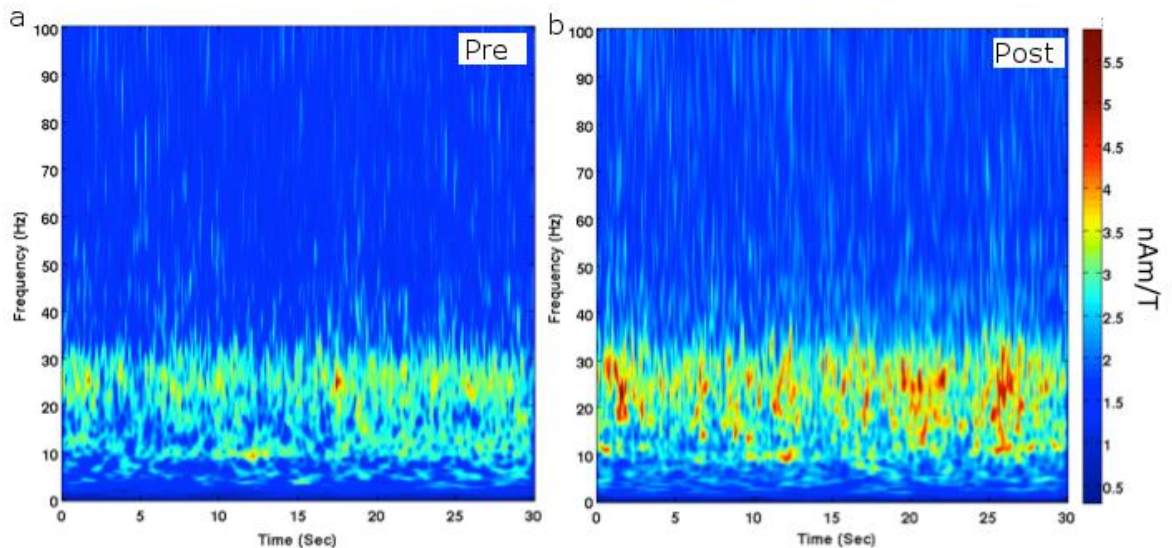
Figure 5. 1a-b. Group-average Morelet-wavelet spectrograms showing human MI (n=8) oscillatory activity before, a (left), and after, b (right) zolpidem administration.
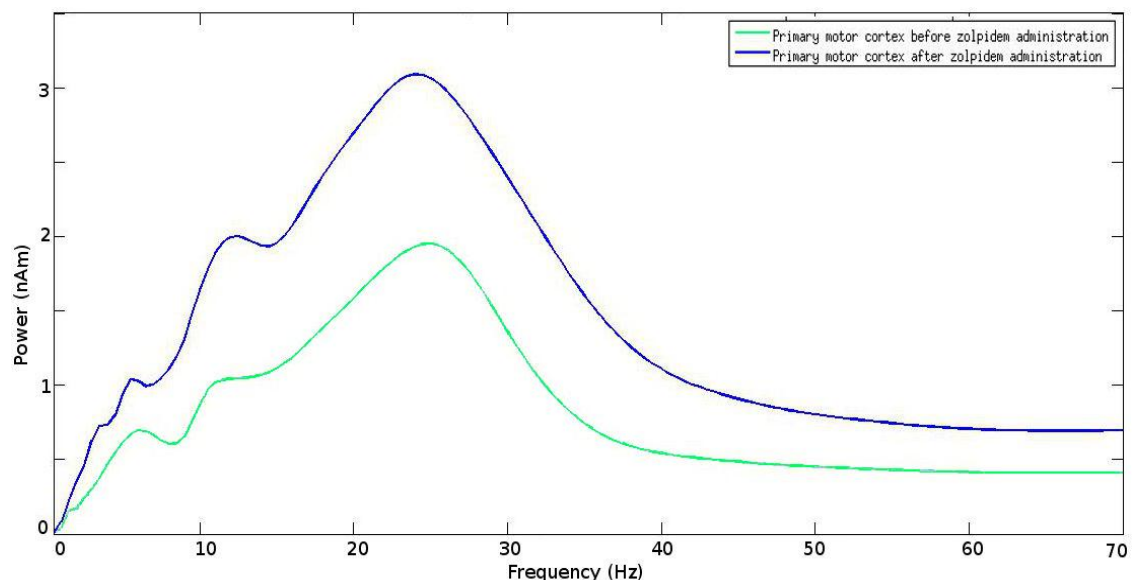
Figure 5. 2. Group- and time-averaged PDS of the ongoing oscillatory activity in MI in humans (n=8) before (green) and after (blue) zolpidem administration. The power increases after zolpidem administration, also shown in figure 5.6a.
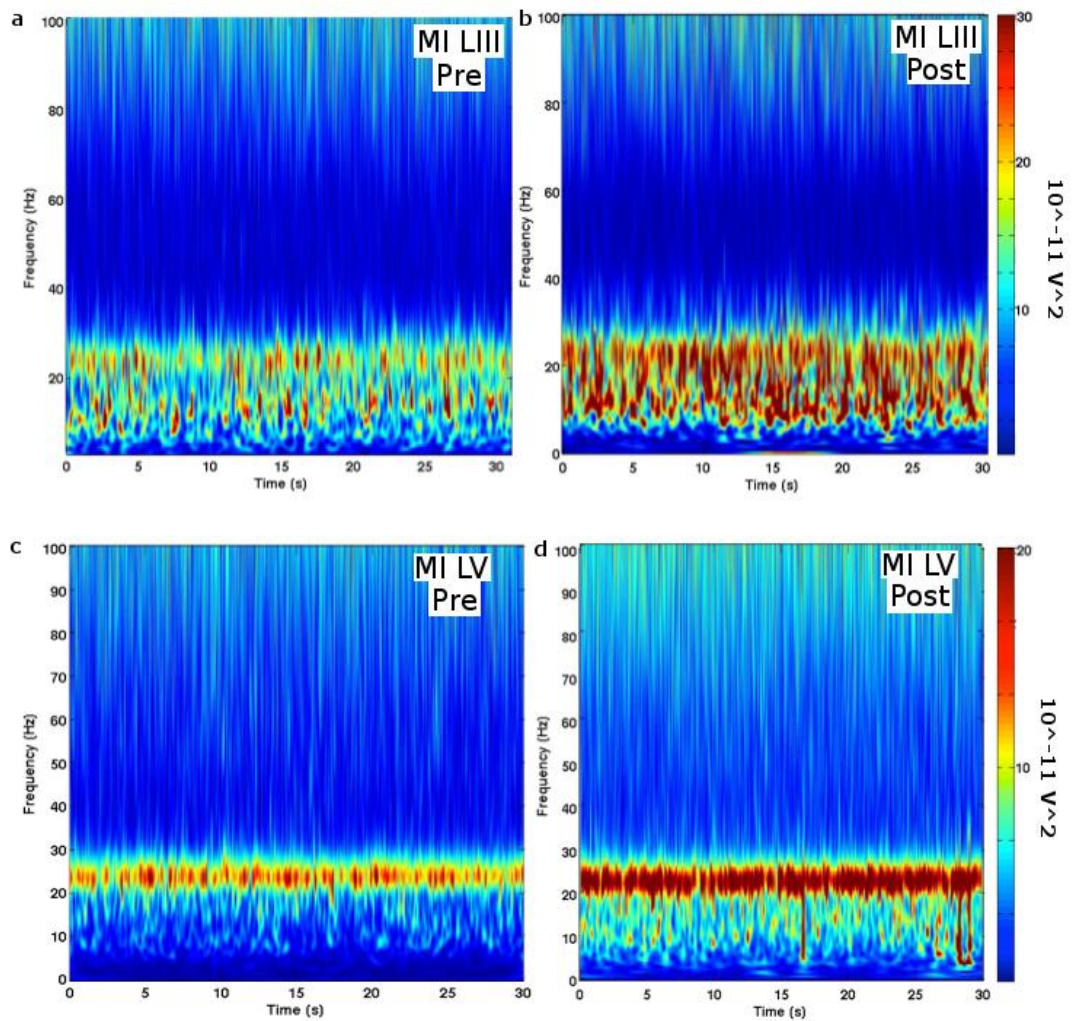
Figure 5. 3a-b. Group-average Morelet-wavelet spectrograms showing oscillatory activity in MI LIII (n=10) and MI LV (n=17) before, a (left), and after, b (right) zolpidem administration, *in vitro*.
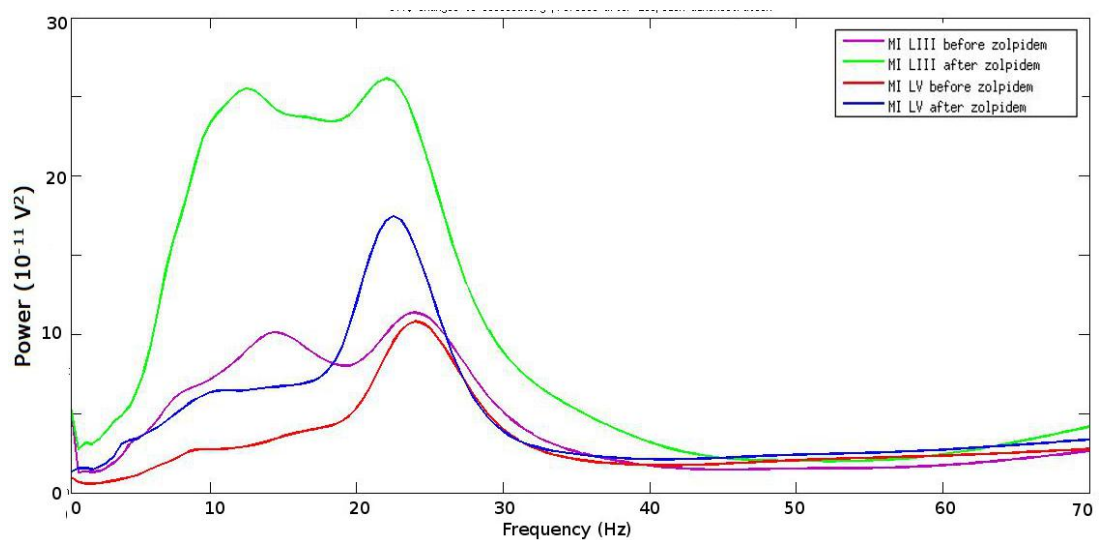
Figure 5. 4. Group- and time-averaged PSD showing oscillatory activity in MI LIII (n=10, purple and green) and MI LV (n=17, red and blue) *in vitro* before and after zolpidem application. The power increases, as seen in figure 5.6b.

5.3.1.1. Frequency and power

In MEG, the mean peak frequency in MI was 20.50±6.07 Hz prior to zolpidem administration; and 22.56±6.23 Hz after zolpidem administration (figure 5.5a). This increase in mean peak frequency was not significant: $t_{[7]}$=-0.7584, p=0.473.

In vitro, the mean peak frequency in MI LIII before zolpidem application was 21.30±11.87 compared to 15.2±6.21 Hz after, this decrease was non-significant: $t_{[9]}$=1.5018, p=0.1674. In MI LV the mean peak frequency decreased significantly from 23.97±8.85 to 19.79±5.98 Hz: $t_{[16]}$=2.3475, p=0.0321 (figure 5.5b).
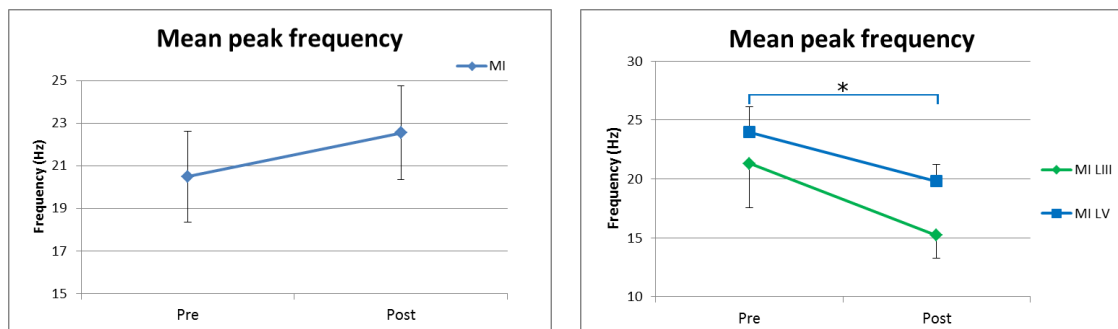
Figure 5. 5a-b. Mean peak frequency in MI (n=8) in MEG recordings, a (left), and *in vitro*, b (right) before and after zolpidem administration (Pre and Post, respectively). The mean peak frequency in MI LV (n=17, blue) decreased significantly following zolpidem application, p<0.05, marked with *. MI LIII (n=10, green) showed no significant difference. Error bars are SEMs.

In the MEG recordings, zolpidem significantly increased the mean peak power in ongoing beta oscillatory activity recorded from MI; 2.48±1.30 nAm compared to 3.66±1.25 nAm, $t_{[7]}$=-3.4975, p=0.01 (figure 5.6a).

In vitro in MI LIII the mean peak power increased significantly from 14.64±13.17, to 33.44±33.82 x10^{-11} V^2, $t_{[9]}$=-2.7837, p=0.0213. In MI LV the mean peak power increased significantly from 12.06±18.34 to 19.16±28.67 x10^{-11} V^2, $t_{[16]}$=-2.3248, p=0.0336 (figure 5.6b).
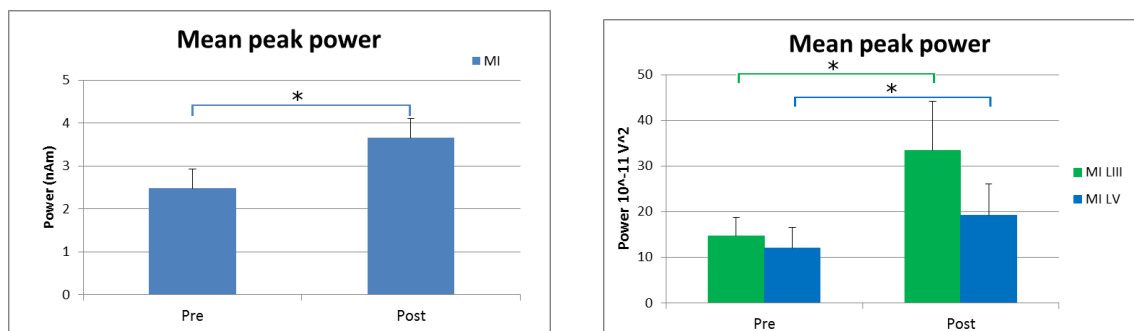
Figure 5. 6a-b. Mean peak power in MI (n=8) in MEG recordings seen in a (left), and *in vitro* MI, seen in b, (right), before and after zolpidem administration (Pre and Post, respectively). The increase in power after zolpidem administration was significant in all locations, p<0.05, marked with *. MI LIII: n=10 (green); MI LIV: n=17 (blue). The error bars represent SEMs.

5.3.1.2. Frequency distribution and variability

There were no significant changes to the mean FWHM in MEG or *in vitro*. In MI from the MEG recordings the mean FWHM was 14.69±6.68 Hz before, and 18.94±7.18 Hz after zolpidem administration (figure 5.7a), $t_{[7]}$=-2.2517, p=0.059. *In vitro,* the mean FWHM in MI LIII was 14.20±10.89 Hz before, and 10.90±5.16 Hz after zolpidem administration, $t_{[9]}$=1.2031, p=0.9657. The mean FWHM in MI LV was 16.59±9.98 Hz before, and 14.56±8.50 Hz after zolpidem administration (figure 5.7b), $t_{[16]}$=0.2596, p=0.3486.
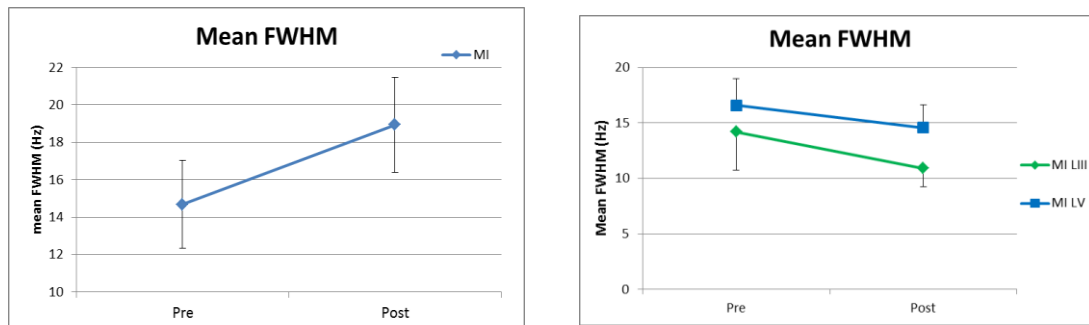
Figure 5. 7a-b. Mean FWHM before and after zolpidem administration showed no significant changes, in human MI (n=8), a (left), or MI *in vitro*, b (right), MI LIII: n=10 (green); MI LV: n=17 (blue). SEMs are represented as error bars.

There were no significant changes to the frequency variability in the MEG and *in vitro* experiments. In MI from the MEG recordings the mean percentage of samples found at the peak frequency was 9.31±4.94 % before and 5.81±1.61 % after zolpidem administration (figure 5.8a), $t_{[7]}$=1.7532, p=0.123.

In vitro, in MI LIII the percentage of samples at the peak frequency was 9.20±9.35 % before and 10.90±5.16 % after zolpidem administration, $t_{[9]}$=1.2861, p=0.2305. In MI LV the percentage of samples at the peak frequency was 16.59±9.98 % before and 14.56±8.50 % after zolpidem administration (figure 5.8b), $t_{[16]}$=0.8454, p=0.4103
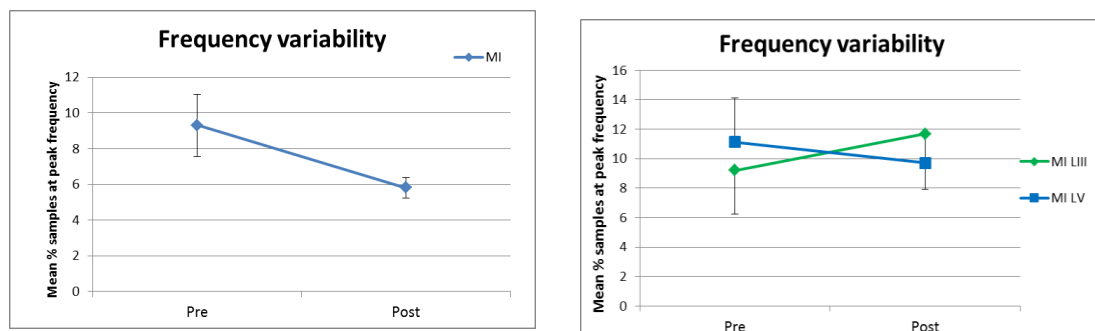
Figure 5. 8a-b. Mean percentage of samples at the peak frequencies did not change significantly after zolpidem administration in human MI (n=8) (a, left) or MI *in vitro* (b, right), MI LIII: n=10 (green); MI LV: n=17 (blue). SEMs are indicated with errorbars.

5.3.1.3. Oscillatory power state

In MEG, the percentage of samples found in the oscillatory upstate was 35.91 % before and 33.98 % after zolpidem administration (figure 5.9), this was non-significant: $t_{[7]}$=1.2848, p=0.2398. The mean power in the upstate increased significantly from 1.3 to 3.41 nAM, $t_{[7]}$=-2.7545, p=0.0283. Similarly, the mean power in the downstate increased significantly from 0.439 to 0.882 nAm, $t_{[7]}$=-2.4407, p=0.0447.
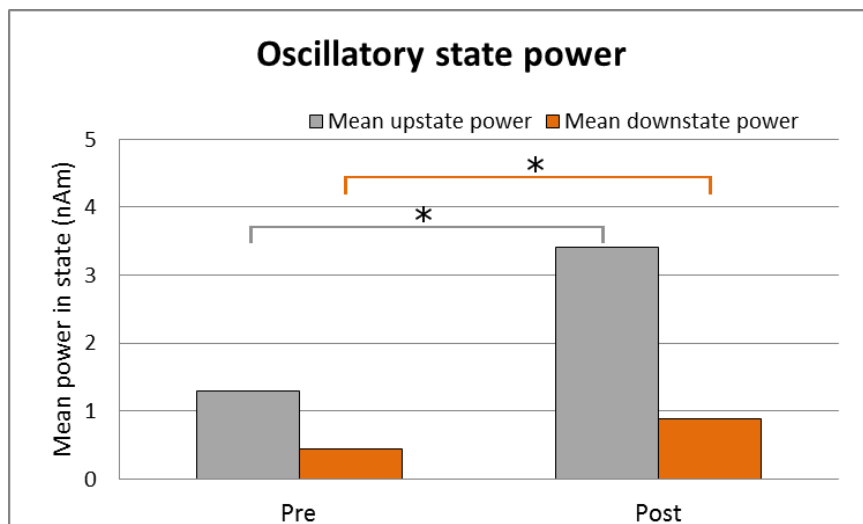
Figure 5. 9. Group-averages of oscillatory up- and downstate mean power in human MI (n=8), before and after zolpidem administration. The mean power in both the upstate (grey) and the downstate (orange) increased significantly, p<0.05, respectively. Dark blue represents mean power in the oscillatory upstate, light blue represents mean power in the oscillatory downstates.

In MI LIII the percentage of samples found in the oscillatory upstate was 38.81 % before and 39.87 % after zolpidem administration. This was not significant, $t_{[9]}$=-1.4776, p=0.1736. The mean upstate power in MI LIII was 10.07 x10^{-11} V^2 before and 19.69 x10^{-11} V^2 after zolpidem application. This was not significant, $t_{[9]}$=-2.131, p=0.0619. The mean downstate power in MI LIII was 3.78 x10^{-11} V^2 before and 7.21 x10^{-11} V^2 after zolpidem application. This was not significant, $t_{[9]}$=-2.0501, p=0.0706.

In MI LV the percentage of samples found in the oscillatory upstate was 38.66 % before and 38.46 % after zolpidem application. This was not significant, $t_{[9]}$=0.1726, p=0.8651. The mean upstate power in MI LV was 4.23 x10^{-11} V^2 before and 9.83 x10^{-11} V^2 after zolpidem application. This was not significant, $t_{[9]}$=-1.6782, p=0.1127.The mean downstate power in MI LV was 9.83 x10^{-11} V^2 before and 3.029 x10^{-11} V^2 after zolpidem application (figure 5.10). This was not significant, $t_{[9]}$=-2.054, p=0.0567.
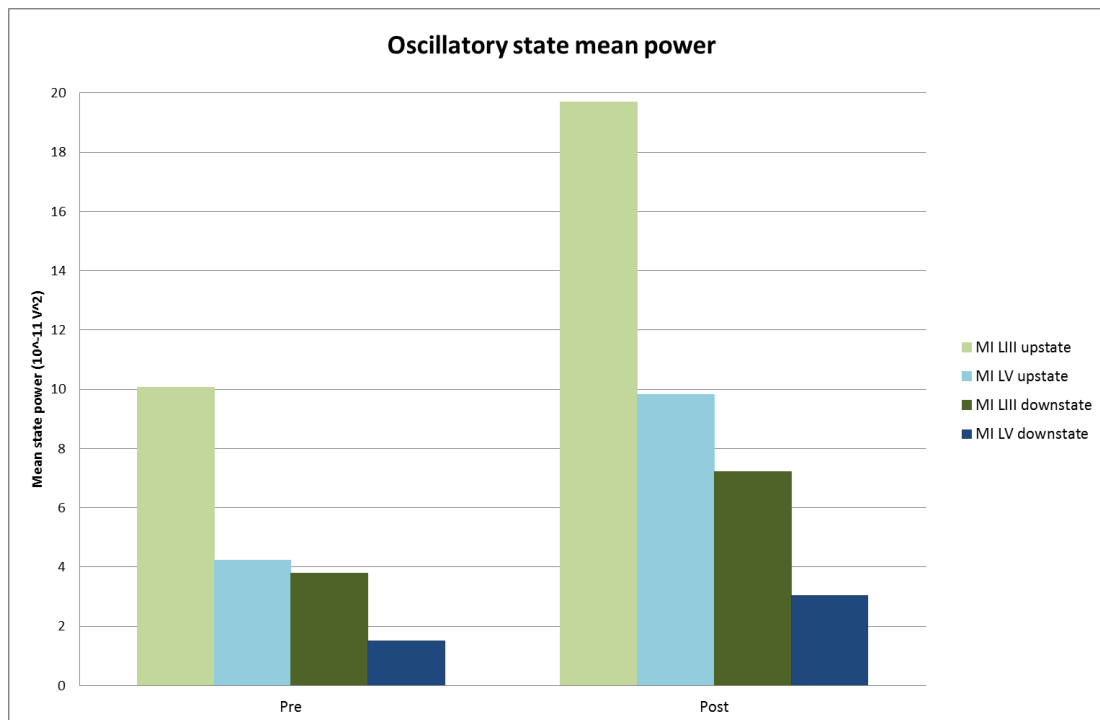
Figure 5. 10. Group-averages of oscillatory up- and downstate mean power in MI LIII (n=10, greens) and MI LV (n=17, blues) *in vitro* before and after zolpidem application *in vitro*. There were no significant changes.

5.3.2. Differential effects of zolpidem in MI and SI

In an attempt to compare the specific effects of $GABA_A$-R modulation of oscillatory activity in MI to SI we undertook LFP recordings in microslices of MI and SI. Figure 5.11 shows an overview.
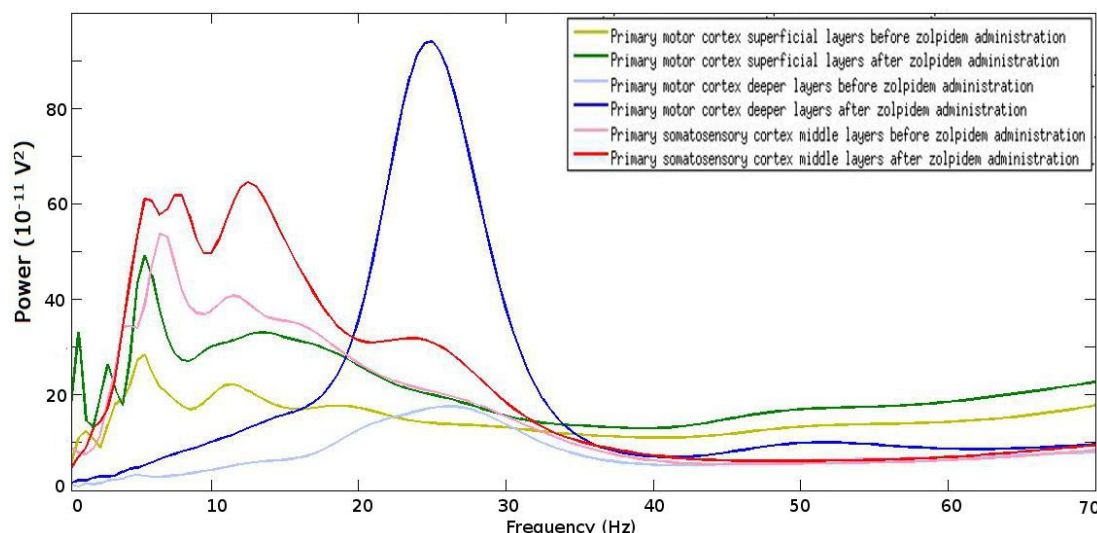
Figure 5. 11. Group- and time-averaged PSD of the oscillatory activity in different laminae in microslices of MI and SI before and after zolpidem application. MI LIII: n=2 (greens), MI LV: n=9 (blues), SI LIV: n=5 (reds).

5.3.2.1. Frequency and power

Mean peak frequency in MI LIII before zolpidem application was 14.5±4.24 Hz, and after 19.25±8.84 Hz. This was not significant, $t_{[1]}$=-1.4615, p=0.382. Mean peak frequency in MI LV before zolpidem application was 25.17±3.90 Hz, and after 23.78±3.25 Hz. This was not significant, $t_{[8]}$=1.2829, p=0.2354. Mean peak frequency in SI LIV before zolpidem application was 28±20.12 Hz, and after 16.25±8.84 Hz (figure 5.12). This was not significant, $t_{[4]}$=1.8106, p=0.1445.
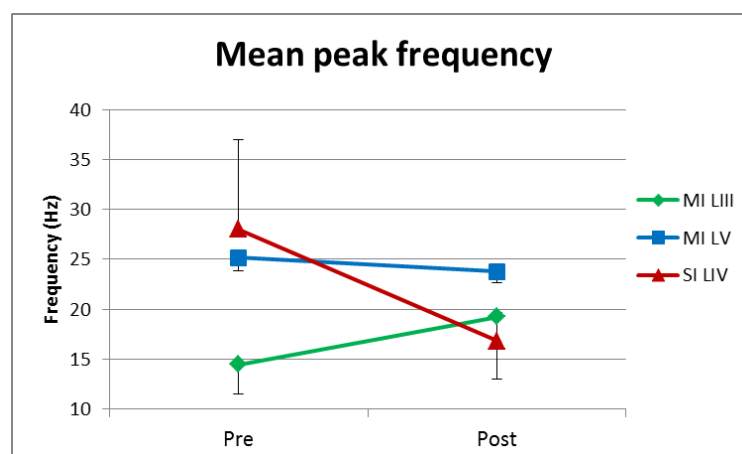
Figure 5. 12. Mean peak frequency before (Pre) and after (Post) zolpidem application in MI LIII (n=2, green), MI LV (n=9, blue) and SI LIV (n=5, red) in the microslice *in vitro* preparation. SEMs are represented as error bars. There were no significant changes.

Mean peak amplitude in MI LIII before was 22.77±27.44 x10^{-11} V^2, and after 33.42±39.02 x10^{-11} V^2. This was not significant, $t_{[1]}$=-1.2009, p=0.4172.Mean peak amplitude in MI LV before was 22.34±28.98 x10^{-11} V^2, and after 100.035±121.694 x10^{-11} V^2. This was not significant, $t_{[8]}$=-2.0101, p=0.0793. In SI LIV the mean peak amplitude was 41.73±77.40 x10^{-11} V^2 before and 68.42±118.88 x10^{-11} V^2 after zolpidem application (figure 5.13). This was not significant, $t_{[4]}$=-1.3888, p=0.2372.
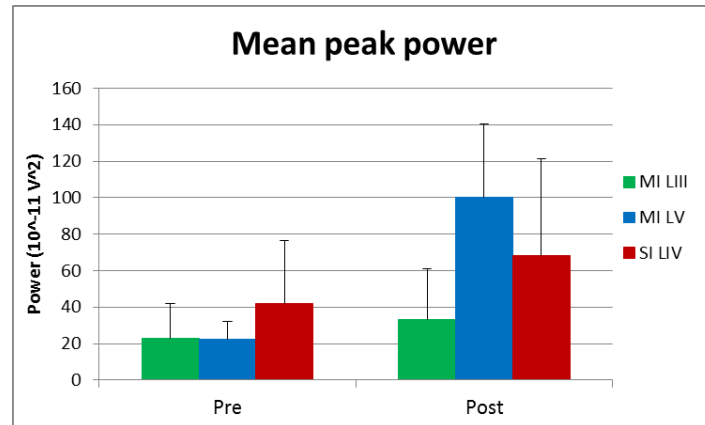
Figure 5. 13. Mean peak power before and after zolpidem application in the microslice *in vitro* preparation. MI LIII: n=2 (green), MI LV: n=9 (blue), SI LIV: n=5 (red). SEMs are represented by error bars. There were no significant changes.

5.3.2.2. Frequency distribution and variability

In MI LIII the mean FWHM was 19.50±7.78 Hz before and 16.25±6.72 Hz after zolpidem application. This was not significant, $t_{[1]}$=4.3333, p=0.1444. In MI LV the mean FWHM was 13.78±5.67 Hz before and 10.56±4.49 Hz after. This was not significant, $t_{[8]}$=1.6138, p=0.1452. In SI LIV the mean FWHM was 28.20±13.88 Hz before and 13.9±5.86 Hz after zolpidem application (figure 5.14). This was not significant, $t_{[4]}$=2.7349, p=0.0522.
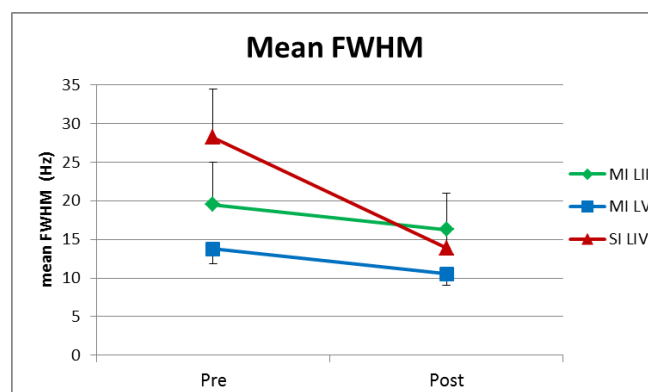
Figure 5. 14. Mean FWHM before and after zolpidem application in MI LIII (n=2, green), MI LV (n=9, blue) and SI LIV (n=5, red) in the *in vitro* microslice preparation. SEMs are plotted as error bars. There were no significant changes.

The peak frequency distribution in MI LV significantly increased after zolpidem application from 8.85±4.25 to 16.92±10.04 %, $t_{[8]}$=-2.4757, p=0.0384, see figure 5.15, and 5.16a-d. In MI LIII the percentage of samples found at the peak frequency was 3.69±0.8469 % before and 3.59±1.4079 % after. In SI LIV the percentage was 2.58±2.43 before and 7.60±5.72 after zolpidem application. There were no significant effects on frequency distribution in MI LIII and SI LIV, $t_{[1]}$=0.0662, p=0.9579 and $t_{[4]}$=-1.7334, p=0.1581, respectively.
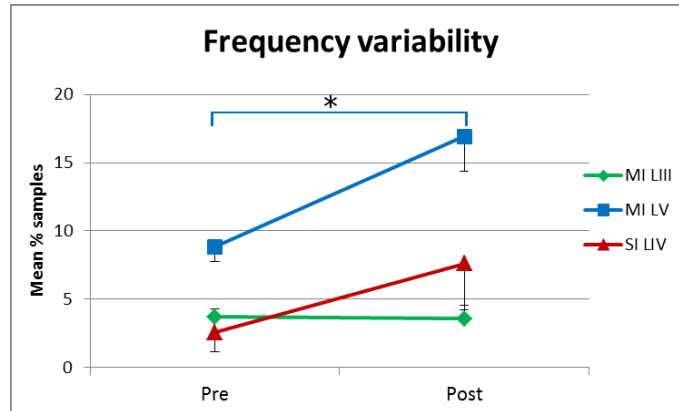
Figure 5. 15. Mean peak frequency distribution before and after zolpidem application in microslices *in vitro*. The mean % of samples at the peak frequency significantly increased in MI LV (n=9, blue), p<0.05, marked with *. MI LIII (n=2, green), SI LIV (n=5, red). SEMs are plotted as error bars.
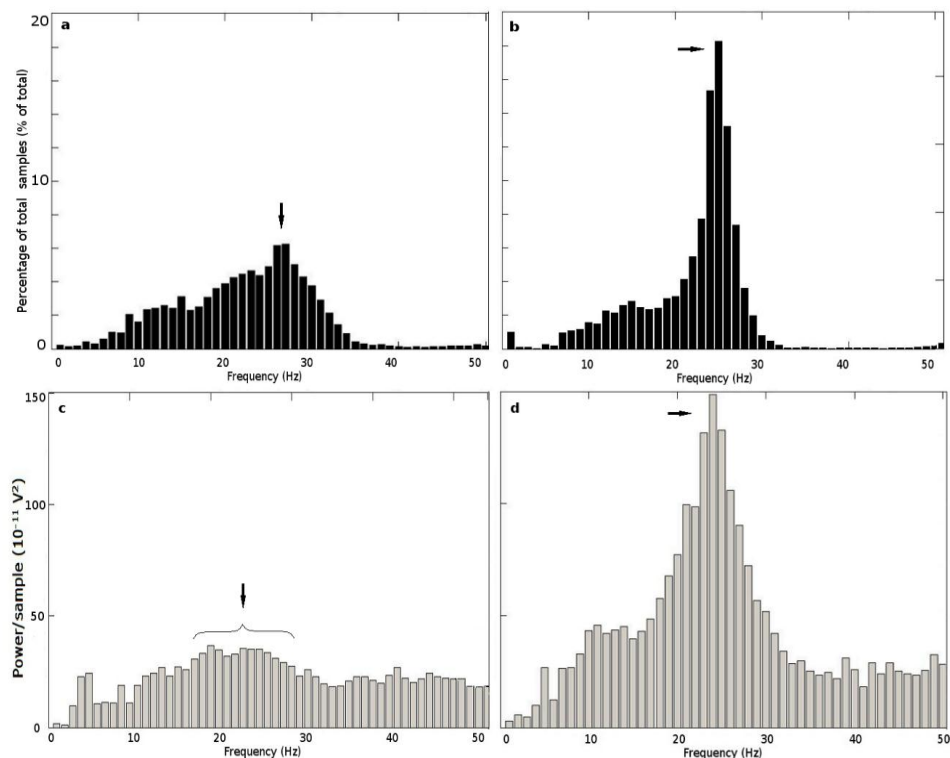
Figure 5. 16a-d. Group-averaged peak frequency, and normalised power to sample, distributions before, (a & c, left) and after (b & d, right) zolpidem application in MI LV (n=9) in microslices *in vitro*. There is a strong increase in number of samples at the peak frequency, as indicated by the black arrows. The change in variance in MI LV was statistically significant, p<0.05.

5.3.2.3. Oscillatory power state

We found significant increases in the mean upstate power in MI LV from 8.69 to 20.34 $x10^{-11}$ V^2, $t_{[8]}$=-3.4147, p=0.0092, and in the mean downstate power also increased significantly from 2.99 to 7.09, $x10^{-11}$ V^2, $t_{[8]}$=-3.2523, p=0.0117. The upstate percentage in MI LV before zolpidem application was 39.36 % and after 38.87 %. This was not significant, $t_{[8]}$=0.8854, p=0.4018. In MI LIII the percentage found in the upstate was 40.07 % before and 41.23 % after. The mean upstate power was 29.10 $x10^{-11}$ V^2 before and 45.98 $x10^{-11}$ V^2. The mean downstate power was $12.39x10^{-11}$ V^2 before and $21.51x10^{-11}$ V^2. These changes were not significant: $t_{[1]}$=-1.3211, p=0.4125; $t_{[1]}$=-1.164, p=0.4519; $t_{[1]}$=-1.1997, p=0.4424, respectively. In SI LIV the percentage found in the upstate was 38.82 % before and 38.61 % after. The mean upstate power was 52.35 $x10^{-11}$ V^2 before and 81.61 $x10^{-11}$ V^2. The mean downstate power was $23.81x10^{-11}$ V^2 before and $30.24x10^{-11}$ V^2 (figure 5.17). These changes were not significant: $t_{[4]}$=0.1201, p=0.9102; $t_{[4]}$=-1.991, p=0.2967; $t_{[4]}$=-1.1951, p=0.2981, respectively.
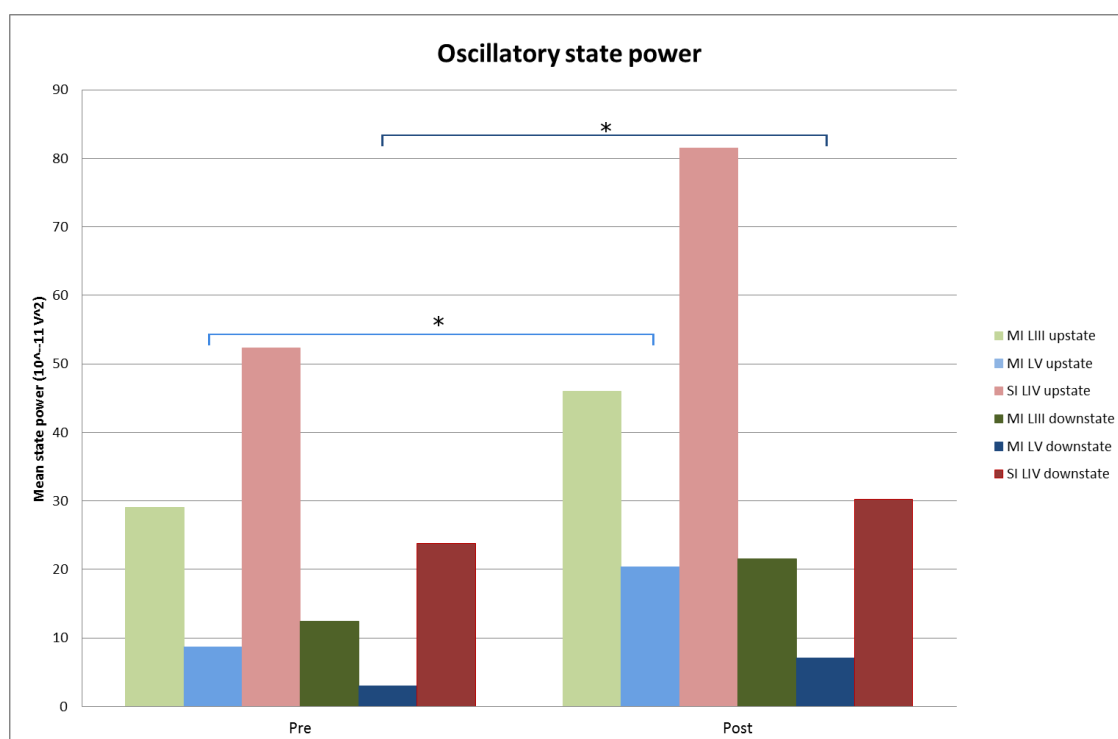
Figure 5. 17. Group-averages of oscillatory state mean power in MI LIII (n=2, greens), MI LV (n=9, blues) and SI LIV (n=5, reds) in the *in vitro* microslice preparation before (Pre) and after (Post) zolpidem application The increases in up- and downstates mean power in MI LV are significant, p<0.01 and p<0.05, respectively, marked with *. (Power is displayed as $x10^{-11}$ V^2).

5.4 Discussion

5.4.1. Summary

We have studied the effects on oscillatory activity in human MI of sub-sedative doses of zolpidem, which significantly increased the mean peak power in MI. Application of zolpidem *in vitro* significantly increased the mean peak power of ongoing beta oscillations in all recorded MI laminae in intact slices. Additionally the frequency in MI LV decreased significantly. Differentiating effects of zolpidem on ongoing activity between MI and SI in microslices showed that, while there were no significant effects on mean peak frequency or power, the peak frequency distribution in MI LV was significantly increased. Moreover, the power in the oscillatory states in MI LV increased significantly.

5.4.2. GABAergic modulation of MI activity *in vitro* compared to MEG

In vitro and *in silico* studies generally report a decrease in peak frequency in the motor cortex after increasing the GABAergic drive and synchronisation, with the characteristic oscillatory power increase (Jensen *et al.*, 2005; Yamawaki *et al.*, 2008; Prokic *et al.*, 2012). In neuroimaging reports, effects on oscillatory frequency from benzodiazepine, and alike, substances, have been reported with more inconsistency (Baker & Baker 2003; Jensen *et al.*, 2005). This is most likely due to differences in the undertaken analysis approaches. We found a significant decrease in the mean peak frequency of the ongoing oscillatory activity in MI LV, but not in any other areas of recording, nor in the human MI. We speculate that this is due to the narrow natural frequency preference that appear characteristic of MI LV oscillatory activity, which this and other studies have reported on (Yamawaki *et al.*, 2008; Prokic *et al.*, under review). Previous research in this project has suggested that the oscillatory activity seen in MI LIII and SI LIV, as well as human MI, arise from more than one oscillator in the underlying neuronal substrate, as determined by the use of distribution and variability analysis. In contrast, the oscillatory network activity distribution in MI LV is centred round the mean peak frequency, instead suggesting that this activity arise from one oscillator. The effects on oscillatory peak frequency from GABAergic modulation on a neuronal network would be less clear if there was modulation of several oscillators of varying frequencies as these amalgamate into one averaged population signal. In MI LV the ongoing oscillatory peak is sharp with a symmetrical and unimodal distribution, thus any GABAergic modulation of the ongoing peak frequency is likely to be seen as a clear shift in peak frequency. Furthermore, the previous chapters have emphasised the difference between MEG and LFP oscillatory signals with regards to number of neuronal networks and source size and frequency. The theories discussed

above, with regards to participating neuronal networks and oscillatory frequencies in the different laminae can be anecdotally scaled up to suit the aggregate MEG signal. We have been unable to locate any other research along these lines, so supporting or refuting these theories is currently difficult. More research on this, as well as the underlying mechanisms of the ongoing activity beta and mu seen in MI LIII and SI LIV, is required to elucidate and substantiate these claims.

In the MEG recordings of oscillatory activity in MI, administration of sub-sedative doses of zolpidem in healthy subjects significantly increased the overall mean beta peak power and oscillatory state power of the recorded oscillatory activity. This is in agreement with previous studies of the effects of benzodiazepine administration in healthy subjects, showing an increase of mean beta power (Domino *et al.* 1989; Glaze, 1990; Baker & Baker 2003; Jensen *et al.*, 2005; Hall *et al.,* 2009; 2010; 2011). The link with increased GABAergic modulation and increased mean beta power in MI recorded with MEG was reported by Gaetz *et al.* (2011). Our findings also agree with previous *in vitro* reports on the increase of beta power after zolpidem and benzodiazepine administration in MI LV (Yamawaki *et al.*, 2008, Prokic *et al.*, under review). In addition, we found that zolpidem significantly increased the mean peak power of the ongoing activity in MI LIII previously not reported. However, there was a non-significant increase in oscillatory state power in *in vitro*; where the non-significance was suspected to be due to low n-numbers. The modulation of the oscillatory mean peak power by zolpidem application suggests similar mechanisms to the oscillatory activity previously reported in MI LV, although the exact mechanisms cannot be determined from these recordings as this would require further pharmacological manipulation *in vitro*. Oscillatory activity has been found to depend on GABAergic interneurons, predominantly FS interneurons (Cobb *et al.*, 1995, Hasenstaub *et al.*, 2005). Effects of benzodiazepines and substances acting on the benzodiazepine site in the $GABA_A$-receptor increase the chloride channel opening time and frequency respectively. These substances affected the features of beta oscillation through increasing the IPSCs in interneurons (Jensen *et al.*, 2005), and in effect by modulating phasic $GABA_A$-R specific inhibition (Yamawaki *et al.*, 2008). It is likely that the GABAergic modulator zolpidem would modulate the overall beta oscillatory activity in all areas we have recorded from. We speculate that it is down to the neuronal network or natural resonance frequency to determine the level of reinforcement and thereby the oscillatory peak power, as the mu amplitude is not significantly changed by zolpidem (data not shown). Previous experiments in this project, discussed in chapter 4, have suggested that oscillatory power is higher in more local networks, although we have not been able to find any other research to substantiate this.

Administration of sub-sedative doses zolpidem to patients with stroke with a sensorimotor lesion reduces the power of the abnormal pathological beta oscillations (Hall *et al.*, 2010). In addition, the 'beta-buzz' in healthy subjects is well-established in the EEG literature as an increase in oscillatory beta power following administration with GABAergic drugs, such as benzodiazepines. *In vitro* experiments have found that the oscillatory beta power in layer V of MI increases after zolpidem application (100nM). Recent research has argued that the effects of zolpidem are dose-dependent and that a lower dose (10 nM) decreases the oscillatory power; this dose was suggested to be more similar to the sub-sedative dose administered to human participants and patients (Prokic *et al.,* 2012). However, the results from this chapter indicate that the oscillatory beta power significantly *increases in healthy subjects* after administration of sub-sedative doses of zolpidem, similar to application of 30 and 100 nM zolpidem in the *in vitro* preparations.

5.4.3. GABAergic modulation of MI activity compared to SI activity *in vitro*

We wanted to determine the specific effects of GABAergic modulation with zolpidem on the oscillatory activity in MI compared to SI in microslices. Although the trends seen in the intact slices were replicated in the microslices, with regards to mean peak frequency and power, we found no significant decrease in mean peak frequency. The effects of GABAergic modulation on the neuronal network activity in MI LV appear different in physically separated MI and SI, compared to intact slices. This was illustrated by the significant increase in peak frequency variability seen after zolpidem administration in MI LV in microslices. This was not seen to the same degree in MI LV in the intact slices. It is difficult to determine whether these differences in effects from GABAergic modulation are down to the intrinsic neuronal network differences between intact and microslices, protocol differences, or simply a combination of factors. We hypothesise that connectivity between MI and SI is an important factor. Further experiments and analysis is required to disentangle this. In addition, the concept of measuring frequency variability is very recent (Little *et al.*, 2012; Hall *et al.*, under review) and has yet to become fully acknowledged and used.

We found no significant increase of oscillatory mean peak power in either location. This is surprising as the experiments by Yamawaki *et al.* (2008) were performed on microslices. Our statistically negative results could be due to low experimental number and subsequent low statistical power. Alternatively, as data from previous *in vitro* studies was band-pass filtered and the peak frequency and power were manually assessed in the before and after conditions in FFT-derived PSD plots; and we used a Morelet-wavelet

sliding window approach with less averaging, the discrepancies in results could be down to differences in analysis approaches. In addition, the increase in mean power in the power states was significant in MI LV in microslices, but not in the intact slices. The full relevance of findings in mean power of oscillatory states is yet to be determined as further investigation of these results is required to understand and relate to the oscillatory patterns seen in neuronal network activity.

5.5. Conclusion

We conclude that the combination of pharmacological manipulation *in vitro* and in MEG has contributed to insight into both the underlying neuronal substrates of oscillatory activity in the sensorimotor cortex. We have shown that MI beta oscillations in healthy humans increase in power after administration of sub-sedative doses of the $GABA_A$-R α1-subunit agonist zolpidem. We have also shown zolpidem application (100nM) increases the beta power of ongoing oscillatory activity in all sensorimotor locations recorded *in vitro.* Furthermore, our results supports the theory of differences in the neuronal networks, as well as the effect of GABA-modulation of the sensorimotor "beta network" and neuronal synchronisation, between healthy subjects and PD patients.

Chapter 6. Effects of frequency specific somatosensory stimulation on ongoing oscillations in the sensorimotor cortex

6.1. Introduction

6.1.1. Background

Beta, mu and gamma oscillations are central phenomena in the sensorimotor cortex and well-documented; as described in previous chapters (Salmelin & Hari 1994; Salmelin *et al.*, 1995; Pfurtscheller & Lopes da Silva 1999; Salenius & Hari 2003, Gaetz & Cheyne 2006; Cheyne 2008; Muthukumaraswamy, 2010; Cheyne 2012). Connectivity studies, both anatomical and functional, have revealed complex connectivity between MI and SI (Brovelli *et al.*, 2004; Douglas & Martin 2004; Thomson & Lamy 2007; Witham *et al.*, 2010; Hooks *et al.*, 2011), supported in particular by the functionally dependent oscillatory dynamics surrounding movement and stimulation (Pfurtscheller 1981; Salmelin & Hari 1994; Salmelin *et al.*, 1995; Stancak & Pfurtscheller 1995; Jurkiewicz *et al.*, 2006; Gaetz & Cheyne 2006; Neuper *et al.*, 2006). The post-movement, or post-stimulation, beta rebound activity seen over MI is believed to reflect somatosensory re-afference and the "resetting" of motor cortex after a sensorimotor event (Salenius *et al.*, 1997b, Schnitzler *et al.*, 1997; Chen *et al.*, 1999; Pfurtscheller *et al.* 2005; Pfurtscheller & Solis-Escalante 2009). However, as was discussed in previous chapters, most sensorimotor research focuses on the oscillatory dynamics surrounding functional changes. There is therefore, less available research on the ongoing beta and mu oscillatory activity in MI and SI and it is unclear to what extent the *ongoing oscillatory activity* in SI influences the *ongoing oscillatory activity* in MI.

The augmented beta activity seen in the beta rebound has also been suggested to temporarily prevent any new movement, underlying some of the symptoms in PD patients (Brown 2006; 2007; Degardin *et al.*, 2009; Eusebio & Brown 2009; Pogosyan *et al.*, 2009). Applying external stimulation at 20 Hz over the motor cortex and entraining ongoing motor cortical oscillations with non-invasive transcranial alternating current stimulation impairs motor function in healthy subjects and was proposed to play an inhibitory role in no-go trials (Pogosyan *et al.*, 2009; Feurra *et al.*, 2011a; Joundi *et al.*, 2012). Driving the motor cortex at gamma frequency facilitated performance (Joundi *et al.*, 2012) and applying stimulation at alpha, gamma and to some degree beta, frequency stimulation over SI resulted in tactile sensations (Feurra *et al.*, 2011b). Suggestions of different functional roles of different oscillation frequencies are far from novel and, in movement disorders, beta frequency oscillations appear to play a central role in the manifestation of abnormal motor outputs (Brown 2006; 2007; Eusebio & Brown 2009; Pogosyan *et al.*, 2009); applying of stimulation of different frequencies has had both beneficial and detrimental effects in movement disorders such as PD (Cantello *et al.*, 2002; Moro *et al.*, 2002;

Benabid 2003; Drout *et al.*, 2004; Lefaucheur *et al.*, 2005; Helmich *et al.*, 2006; Kuncel *et al.*, 2006; Priori *et al.*, 2006; Eusebio *et al.*, 2008; Filipović *et al.*, 2011; Yamawaki *et al.*, 2012). Similarly, different frequencies are known to affect motor excitability in distinct ways; application of transcranial stimulation with high frequencies over the motor cortex e.g. >5 Hz, increase motor cortex excitability and facilitates motor output, whereas low frequency stimulation is reported to depress motor cortex excitability (Pascual-Leone *et al.*, 1994; Chen *et al.*, 1999; Muellbacher *et al.*, 2000; Gangitano *et al.*, 2002; Romero *et al.*, 2002; Fitzgerald *et al.*, 2006; Jung *et al.*, 2008; Feurra *et al.*, 2011a).

Different areas are believed to oscillate at specific natural frequencies due to their distinct electrophysiological setup (Chagnac-Amitai & Connors 1982; Flint & Connors 1996; Rosanova at al., 2009, Zaehle *et al.*, 2010); evidenced by single pulse experiments. Applying an external rhythm is more likely to drive the underlying neural substrate if the applied rhythm is close to the natural frequency (Fries 2005; Schnitzler & Gross 2005; Rosanova *et al.*, 2009; Thut *et al.*, 2011a). Conventionally, oscillatory activity in the mu frequency range is representative of SI and beta frequency oscillations are believed to originate from MI (Salmelin & Hari 1994; Salmelin *et al.*, 1995; Pfurtscheller & Lopes da Silva 1999; Salenius & Hari 2003, Gaetz & Cheyne 2006; Cheyne 2012). The natural resonance frequencies are enhanced temporarily when applying for example single pulse TMS. Single pulse TMS applied to the motor cortex increased the 15-30 Hz synchronised activity in motor cortex (Paus *et al.*, 2001; Fugetta *et al.*, 2005; van der Warf & Paus 2006; Thut & Miniussi 2011). Distinct frequency bands, with anecdotal inter-individual frequency specificity and variability within the distinct band, are suggested to be relevant for particular functions (Neuper & Pfurtscheller 2001a; 2001b: Steriade, 2006; Mantini *et al.*, 2007; Thut *et al.*, 2011b; Thut & Miniussi 2011; Cheyne 2012). Few studies in humans look at long-lasting effects on the ongoing oscillatory activity, e.g. lasting after stimulation offset, of stimulating at different frequencies, although one recent study noted that rTMS at 20 Hz resulted in an increase in alpha power, e.g. 10Hz, over the motor cortex lasting for 5 minutes after stimulation offset (Veniero *et al.*, 2011).

Mechanisms underlying any long-term changes are largely unknown. One recent report by Zhaele *et al.* (2010) used transcranial alternating current stimulation and a network model to show that spike-timing dependent plasticity plays an important role, even after stimulation has ended. The resonant frequencies of the stimulated neural circuits determined the modulation of the constituent synapses in the circuit; the closer to the inherent resonance frequency the stimulation was, the more the synapses were strengthened. While studies in humans with transcranial stimulation have focused on the driven and entrainment effects on oscillatory activity during the stimulation itself, *in vitro*

studies have predominantly focused on the effects after stimulation offset. This is due to the large artefacts that surround the *in vitro* experimental stimulation. Yamawaki *et al.* (2008) applied electrical stimulation of the superficial layers of MI at 4, 20 and 125 Hz and reported a frequency dependent effect after the stimulation offset. Specifically, beta oscillatory activity in MI was reinforced following gamma and theta stimulation frequencies, while 20 Hz stimulation promoted gamma and theta frequencies. These findings are supported by the observations of Yazdan-Shahmorad *et al.* (2011), who found that specific frequencies of stimulation over MI *in vivo* have different effects on the neuronal spike activity in the individual laminae of MI.

While strong connectivity exists between SI and MI and somatosensory inputs are known to incur changes in MI, it is unclear to what extent specific frequency plays a role in this connectivity. Here, we address this question directly, using parallel experiments in MEG and *in vitro* to determine the effects of frequency specific somatosensory stimulation on the activity of MI. We explore: (1) the effects of somatosensory stimulation across the frequency range on MI oscillations, between MEG and *in vitro* experiments and (2) the effects of SI and MI stimulation on SI and MI activity *in vitro* to determine the relevance of cortico-cortical connectivity.

6.1.2. Aims and research objectives

Previous studies have described strong physiological and functional coupling between MI and SI, and imply the involvement of beta, mu and gamma oscillations. However, it is unclear to what extent specific oscillatory inputs from one area are important in influencing the activity of the other. Furthermore, in movement disorders, beta oscillations appear to play a central role in the manifestation of abnormal motor outputs. However, it is not clear to what extent SI oscillations influence those in MI. We aim to better understand these relationships by addressing the following questions:

- o How does somatosensory stimulation affect the spontaneous oscillations in human MI and SI?
- o How does SI stimulation effect the spontaneous oscillations of MI and SI in the *in vitro* recordings?
- o To what extent is the specific frequency of stimulation important in eliciting effects in MEG and *in vitro*?

6.2. Methods

6.2.1. MEG

15 subjects (8F), age range 24-45 years, were seated upright in the MEG scanner for a period of 10 mins. The study was performed in accordance with the Declaration of Helsinki, and approved by the Ethics Committee of the School of Life and Health Sciences at Aston University. Written informed consent was obtained from all participants. The participants received visual instructions from a computer screen, in addition to audio instructions from the experiementer. Participants performed voluntary and self-paced finger movements every 5 seconds with left index finger for 1-2 minutes. Primary motor cortex was localised with a SAM beamformer approach based on the PMBR seen after voluntary finger movements (Jurkiewicz et al., 2006). The PMBR was identified by an increase in the 15-30 Hz frequency band 0.5 to 1.5 seconds following movement offset compared to and -2.0 to -1.0 seconds before movement. EMG electrodes were placed on the FDI muscle to determine the onset and offset of finger movements. Primary somatosensory cortex was localised in participants using the ERSAM approach (Cheyne et al., 2006), using the stimulation events in a 2 Hz electrical stimulation train delivered through two electrodes (Digitimer Ltd.) to the median nerve at 50% of the thumb-twitch threshold. We focused the ERSAM on gamma (30-100Hz) activity around the evoked potential latency. Participants received somatosensory stimulation at different frequencies via galvanic stimulation of the median nerve, at 50% of the intensity required to elicit a thumb-twitch. Stimuli were generated with a clinical current stimulator (Model DS7a, Digitimer, Ltd, UK) and delivered through two electrodes, placed over the dorsal part of the median nerve. There were 10 stimulation events per frequency, 2s each, interspersed with 4-6 seconds of rest. 12 different frequencies were randomly delivered (5, 10, 15, 20, 26, 31, 36, 42, 47, 53, 59, 67 Hz), with a pulse width of 200 µs (figure 6.1). The stimulation was externally controlled by the Presentation software (Neurobehavioural systems, UK). Throughout the recording, participants were instructed to sit at rest and were allowed to watch a movie of their choice, displayed on screen outside the shielded room, in order to maintain attention throughout the lengthy recording session. This was intended to reduce the potential effects on ongoing oscillations of individuals focusing to different degrees on the stimulation. None of the participants reported the stimulation as painful. Trials containing artefacts were discarded and the data was filtered to 1-200 Hz, with additional notch filters at 50 and 60 Hz.
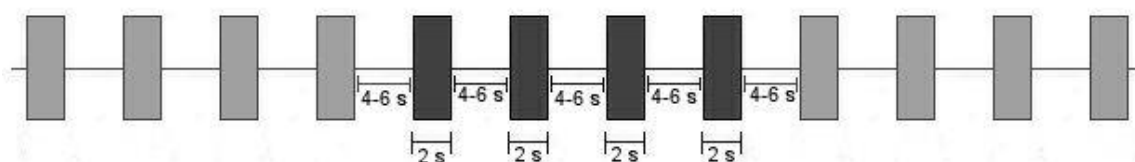
Figure 6. 1 Schematic of the stimulation protocol used in the frequency stimulation experiments in humans. The stimulation events, shown in black/grey blocks, were 2s in length, and interspersed with 4-6s. Different frequencies were randomised throughout the recording. There were ten stimulation events of each of the 12 frequencies in each subject.

Data were screened for artefacts and head movement errors. 7 participants were excluded from further offline analysis; two were removed due to artefacts during data acquisition, two were removed due to exceeding movement limitation in the scanner, two were removed as there was no high quality MRI to proceed with an acceptable SAM localisation, and one participant was on sick leave. Data from virtual electrodes in MI and SI were reconstructed before and after stimulation and analysed using Matlab (Mathworks). Specifically, the oscillatory activity 2 seconds prior to stimulation was compared with activity 2 seconds post-stimulation for each stimulation frequency. The effects of each stimulation frequency were analysed for changes in oscillatory power and frequency, for frequency distribution and variability and power state change, using the custom analysis software described in chapter 2. Statistical differences in each of these attributes before and after stimulation were determined by Student's t-test.

6.2.2. *In vitro*

Intact sensorimotor slices were prepared using protocol 2, described in chapter 2. All animal experiments were performed in accordance with the Aston University ethical review board regulations, as well as the Animals Scientific Procedures Act 1986; European Communities Directive (86/609/EEC). Brains from p18-p22 (50-60g) male Wistar rats were extracted. 450 μm thick sagittal sensorimotor slices were stored in a tissue interface chamber at room temperature for >1h. The slices were then transferred to a recording chamber with a temperature of 33-34°C and a continuous flow rate of 2 ml/min aCSF with added KA and CCh; concentrations and preparations according to protocol 2. Recordings of LFPs from superficial layers (II/III) and deeper layers (V) of MI and middle layer (IV) of SI (figure 2.6) were made. The electrodes were placed in relevant layers, identified by using a dissecting microscope and the Rat Brain Atlas (Paxinos & Watson 1986) as reference. LFP recording started after the KA- and CCh-induced oscillatory activity had stabilised, >1h in the recording chamber with KA and CCh in the aCSF flow, and lasted for >3h.

Electrical stimulation was delivered through a wire electrode inserted into SI LIV and generated with a current stimulator (Model DS3, Digitimer, Ltd, UK). Each stimulation event was 2s, interspersed with 60s of rest (figure 6.2). 12 different frequencies were used (5, 10, 15, 20, 25, 30, 35, 40, 45, 50, 55, 60 Hz).
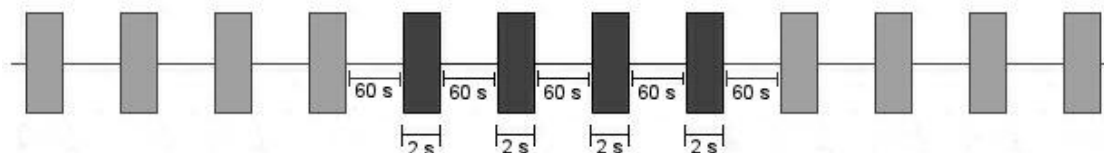
Figure 6. 2 Schematic of the stimulation protocol used in the frequency stimulation experiments *in vitro*. The stimulation events, shown in black/grey blocks, were 2s in length, and interspersed with 60s. Different frequencies were randomised throughout the recording.

The intensity of the constant current stimulator was set at 1.5mA with a pulse width of 100 µs. The stimulation protocol was programmed and controlled through Spike2 (CED, Ltd), which was also used for recording the LFPs and online FFT analysis. Total and used number of recordings, in 10 slices, per frequency can be seen in table 6.1. Recorded data was exported to MatLab and 30s time periods, pre and post of each stimulation event were exported as separate trials to MatLab in spreadsheet format. From these trials Morelet-Wavelet spectrograms were derived and used for the offline analysis with the previous described analysis approach, for details see chapter 2.

Table 6. 1 Number of recordings in the *in vitro* experiments at different stimulation frequencies

Stimulation Frequency	Total no. (x3)	Number of recordings:		
		MI LIII	MI LV	SI LIV
5	24	15	23	24
10	39	26	36	42
15	44	33	41	45
20	42	31	37	43
25	26	15	26	26
30	18	14	17	20
35	24	16	23	25
40	20	14	17	21
45	18	14	18	20
50	26	21	26	25
55	41	22	39	43
60	21	17	19	23
Total	343	238	322	357

The effects of each stimulation frequency were analysed for changes in oscillatory power and frequency, for frequency distribution and variability and power state change.

6.2.3. Analysis approach

The mean peak frequency and peak power was determined for each sample in the epoch (30s = 30000 samples for *in vitro* and 2s = 1200 samples for MEG data) with a sliding window approach applied to the Morelet-wavelet spectrograms. The frequency distribution of the oscillations was determined using FWHM. The frequency variability was computed using the amplitude-independent peak frequency distribution, where the peak frequency of each sample was sorted into frequency bins of 1 Hz. Variability in oscillatory power was determined using an amplitude sorting measurement to determine the time and amplitude changes of oscillatory up and down states. We used student's T-tests to statistically test for differences between before and after stimulation for each stimulation frequency and location, these were not compared in between each other. Further details regarding this analysis approach can be found in chapter 2.

6.3. Results

6.3.1. Somatosensory stimulation and oscillatory power

6.3.1.1. MEG

The mean peak power in SI decreased significantly after 10 Hz stimulation; $t_{[7]}=2.4862$, $p=0.0418$ (figure 6.3). See table 6.2-3 for non-significant changes.
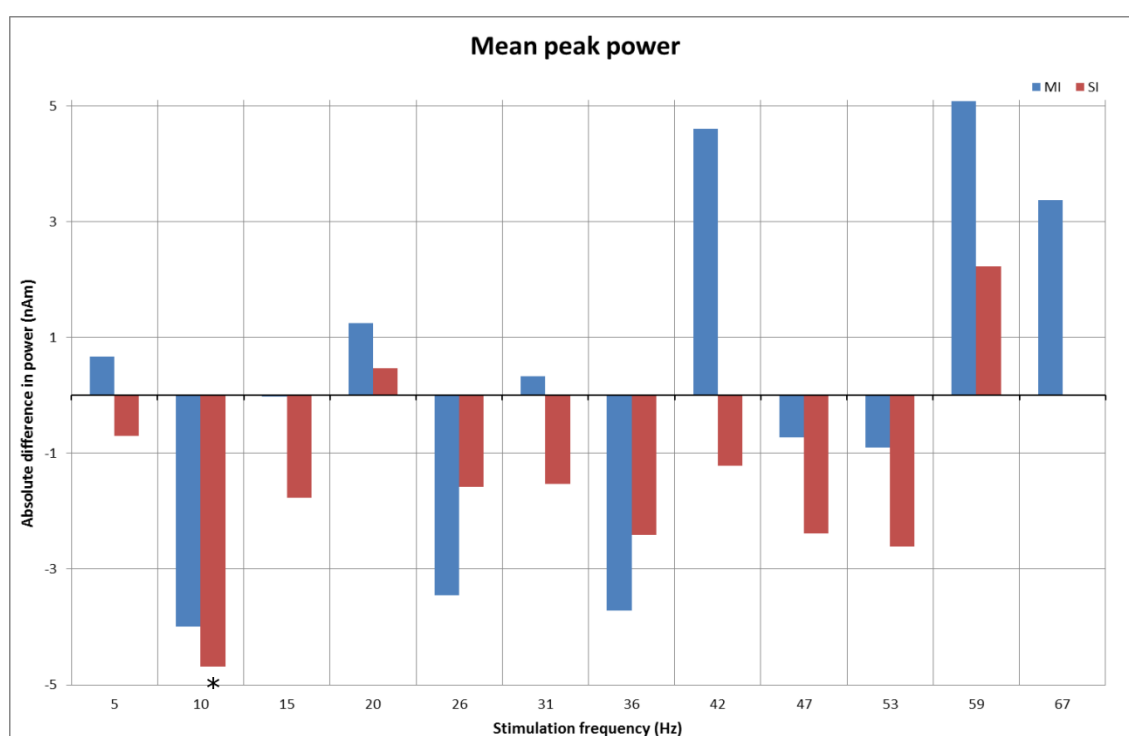
Figure 6. 3. Group-averages of significant and non-significant absolute differences in mean peak power after stimulation with different frequencies in MI (n=8, blue) and SI (n=8, red). The decrease in power in SI was significant after 10 Hz stimulation, $p<0.05$, indicated with *.

Table 6. 2. Mean peak power before and after stimulation with different frequencies

Mean peak power before and after stimulation ± SD (nAm)				
		Pre		**Post**	
Stim.	**F**	**MI**	**SI**	**MI**	**SI**
	5	18.22±9.12	9.63±3.48	18.89±11.29	8.93±4.21
	10	22.58±15.98	13.10±6.98	18.59±12.75	8.41±4.20
	15	19.82±12.58	11.75±6.56	19.80±13.68	9.97±5.62
	20	20.93±14.85	9.22±5.15	22.18±15.90	9.69±5.89
	26	24.98±20.14	10.17±7.04	21.53±13.94	8.59±4.12
	31	20.21±13.07	10.02±6.05	20.54±13.02	8.49±3.72
	36	23.90±17.03	10.59±6.32	20.19±15.48	8.18±3.98
	42	18.27±12.10	10.04±5.03	22.88±16.71	8.82±4.23
	47	20.00±14.5	10.62±5.78	19.28±13.94	8.24±3.67
	53	22.64±15.67	10.73±5.57	21.74±15.48	8.12±4.48
	59	19.46±12.36	19.43±32.35	24.55±16.59	21.67±36.48
	67	19.39±13.31	8.94±3.53	22.76±16.92	8.96±4.33

Grey highlight indicates statistical significance, $p<0.05$.

Table 6. 3. T-statistics: mean peak power in humans

T-statistics: Mean peak power							
Stim F.		MI	SI	Stim F.		MI	SI
5	*T*	-0.3216	0.6402	36	*T*	0.8317	1.4687
	p	0.7571	0.5424		*p*	0.433	0.1854
10	*T*	1.6726	2.4862	42	*T*	-2.2363	0.8015
	p	0.1383	0.0418 (*)		*p*	0.0604	0.4492
15	*T*	0.0131	0.803	47	*T*	0.2979	1.3551
	p	0.9899	0.4484		*p*	0.7744	0.2175
20	*T*	-0.6865	-1.0247	53	*T*	0.3433	2.5374
	p	0.5145	0.3396		*p*	0.7415	0.0388
26	*T*	0.7027	1.3685	59	*T*	-1.962	-1.3716
	p	0.505	0.2134		*p*	0.0906	0.2125
31	*T*	-0.1376	1.4483	67	*T*	-0.9412	-0.0287
	p	0.8944	0.1908		*p*	0.3779	0.9779

Significance, p<0.05, is marked with *.

6.3.1.2. *In vitro*

Mean peak power increased significantly in MI LIII after 5, 40 and 55 Hz stimulation, $t_{[14]}$=-0.1168, p=0.0312; $t_{[13]}$=-2.4368, p=0.0299 and $t_{[21]}$=-2.6579, p=0.0147, respectively (figure 6.4). See table 6.4-5 for non-significant changes.
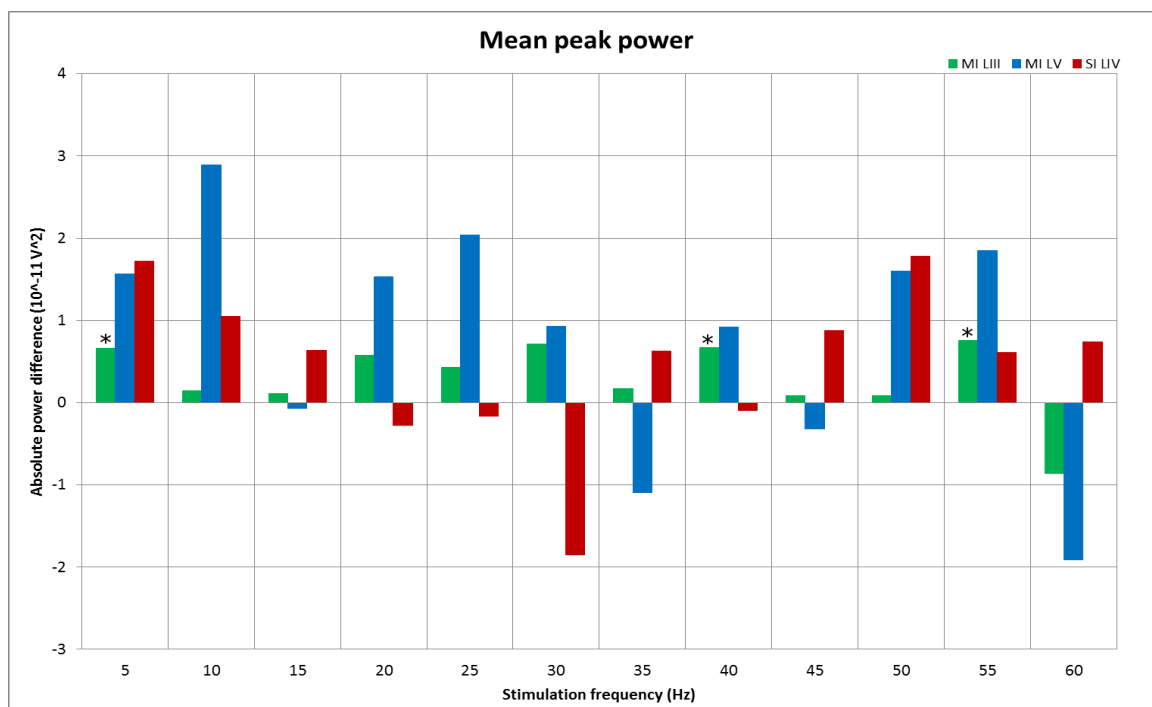
Figure 6. 4. Group-averages of significant and non-significant absolute mean peak power difference after stimulation with different frequencies. MI LIII (green) showed significant increases in oscillatory peak power at 5 (n=15), 40 (n=14) and 55 (n=22) Hz, p<0.05, marked with *. MI LV is marked with blue and SI LIV is marked with red.

Table 6. 4. Mean peak power before and after stimulation *in vitro*

Mean peak power before and after stimulation ± SD						
Stim.		Pre			Post	
(Hz)	MI LIII	MI LV	SI LIV	MI LIII	MI LV	SI LIV
5	11.58±11.04	56.14±59.09	50.72±46.94	12.24±11.70	57.70±64.86	52.45±49.61
10	11.02±12.30	46.21±72.44	45.18±40.77	11.16±12.43	49.11±74.37	46.23±41.37
15	9.13±9.10	46.41±63.45	42.18±41.15	9.24±9.34	46.33±63.20	42.82±41.84
20	10.00±10.42	39.84±51.89	44.37±4.72	10.57±11.47	41.37±55.86	44.09±40.53
25	12.24±11.68	51.74±57.31	50.63±48.04	12.67±14.04	53.78±61.64	50.47±48.21
30	8.16±10.85	29.83±5.56	37.91±47.75	8.87±12.14	30.75±51.86	36.06±38.04
35	12.93±10.35	58.32±65.87	51.15±48.18	13.10±10.41	57.23±66.93	51.77±50.11
40	7.67±11.15	31.37±60.18	32.87±24.51	8.34±11.90	32.29±59.93	32.77±25.06
45	8.38±12.27	46.46±84.02	31.90±24.72	8.47±12.20	46.14±84.31	32.77±26.84
50	10.45±9.76	51.45±57.26	44.51±44.83	10.53±10.41	53.05±60.09	46.29±45.59
55	12.95±11.71	44.24±64.02	44.60±41.30	13.71±11.93	46.10±66.01	45.20±41.57
60	8.96±11.46	37.59±76.33	31.58±23.73	8.09±110.62	35.68±67.17	32.31±24.59

Grey highlight indicates statistical significance, p<0.05.

Table 6. 5. T-statistics: mean peak power *in vitro*

T-statistics: Mean peak power									
Stim F.		MI LIII	MI LV	SI LIV	Stim F.		MI LIII	MI LV	SI LIV
5	*T*	-2.3937	-0.8716	-2.2187	35	*T*	-0.4049	0.5972	-0.5357
	p	0.0312 (*)	0.3929	0.0424 (*)		*p*	0.6913	0.5565	0.6006
10	*T*	-0.5215	-1.0629	-0.2008	40	*T*	-2.4368	-0.1705	-0.6537
	p	0.6066	0.2951	0.8432		*p*	0.0299 (*)	0.8668	0.5226
15	*T*	-0.4781	0.1353	0.1292	45	*T*	-0.5988	0.4607	0.2221
	p	0.6358	0.893	0.8982		*p*	0.5596	0.6508	0.8277
20	*T*	-1.8046	-1.4911	-1.8046	50	*T*	-0.3385	-1.9502	-0.5114
	p	0.0812	0.1446	0.0812		*p*	0.7385	0.0625	0.6153
25	*T*	-0.5639	-1.6315	-0.5443	55	*T*	-2.6579	-1.9604	-1.886
	p	0.5817	0.1153	0.5933		*p*	0.0147 (*)	0.0573	0.0747
30	*T*	-1.748	-1.4404	-1.748	60	*T*	1.4906	0.8227	1.4906
	p	0.104	0.169	0.104		*p*	0.1555	0.4214	0.1555

Abbreviations: *T*=t-statistic, *p*=p-value. Significance p<0.05, is marked with *.

6.3.2. Somatosensory stimulation and oscillatory frequency

6.3.2.1. MEG

The increase in mean peak frequency in SI after 36 and 53 Hz stimulation were significant: $t_{[7]}$=-2.673, p=0.0319, and $t_{[7]}$=-2.4346, p=0.0451, respectively (figure 6.5). See talbe 6.6-7 for non-significant changes.
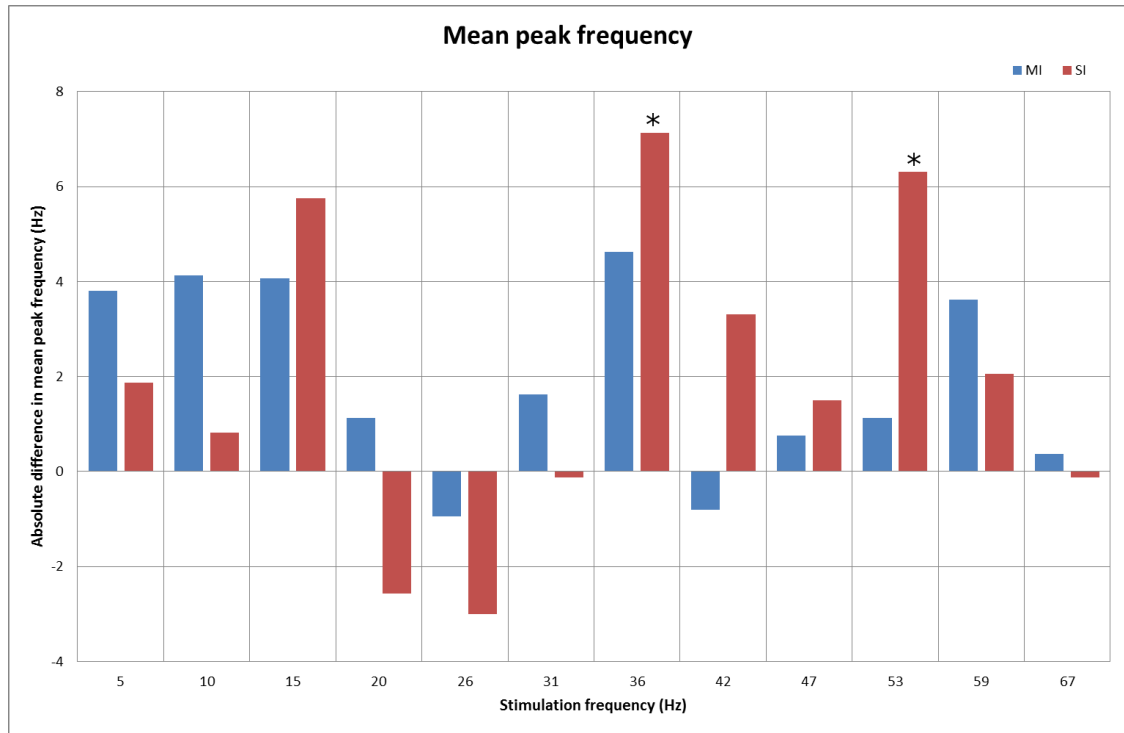
Figure 6. 5. Group-averages of significant and non-significant absolute differences in mean peak frequency in MI (blue) and SI (red) after stimulation with different frequencies. In SI (n=8), the increases in mean peak frequency at 36 and 53 Hz were significant, p<0.05, marked with *.

Table 6. 6. Mean peak frequency before and after stimulation with different frequencies

Mean peak frequency before and after stimulation ± SD (Hz)				
	Pre		Post	
Stim. F	MI	SI	MI	SI
5	19.50±7.19	17.31±6.94	23.31±5.90	19.19±6.84
10	19.38±6.66	16.69±6.14	23.50±6.11	17.50±7.25
15	19.19±6.89	14.88±5.20	23.25±5.78	20.63±6.47
20	21.50±6.80	19.69±6.60	22.63±5.3	17.13±6.69
26	23.44±6.10	19.31±7.24	22.50±5.39	16.31±5.68
31	23.19±5.58	19.00±6.89	24.81±3.39	18.88±7.41
36	18.38±7.31	15.63±7.63	23.01±7.50	22.75±5.55
42	25.81±3.60	19.19±7.26	25.00±4.31	22.5±5.95
47	21.75±6.90	18.94±6.78	22.50±6.05	20.44±6.83
53	23.88±6.53	15.69±6.39	25.02±4.33	22.00±7.72
59	20.75±7.98	22.19±11.39	24.38±3.97	24.25±12.49
67	24.00±5.74	19.00±6.69	24.38±6.36	18.88±7.26

Grey highlight indicates statistical significance, p<0.05.

Table 6. 7. T-statistics: mean peak frequency in humans

T-statistics: Mean peak frequency					
Stim F.		MI	SI	Stim F.		MI	SI
5	*T*	-1.3938	-1.2658	36	*T*	-1.2482	-2.673
	p	0.206	0.2461		*p*	0.2521	0.0319 (*)
10	*T*	-1.4949	-0.2555	42	*T*	0.974	-1.1989
	p	0.1786	0.8057		*p*	0.3625	0.2696
15	*T*	-1.6494	-2.2476	47	*T*	-0.2798	-0.5875
	p	0.1431	0.0594		*p*	0.7878	0.5753
20	*T*	-0.7445	1.1266	53	*T*	-0.7657	-2.4346
	p	0.4808	0.297		*p*	0.4689	0.0451 (*)
26	*T*	0.3272	0.9294	59	*T*	-1.1414	-0.8038
	p	0.7531	0.3836		*p*	0.2913	0.448
31	*T*	-0.9442	0.0408	67	*T*	-0.1697	0.1876
	p	0.3765	0.9686		*p*	0.87	0.8565

Abbreviations: *T*=t-statistic, *p*=p-value. Significance p<0.05, is marked with *.

6.3.2.2 *In vitro*

20 Hz stimulation significantly decreased the ongoing oscillatory mean peak frequency in MI LIII, $t_{[30]}$=2.6382, p=0.0131 (figure 6.6). See table 6.8-9 for non-significant changes.
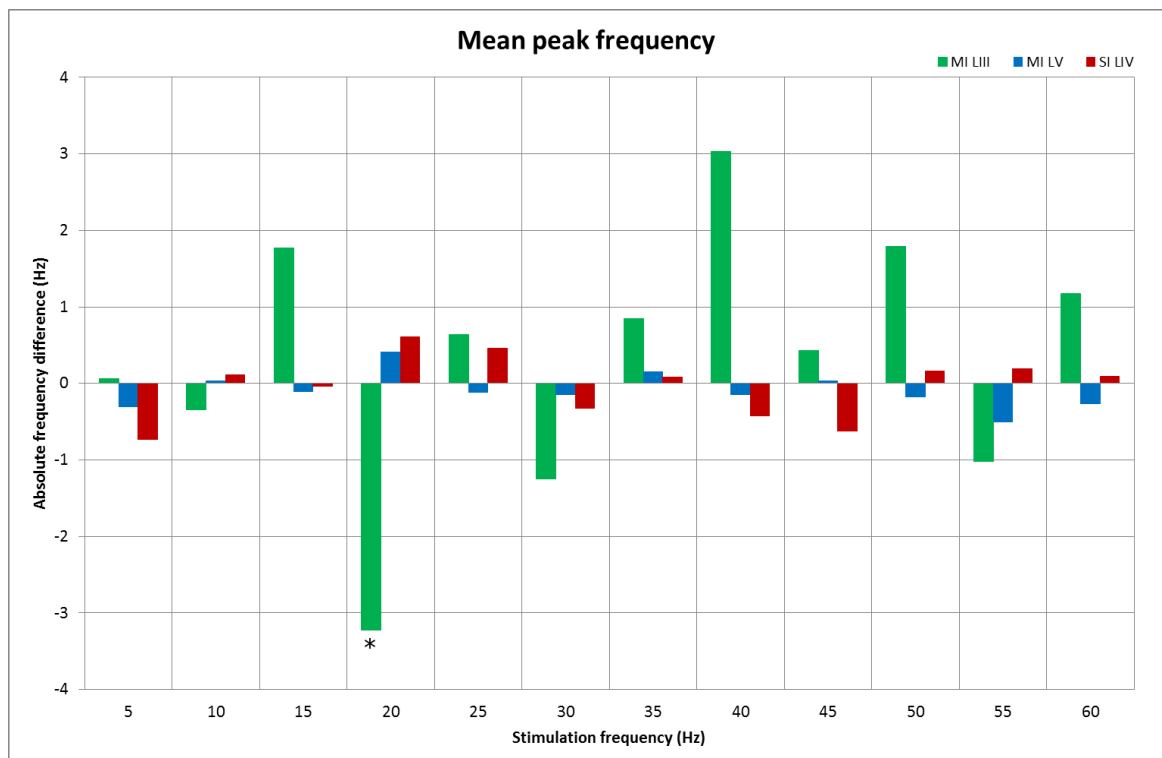
Figure 6. 6. Group-averages of significant and non-significant absolute differences in mean peak frequency after stimulation. The decrease after 20 Hz stimulation in MI LIII (n=31, green) was significant, p<0.05. MI LV is indicated by blue, SI LIV by red.

Table 6. 8. Mean peak frequency before and after stimulation at different frequencies *in vitro*

Mean peak frequency before and after stimulation ± SD					
Stim.		Pre			Post	
(Hz)	MI LIII	MI LV	SI LIV	MI LIII	MI LV	SI LIV
5	20.17±9.59	29.89±2.50	27.23±2.85	20.23±9.71	29.59±2.63	26.50±3.54
10	20.46±9.25	29.86±3.36	26.67±3.36	20.12±9.13	29.89±3.50	26.77±3.44
15	17.59±8.97	30.51±2.05	26.25±3.99	19.36±8.95	30.40±2.06	26.22±3.68
20	20.76±9.16	29.69±4.28	25.79±4.60	17.53±8.62	30.09±3.89	26.40±3.67
25	19.13±9.67	29.27±4.47	26.11±4.43	19.77±9.32	29.15±4.57	26.58±4.42
30	19.61±9.75	30.97±1.48	25.78±3.80	18.36±9.38	30.82±1.67	25.45±3.54
35	18.19±9.90	29.87±2.15	26.38±4.68	19.03±10.14	30.02±2.20	26.46±4.59
40	18.29±9.24	29.91±5.02	25.36±3.20	21.32±8.13	29.76±4.69	24.93±4.97
45	19.57±9.77	30.67±1.53	25.38±3.37	20.00±9.77	30.69±1.51	24.75±3.82
50	18.24±9.12	29.31±4.56	26.58±4.63	20.02±9.10	29.13±4.65	26.74±3.74
55	21.89±9.06	30.58±1.93	25.29±5.07	20.86±8.93	30.08±3.75	25.48±4.76
60	16.00±8.33	31.18±1.24	25.63±3.96	17.18±8.39	30.92±1.47	25.72±3.59

Grey highlight indicates statistical significance, p<0.05.

Table 6. 9. T-statistics: mean peak frequency *in vitro*

T-statistics: Mean peak frequency								
Stim F.		MI LIII	MI LV	SI LIV	Stim F.		MI LIII	MI LV	SI LIV
5	*T*	-0.1168	1.7186	-0.4336	35	*T*	-0.4269	-0.8372	-0.4262
	p	0.9087	0.0997	0.6708		*p*	0.6755	0.4115	0.6765
10	*T*	0.3993	-0.2507	0.2109	40	*T*	-1.3616	0.0973	-1.4042
	p	0.693	0.8035	0.8355		*p*	0.1965	0.9237	0.1794
15	*T*	-1.8764	1.2445	-1.2882	45	*T*	-0.1927	-0.2514	0.5496
	p	0.0697	0.2206	0.2086		*p*	0.8502	0.8045	0.5919
20	*T*	2.6382	-1.0349	2.6382	50	*T*	-1.5179	1.1218	-1.3549
	p	0.0131 (*)	0.3076	0.0131		*p*	0.1447	0.2726	0.1922
25	*T*	-0.837	1.3636	-0.5047	55	*T*	0.6769	1.0447	0.6185
	p	0.4166	0.1848	0.6203		*p*	0.5059	0.3028	0.5436
30	*T*	1.6051	1.5713	1.6051	60	*T*	-0.6479	2.0412	-0.6479
	p	0.1325	0.1357	0.1325		*p*	0.5263	0.0562	0.5263

Abbreviations: *T*=t-statistic, *p*=p-value. Significance p<0.05, is marked with *.

6.3.3. Somatosensory stimulation and frequency distribution

6.3.3.1. MEG

There were no significant effects on mean FWHM in MI or SI after MSN of any frequency in humans (figure 6.7, table 6.10-11).
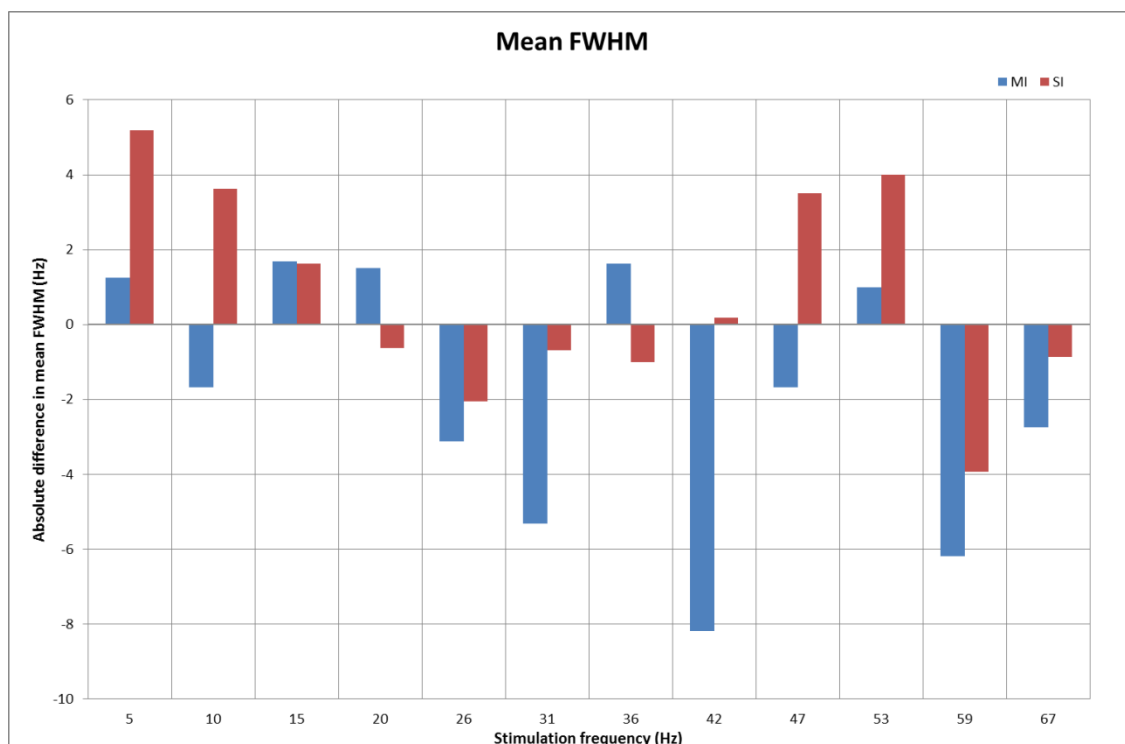
Figure 6. 7 Group-averages of non-significant absolute differences in mean FWHM between before and after stimulation with different frequencies. MI is indicated by blue, SI by red.

Table 6. 10. Mean FWHM before and after stimulation with different frequencies in humans

Mean FWHM before and after stimulation ± SD (Hz)				
	Pre		Post	
Stim. F	MI	SI	MI	SI
5	19.13±8.98	14.25±4.54	20.38±11.22	19.44±10.50
10	18.50±9.12	14.06±11.79	16.81±8.88	17.69±7.77
15	16.25±5.02	15.19±11.02	17.94±9.59	16.81±6.11
20	19.38±9.94	19.50±11.09	20.88±10.80	18.88±11.11
26	19.00±11.48	19.13±8.64	15.88±6.43	17.06±9.04
31	19.56±9.53	18.81±8.79	14.25±3.83	18.13±6.82
36	15.50±8.78	19.81±10.85	17.13±5.73	18.81±7.96
42	24.56±11.03	21.75±13.61	16.37±7.77	21.94±8.54
47	19.63±9.72	15.94±7.49	17.94±10.46	19.44±10.18
53	18.00±8.75	18.44±7.78	19.00±9.40	22.44±11.69
59	20.25±9.70	20.69±7.50	14.06±4.66	16.75±7.16
67	21.06±9.11	20.50±8.43	18.31±9.75	19.63±10.47

Table 6. 11. T-statistics: mean FWHM in humans

T-statistics: Full-width half maximum							
Stim F.		**MI**	**SI**	**Stim F.**		**MI**	**SI**
5	*T*	-0.3637	-1.2628	36	*T*	-0.5359	0.3019
	p	0.7268	0.2471		*p*	0.6086	0.7715
10	*T*	0.4193	-0.9219	42	*T*	2.4577	-0.0413
	p	0.6876	0.3873		*p*	0.0436	0.9682
15	*T*	-0.6222	-0.4102	47	*T*	0.5437	-0.9651
	p	0.5536	0.6939		*p*	0.6035	0.3666
20	*T*	-0.4596	0.5018	53	*T*	-0.6325	-1.274
	p	0.6597	0.6312		*p*	0.5472	0.2433
26	*T*	0.8597	1.1032	59	*T*	1.9202	1.0012
	p	0.4184	0.3064		*p*	0.0963	0.3501
31	*T*	2.1819	0.1512	67	*T*	1.2478	0.2052
	p	0.0655	0.8841		*p*	0.2522	0.8433

Abbreviations: *T*=t-statistic, *p*=p-value.

6.3.3.2. *In vitro*

There were no significant effects on mean FWHM after somatosensory stimulation *in vitro* in any laminae at any frequency (figure 6.8, table 6.12-13).
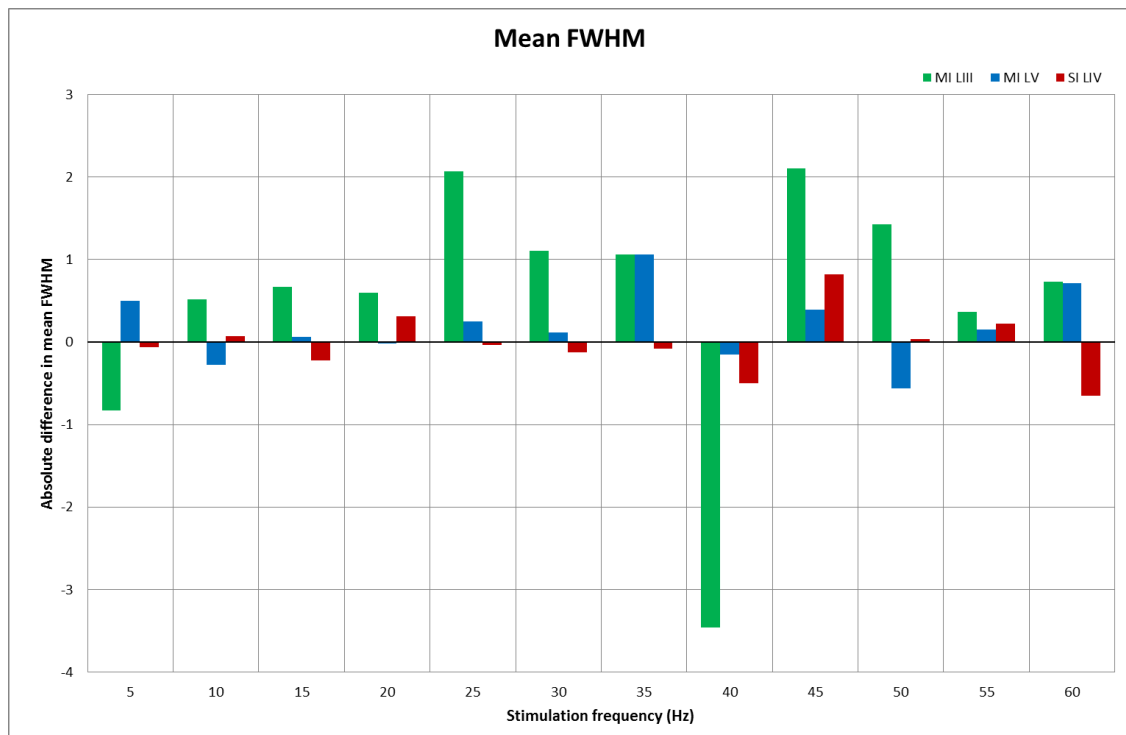
Figure 6. 8. Group-averages of non-significant absolute differences in FWHM between before and after stimulation *in vitro*. MI LIII is indicated by green, MI LV by blue and SI LIV by red.

Table 6. 12. Mean FWHM before and after stimulation with different frequencies *in vitro*

Mean FWHM before and after stimulation ± SD (Hz)						
Stim. F	Pre			Post		
(Hz)	MI LIII	MI LV	SI LIV	MI LIII	MI LV	SI LIV
5	15.70±6.58	13.61±5.35	18.90±5.14	14.87±7.50	14.11±5.66	18.83±4.58
10	16.06±7.14	15.03±5.62	18.21±4.94	16.58±6.05	14.75±5.62	18.29±4.93
15	14.50±7.03	14.00±5.17	19.10±5.27	15.17±7.32	14.06±4.92	18.88±4.96
20	15.42±6.86	14.07±4.73	18.67±5.31	16.02±5.97	14.05±5.02	18.99±5.25
25	15.67±7.51	13.65±4.57	18.88±4.73	17.73±7.69	13.90±5.09	18.85±4.76
30	15.71±8.27	14.26±4.69	19.50±4.22	16.82±6.22	14.38±5.08	19.38±4.31
35	15.34±6.32	12.91±4.10	18.32±4.86	16.41±6.85	13.98±5.64	18.24±5.08
40	19.21±9.51	15.35±5.29	19.24±4.74	15.75±7.92	15.21±5.55	18.74±5.10
45	14.79±8.83	13.81±4.63	18.95±4.16	16.89±8.23	14.19±4.62	19.78±4.19
50	14.67±7.12	14.12±5.13	19.24±4.75	16.10±5.61	13.56±4.61	19.28±4.53
55	17.75±6.81	13.60±5.26	18.80±5.04	18.11±6.60	13.76±5.16	19.02±5.06
60	16.24±7.50	14.58±5.57	19.70±4.99	16.97±6.83	15.29±6.25	19.04±5.10

Table 6. 13. T-statistics: mean FWHM *in vitro*

T-statistics: Full-width half-maximum								
Stim F.		MI LIII	MI LV	SI LIV	Stim F.		MI LIII	MI LV	SI LIV
5	*T*	1.3309	-0.7424	0.1596	35	*T*	-1.147	-1.8934	0.1582
	p	0.2045	0.4657	0.8746		*p*	0.2693	0.0715	0.8756
10	*T*	-0.51	0.647	-0.1609	40	*T*	1.4071	0.1239	0.5693
	p	0.6145	0.5218	0.8729		*p*	0.1829	0.9029	0.5755
15	*T*	-0.6254	-0.1264	0.5954	45	*T*	-1.0439	-0.9191	-1.8615
	p	0.5361	0.9	0.5546		*p*	0.3156	0.3709	0.0782
20	*T*	-0.7302	0.0329	-0.8985	50	*T*	-1.3923	1.2684	-0.0811
	p	0.4709	0.9739	0.3741		*p*	0.1791	0.2163	0.936
25	*T*	-1.5897	-0.3994	0.11	55	*T*	-0.4439	-0.3571	-0.4647
	p	0.1342	0.693	0.9133		*p*	0.6617	0.723	0.6445
30	*T*	-0.7661	-0.3527	0.2028	60	*T*	-0.4299	-1.5363	1.2367
	p	0.4573	0.7289	0.8415		*p*	0.673	0.1419	0.2292

Abbreviations: *T*=t-statistic, *p*=p-value.

6.3.4. Somatosensory stimulation and frequency variability

6.3.4.1. MEG

In MEG stimulation at 36 Hz significantly decreased the frequency variability in both MI and SI; $t_{[7]}=2.4534$, $p=0.0439$; $t_{[7]}=2.4823$, $p=0.0421$, respectively (figure 6.9).
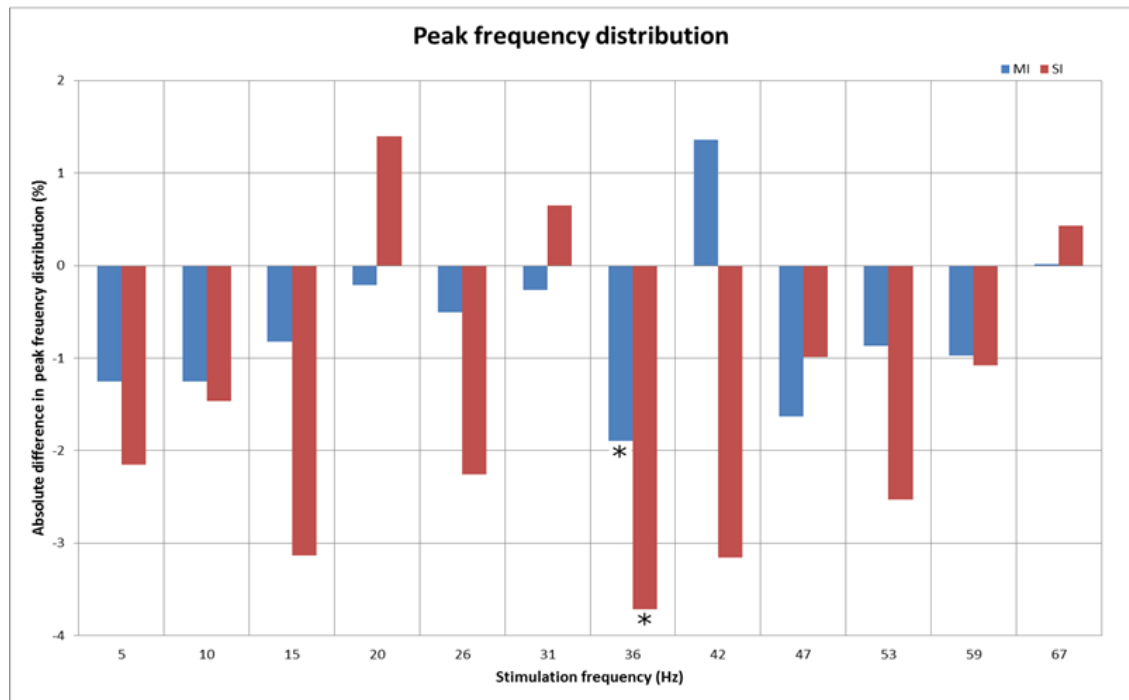
Figure 6. 9. Group-averages of significant and non-significant absolute differences in the mean percentage of samples at the peak frequency stimulation with different frequencies. After 36 Hz stimulation in MI (n=8, blue) and SI (n=8, red), the decrease in peak frequency distribution was significant, $p<0.05$, marked with *.

Table 6. 14. Peak frequency distribution before and after stimulation with different frequencies

Frequency distribution before and after stimulation: % samples at peak				
	Pre		Post	
Stim. F	MI	SI	MI	SI
5	7.40±4.75	7.84±4.74	6.15±6.76	5.68±4.32
10	6.12±3.49	7.24±4.20	4.86±2.22	5.77±2.90
15	5.73±2.52	9.03±7.82	4.91±2.08	5.89±3.70
20	5.42±3.20	6.23±3.92	5.21±2.77	7.63±3.95
26	5.49±4.87	6.23±5.84	4.99±2.64	3.97±1.43
31	4.79±2.52	4.84±2.17	4.52±2.83	5.49±2.30
36	6.58±6.58	8.20±5.16	4.68±1.25	4.48±2.92
42	3.88±1.32	7.41±5.82	5.24±2.80	4.25±1.63
47	6.22±4.45	6.77±3.28	4.59±1.96	5.78±5.12
53	4.96±2.60	7.89±5.07	4.09±2.86	5.36±5.00
59	6.24±5.95	6.19±4.33	5.27±2.67	5.12±4.05
67	4.99±2.84	5.74±3.12	5.00±2.56	6.17±3.98

Grey highlight indicates statistical significance, $p<0.05$.

Table 6. 15. T-statistics: peak frequency distribution in humans

T-statistics: Frequency variability						
Stim F.		MI	SI	Stim F.		MI	SI
5	*T*	0.5762	1.4093	36	*T*	2.4534	2.4823
	p	0.5826	0.2016		*p*	0.0439 (*)	0.0421 (*)
10	*T*	1.4279	0.9097	42	*T*	-1.2377	1.5576
	p	0.1964	0.3932		*p*	0.2557	0.1633
15	*T*	0.6001	1.1314	47	*T*	1.0885	0.5506
	p	0.5674	0.2951		*p*	0.3124	0.599
20	*T*	0.182	-1.6543	53	*T*	1.166	1.4136
	p	0.8608	0.142		*p*	0.2818	0.2004
26	*T*	0.3324	1.253	59	*T*	0.5543	0.7347
	p	0.7493	0.2504		*p*	0.5966	0.4864
31	*T*	0.2311	-0.8402	67	*T*	-0.012	-0.3459
	p	0.8239	0.4286		*p*	0.9908	0.7396

Abbreviations: *T*=t-statistic, *p*=p-value. Significance $p < 0.05$, is marked with *.

6.3.4.2. *In vitro*

The frequency variability in MI LIII increased significantly after 20 Hz stimulation: $t_{[30]}=-3.22309$, p=0.003. There was a significant increase after 55 Hz stimulation as well: $t_{[21]}=-2.1863$, p=0.0403 (figure 6.10). See table 6.16-17 for non-significant changes.
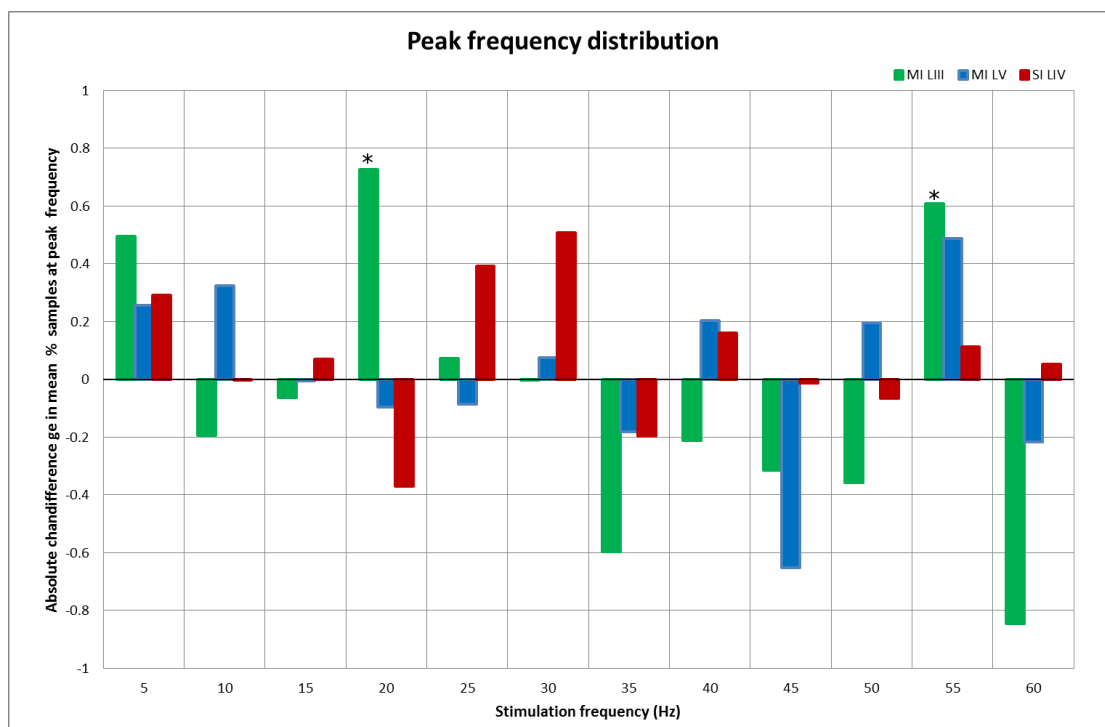
Figure 6. 10. Group-averages of significant and non-significant absolute differences in mean percentage of samples found at the peak frequency. The increases in mean % samples found at peak frequencies in MI LIII (green) after 20 (n=31) and 55 (n=22) Hz stimulation were significant, $p < 0.05$, marked with *. MI LV is indicated by blue and SI LIV by red.

Table 6. 16. Frequency distribution before and after stimulation with different frequencies *in vitro*

Stim. F	Pre			Post		
(Hz)	MI LIII	MI LV	SI LIV	MI LIII	MI LV	SI LIV
5	5.10±3.17	9.34±4.02	6.35±2.36	5.60±3.34	9.60±4.60	6.64±2.50
10	5.40±4.48	8.22±4.30	6.68±2.33	5.20±4.19	8.54±4.27	6.67±2.23
15	4.93±3.40	8.69±3.64	6.14±2.39	4.87±3.82	8.69±3.82	6.21±2.52
20	4.58±3.60	8.84±8.83	6.65±2.29	5.31±3.53	8.75±3.69	6.28±2.62
25	5.43±3.43	9.14±3.40	6.30±2.45	5.51±3.54	9.06±4.21	6.69±2.22
30	4.83±4.30	8.12±3.59	5.61±1.78	4.83±4.11	8.19±3.12	6.12±2.42
35	6.20±3.53	9.84±4.28	6.70±2.21	5.60±3.62	9.66±3.94	6.51±1.87
40	4.28±3.86	7.82±3.51	5.64±1.98	4.07±4.44	8.03±3.58	5.80±2.05
45	4.67±4.49	8.37±3.76	5.70±1.99	4.35±4.21	7.72±3.22	5.69±1.88
50	5.15±3.25	9.19±3.57	6.59±2.06	4.80±3.04	9.39±4.00	6.52±2.31
55	5.38±4.34	8.80±4.21	5.87±2.12	5.99±4.28	9.29±4.14	5.98±1.90
60	5.30±3.56	8.45±3.40	5.89±2.09	4.46±3.42	8.24±3.91	5.95±1.75

Grey highlight indicates statistical significance, p<0.05.

Table 6. 17. T-statistics: frequency distribution *in vitro*

Stim		MI LIII	MI LV	SI LIV	Stim		MI LIII	MI LV	SI LIV
5	*T*	-1.3428	-0.8033	-1.0035	35	*T*	1.2771	0.5125	0.5533
	p	0.2007	0.4304	0.3261		*p*	0.221	0.6134	0.5852
10	*T*	0.536	-1.2213	0.0085	40	*T*	0.4921	-0.4748	-0.5203
	p	0.5967	0.2301	0.9932		*p*	0.6308	0.6414	0.6085
15	*T*	0.161	0.0199	-0.3392	45	*T*	0.5871	1.4291	0.061
	p	0.8731	0.9842	0.7361		*p*	0.5672	0.1711	0.952
20	*T*	-3.2302	0.3597	1.2928	50	*T*	1.0899	-0.5956	0.3202
	p	0.003 (**)	0.7212	0.2032		*p*	0.2887	0.5568	0.7516
25	*T*	-0.1639	0.2278	-1.1512	55	*T*	-2.1863	-1.5401	-0.5543
	p	0.8721	0.8217	0.2605		*p*	0.0403 (*)	0.1318	0.5823
30	*T*	0.0065	-0.2251	-1.0359	60	*T*	1.9554	0.5356	-0.8202
	p	0.9949	0.8247	0.3133		*p*	0.0682	0.5988	0.4209

Abbreviations: *T*=t-statistic, *p*=p-value. Significance p<0.05 is marked with *, p<0.01 with **.

6.3.5. Somatosensory stimulation and oscillatory power state

6.3.5.1. MEG

In the MEG recordings, in MI the decrease in the upstate percentage after 15 Hz stimulation was significant, $t_{[7]}=2.9982$, p=0.02 (figure 6.11).

In the MEG recordings, in SI the mean oscillatory power in the upstate in SI significantly decreased following 10 Hz stimulation, $t_{[7]}=3.2937$, p=0.0132. The mean oscillatory power in the downstates significantly decreased in SI, after 10 Hz stimulation, $t_{[7]}=2.7426$, p=0.0288. The increase in the upstate percentage after 47 Hz stimulation was significant, $t_{[7]}=-31376$, p=0.0164 (figure 6.11-13).
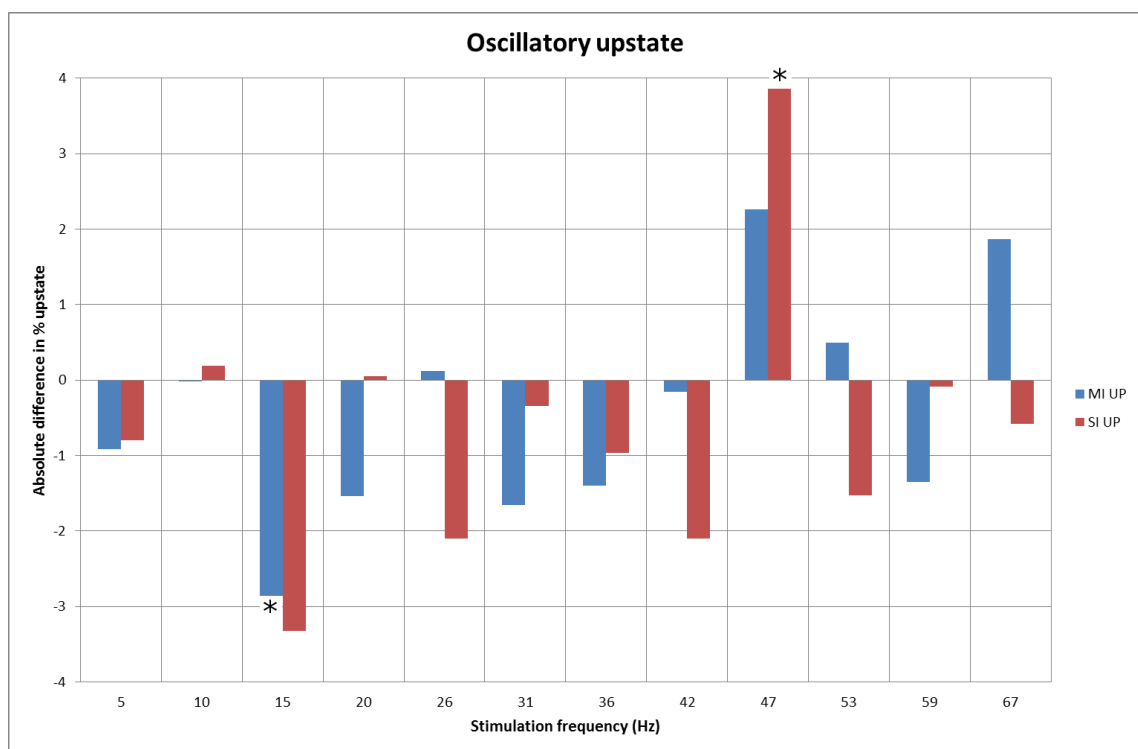
Figure 6. 11. Group-averages of significant and non-significant absolute differences in oscillatory upstate between before and after stimulation at different frequencies. In MI (n=8, blue) the decrease in the upstate percentage after 15 Hz stimulation was significant, p<0.05. In SI (n=8, red) the increase in the upstate percentage after 47 Hz stimulation was significant, p<0.05, marked with *.
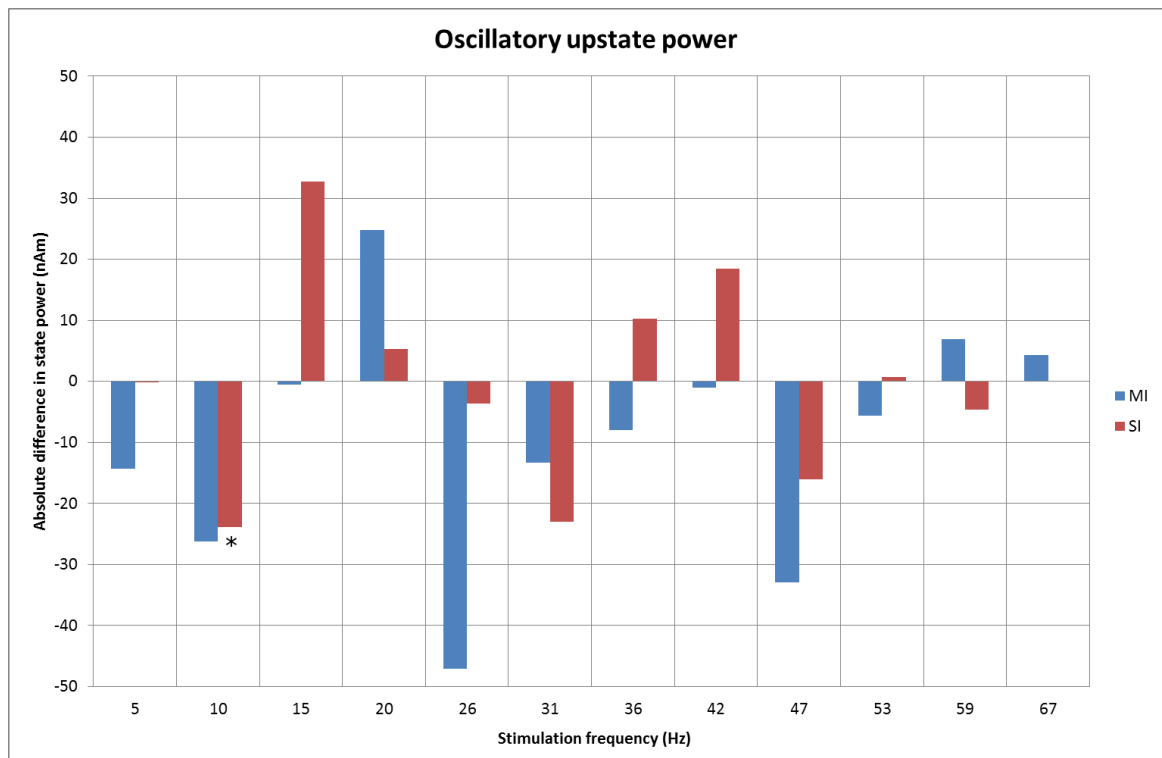
Figure 6. 12. Group-averages of significant and non-significant absolute differences in the oscillatory upstate power between before and after stimulation. The mean oscillatory power in the upstate in SI (n=8, red) significantly decreased following 10 Hz stimulation, p<0.05, marked with *. MI is indicated by blue.
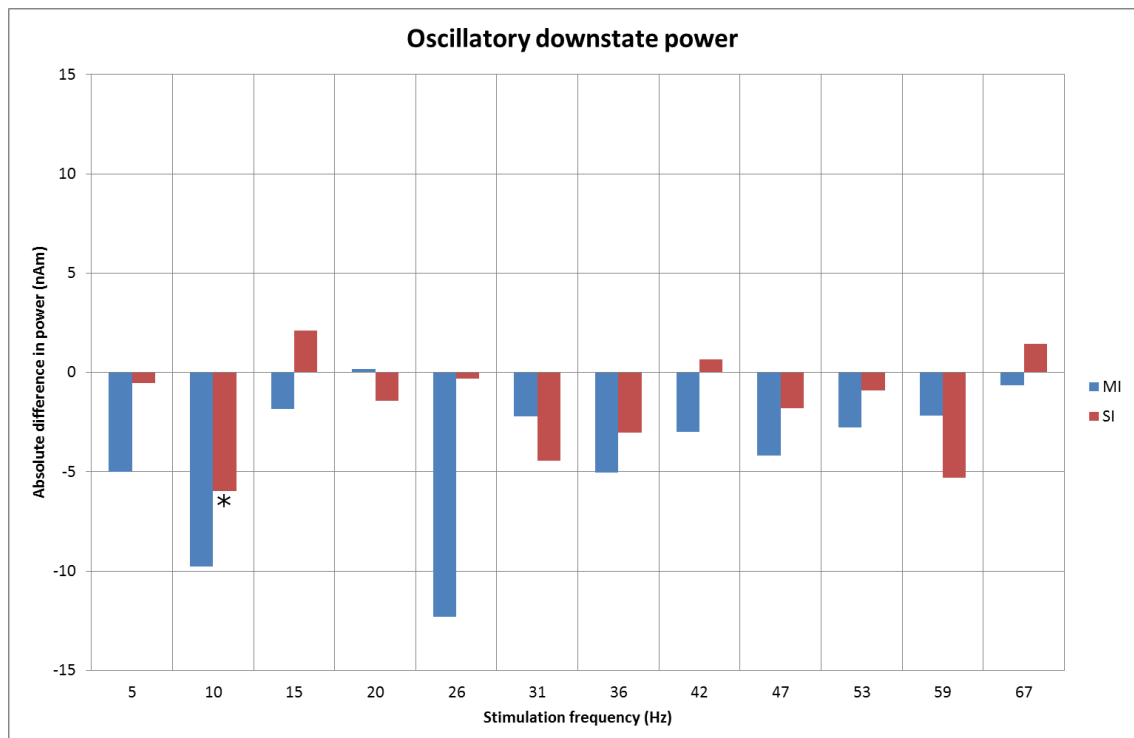
Figure 6. 13. Group-averages of significant and non-significant absolute differences in oscillatory downstate power between before and after stimulation. The mean oscillatory power in the downstate significantly decreased in SI (n=8, red), after 10 Hz stimulation, p<0.05, marked with *. MI is indicated by blue.

154

Table 6. 18. Oscillatory state and power before and after stimulation in humans

Stim. F			% samples at peak F ± SD			
			Pre		Post	
			MI	SI	MI	SI
5		UP%	36.21	36.53	35.30	35.73
		Mean UP power	161.71	83.38	147.42	83.32
		Mean DN power	46.79	24.84	41.81	24.29
10		UP%	35.64	34.82	35.62	35.00
		Mean UP power	170.84	92.34	144.64	68.52
		Mean DN power	51.91	27.51	42.14	21.55
15		UP%	37.46	38.15	34.60	34.83
		Mean UP power	147.47	69.27	146.97	102.00
		Mean DN power	45.51	22.52	43.68	24.62
20		UP%	36.80	35.109	35.25	35.16
		Mean UP power	160.36	88.20	185.10	93.50
		Mean DN power	45.62	25.55	45.78	24.12
26		UP%	35.32	37.15	35.44	35.05
		Mean UP power	229.18	83.07	182.11	79.39
		Mean DN power	56.76	24.67	44.44	24.36
31		UP%	34.31	37.726	32.65	37.38
		Mean UP power	193.96	93.66	180.66	70.70
		Mean DN power	48.15	25.81	45.94	21.35
36		UP%	35.87	36.22	34.46	35.26
		Mean UP power	156.26	78.68	148.30	88.93
		Mean DN power	48.21	25.99	43.17	22.94
42		UP%	36.02	37.73	35.86	35.63
		Mean UP power	167.80	76.32	166.78	94.80
		Mean DN power	47.92	23.30	44.92	23.95
47		UP%	34.78	34.92	37.04	38.77
		Mean UP power	160.01	90.80	127.04	74.77
		Mean DN power	42.33	24.33	38.15	22.53
53		UP%	35.10	38.37	35.59	36.84
		Mean UP power	180.39	72.93	174.83	73.64
		Mean DN power	51.72	24.30	48.96	23.38
59		UP%	36.85	35.37	34.509	35.28
		Mean UP power	111.87	324.28	118.78	319.68
		Mean DN power	39.18	72.10	36.99	66.78
67		UP%	34.86	36.56	36.73	35.99
		Mean UP power	156.69	83.51	161.05	83.59
		Mean DN power	46.15	23.28	45.47	24.73

Grey highlight indicates statistical significance, p<0.05.

Table 6. 19. T-statistics: oscillatory upstate in humans

T-statistics: Upstate percentage in humans							
Stim F.		**MI**	**SI**	**Stim F.**		**MI**	**SI**
5	*T*	0.3478	0.6075	36	*T*	1.2111	0.7259
	p	0.7382	0.5627		*p*	0.2652	0.4915
10	*T*	0.0096	-0.103	42	*T*	0.0712	1.0583
	p	0.9926	0.9208		*p*	0.9452	0.3251
15	*T*	2.9982	1.6693	47	*T*	-1.0053	-3.1376
	p	0.02 (*)	0.139		*p*	0.3482	0.0164 (*)
20	*T*	0.9098	-0.0405	53	*T*	-0.3134	0.796
	p	0.3932	0.9688		*p*	0.7631	0.4522
26	*T*	-0.0748	1.4247	59	*T*	0.9684	0.0631
	p	0.9424	0.1973		*p*	0.3651	0.9515
31	*T*	0.8593	0.1981	67	*T*	-0.9804	0.5049
	p	0.4186	0.8486		*p*	0.3596	0.6291

Abbreviations: *T*=t-statistic, *p*=p-value. Significance $p < 0.05$ is marked with *.

Table 6. 20. T-statistics: oscillatory state mean power in humans

T-statistics: Up- and downstate power in humans									
Stim F.			**MI**	**SI**	**Stim F.**			**MI**	**SI**
5	U	*T*	0.5437	0.0033	36	U	*T*	0.4459	-0.7149
		p	0.6035	0.9975			*p*	0.6691	0.4978
	D	*T*	1.2912	0.147		D	*T*	1.358	0.7749
		p	0.2376	0.8873			*p*	0.2166	0.4637
10	U	*T*	1.3012	3.2937	42	U	*T*	0.0546	-1.3068
		p	0.2344	0.0132 (*)			*p*	0.958	0.2326
	D	*T*	1.8276	2.7426		D	*T*	0.875	-0.3795
		p	0.1103	0.0288 (*)			*p*	0.4106	0.7156
15	U	*T*	0.0382	-1.1972	47	U	*T*	1.1011	0.7237
		p	0.9706	0.2702			*p*	0.3073	0.4927
	D	*T*	0.4805	-0.7414		D	*T*	1.0793	0.564
		p	0.6455	0.4826			*p*	0.3162	0.5903
20	U	*T*	-1.0683	-0.2688	53	U	*T*	0.2946	-0.0563
		p	0.3208	0.7958			*p*	0.7768	0.9567
	D	*T*	-0.0394	2.2073		D	*T*	0.7374	0.3424
		p	0.9697	0.063			*p*	0.4849	0.7421
26	U	*T*	2.245	0.5585	59	U	*T*	-1.9983	0.8981
		p	0.0596	0.5939			*p*	0.0858	0.399
	D	*T*	1.7603	0.1322		D	*T*	0.5723	0.6778
		p	0.1217	0.8986			*p*	0.6653	0.5196
31	U	*T*	1.0955	1.0785	67	U	*T*	-0.1424	-0.0112
		p	0.3095	0.3166			*p*	0.8908	0.9914
	D	*T*	1.0585	0.8393		D	*T*	0.1381	-0.3984
		p	0.325	0.429			*p*	0.8941	0.7022

Abbreviations: U=upstate mean power, D=downstate mean power, *T*=t-statistic, *p*=p-value. Significance $p < 0.05$ is marked with *.

6.3.5.2. *In vitro*

In vitro, in MI LIII the decrease in the upstate percentage after 40 Hz stimulation was significant, $t_{[13]}$=2.627, p=0.0209; After 45 Hz stimulation the mean oscillatory power in the upstate in MI LIII increased significantly, $t_{[13]}$=-2.5356, p=0.0249 (figure 6.14-16). *In vitro*, in MI LV the decrease in the upstate percentage after 40 Hz stimulation was significant $t_{[16]}$=2.3748, p=0.0304. In MI LV the mean upstate power increased significantly after 50 Hz stimulation, $t_{[25]}$=-2.6135, p=0.015 (figure 6.14-16). Non-significant changes are summarised in table 6.21-23.

In vitro, in SI LIV the percentage in the upstate decreased significantly $t_{[19]}$=2.261, p=0.0357 following 45 Hz stimulation. The mean oscillatory power in the upstate significantly increased following 10 Hz stimulation, $t_{[41]}$=-2.2309, p=0.0312. The mean oscillatory power in the downstates significantly decreased after 25 Hz stimulation, $t_{[25]}$=2.3233, p=0.0286. The upstate percentage decreased significantly after 45 Hz stimulation, $t_{[19]}$=2.2611, p=0.0357. Additionally, after 45 Hz stimulation the mean oscillatory power in the upstate increased significantly: $t_{[19]}$=-2.6189, p=0.0169. The mean oscillatory power in the downstates also increased significantly after 45 Hz stimulation, $t_{[19]}$=-2.558, p=0.0192 (figure 6.14-16).
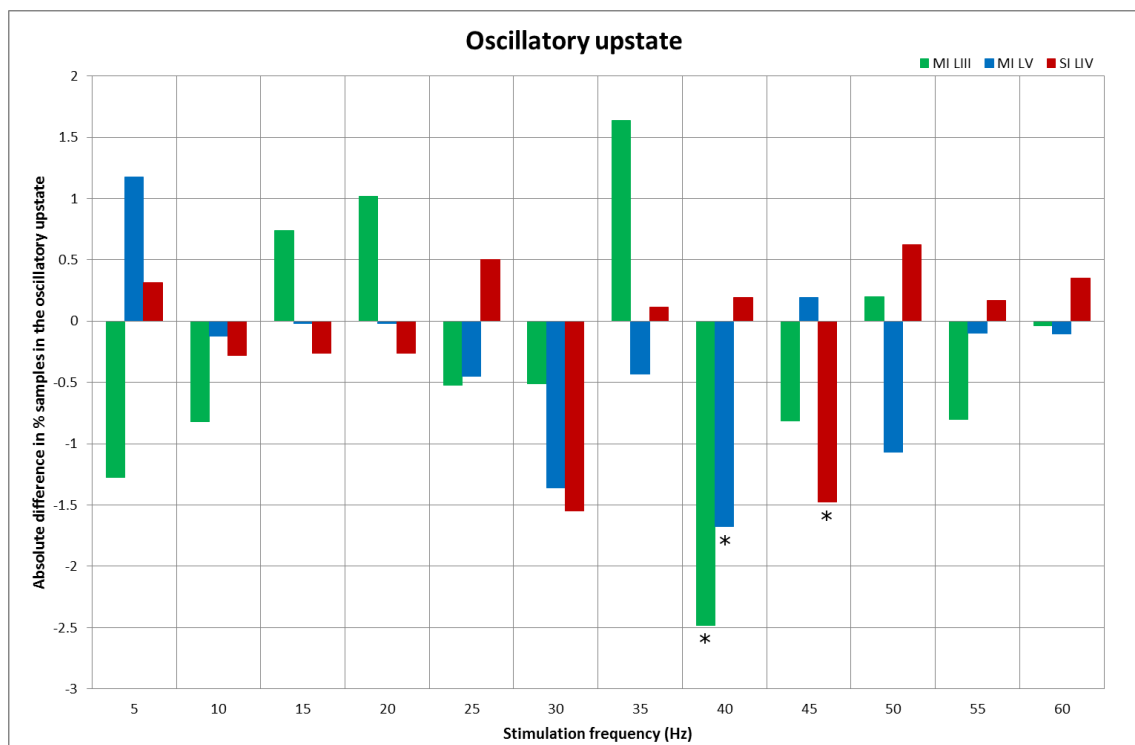
Figure 6. 14. Group-averages of significant and non-significant absolute differences in oscillatory upstate after stimulation with different frequencies. In MI LIII (n=14, green) and MI LV (n=17, blue) the decrease in the upstate percentage after 40 Hz stimulation was significant, p<0.05. In SI LIV (n=20, red) the decrease in the upstate percentage after 45 Hz stimulation was significant, p<0.05. Significant differences are marked with *.
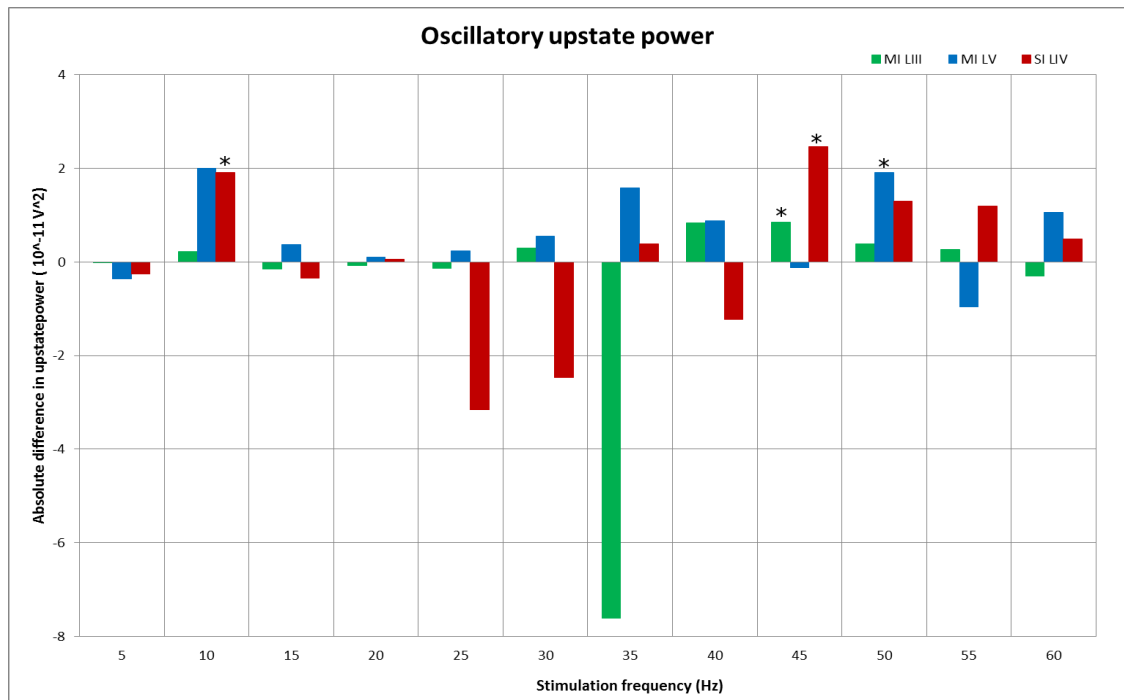
Figure 6. 15. Group-averages of significant and non-significant absolute differences in mean oscillatory upstate power after stimulation with different frequencies. In SI LIV (n=42, red) there was a significant increase following 10 Hz stimulation, p<0.05. After 45 Hz stimulation there was a significant increase in in MI LIII (n=14, green) and SI LIV (n=20), p<0.05. In MI LV (blue) the mean upstate power increased significantly after 50 Hz stimulation (n=26), p=0.05. Significant differences are marked with *.
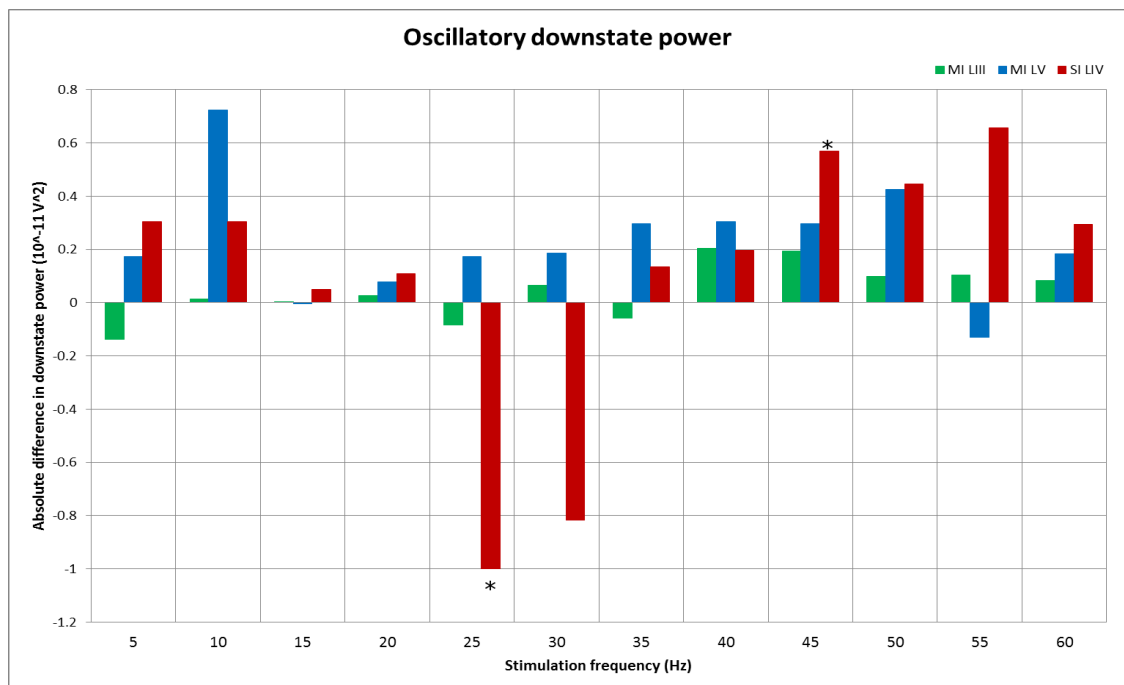
Figure 6. 16. Group-averages of significant and non-significant absolute differences in mean oscillatory downstate power after stimulation with different frequencies. Significant decrease is in SI LIV (red) after 25 Hz stimulation (n=26) and significant increase in SI LIV after 45 Hz (n=20) stimulation, p<0.05. Significant differences are marked with *. MI LIII is indicated by green and MI LV by blue.

Table 6. 21. Oscillatory states and power before and after stimulation *in vitro*

Oscillatory states and power: percentage (%) and power (10^{-11} V^2) change							
Stim. F		Pre			Post		
(Hz)		MI LIII	MI LV	SI LIV	MI LIII	MI LV	SI LIV
5	UP%	39.91	36.69	37.01	38.63	37.87	37.33
	Mean UP power	11.44	25.43	40.73	11.42	25.07	40.48
	mean DN power	4.23	7.61	12.35	4.09	7.78	12.65
10	UP%	39.01	37.16	37.25	38.19	37.04	36.97
	Mean UP power	9.01	22.10	35.24	9.25	24.10	37.15
	mean DN power	3.23	6.74	10.96	3.24	7.46	11.27
15	UP%	37.92	37.28	37.67	38.66	37.26	37.41
	Mean UP power	9.18	22.44	33.92	9.03	22.82	33.57
	mean DN power	3.17	6.79	10.65	3.17	6.79	10.70
20	UP%	37.41	37.51	37.38	38.42	37.49	37.11
	Mean UP power	9.84	19.74	35.51	9.77	19.85	35.56
	mean DN power	3.40	6.13	11.19	3.43	6.21	11.29
25	UP%	37.98	37.86	37.03	37.46	37.41	37.53
	Mean UP power	11.92	24.70	42.67	11.79	24.94	39.51
	mean DN power	4.17	7.55	13.12	4.09	7.73	12.12
30	UP%	39.31	38.25	38.20	38.80	36.89	36.65
	Mean UP power	7.00	16.57	33.46	7.30	17.12	30.99
	mean DN power	2.54	4.97	10.81	2.61	5.16	10.00
35	UP%	36.82	37.82	36.89	38.46	37.39	37.00
	Mean UP power	20.10	25.08	39.06	12.49	26.66	39.46
	mean DN power	4.55	7.81	11.95	4.49	8.11	12.09
40	UP%	39.89	38.58	37.02	37.41	36.91	37.22
	Mean UP power	6.30	16.95	29.71	7.13	17.83	28.49
	mean DN power	2.28	5.50	9.43	2.49	5.81	9.62
45	UP%	38.61	37.55	38.37	37.80	37.74	36.89
	Mean UP power	6.05	21.50	26.89	6.90	21.38	29.35
	mean DN power	2.21	6.36	8.85	2.41	6.66	9.41
50	UP%	38.18	37.64	36.61	38.38	36.57	37.23
	Mean UP power	10.72	23.93	35.17	11.10	25.85	36.48
	mean DN power	3.90	7.40	10.68	4.00	7.82	11.12
55	UP%	38.78	37.24	37.49	37.97	37.14	37.66
	Mean UP power	11.02	21.32	37.36	11.29	20.37	38.55
	mean DN power	3.86	6.47	11.84	3.96	6.34	12.50
60	UP%	38.19	37.68	37.11	38.15	37.58	37.46
	Mean UP power	7.75	19.00	27.71	7.45	20.06	28.19
	mean DN power	2.64	6.01	8.79	2.73	6.20	9.08

Grey highlights indicate statistical significance $p < 0.05$

Table 6. 22. T-statistics: oscillatory upstate percentage *in vitro*

Stim F.		MI LIII	MI LV	SI LIV	Stim F.		MI LIII	MI LV	SI LIV
T-statistics: Upstate percentage *in vitro*									
5	*T*	1.5956	-1.7729	-0.4679	35	*T*	-0.7779	0.6695	-0.0999
	p	0.1329	0.0901	0.6443		*p*	0.4487	0.5101	0.9213
10	*T*	1.0082	0.2796	0.5089	40	*T*	2.627	2.3748	-0.3548
	p	0.323	0.7814	0.6136		*p*	0.0209(*)	0.0304(*)	0.7265
15	*T*	-0.6931	0.0387	0.5663	45	*T*	0.9209	-0.3595	2.2611
	p	0.4932	0.9693	0.5741		*p*	0.3739	0.7236	0.0357(*)
20	*T*	-1.2319	0.0428	0.3842	50	*T*	-0.2658	2.0459	-0.8402
	p	0.2276	0.9661	0.7027		*p*	0.7931	0.0514	0.4091
25	*T*	0.4929	0.793	-0.6711	55	*T*	1.0232	0.1818	-0.3597
	p	0.6297	0.4353	0.5083		*p*	0.3178	0.8567	0.7208
30	*T*	0.4418	1.5851	1.8024	60	*T*	0.0376	0.1314	-0.3895
	p	0.6659	0.1325	0.0874		*p*	0.9705	0.8969	0.7007

Abbreviations: *T*=t-statistic, *p*=p-value. Significance p<0.05 is marked with *.

Table 6. 23. T-statistics: oscillatory upstate percentage *in vitro*

Stim F			MI LIII	MI LV	SI LIV	Stim F			MI LIII	MI LV	SI LIV
T-statistics: Oscillatory state mean power											
5	U	*T*	0.0441	0.5489	0.1616	35	U	*T*	0.942	-1.3188	-0.2844
		p	0.9655	0.5886	0.873			*p*	0.3611	0.2008	0.7785
	D	*T*	0.978	-1.4651	-0.9571		D	*T*	0.3195	-1.2784	-0.4666
		p	0.3447	0.157	0.3485			*p*	0.7538	0.2144	0.645
10	U	*T*	-0.7891	-1.1606	-2.2309	40	U	*T*	-1.5147	-0.3141	0.5936
		p	0.4375	0.2537	0.0312(*)			*p*	0.1538	0.7575	0.5594
	D	*T*	-0.2142	-1.2949	-1.2606		D	*T*	1.7486	-0.4835	-0.4333
		p	0.8321	0.2038	0.2146			*p*	0.1039	0.6353	0.6694
15	U	*T*	0.3015	-0.5091	0.3147	45	U	*T*	-2.5356	0.3026	-2.6189
		p	0.765	0.6135	0.7545			*p*	0.0249(*)	0.7659	0.0169(*)
	D	*T*	-0.0496	0.0283	-0.2808		D	*T*	-1.5769	-1.2631	-2.558
		p	0.9607	0.9775	0.7801			*p*	0.1388	0.2236	0.0192(*)
20	U	*T*	0.2638	-0.2694	-0.0445	50	U	*T*	-0.873	-2.6135	-1.2514
		p	0.7937	0.7891	0.9647			*p*	0.393	0.015(*)	0.2229
	D	*T*	-0.3694	-0.6141	-0.3806		D	*T*	-1.0719	-1.652	-1.9463
		p	0.7144	0.543	0.7054			*p*	0.2965	0.111	0.0634
25	U	*T*	0.1766	-0.2501	1.8967	55	U	*T*	-0.6358	0.996	-1.0928
		p	0.8624	0.8045	0.0695			*p*	0.5318	0.3255	0.2807
	D	*T*	0.4127	-0.7599	2.3233		D	*T*	-0.9848	0.7044	-1.3437
		p	0.6861	0.4544	0.0286(*)			*p*	0.336	0.4855	0.1863
30	U	*T*	-1.1744	-1.5272	0.4908	60	U	*T*	0.3654	-1.1344	-0.284
		p	0.2613	0.1462	0.6292			*p*	0.7196	0.2715	0.779
	D	*T*	-0.9194	-1.921	0.6072		D	*T*	-0.648	-1.3559	-0.8495
		p	0.3746	0.0727	0.5509			*p*	0.5262	0.1919	0.4048

Abbreviations: U=upstate mean power, D= downstate mean power, *T*=t-statistic, *p*=p-value. Significance p<0.05 is marked with *.

6.3.6. Summary of results

There are several differences in the effects of different frequencies in stimulation and between modalities. Here we summarise the significant effects on frequency, power, variability and state.

6.3.6.1. Power

In MEG recordings, 10 Hz stimulation significantly decreases the mean peak power of the beta activity in SI. In the *in vitro* recordings in MI LIII 5, 40 and 55 Hz stimulation significantly increases the mean peak power of beta activity.

6.3.6.2. Frequency

In MEG recordings 36 and 53 Hz stimulation significantly increases the mean beta peak frequency in SI. In the *in vitro* recordings 20 Hz stimulation significantly decreases the mean beta peak frequency in MI LIII.

6.3.6.3. Frequency variability

In MEG recordings 36 Hz stimulation significantly decreases the variability in MI and SI. *In vitro* recordings 20 and 55 Hz stimulation significantly increases the variability in MI LIII.

6.3.6.4. Power state

In MEG recordings 15 Hz stimulation significantly decreases the percentage of samples found in the upstate in MI. In SI 47 Hz stimulation significantly increases the upstate percentage. The up- and downstate mean power in SI significantly decreases after 10 Hz stimulation. In the *in vitro* recordings 40 and 45 Hz stimulation significantly decreases the upstate percentage in MI LIII, LV and SI LIV. The upstate mean power is significantly increased after 45 Hz stimulation in MI LIII, after 50 Hz in MI LV and after 10 and 45 Hz stimulation in SI LIV. The mean downstate power is significantly decreased in SI LIV after 25 Hz and increased after 45 Hz stimulation.

6.4. Discussion

6.4.1. Somatosensory stimulation affects SI activity in humans and MI LIII *in vitro*

Early studies using MNS detected sensory evoked fields in SI using MEG (Forss *et al.*, 1994a; 1994b), and MNS is reported to functionally activate both MI and SI in fMRI (Speigel *et al.*, 2000). The functionally related effects on oscillatory activity in MI and SI, e.g. ERD and ERS/PMBR, after single pulse MNS and tactile stimulation are well-established (Salmelin & Hari 1994; Salenius *et al.* 1997; Schnitzler *et al.* 1997; Chen *et al.*, 1999; Nikouline *et al.*, 2000; Cheyne *et al.*, 2003). While we found both beta ERD and ERS after MSN of all frequencies (data not shown), in agreement with the cited beta ERD/ERS studies, we focused on the long-lasting effects on ongoing sensorimotor oscillations from somatosensory stimulation of varying frequencies. In our experiments, MNS resulted in significant long-lasting effects, e.g. significant effects after stimulation offset. These are predominantly found on the mean peak frequency and power of the ongoing oscillatory activity in SI, but not in MI.

In contrast, the significant changes in mean peak frequency and power after electrical stimulation in SI LIV *in vitro* were seen only in MI LIII. A previous study applying stimulation in MI LIII, noted frequency specific long-lasting effects both in MI LIII and MI LV, although the effect in MI LV was delayed (Yamawaki *et al.*, 2008). Application of TMS over MI is also suggested to exert its main effect on the superficial layers (Rothwell 1991; Fugetta *et al.*, 2005; Di Lazzaro *et al.*, 2012). The lack of significant changes in MI LV after stimulation in SI LIV suggests there is little possibility of lasting effects from driving oscillations between MI LIII and MI LV with input in SI LIV. As MI LV is considered an output station, containing cortico-spinal cell soma (Rivara *et al.*, 2003), this also suggests that there is little ability for indirect driving of motor output from SI LIV.

6.4.2. Distinct effects of specific stimulation frequencies

Our experiments show that regardless of similarities in results between MEG and *in vitro*, beta and mu stimulation frequencies are preferential in eliciting effects in MI and SI. Applying an external rhythm is more likely to drive the underlying neural substrate if the applied rhythm is close to the natural frequency (Fries 2005; Schnitzler & Gross 2005; Rosanova *et al.*, 2009; Thut *et al.*, 2011a). rTMS over the occipital or parietal cortex at alpha frequency entrains the local alpha activity with subsequent power increase during stimulation (Thut *et al.*, 2011a), but also <3 min after (Zahele *et al.*, 2010). 20 Hz rTMS

over MI resulted in a long-lasting (<5 min) significant increase in alpha power (Veniero *et al.*, 2011). In contrast, our experiments found that applying somatosensory stimulation at 10 Hz significantly decreased the peak power of the ongoing activity in SI after the stimulation; addition of a peripheral 10 Hz rhythm desynchronises the ongoing oscillatory activity in SI. Other frequencies are less effective at this in SI, or not at all in MI. The significant decrease in mean peak power in SI after 10 Hz also encompassed significant decreases in both the oscillatory up- and downstate.

Application of beta rhythms over MI is reported to increase the beta power of the ongoing MI activity and have effects on functional tasks (Paus *et al.*, 2001; Fugetta *et al.*, 2005; van der Warf & Paus 2006; Pogosyan *et al.*, 2009; Feurra *et al.*, 2011; Thut & Miniussi 2011; Joundi *et al.*, 2012). We found no significant effects on oscillatory peak power in MI after any of the stimulation frequencies. This difference in results could be due to the difference in analysis approach or too few recordings; although we speculate that it is due to the stimulation method. Importantly we noted significant changes of the oscillatory power state distribution in MI after 15 Hz stimulation; the pattern of oscillatory activity changes.

Previous *in vitro* reports have investigated the long-lasting effects on peak power of the oscillatory activity in MI LIII and MI LV. Effects after MI LIII stimulation was studied specifically after 4, 20 and 125 Hz. Activity in MI was reinforced at the gamma and theta stimulation frequencies, and 20 Hz stimulation also promoted gamma and theta frequency activity (Yamawaki *et al.*, 2008). We found significant increases of the mean peak power of the ongoing oscillatory activity in MI LIII after 5, 40 and 55 Hz stimulation, suggesting increased synchronisation after these frequencies. We did not find any significant effects of different frequency stimulations on the mean peak power in MI LV, or from the beta frequency range of stimulation. This could be due to the difference in slice preparation, stimulation location and/or application; we used 1-site bipolar stimulation in SI LIV in intact slices compared to 2-site bipolar stimulation in MI LIII in microslices. The analysis approaches are also different, it is plausible that our results would support cited if band-pass filtering was employed, or focus on specific frequencies. However, our focus has been on determining specific effects of different stimulation frequencies on the *ongoing oscillatory activity* in sensorimotor areas.

Effects on the peak frequency have generally not been considered in detail previously. In addition, as we determine the mean peak frequency of MI and SI differently in this study compared to most published reports, the extrapolation of our reported effects on ongoing frequencies onto other studies become difficult. Nevertheless, we found that MNS at 36

and 53 Hz significantly increased the frequency of ongoing oscillatory activity in SI. These effects suggest that the neuronal network, or oscillator(s), responsible for the oscillatory activity in SI are more easily perturbed by these frequencies. *In vitro*, there was also a significant effect on the mean peak frequency, but in MI LIII; a significant decrease after 20 Hz stimulation. The significant effects on oscillatory frequency were further reinforced by the significant decrease in frequency variability after 36 Hz stimulation in both MI and SI in the MEG recordings. In addition, the frequency distribution was significantly increased after 20 and 55 Hz stimulation in MI LIII *in vitro*.

Most studies in humans do not look at long-lasting effects on the ongoing sensorimotor oscillatory activity apart from cited functional changes. Given the role of MI as a motor centre, with less importance in somatosensory processing, it is possible that effects in MI are particularly transient and would not be seen after stimulation offset. Indeed, preliminary results investigating peak power changes in the ongoing activity in MI at the frequencies of stimulation indicate that there are frequency specific effects to be found in MI, see figure 6.17 below.
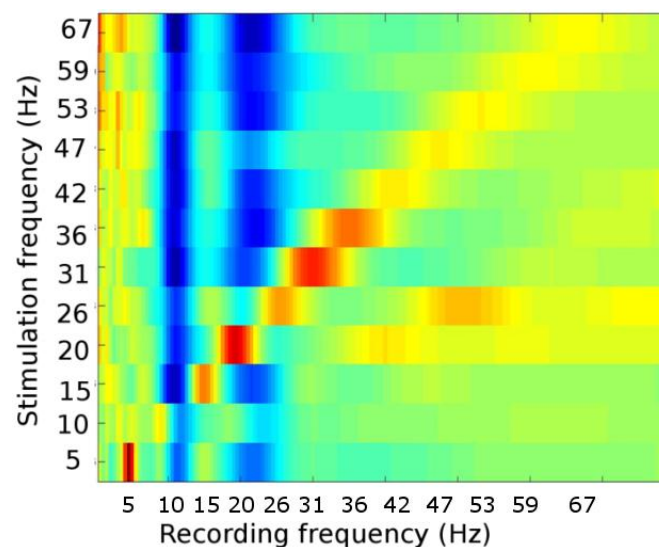
Figure 6. 17. Group-average Morelet-wavelet combination spectrogram summarising the oscillatory activity at the stimulation frequency in MI during MNS of different frequencies.

We have not yet investigated long-term effects on the specific frequency bands of stimulation due to time restrictions. It is possible that there are long-lasting effects after certain frequencies of stimulation. Further analysis of these experiments would determine that.

6.4.3. Comparisons between *in vitro* and MEG

An important point to make when comparing these modalities is that the amplitude of stimulation is not necessarily comparable between MEG and *in vitro*, which could be one reason for differences in results. As the connectivity between MI and SI is vast and complex, we speculate that the lack of long-lasting effects on oscillatory power and frequency in MI from MNS is due to the processing of the somatosensory information prior to reaching SI. This could also be an underlying reason for differences in results between MEG and *in vitro* recordings. There are several input routes from the median nerve to the cortex that do not pass MI. In addition, peripheral somatosensory stimulation passes through thalamus before arriving in the somatosensory areas. The thalamocortical axons terminate mainly in layer IV, but also in the deep part of layer III of SI (Herkenham 1980; Shipp 2007). Reciprocal connections like these are lost in the *in vitro* preparation; their importance in maintaining oscillations is unknown. Here, *in vitro* stimulation was delivered straight into middle layers of SI, with nowhere else to go but in the local sensorimotor network in the sensorimotor slice. A comparison between TMS applied stimulation and our *in vitro* protocol would further the comparison since TMS pulses are believed to affect the superficial layers of motor cortex (Rothwell 1991; Fugetta *et al.*, 2005; Di Lazzaro *et al.*, 2012).

6.5. Conclusion

There appears to be limited ability of the cortex in any modality to sustain activity of an imposed frequency for longer periods of time, e.g. after stimulation offset. There are effects on the ongoing oscillations after stimulation of different frequencies, but only a few examples of continued activity such as rearrangement, or reinforcements of ongoing rhythms with increased synchronisation. Previous neuroimaging literature has focused on the effects during stimulation, with reported entrainment. Here, there are observed significant differences after stimulation at different frequencies in both modalities, but they are not consistent between recording methods. This indicates that the differences in complexity of the studied neuronal networks, protocol, and underlying source size make it difficult to disentangle details. There is evidence in these studies suggesting that that the beta or mu range rhythms in the sensorimotor neuronal networks are more prone to long-lasting effects of somatosensory stimulation, but the details of these effects are unclear.

Chapter 7. Effects of theta burst stimulation on ongoing oscillations in the sensorimotor cortex

7.1. Introduction

7.1.1. Background

In the previous chapters we showed that connectivity is important for the oscillatory activity in the sensorimotor cortex. We showed that applying stimulation in distant areas affects oscillatory activity even far away. Here we will consider another stimulation protocol, reported to affect the sensorimotor cortex excitability in a well-established fashion, although the detailed effects on the ongoing oscillatory neuronal network activity is less reported.

TMS has been around for a few decades and has showed great potential in fundamental neuroscientific research and neurological therapeutic settings (Wassermann & Ziemann 2012). Applying TMS over MI is believed to primarily excite pyramidal neurons in the superficial layers and thereby indirectly activate layer V pyramidal cells and local interneurons (figure 7.1.) (Di Lazzaro *et al.*, 2012).
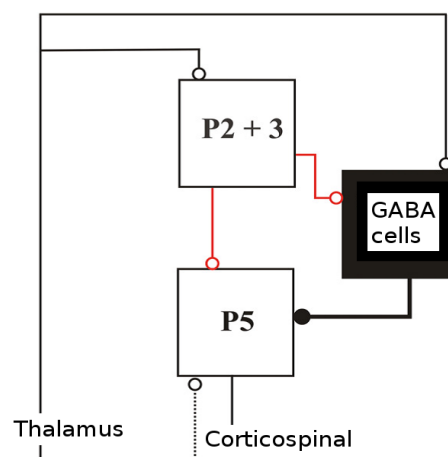
Figure 7. 1. TMS over MI is suggested to result in a descending volley effectively starting at the pyramidal cells in layer II and III (P2 and P3). Figure modified from Di Lazzaro *et al.* (2012).

7.1.1.1. Continuous theta burst stimulation

Theta burst stimulation (TBS) is a repetitive TMS protocol. Repetitive TMS protocols have different effects on function depending on the pattern of repetition. The effect duration is variable and according to some researchers depends on the duration of the stimulation (Hoogendam *et al.*, 2010). In TBS the TMS pulses are delivered at theta frequency (figure 7.2). Here we use continuous theta burst stimulation (cTBS) which is an effective protocol with stimulation for 40s and long-lasting effect on motor cortical excitability of <45 min (Huang *et al.*, 2005). TMS-applied cTBS has been shown to depress motor cortex excitability and impair motor function in healthy subjects, while a different, intermittent, pattern of theta burst stimulation is reported to increase the excitability of MI (Huang *et al.*,

2005; Lazzaro *et al.* 2005; 2008; Suppa *et al.*, 2008). The concentration of GABA in MI has been found to be increased after cTBS; indicating that that the motor cortex is more inhibited during this time and that cTBS indeed can modulate motor cortex activity (Stagg *et al.*, 2009). Association between MI beta oscillations and motor excitability have been suggested by Mäki & Ilmoniemi (2010), although the exact nature of this association is less clear.
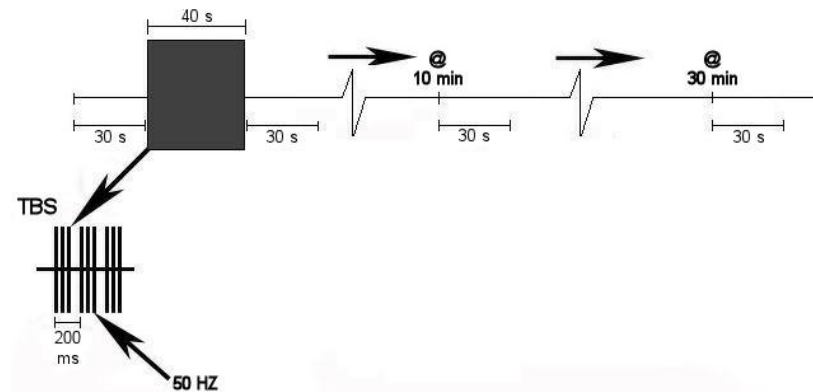
Figure 7. 2. cTBS protocol. Three pulses of 50 Hz interspersed with 200 ms from the first burst to the next one, e.g. 5 Hz over all. The stimulation lasts for 40s, corresponding to 600 pulses. The oscillatory activity at different time points after cTBS was characterised offline.

The idea of altering cortical activity and excitability using stimulation is far from new, it was described by Penfield already in 1950's (Sanes & Donoghue 2000). Mechanisms underlying the effects seen after different burst stimulation patterns have been intensively studied *in vitro* and *in vivo* for several decades (Diamond *et al.*, 1988, Kirkwood *et al.,* 1993).

7.1.1.2. TBS *in vitro*

TBS was initially applied in hippocampal studies to study long-term potentiation (LTP) and long-term depression (LTD) (Larson & Lynch 1988; Capocchi *et al.*, 1992; Ngyen & Kandel 1997; reviewed by Malenka & Bear 2004). Studies investigating LTP and LTD in motor cortex followed quickly as plasticity is extremely relevant to the dynamic nature of the cortex particularly MI (Hess *et al.*. 1994; Castro-Alamancas *et al.*, 1995; Hess & Donoghue 1996; 1999). Motor cortex flexibility and plasticity is a century old topic of research, described initially by Brown and Sherrington in 1912 (Sanes & Donoghue 2000), and the LTP phenomenon saw the printed light in 1973 by Lømo and Bliss (Lømo, 2003). Equally, suggested mechanisms underlying plasticity in motor cortex, e.g. NMDA-dependency, are well-established *in vitro* (Hess *et al.*, 1994; Ziemann *et al.*, 1998; Stefan *et al.*, 2000, Huang *et al.*, 2007a).

7.1.1.3. Mechanisms of TBS

The underlying physiological mechanisms of TBS are believed to be the result of the same neuroplastic effects elicited by LTP/PTD paradigms (Hoogendam *et al.* 2010; Funke & Benali 2011). Different TBS patterns have different effects on the motor excitability; some more obvious than others. Small modifications of the cTBS pattern described by Huang *et al.* (2005), resulted in longer depression of the excitability and subsequently suggested differences in plasticity (Goldsworthy *et al.*, 2012); other studies have found that the excitability and plasticity of MI can be reversed quickly and is dependent on the prior state of activity in MI (Gentner *et al.*, 2007).

While cTBS has been shown to elicit profound effects on both cortico-spinal excitability and motor performance (Huang *et al.*, 2005), the effects of this stimulation on neuronal network activity is unclear. A recent study in humans reported that cTBS enhanced synchronisation in the lower beta band (13-19.5 Hz), e.g. power in this band increased after cTBS (Noh *et al.*, 2012), while another found no effect on alpha or beta power in MI (McAllister *et al.*, 2011). Both these studies used EEG and implemented a limited spatial approach with only a few electrodes at relevant areas. Furthermore, there is no research on the effects of applying cTBS patterns on oscillations at the laminar level of the sensorimotor cortex.

7.1.2. Aims and research objectives

Stimulation of MI using cTBS is shown to elicit transient motor impairment in human lasting up to an hour. The effects of this stimulation on neuronal network activity are unknown. Disorders affecting motor function, such as Parkinson's disease have an accompanying increase in beta power. It is unclear whether these same effects can be observed as a result of the cTBS model of transient motor impairment. Furthermore, given the potentially broad effects of TMS, it is unclear to what extent the specific cortical laminae are responsible for the changes in neuronal network activity following cTBS. Here we aim to clarify these attribute by addressing the following questions:

- o What are the effects of cTBS stimulations on spontaneous MI oscillations in humans?
- o What are the effects of cTBS stimulation on spontaneous oscillations in the various laminae of MI *in vitro*?

7.2 Methods

7.2.1. Neuroimaging experiments

These experiments were done in collaboration with Dr Craig McAllister at the Brain stimulation laboratory at Aston Brain Centre. Sixteen right handed healthy volunteers (19–44 years, 9F) with normal or corrected to normal vision participated in the study. The study was performed in accordance with the Declaration of Helsinki, and approved by the Ethics Committee of the School of Life and Health Sciences at Aston University. Written informed consent was obtained from all participants. The electromyographic (EMG) activity of the first dorsal interosseous (FDI) muscle in the right hand was recorded using bipolar, single differential surface EMG electrodes (DE-2.1, Delsys Inc, Boston, MA), and measured as a motor evoked potential (MEP). The surface electrodes comprised two 10 mm x 1 mm silver bar strips, spaced 10 mm apart, with a 20 Hz to 450 kHz bandwidth, 92 dB common mode rejection ratio, and $>10^{15}$ Ω input impedance. The electrodes were placed over the muscle and a reference ground electrode was placed over the ulnar process of the right wrist. The EMG signal was digitized with a sampling rate of 2 kHz using a Micro 1401 analogue-digital converter and analysed using Signal version 4 (Cambridge Electronic Design, Cambridge, UK). Single pulse TMS was performed using a Magstim 2002 stimulator and continuous theta burst stimulation (cTBS) was performed using a Magstim Super Rapid stimulator (Magstim Co. Ltd, Whitland, UK), both performed using a 70 mm diameter figure-of-eight coil, held tangentially to the scalp with the coil handle pointing backwards approximately 45º laterally. The optimal position for evoking a response in the FDI muscle was marked on the scalp and the coil position was then fixed using a mechanical arm (Manfrotto & Co., Cassola, Italy). Active motor threshold (AMT) was defined as the minimum stimulator output necessary to evoke an MEP of at least 200 μV in five out of 10 consecutive trials from the FDI muscle as participants used visual feedback to maintain a force level corresponding to approximately 5% maximum voluntary contraction. Participants were instructed to open their eyes and to relax their hand and finger muscles during all other TMS procedures.

The effects of cTBS on ongoing oscillatory activity in the human motor cortex were investigated using MEG before and after cTBS sessions. The participants were instructed via visual cues to make right or left finger abductions. These were later on used to establish PMBR and localise MI through the VE SAM approach described in chapter 2, 3, 5 and 6.
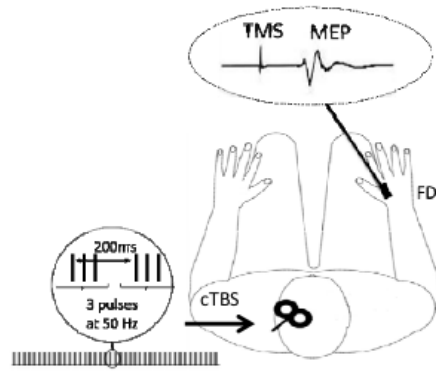
Figure 7. 3. Schematic showing the position of the coil over MI with a summarized view of the cTBS protocol. The EMG electrode was placed over the first dorsal interosseos muscle and the motor evoked potentials were recorded here after single pulse TMS over MI.

The peak amplitude of spontaneous oscillatory power within the beta band (15-35Hz) was calculated for three 60s rest periods from three MEG recording blocks, pre-TBS, post-TBS1 (10-25 minutes after cTBS) and post-TBS2 (30-45 minutes after cTBS), for both left and right MI. Repeated measures (RM) ANOVA was used to test for significant changes in beta power. The cTBS protocol consisted of 3 pulses of 50 Hz, interspersed with 200 ms, and continued for 40s (figure 7.3). The pulses were applied at 80% of the active motor threshold and over the left motor hot spot. The measurements from the ipsilateral hemispheres and finger (e.g. left) served as controls for the MEG experiments.

7.2.2. *In vitro*

In an attempt to specifically seek out which area in the sensorimotor cortex would be most affected by cTBS treatment, as well as how neighbouring areas respond to this, we employed a protocol similar to the neuroimaging cTBS experiment. Intact sensorimotor slices were prepared using protocol 2, described in chapter 2. All animal experiments were performed in accordance with the Aston University ethical review board regulations, as well as the Animals Scientific Procedures Act 1986; European Communities Directive (86/609/EEC). Brains from p18-p22 (50-60g) male Wistar rats were extracted. 450 μm thick sagittal sensorimotor slices were stored in a tissue interface chamber at room temperature for >1h. The slices were then transferred to a recording chamber with a temperature of 33-34°C and a continuous flow rate of 2 ml/min aCSF with added KA and CCh; concentrations and preparations according to protocol 2. Recordings of LFPs from superficial layers (II/III) and deeper layers (V) of MI and middle layer (IV) of SI (figure 2.6) were made. The electrodes were placed in relevant layers, identified by using a dissecting microscope and the Rat Brain Atlas (Paxinos & Watson 1986) as reference. LFP recording started after the KA- and CCh-induced oscillatory activity had stabilised, >1h in the recording chamber with KA and CCh in the aCSF flow, and lasted for >3h.

We used electrical stimulation instead of TMS, but the cTBS still lasted for 40s. The cTBS pattern was applied to MI LIII (cTBS$_{MI\,LIII}$), MI LV (cTBS$_{MI\,LV}$) and SI LIV (cTBS$_{SI\,LIV}$). Once the LFP recordings had been pre-processed and converted to MatLab format, datasets with artefacts were discarded. This left the following numbers for analysis, for cTBS$_{MI\,LIII}$, MI LIII: n=7; MI LV: n=10; SI LIV=10. For cTBS$_{MI\,LV}$, MI LIII: n=8; MI LV: n=10; SI LIV: 9. For cTBS$_{SI\,LIV}$, MI LIII: n=8; MI LV: n=10; SI LIV=9. Analysis of these recordings was centred around five different time points. 30 s immediately before stimulation was defined as the baseline (Pre). The oscillatory activity (during 30 s) in the different areas was compared to this baseline immediately, 10, 20 and 30 minutes after cTBS; post 0 min, post 10 min, post 20 min and post 30 min, respectively. Morelet-wavelet average spectrograms of recordings from specific locations were calculated and used for further analysis.

The intensity of the constant current stimulator was set at 1.5mA with a pulse width of 100 µs. The stimulation protocol was programmed and controlled through Spike2 (CED, Ltd), which was also used for recording the LFPs and online FFT analysis. Recorded data was exported to MatLab and 30s time periods, pre and post of each stimulation event were exported as separate trials to MatLab in spreadsheet format. From these trials Morelet-Wavelet spectrograms were derived and used for the offline analysis with the previous described analysis approach, for details see chapter 2.

The data from the *in vitro* experiments underwent the analysis approach we developed for this project (which was not the case at the time of writing for the MEG data). The mean peak frequency and peak power was determined for each sample in the 30s epoch (30000 samples) with a sliding window approach applied to the Morelet-wavlet spectrograms. The frequency distribution of the oscillations was determined using FWHM. The frequency variability was computed using the amplitude-independent peak frequency distribution, where the peak frequency of each sample was sorted into frequency bins of 1 Hz. Variability in oscillatory power was determined using an amplitude sorting measurement to determine the time and amplitude changes of oscillatory up and down states. We used student's T-tests to statistically test for differences between before and after stimulation. The pre time period was individually compared to each one of the 4 post-conditions, but not in between each other as this would require a different statistical approach. Further details regarding analysis can be found in chapter 2.

7.3 Results

7.3.1. cTBS in humans

7.3.1.1. Functional effects of cTBS

In the TMS-based cTBS study we applied cTBS over MI. 8 participants demonstrated a significant decrease in MEP amplitudes, e.g. <90% mean reduction from baseline recorded from the FDI muscle in the 5-45 minutes following cTBS application; the responders. The other 8 participants did not show an increase or indeed any response; the non-responders. There was no significant difference in the baseline MEP amplitude between the two groups of participants. RM ANOVA revealed significant interaction of group x block on MEP amplitude: $F_{(2,28)}=16.8$, $p<0.001$. Compared to baseline, MEP amplitudes of the responder participants were reduced by 243 µV at post-TBS1, $p=0.03$; and by 263 µV at post-TBS2, $p=0.01$,. In contrast, MEP amplitudes of the non-responder participants showed a non-significant increase at post-TBS1 and a significant increase of 308 µV, $p=0.003$, at post-TBS2 (figure 7.4).
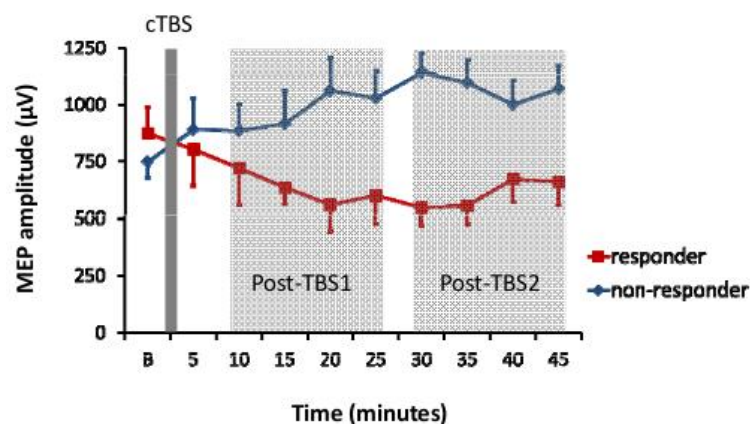
Figure 7. 4. Functional effects of cTBS. In responders (n=8) the MEP significantly decreased at post-TBS1 and post-TBS2, $p<0.05$ and <0.01 respectively. Non-responders (n=8) showed a significant increase only at post-TBS2, $p<0.05$.

7.3.1.2. cTBS effects on ongoing beta power in MI

The RM ANOVA confirmed a significant interaction of hemisphere x group $F_{(1,14)}=6.32$, $p=0.025$. The interaction effect was due to the responder participants having a significant increase in left MI beta-band power from pre-TBS to post-TBS recordings, $p=0.012$. No such effect was detected in the right MI of responder participants or either MI of non-responder participants. The non-responding group of participants showed no significant effect on the ongoing beta power (figure 7.5).
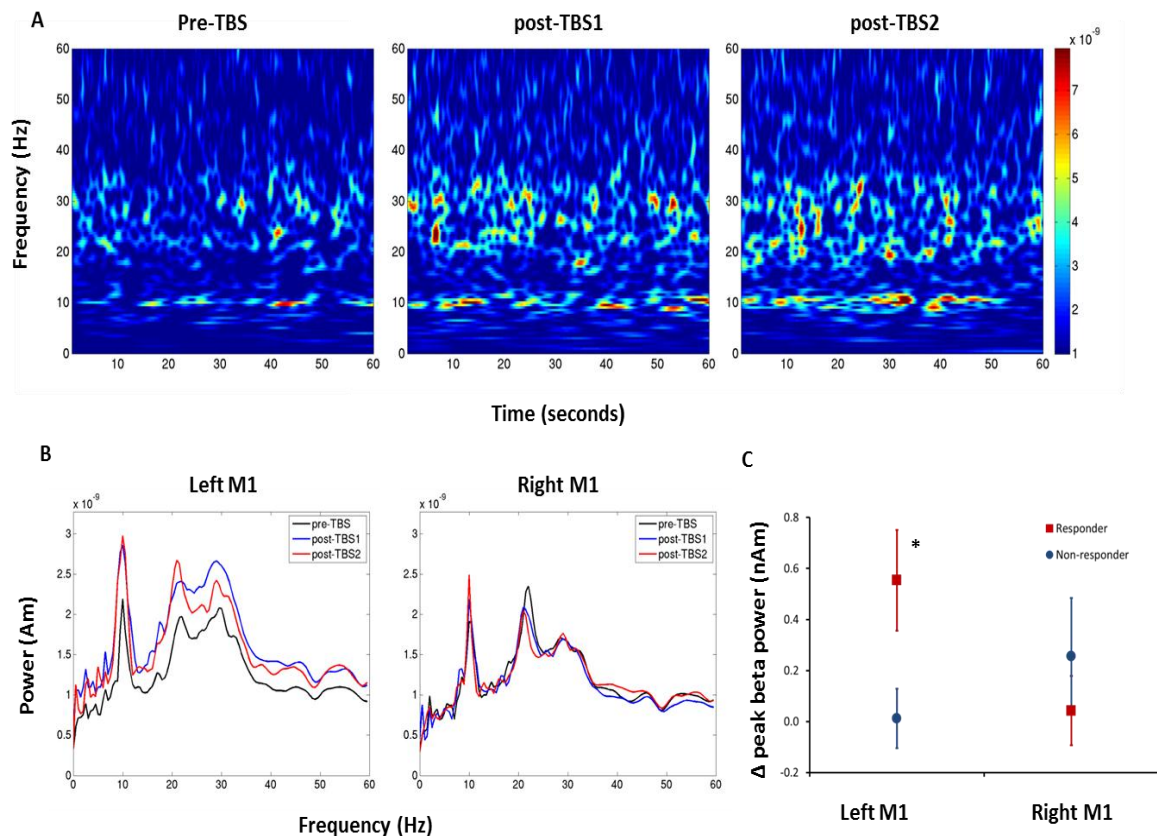
Figure 7. 5a-c. The averaged time-frequency spectrograms from the stimulated MI in one participant show the increase in spontaneous beta power at two different time points after cTBS, seen in A (top row). In B (bottom right and middle), the time-averaged PSD plots further illustrate the increase in spontaneous overall oscillatory power seen in the stimulated left MI (right), compared to the non-stimulated right MI (middle) from one participant. The effects on spontaneous beta power (15-30 Hz) is summarized in C, (bottom left), showing the significant increase beta power in left MI of responders (n=8), indicated by *, p<0.05. SEMs are indicated by error bars.

7.3.2. Effects of cTBS on oscillatory power and frequency *in vitro*

Next, we wanted to localise the source of the increased beta activity seen in MI after cTBS so we used a similar protocol *in vitro*. We stimulated MI LIII and LV, as well as SI LIV, with the cTBS protocol and recorded oscillatory activity up to 30 minutes after cTBS. Applying cTBS to the different areas of interest in the sensorimotor cortex *in vitro* indicated that the effects of cTBS are predominantly local with some differences in effects between areas of stimulation.   Figure 7.6-8 show overviews of these experiements. In an effort to quantify any changes to the variables we were measuring we used Student's t-test to distinguish between two time-points: before and one of the post-stimulation time points.
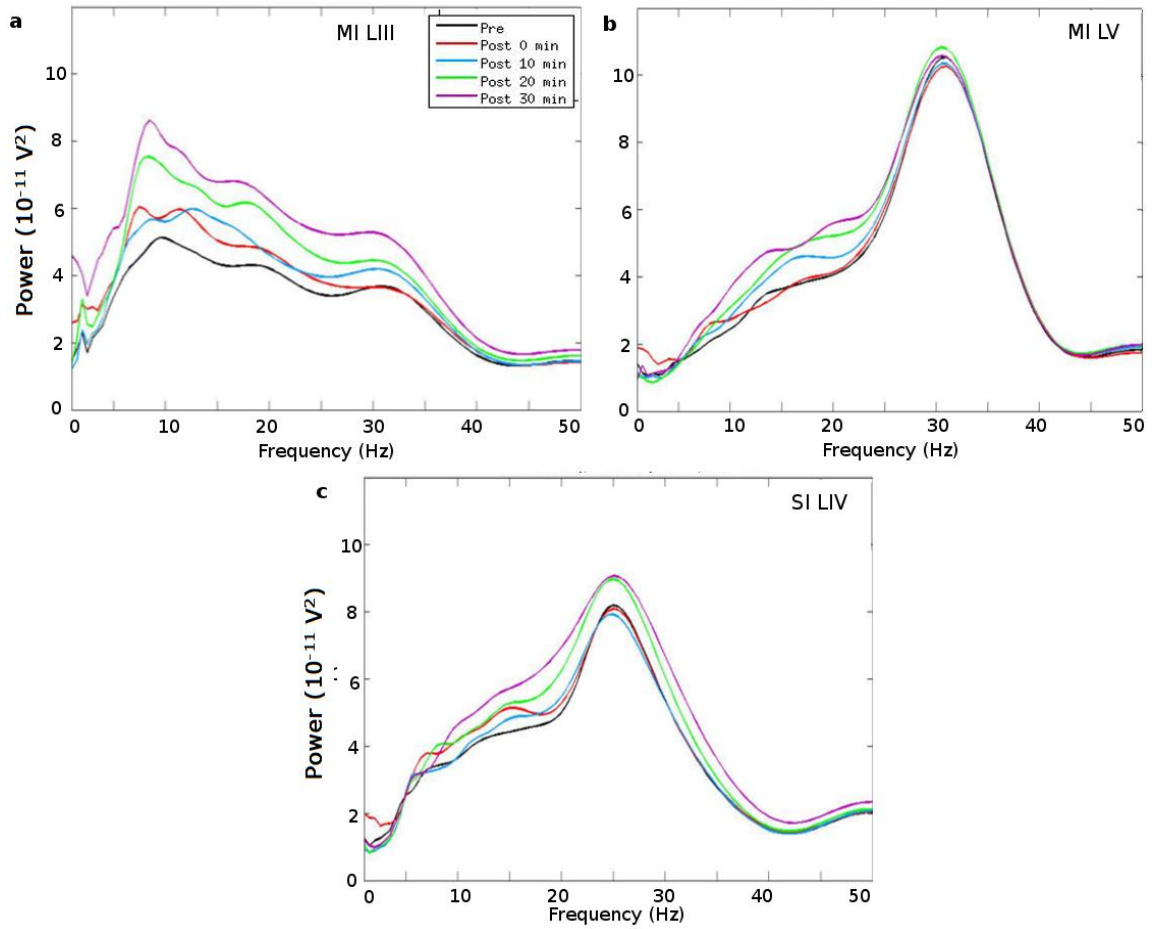
Figure 7. 6a-c. Group- and time-averaged PSDs showing the oscillatory profiles at different time points after cTBS$_{MI\ LIII}$, recorded in in MI LIII (n=7), seen in a (top left); MI LV (n=10), seen in b (top right); and SI LIV (n=10), seen in c (bottom). The PSD from the time period before cTBS$_{MI\ LIII}$ (Pre) is illustrated with a black line, .the time period immediately after cTBS$_{MI\ LIII}$ (Post 0 min) is illustrated by red, 10 minutes after cTBS$_{MI\ LIII}$ (Post 10 min) by blue, 20 minutes after cTBS$_{MI\ LIII}$ (Post 20 min) by green and 30 minutes after cTBS$_{MI\ LIII}$ (Post 30 min) by purple.
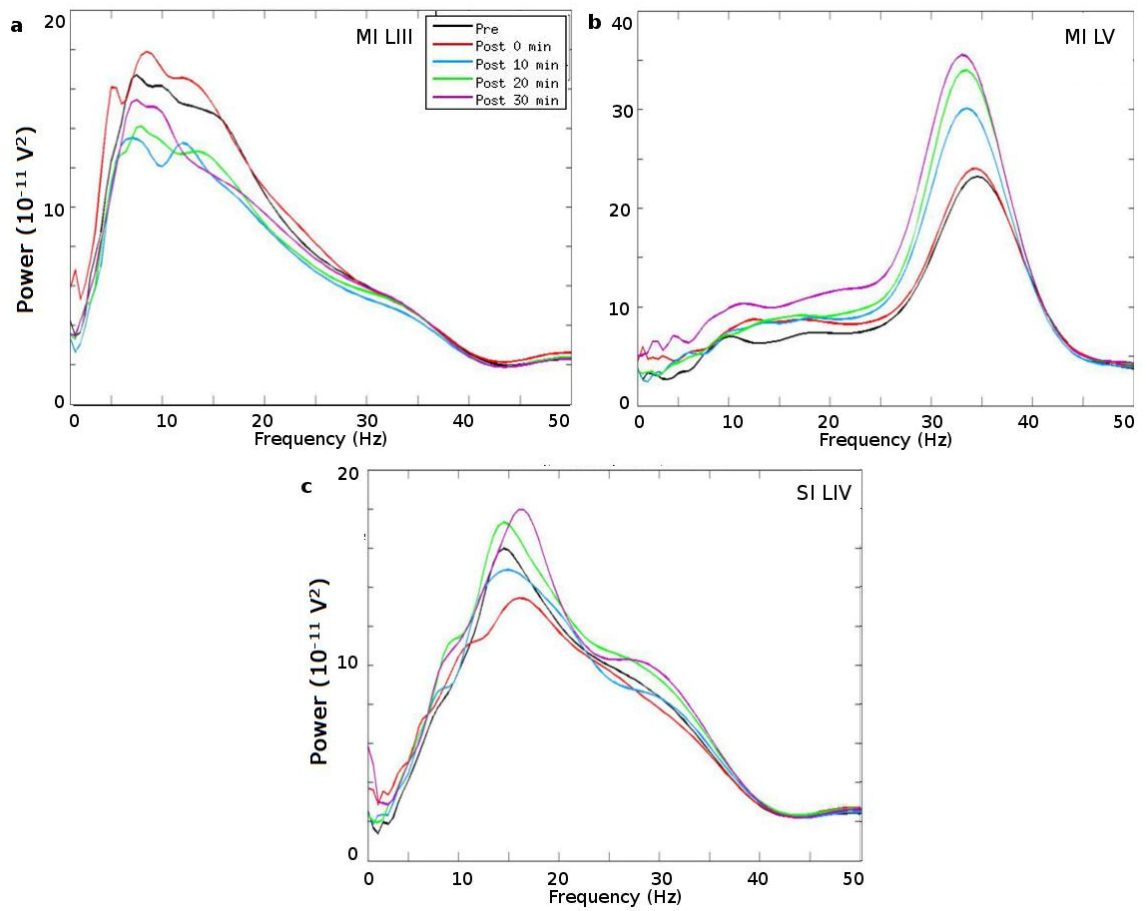
Figure 7. 7a-c. Group- and time-averaged PSDs showing the oscillatory profiles before and at different time points after cTBS$_{MI LV}$, recorded in MI LIII (n=8), in a (top left), MI LV (n=10), seen in b (top right), and SI LIV (n=9), seen in c (bottom). The PSD from the time period before cTBS$_{MI LV}$ (Pre) is illustrated with a black line, the time period immediately after cTBS$_{MI LV}$ (Post 0 min) is illustrated by red, 10 minutes after cTBS$_{MI LV}$ (Post 10 min) by blue, 20 minutes after cTBS$_{MI LV}$ (Post 20 min) by green and 30 minutes after cTBS$_{MI LV}$.

177
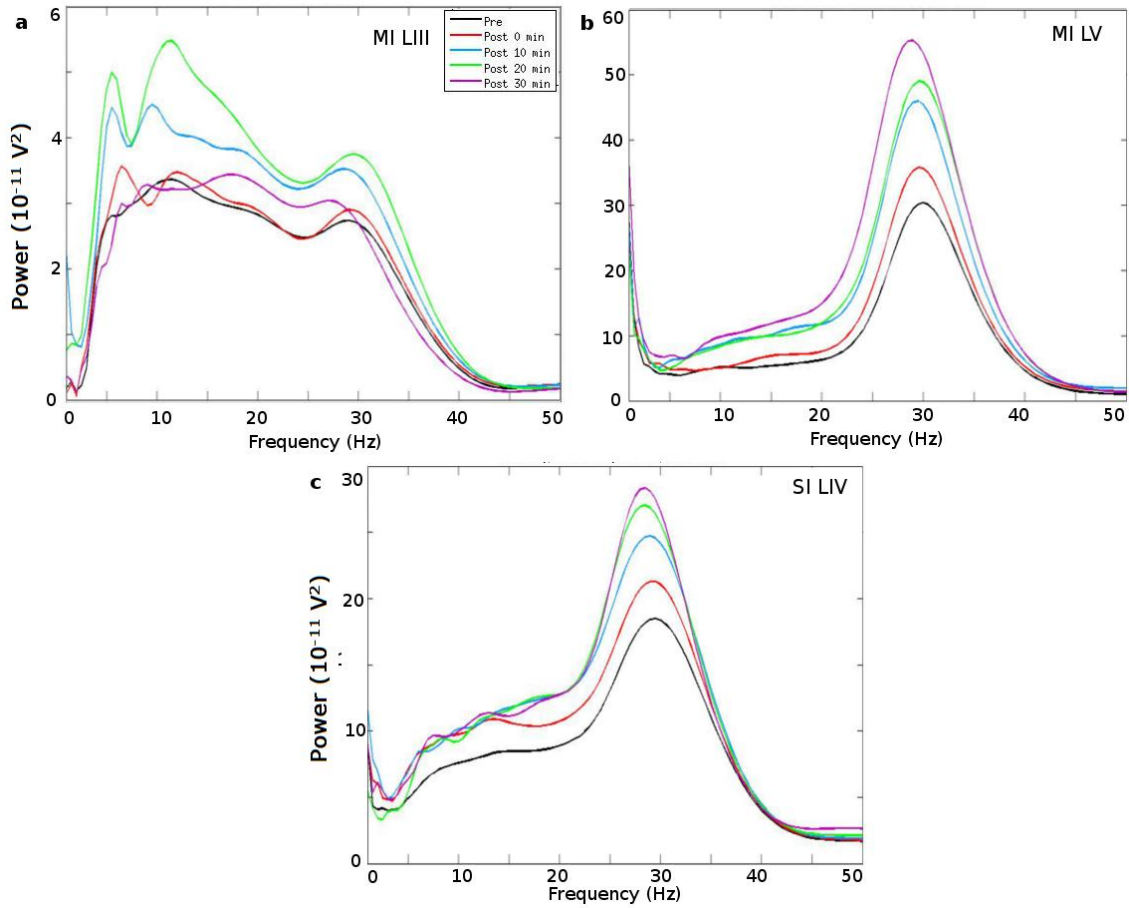
Figure 7. 8a-c. Group- and time-averaged PSDs showing the oscillatory profiles before and at different time points after cTBS$_{SI\ LIV}$, recorded in MI LIII (n=8), seen in a (top left), MI LV (n=10), seen in b (top right), and SI LIV (n=9), seen in c (bottom). The PSD from the time period before cTBS$_{SI\ LIV}$ (Pre) is illustrated with a black line, the time period immediately after cTBS$_{SI\ LIV}$ (Post 0 min) is illustrated by red, 10 minutes after cTBS$_{SI\ LIV}$ (Post 10 min) by blue, 20 minutes after cTBS$_{SI\ LIV}$ (Post 20 min) by green and 30 minutes after cTBS$_{SI\ LIV}$.

7.3.2.1. Frequency and power

cTBS$_{MI\ LIII}$ did not result in significant time-dependent changes in any laminae on mean peak frequency. cTBS$_{MI\ LV}$ significantly decreased the peak frequency in MI LV after 30 minutes, from 31.00±7.59 to 30.20±6.97 Hz, t$_{[9]}$=2.3881, p=0.0407, but not in MI LIII or SI LIV. cTBS$_{SI\ LIV}$ significantly decreased the mean peak frequency after 30 minutes in SI LIV: from 25.61±7.83 Hz to 21.22±8.91 Hz, t$_{[8]}$=2.397, p=0.0434, but not in the other laminae.

cTBS$_{MI\ LIII}$, cTBS$_{MI\ LV}$ and cTBS$_{SI\ LIV}$ did not result in significant time-dependent changes in any laminae on mean peak power.

The detailed results on mean peak frequency and power from cTBS in different laminae are listed in table 7.1-3 and figure 7.9-10 presents overviews.

178
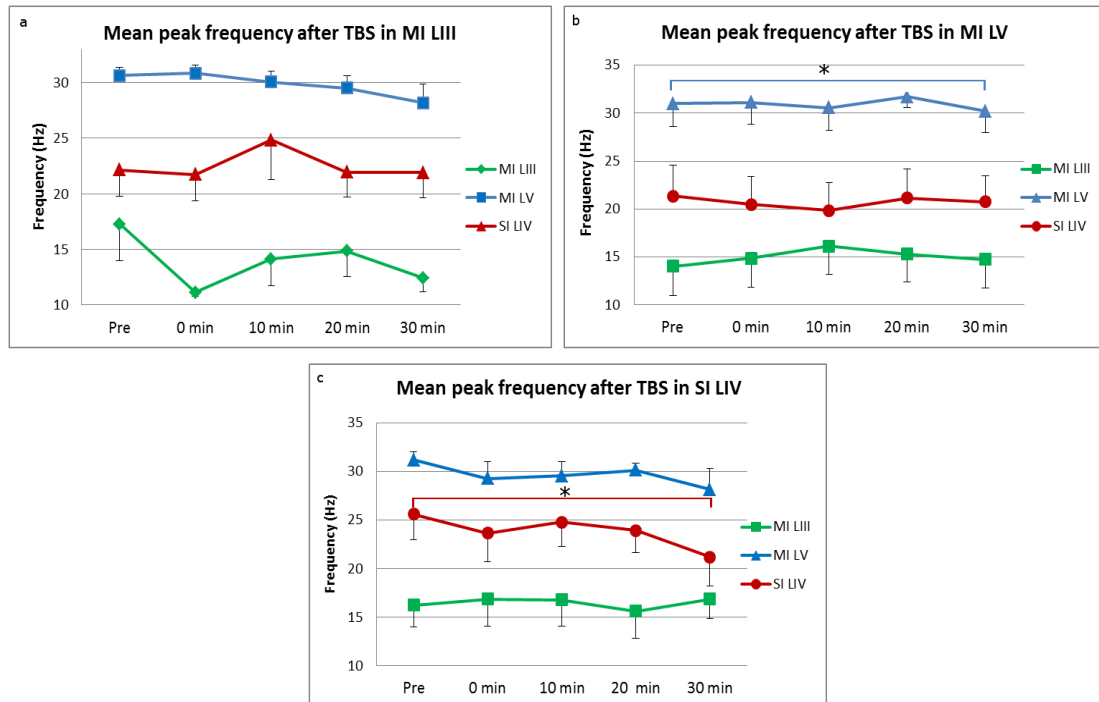
Figure 7. 9a-c. Mean peak frequency before and after cTBS in different laminae. The peak frequency decreased significantly in MI LV 30 minutes after cTBS$_{MI\ LV}$, p<0.05. The peak frequency decrease in SI LIV 30 minutes after cTBS was also significant, p<0.05. SEMs are plotted as error bars. cTBS$_{MI\ LIII}$: MI LIII n=6, MI LV n=9. SI LIV n=9. cTBS$_{MI\ LV}$: MI LIII n=7, MI LV n=9, SI LIV n=8. cTBS$_{SI\ LIV}$: MI LIII n=7, MI LV n=9, SI LIV n=8. MI LIII values are shown in green, MI LV in blue and SI LIV in red.
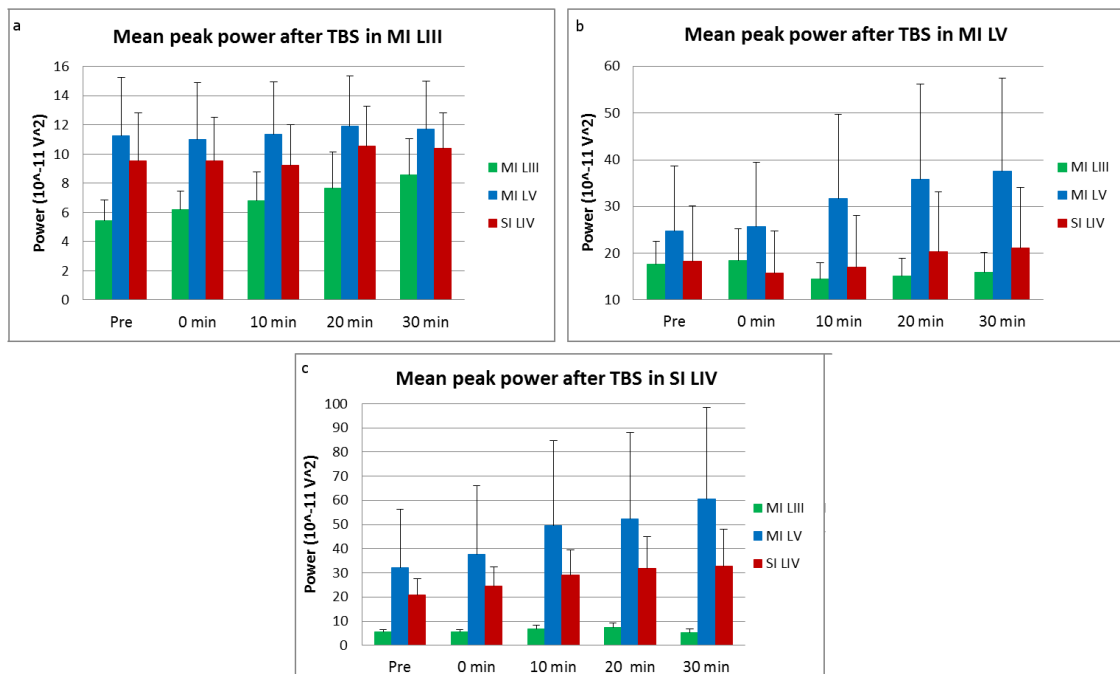
Figure 7. 10a-c. Mean peak power before and after cTBS in different laminae. There were no significant effects. SEMs are plotted as error bars. cTBS in MI LIII: MI LIII n=6, MI LV n=9. SI LIV n=9. cTBS$_{MI\ LIII}$: MI LIII n=6, MI LV n=9. SI LIV n=9. cTBS$_{MI\ LV}$: MI LIII n=7, MI LV n=9, SI LIV n=8. cTBS$_{SI\ LIV}$: MI LIII n=7, MI LV n=9, SI LIV n=8. MI LIII values are shown in green, MI LV in blue and SI LIV in red.

Table 7. 1. Mean oscillatory peak frequency and power before and after cTBS in MI LIII.

MI LIII	Pre	Post 0	Post 10	Post 20	Post 30
mean F ±SD (Hz)	17.29±9.2	11.14±0.9	14.14±6.8	14.86±6.5	12.43±3.5
mean A ±SD (10^{-11} V^2)	5.43±3.9	6.17±3.6	6.78±5.6	7.68±6.9	8.56±7.0
MI LV	**Pre**	**Post 0**	**Post 10**	**Post 20**	**Post 30**
mean F ±SD (Hz)	30.65±2.2	30.85±2.2	30.05±3.1	29.50±3.5	28.2±5.2
mean A ±SD (10^{-11} V^2)	11.25±12.5	10.97±12.3	11.36±11.2	11.89±10.9	11.71±10.2
SI LIV	**Pre**	**Post 0**	**Post 10**	**Post 20**	**Post 30**
mean F ±SD (Hz)	22.15±7.5	21.75±7.4	24.85±11.2	21.95±6.9	21.90±7.0
mean A ±SD (10^{-11} V^2)	9.54±10.2	9.52±9.4	9.19±8.8	10.53±8.5	10.37±7.7

Table 7. 2. T-statistics: mean peak frequency and power *in vitro* after cTBS in MI LIII.

cTBS: MI LIII		Post 0 min			Post 10 min		
		MI LIII	MI LV	SI LIV	MI LIII	MI LV	SI LIV
	d.f.	6	9	9	6	9	9
Peak F	t-statistic	1.796	-1.8091	0.4356	1.3479	1.4275	-1.327
	p-value	0.1226	0.1039	0.6734	0.2264	0.1872	0.2172
Peak A	t-statistic	-2.0946	1.2461	0.0622	-1.8478	-0.1303	0.6238
	p-value	0.0811	0.2442	0.9518	0.1141	0.8992	0.5483
		Post 20 min			**Post 30 min**		
		MISL	MIDL	SIML	MISL	MIDL	SIML
	d.f.	6	9	9	6	9	9
Peak F	t-statistic	1.2842	2.1594	0.647	1.5353	2.1892	0.3946
	p-value	0.2464	0.0591	0.5338	0.1756	0.0563	0.7023
Peak A	t-statistic	-1.6818	-0.5247	-0.8089	-2.0089	-0.2311	-0.455
	p-value	0.1436	0.6125	0.4394	0.0913	0.8224	0.6599

Table 7. 3. Mean oscillatory peak frequency and peak power after cTBS in MI LV.

MI LIII	Pre	Post 0	Post 10	Post 20	Post 30
mean F ±SD (Hz)	14.06±8.8	14.88±8.6	16.13±8.3	15.31±8.2	14.75±8.4
mean A ±SD ($10^{-11}V^2$)	17.67±13.8	18.47±19.0	14.56±9.4	15.05±11.1	15.90±11.9
MI LV	**Pre**	**Post 0**	**Post 10**	**Post 20**	**Post 30**
mean F ±SD (Hz)	31.00±7.5	31.10±7.1	30.55±7.4	31.70±3.5	30.20±6.9
mean A ±SD ($10^{-11}V^2$)	24.76±43.8	25.75±43.4	31.67±57.0	35.77±64.5	37.58±62.7
SI LIV	**Pre**	**Post 0**	**Post 10**	**Post 20**	**Post 30**
mean F ±SD (Hz)	21.33±9.6	20.50±8.7	19.83±8.8	21.17±9.0	20.78±7.9
mean A ±SD ($10^{-11}V^2$)	18.23±35.6	15.82±26.8	17.10±33.0	20.36±38.5	21.08±39.2

Grey highlights indicates statistical significance, p<0.05.

Table 7. 4. T-statistics: mean peak frequency and power after cTBS in MI LV.

cTBS: MI LV		Post 0 min			Post 10 min		
		MI LIII	MI LV	SI LIV	MI LIII	MI LV	SI LIV
	d.f.	7	9	8	7	9	8
Peak F	t-statistic	-0.7918	-0.4523	0.527	-1.8551	2.0769	0.7963
	p-value	0.4545	0.6618	0.6125	0.106	0.0676	0.4489
Peak A	t-statistic	-0.3977	-2.1523	0.7884	1.6638	-1.615	0.973
	p-value	0.7027	0.0598	0.4532	0.1401	0.1408	0.359
		Post 20 min			Post 30 min		
		MI LIII	MI LV	SI LIV	MI LIII	MI LV	SI LIV
	d.f.	7	9	8	7	9	8
Peak F	t-statistic	-1.452	-0.5047	0.417	-0.5883	2.3881	0.3114
	p-value	0.1898	0.6259	0.6876	0.5748	0.0407 (*)	0.7635
Peak A	t-statistic	1.7808	-1.662	-1.2645	1.2761	-2.0752	-1.2579
	p-value	0.1182	0.1309	0.2416	0.2426	0.0678	0.2439

Statistical significance p<0.05 is marked with *.

Table 7. 5. Mean peak frequency and power before and after cTBS in SI LIV.

MI LIII	Pre	Post 0	Post 10	Post 20	Post 30
mean F ±SD (Hz)	16.25±6.3	16.88±7.8	16.81±7.7	15.63±7.9	16.88±5.5
mean A±SD (10^{-11} V^2)	5.69±2.5	5.67±2.5	6.93±3.8	7.31±5.3	5.37±3.6
MI LV	Pre	Post 0	Post 10	Post 20	Post 30
mean F ±SD (Hz)	31.20±2.5	29.30±5.5	29.55±4.7	30.15±2.2	28.15±6.7
mean A±SD (10^{-11} V^2)	32.18±76.0	37.70±89.5	49.53±110.9	52.46±112.2	60.69±119.2
SI LIV	Pre	Post 0	Post 10	Post 20	Post 30
mean F ±SD (Hz)	25.61±7.8	23.67±8.9	24.78±7.4	23.94±6.8	21.22±8.9
mean A±SD (10^{-11} V^2)	20.94±19.7	24.44±24.3	29.11±30.9	31.91±39.1	32.84±45.5

Grey highlights indicates statistical significance, p<0.05.

Table 7. 6. Mean peak frequency and power before and after cTBS in SI LIV.

cTBS: SI LIV		Post 0 min			Post 10 min		
		MI LIII	MI LV	SI LIV	MI LIII	MI LV	SI LIV
	d.f.	7	9	8	7	9	8
Peak F	t-statistic	-0.3716	1.0586	1.108	-0.4133	1.065	2.1822
	p-value	0.7211	0.3173	0.3	0.6917	0.3146	0.0607
Peak A	t-statistic	0.0378	-1.2742	-2.0487	-1.8329	-1.5159	-2.1521
	p-value	0.9709	0.2345	0.0747	0.1095	0.1638	0.0636
		Post 20 min			Post 30 min		
		MI LIII	MI LV	SI LIV	MI LIII	MI LV	SI LIV
	d.f.	7	9	8	7	9	8
Peak F	t-statistic	0.4144	2.2429	1.3245	-0.7407	1.3614	2.397
	p-value	0.691	0.0516	0.2219	0.483	0.2065	0.0434 (*)
Peak A	t-statistic	-1.0155	-1.6926	-1.626	0.2714	-1.8632	-1.2674
	p-value	0.3437	0.1248	0.1426	0.7939	0.0953	0.2407

Statistical significance p<0.05 is marked with *.

7.3.2.2. Frequency distribution and variability

There were no significant changes over time in the mean FWHM or peak frequency distribution in MI LIII, MI LV or SI LIV after cTBS in any of the three locations.

Additionally, there were no significant effects over time of cTBS in any laminae on the frequency variability. The detailed results on mean FWHM and frequency variability from cTBS in different laminae are listed in table 7.4-6 and figure 7.11-12 presents overviews.
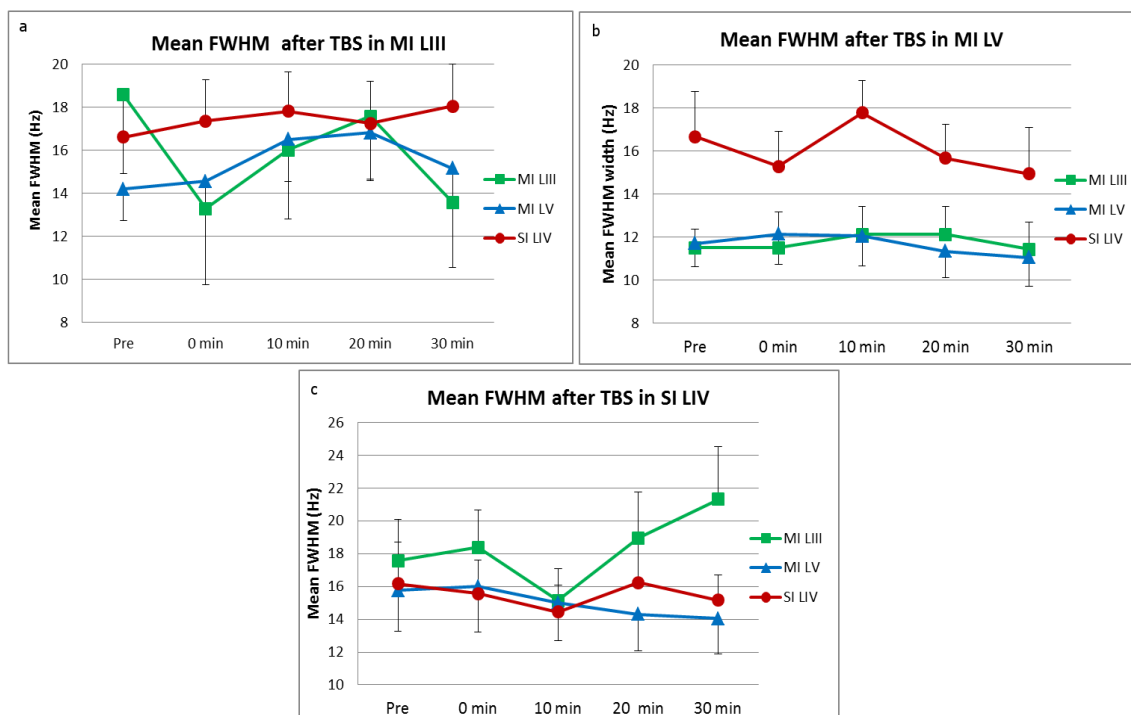
Figure 7. 11a-c. Mean FWHM after cTBS in all laminae. No significant effects were seen. SEMs are represented by error bars. $cTBS_{MI\ LIII}$: MI LIII n=6, MI LV n=9. SI LIV n=9. $cTBS_{MI\ LV}$: MI LIII n=7, MI LV n=9, SI LIV n=8. $cTBS_{SI\ LIV}$: MI LIII n=7, MI LV n=9, SI LIV n=8. MI LIII values are shown in green, MI LV in blue and SI LIV in red.

Table 7. 7. Mean FWHM and frequency distribution before and after cTBS in MI LIII.

MI LIII	Pre	Post 0	Post 10	Post 20	Post 30
mean FWHM ±SD (Hz)	18.57±10.3	13.29±9.9	16.00±9.0	17.57±8.4	13.57±8.5
Mean % at peak±SD	4.55±2.6	4.75±2.6	5.55±3.1	4.45±2.8	5.11±2.3
MI LV	**Pre**	**Post 0**	**Post 10**	**Post 20**	**Post 30**
mean FWHM (Hz)	14.20±4.6	14.55±4.0	16.50±6.1	16.80±6.7	15.15±4.5
Mean % at peak±SD	9.63±4.1	9.49±3.7	10.31±4.0	10.04±4.8	8.75±2.8
SI LIV	**Pre**	**Post 0**	**Post 10**	**Post 20**	**Post 30**
mean FWHM (Hz)	16.60±5.5	17.35±6.0	17.80±5.8	17.25±6.1	18.05±6.1
Mean % at peak±SD	7.60±8.4	7.91±6.2	8.33±6.4	7.73±6.6	7.09±5.4
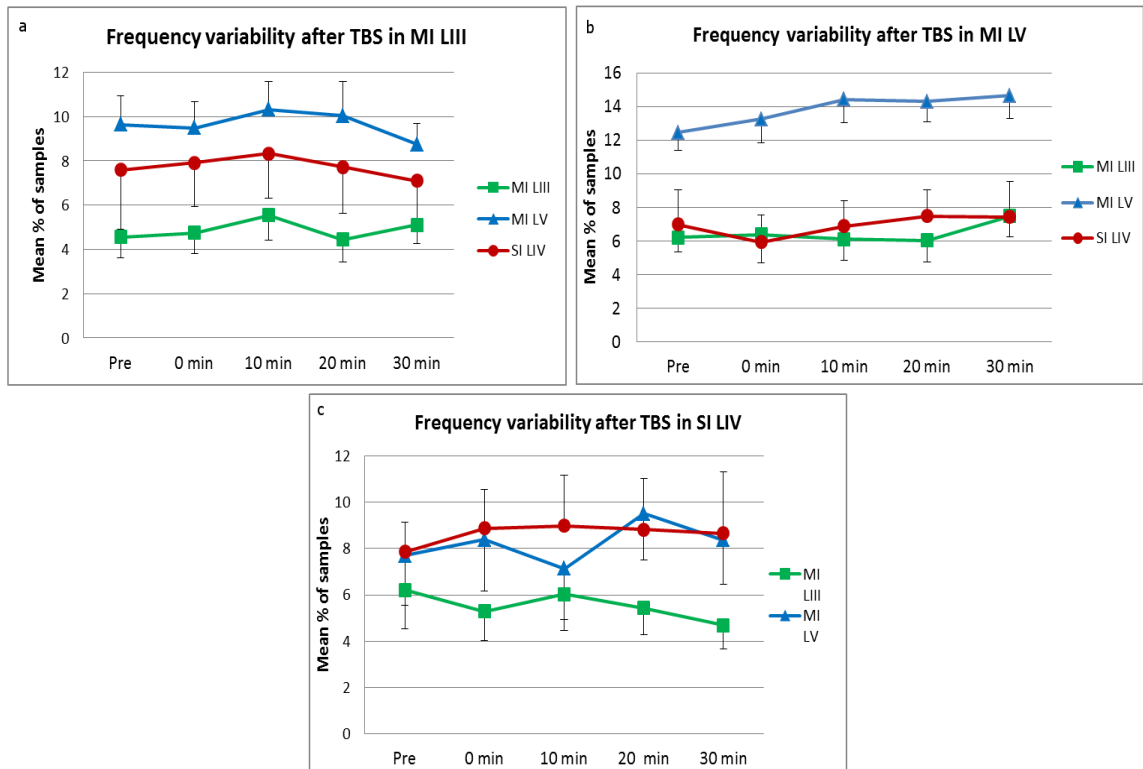
Figure 7. 12a-c. Mean frequency variability after cTBS in all laminae. No significant effects were seen. SEMs are represented by error bars. $cTBS_{MI\ LIII}$: MI LIII n=6, MI LV n=9. SI LIV n=9. $cTBS_{MI\ LV}$: MI LIII n=7, MI LV n=9, SI LIV n=8. $cTBS_{SI\ LIV}$: MI LIII n=7, MI LV n=9, SI LIV n=8. MI LIII values are shown in green, MI LV in blue and SI LIV in red.

Table 7. 8. T-statistics: mean FWHM and frequency distribution after cTBS in MI LIII

cTBS: MI LIII		Post 0 min			Post 10 min		
		MI LIII	MI LV	SI LIV	MI LIII	MI LV	SI LIV
	d.f.	6	9	9	6	9	9
FWHM	t-statistic	1.655	-0.2461	-0.7601	1.7034	-1.4307	-1.206
	p-value	0.149	0.8111	0.4666	0.1394	0.1863	0.2585
FV	t-statistic	-0.4642	0.1569	-0.3141	-1.4955	-0.7475	-0.6479
	p-value	0.6589	0.8788	0.7606	0.1854	0.4739	0.5332
		Post 20 min			Post 30 min		
		MI LIII	MI LV	SI LIV	MI LIII	MI LV	SI LIV
	d.f.	6	9	9	6	9	9
FWHM	t-statistic	0.7385	-1.5169	-0.7143	1.329	-0.8958	-1.6593
	p-value	0.4881	0.1636	0.4931	0.2322	0.3937	0.1314
FV	t-statistic	0.1134	-0.3241	-0.1652	-0.6917	0.8423	0.4196
	p-value	0.9134	0.7533	0.8724	0.515	0.4215	0.6846

Table 7. 9. Mean FWHM and peak frequency distribution after cTBS in MI LV.

MI LIII	Pre	Post 0	Post 10	Post 20	Post 20
mean FWHM ±SD (Hz)	11.50±2.4	11.50±4.7	12.13±3.6	12.13±3.6	11.44±3.5
mean % at peak ±SD	6.24±1.6	6.40±2.7	6.13±2.8	6.06±3.6	7.50±3.6
MI LV	**Pre**	**Post 0**	**Post 10**	**Post 20**	**Post 20**
mean FWHM ±SD (Hz)	11.70±3.3	12.15±4.4	12.05±4.3	11.35±3.8	11.05±4.2
mean % at peak ±SD	12.48±3.1	13.28±3.7	14.45±4.4	14.32±6.3	14.67±5.2
SI LIV	**Pre**	**Post 0**	**Post 10**	**Post 20**	**Post 20**
mean FWHM ±SD (Hz)	16.67±6.2	15.28±4.8	17.78±4.4	15.67±4.6	14.94±6.4
mean % at peak ±SD	7.00±3.4	5.96±3.3	6.90±3.3	7.50±3.5	7.44±4.3

Table 7. 10. T-statistics: mean FWHM and peak frequency distribution after cTBS in MI LV.

cTBS: MI LV		Post 0 min			Post 10 min		
		MI LIII	MI LV	SI LIV	MI LIII	MI LV	SI LIV
	d.f.	7	9	8	7	9	8
FWHM	t-statistic	0.001	-0.7406	0.9306	-0.9674	-0.7612	-0.6132
	p-value	0.999	0.4778	0.3793	0.3656	0.466	0.5568
FV	t-statistic	-0.1966	-0.728	1.5624	0.1122	-1.7155	0.1135
	p-value	0.8497	0.4851	0.1568	0.9138	0.1204	0.9124
		Post 20 min			**Post 30 min**		
		MI LIII	MI LV	SI LIV	MI LIII	MI LV	SI LIV
	d.f.	7	9	8	7	9	8
FWHM	t-statistic	-0.7977	1.1053	0.3963	0.0598	1.8571	0.5027
	p-value	0.4512	0.2977	0.7023	0.954	0.0963	0.6287
FV	t-statistic	0.1492	-1.226	-0.5123	-1.0524	-1.7693	-0.4463
	p-value	0.8856	0.2513	0.6223	0.3276	0.1106	0.6672

Table 7. 11. Mean FWHM and peak frequency distribution before and after cTBS in SI LIV.

MI LIII	Pre	Post 0	Post 10	Post 20	Post 30
mean FWHM ±SD (Hz)	17.56±7.0	18.38±6.4	15.13±5.4	18.94±7.9	21.31±9.0
Mean % at peak ±SD	6.21±4.7	5.28±3.5	6.04±4.4	5.42±3.4	4.69±2.9
MI LV	**Pre**	**Post 0**	**Post 10**	**Post 20**	**Post 30**
mean FWHM ±SD (Hz)	15.75±7.8	16.00±8.8	15.00±7.2	14.30±7.0	14.05±6.8
Mean % at peak ±SD	7.70±6.8	8.39±7.0	7.13±6.6	9.52±6.4	8.36±6.0
SI LIV	**Pre**	**Post 0**	**Post 10**	**Post 20**	**Post 30**
mean FWHM ±SD (Hz)	16.17±7.6	15.56±6.1	14.44±4.8	16.22±7.3	15.17±4.6
Mean % at peak ±SD	7.85±3.8	8.87±5.0	8.99±6.5	8.83±6.6	8.65±8.0

Table 7. 12. T-statistics: mean FWHM and peak frequency distribution after cTBS in SI LIV.

cTBS: SI LIV		Post 0 min			Post 10 min		
		MI LIII	MI LV	SI LIV	MI LIII	MI LV	SI LIV
	d.f.	7	9	8	7	9	8
FWHM	**t-statistic**	-0.4539	-0.1297	0.5645	1.7414	0.4596	0.8819
	p-value	0.6637	0.8996	0.5879	0.1252	0.6567	0.4035
FV	**t-statistic**	0.9504	-0.5909	-1.5188	0.221	1.1705	-1.056
	p-value	0.3736	0.5691	0.1673	0.8314	0.2719	0.3218
		Post 20 min			**Post 30 min**		
		MI LIII	MI LV	SI LIV	MI LIII	MI LV	SI LIV
	d.f.	7	9	8	7	9	8
FWHM	**t-statistic**	-0.6721	0.6461	-0.0495	-1.6846	0.712	0.4259
	p-value	0.5231	0.5343	0.9617	0.1359	0.4945	0.6814
FV	**t-statistic**	0.5203	-0.9364	-0.6698	1.7471	-0.4289	-0.4123
	p-value	0.6189	0.3735	0.5218	0.1241	0.6781	0.6909

7.3.2.3. Power state

After cTBS in MI LIII, the mean power in the upstate in MI LIII increased significantly from 6.65×10^{-11} V^2 to 10.62×10^{-11} V^2, 30 minutes after cTBS, $t_{[6]}$=-3.0322, p=0.023. In addition, in SI LIV the mean downstate power increased significantly from 2.13 to 2.69 $\times 10^{-11}$ V^2, $t_{[9]}$=-2.4134, p=0.039. There were no significant effects on oscillatory state or state power in MI LV after cTBS in SI LIV.

After cTBS in MI LV, there were no significant effects in any laminae.

After cTBS in SI LIV the mean upstate power in SI LIV showed a significant increase at 10 minutes after, $t_{[8]}$=-2.3778, p=0.0447. The mean downstate power significantly increased at 20 and 30 minutes post cTBS, $t_{[8]}$=-3.455, p=0.0086, and $t_{[8]}$=-2.3731, p=0.045, respectively. There were no significant changes in MI LIII and MI LV after cTBS$_{SI LIV}$. The detailed results on oscillatory state and state power from cTBS in different laminae are listed in table 7.7-9 and figure 7.12-15 presents overviews.
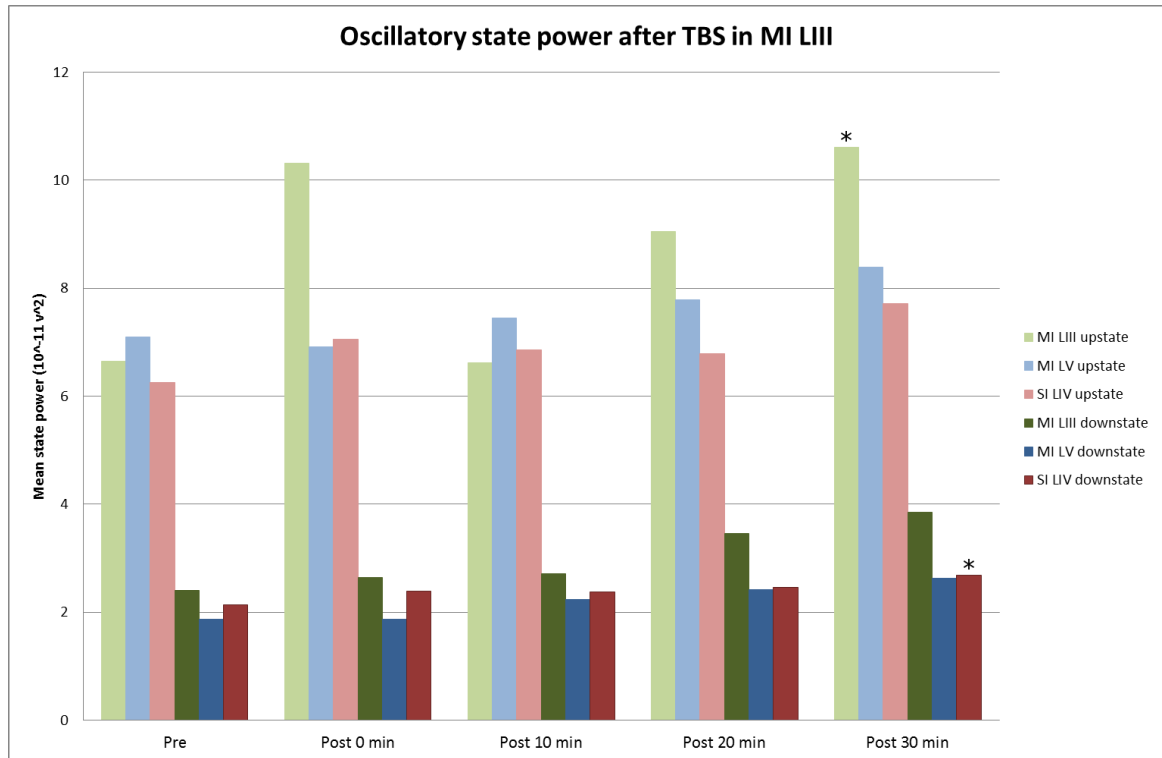
Figure 7. 13. Mean oscillatory state power before and after cTBS$_{MI\ LIII}$, recorded in MI LV (blues), MI LIII (greens) and SI LIV(reds). The difference in the mean up- and downstate power, in MI LIII and SI LIV respectively, after 30 minutes was significant, $p<0.05$, illustrating the gradual increase in power. The values shown are in amplitude (x10^{-11} V^2). cTBS$_{MI\ LIII}$: MI LIII n=6, MI LV n=9. SI LIV n=9. cTBS$_{MI\ LV}$: MI LIII n=7, MI LV n=9, SI LIV n=8. cTBS$_{SI\ LIV}$: MI LIII n=7, MI LV n=9, SI LIV n=8.

Table 7. 13. Oscillatory state and power before and after cTBS application in MI LIII.

MI LIII	Pre	Post 0 min	Post 10 min	Post 20 min	Post 30 min
% Upstate	40.05	34.63	41.36	39.70	36.29
Mean upstate power	6.65	10.32	6.62	9.05	10.62
Mean downstate power	2.41	2.65	2.71	3.46	3.85
MI LV	**Pre**	**Post 0 min**	**Post 10 min**	**Post 20 min**	**Post 30 min**
% Upstate	34.58	36.31	37.32	38.41	36.94
Mean upstate power	7.09	6.91	7.46	7.78	8.40
Mean downstate power	1.87	1.87	2.23	2.42	2.63
SI LIV	**Pre**	**Post 0 min**	**Post 10 min**	**Post 20 min**	**Post 30 min**
% Upstate	36.94	38.74	38.63	40.14	39.17
Mean upstate power	6.26	7.05	6.86	6.79	7.72
Mean downstate power	2.13	2.39	2.38	2.46	2.69

Grey highlights indicate statistical significance, $p<0.05$

Table 7. 14. T-statistics: oscillatory state and power after cTBS in MI LIII

cTBS: MI LIII		Post 0 min			Post 10 min		
		MI LIII	MI LV	SI LIV	MI LIII	MI LV	SI LIV
	d.f.	6	9	9	6	9	9
UP %	t-statistic	1.1526	-0.5314	-0.7019	-0.9905	-0.9791	-0.8181
	p-value	0.2929	0.608	0.5005	0.3602	0.3531	0.4344
UP pow	t-statistic	-1.0282	0.1438	-0.6778	0.0498	-0.2961	-0.6277
	p-value	0.3435	0.8889	0.5149	0.9619	0.7739	0.5458
DN pow	t-statistic	-1.4284	-0.0064	-1.8495	-1.1723	-1.4861	-1.6584
	p-value	0.2031	0.995	0.0974	0.2855	0.1714	0.1316
		Post 20 min			Post 30 min		
		MI LIII	MI LV	SI LIV	MI LIII	MI LV	SI LIV
	d.f.	6	9	9	6	9	9
UP %	t-statistic	0.3249	-1.4288	-1.8289	1.2052	-1.6357	-1.5654
	p-value	0.7563	0.1868	0.1007	0.2735	0.1363	0.1519
UP pow	t-statistic	-2.1935	-0.5729	-0.6389	-3.0322	-1.1881	-1.4923
	p-value	0.0707	0.5807	0.5388	0.023 (*)	0.2652	0.1698
DN pow	t-statistic	-1.7604	-1.9078	-2.0934	-2.1291	-2.01	-2.4134
	p-value	0.1288	0.0888	0.0658	0.0773	0.0753	0.039 (*)

Statistical significance p<0.05 is marked with *.
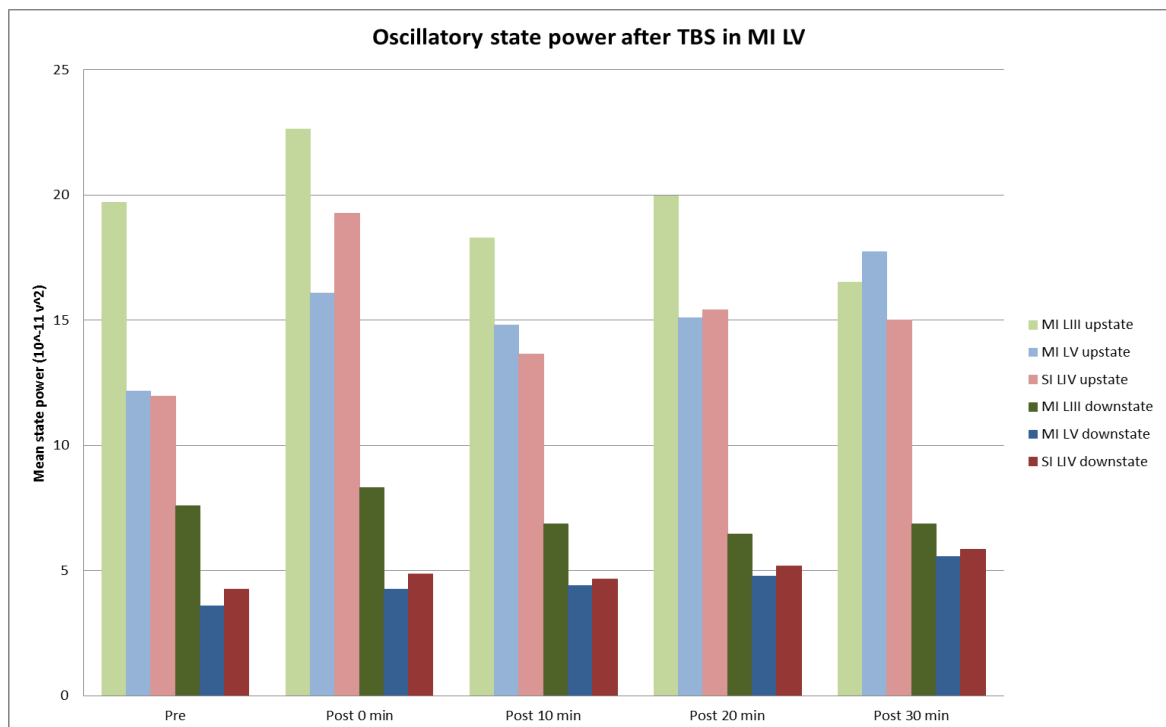
Figure 7. 14. Mean oscillatory state power after cTBS$_{MI\ LV}$. There were no significant differences in the oscillatory state power after cTBS. cTBS$_{MI\ LIII}$: MI LIII n=6, MI LV n=9. SI LIV n=9. cTBS$_{MI\ LV}$: MI LIII n=7, MI LV n=9, SI LIV n=8. cTBS$_{SI\ LIV}$: MI LIII n=7, MI LV n=9, SI LIV n=8. MI LIII is illustrated by green colours, MI LV by blue colours and SI LIV by red colours.

Table 7. 15. Oscillatory state and power before and after cTBS in MI LV

MI LIII	Pre	Post 0 min	Post 10 min	Post 20 min	Post 30 min
% Upstate	38.79	37.31	37.93	33.81	39.42
Mean upstate power	19.71	22.64	18.27	19.95	16.50
Mean downstate power	7.58	8.32	6.86	6.46	6.87
MI LV	**Pre**	**Post 0 min**	**Post 10 min**	**Post 20 min**	**Post 30 min**
% Upstate	37.06	36.81	36.77	38.32	37.15
Mean upstate power	12.16	16.07	14.80	15.09	17.72
Mean downstate power	3.60	4.25	4.40	4.77	5.57
SI LIV	**Pre**	**Post 0 min**	**Post 10 min**	**Post 20 min**	**Post 30 min**
% Upstate	39.18	35.83	39.57	36.60	38.73
Mean upstate power	11.96	19.27	13.64	15.41	15.01
Mean downstate power	4.26	4.85	4.67	5.18	5.85

Table 7. 16. T-statistics: oscillatory state and power after cTBS in MI LV

cTBS: MI LV		**Post 0 min**			**Post 10 min**		
		MI LIII	**MI LV**	**SI LIV**	**MI LIII**	**MI LV**	**SI LIV**
	d.f.	7	9	8	7	9	8
UP %	**t-statistic**	0.6294	0.2372	1.0262	0.2783	0.3107	-0.2319
	p-value	0.5491	0.8178	0.3348	0.7888	0.7631	0.8224
UP pow	**t-statistic**	-0.5659	-0.9692	-1.1183	0.4066	-1.1548	-0.6586
	p-value	0.5891	0.3578	0.2959	0.6965	0.2779	0.5287
DN pow	**t-statistic**	-0.8175	-0.9436	-1.1289	1.2561	-1.248	-0.7279
	p-value	0.4406	0.37	0.2917	0.2494	0.2435	0.4875
		Post 20 min			**Post 30 min**		
		MI LIII	**MI LV**	**SI LIV**	**MI LIII**	**MI LV**	**SI LIV**
	d.f.	7	9	8	7	9	8
UP %	**t-statistic**	1.5408	-0.9261	2.1868	-0.272	-0.0702	0.3306
	p-value	0.1673	0.3786	0.0602	0.7935	0.9456	0.7495
UP pow	**t-statistic**	-0.0841	-2.0212	-0.9128	1.383	-1.8191	-0.8674
	p-value	0.9354	0.074	0.388	0.2092	0.1023	0.411
DN pow	**t-statistic**	1.3708	-1.9078	-0.9132	1.058	-1.7579	-1.0615
	p-value	0.2128	0.0888	0.3878	0.3252	0.1126	0.3195

Table 7. 17. Oscillatory state and power before and after cTBS in SI LIV

MI LIII	Pre	Post 0 min	Post 10 min	Post 20 min	Post 30 min
% Upstate	39.21	40.82	40.06	40.14	40.33
Mean upstate power	5.71	5.96	6.86	7.42	6.36
Mean downstate power	2.27	2.46	2.76	3.07	2.46
MI LV	**Pre**	**Post 0 min**	**Post 10 min**	**Post 20 min**	**Post 30 min**
% Upstate	36.19	37.07	37.18	36.15	36.84
Mean upstate power	9.56	11.13	15.79	17.90	19.18
Mean downstate power	2.89	3.57	5.43	5.26	5.78
SI LIV	**Pre**	**Post 0 min**	**Post 10 min**	**Post 20 min**	**Post 30 min**
% Upstate	36.82	36.99	36.01	38.97	36.79
Mean upstate power	14.56	16.35	19.09	15.60	17.26
Mean downstate power	4.43	4.73	6.07	5.74	5.91
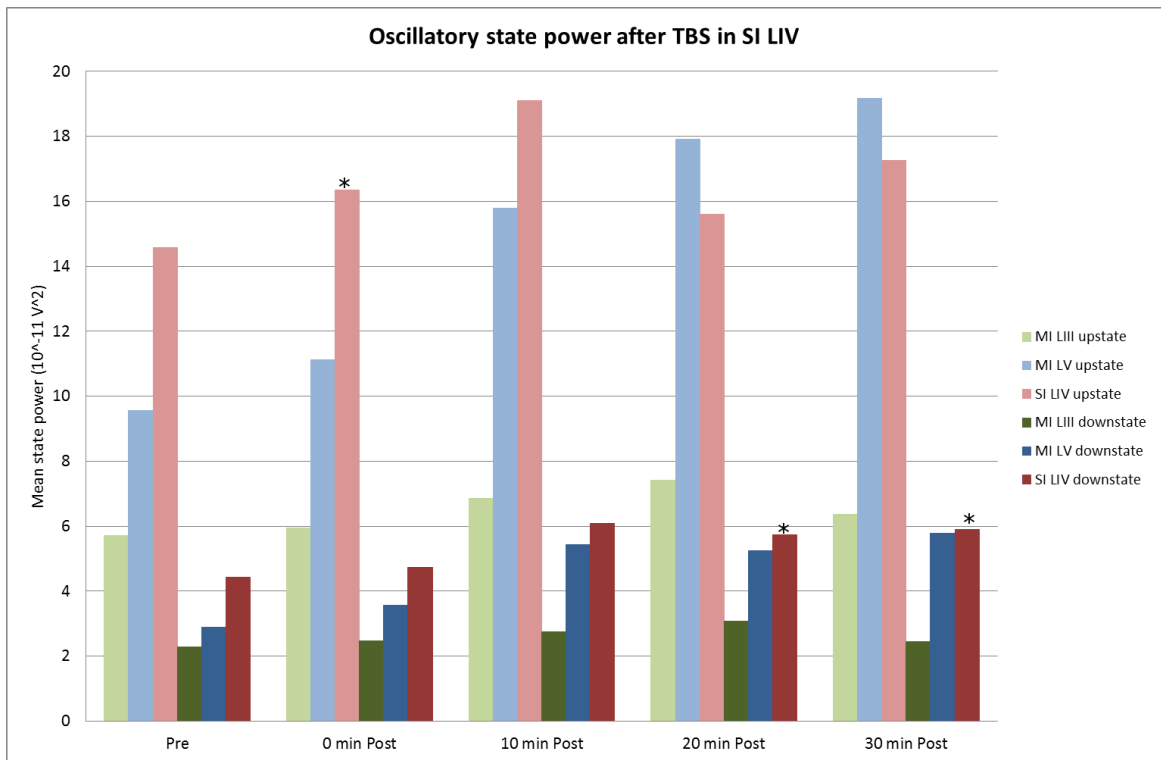
Figure 7. 15. Mean oscillatory state power before and after cTBS$_{SI\ LIV}$. The increase in mean upstate power in SI LIV at 10 minutes after cTBS$_{SI\ LIV}$ was significant, p<0.05. In addition, the increases in mean downstate power at 20 and 30 minutes in SI LIV were also significant, p<0.05. cTBS$_{MI\ LIII}$: MI LIII n=6, MI LV n=9. SI LIV n=9. cTBS$_{MI\ LV}$: MI LIII n=7, MI LV n=9, SI LIV n=8. cTBS$_{SI\ LIV}$: MI LIII n=7, MI LV n=9, SI LIV n=8. MI LIII is shown in green colours, MI LV in blue and SI LIV in blue.

Table 7. 18. T-statistics: oscillatory state and power after cTBS in SI LIV

cTBS: SI LIV		Post 0 min			Post 10 min		
		MI LIII	MI LV	SI LIV	MI LIII	MI LV	SI LIV
	d.f.	7	9	8	7	9	8
UP %	t-statistic	-1.2706	-0.8769	-0.2016	-0.4842	-1.0961	0.3652
	p-value	0.2445	0.4033	0.8452	0.643	0.3015	0.7244
UP pow	t-statistic	-0.6373	-1.2975	-1.4434	-2.323	-1.4048	-2.3778
	p-value	0.5442	0.2267	0.1869	0.0532	0.1936	0.0447 (*)
DN pow	t-statistic	-0.9688	-1.2678	-1.1884	-1.69	-1.3348	-1.7062
	p-value	0.3649	0.2367	0.2688	0.1349	0.2147	0.1264
		Post 20 min			Post 30 min		
		MI LIII	MI LV	SI LIV	MI LIII	MI LV	SI LIV
	d.f.	7	9	8	7	9	8
UP %	t-statistic	-0.8969	0.0377	-1.5812	-0.7675	-0.6144	0.0196
	p-value	0.3996	0.9708	0.1525	0.4679	0.5542	0.9849
UP pow	t-statistic	-1.1988	-1.7845	-0.4863	-0.3931	-1.8902	-0.8206
	p-value	0.2696	0.108	0.6398	0.7059	0.0913	0.4357
DN pow	t-statistic	-1.1406	-1.8063	-3.4557	-0.3119	-2.0857	-2.3731
	p-value	0.2916	0.1043	0.0086 (**)	0.7642	0.0666	0.045 (*)

Significance p<0.05 is marked with *.

7.4 Discussion

7.4.1. Summary of findings

Applying cTBS over the left MI significantly increased the power of the ongoing beta activity in the stimulated hemisphere, and in responders, only. The responders also showed a significant decrease in the MEP amplitude. The *in vitro* experiments showed that the peak frequency in the stimulated laminae significantly decreased after cTBS, and while there was no significant effect on peak power, there were significant changes to the power states.

7.4.2. cTBS increases beta power in the stimulated hemisphere in humans

cTBS application over MI increased the power of the ongoing beta oscillations in the stimulated hemisphere in 50% of the participants; the responders. Previous reports have suggested that the differential response depends on the individual genetic differences in the polymorphism of brain-derived neurotrophic factor (BDNF). Cortico-spinal excitability is reported to reduce after cTBS in participants with Val66Val polymorphism, but not in individuals with the Val66Met polymorphism. The prevalence of Val66Val is approximately 65% in a population (Cheeran *et al.*, 2008). BDNF is reported to depress the postsynaptic $GABA_A$ responses (Tanaka *et al.*, 1997; Frerking *et al.*, 1998). $GABA_A$ transmission is essential for the oscillatory beta activity found in MI (Yamawaki *et al.*, 2008). In addition, BDNF has also recently been reported to exert effects NMDA-mediated transmission and plasticity, and in the subject with the polymorphism the plasticity is altered (Pattwell *et al.*, 2012). Our results support the theory that genetic differences underlie the differences seen in cTBS effects, as the reduction in cortico-spinal excitability and increase in ongoing beta power was absent in the participants without a response to cTBS. There are different effects of cTBS on the cell biological level, which could explain differences over time, as well as anatomical differences.

Previous reports on the effects on beta oscillations in MI after cTBS have shown dissimilar results. Activity in the lower beta frequency range (13-19.5 Hz) in MI was enhanced by cTBS, reported by Noh *et al.* (2012) but there were no significant enhancement in the higher beta band (20-30 Hz). In the study by McAllister *et al.*, (2011) there were no effects on beta power. Our results are only supportive of these findings to a small extent and there are several essential differences between our methods and analysis compared to those reported in these studies. Firstly, these two studies used a more limited spatial EEG approach, while we used MEG with good spatial accuracy. Second, the analysis of power

in the beta band was in Noh *et al.*'s article focused on dividing up the beta frequency range into two bands, while in our study we used one beta frequency range. It is possible that the increase in beta power Noh *et al.* reported is comparable to our results. Lastly, both of these groups used only 2s of oscillatory activity, which was subsequently averaged over several trials, and analysed with FFT-algorithms. Our analysis was based on 60s of resting data and analysed with a Morelet-wavelet algorithm. We chose a longer period of time for our analysis of ongoing activity and a Morelet-wavelet approach since previous experience and results have indicated that the FFT algorithm is more insensitive and the oscillatory signals contain stark variability in both oscillatory power and frequency (discussed in chapter 2 and 3).

Mäki & Ilmoniemi (2010) reported an association between MI excitability and beta oscillations measured with EEG, but also emphasised that the two features arise from different mechanisms, which essentially results in a weak correlation. With regards to differences in analysis approach, this group used 1s time windows, which were averaged, and three band-filters (12-15, 15-18, 15-30 Hz) for their beta oscillations were applied. Similarly, Zarkowski *et al.* (2006) also showed a statistically significant association between MI excitability and alpha and gamma activity. This group used 2s analysis and an undefined method of frequency spectrum analysis in MatLab. In addition the studies by Stagg *et al.* (2009) and Gaetz *et al.* (2011), the discussed results above and our own, provides evidence that the GABAergic system indeed is linked to the level of excitability in MI, as well as the beta power. However, the specific correlations between the features of human MI beta oscillations and MI excitability are still unclear and require further work.

7.4.3. cTBS *in vitro*

The significant effects of cTBS *in vitro* were predominantly local to the stimulated laminae. To date there are no studies reporting the effects of cTBS on ongoing oscillatory activity in the sensorimotor laminae *in vitro;* literature on the effects of cTBS on oscillations *in vitro* is sparse. In the *in vivo* study by Benali *et al.*, (2011) TBS was applied over the frontal cortex of rats. This group reported a significant increase in gamma power, in addition to a non-significant increase in beta power, after intermittent TBS, but not cTBS. However, the lack of spatial specificity when applying TMS-based cTBS onto the scalp of a rat is confounding; there is no procedure to establish that the findings were related to stimulation of one area in particular. Regardless, the reported effects of intermittent TBS were those, which if compared to the human studies, would have been expected for the cTBS, e.g. an increase in the beta/gamma power of ongoing oscillatory activity. There were no significant effects of cTBS on the oscillatory power in the study by Benali *et al.*. In

our study, there were no significant effects of cTBS on peak power in any area *in vitro*. However, there were significant effects on the mean power in the oscillatory states. This indicates that the effect of cTBS on power depends on the intrinsic power variability. This change in activity pattern and subsequent increase in variability suggests that the changes from cTBS cannot be reliably assessed with a defined band-approach or peak approach. These analysis methods were used in the EEG studies previously discussed, which reported an increase in sensorimotor beta power after cTBS (Noh *et al.*, 2012), or no change (McAllister *et al.*, 2011).

The local effects seen *in vitro* were time-dependent, e.g. they predominantly increased or decreased gradually over 30 minutes after cTBS. In most cases, however, they did not reach significance until 30 minutes after cTBS. Particularly interesting is the non-significant observation that oscillatory activity in some areas was only reinforced in one part of their frequency range. For example, cTBS applied in MI LIII appeared to only increase the power in the lower beta and mu ranges in MI LV, while the ongoing beta activity appeared unaffected. In MI LIII after $cTBS_{MI LIII}$ the broad ongoing activity increased in power. This could also be supportive of the idea that the local activity is reinforced and could be seen reflected in other connected areas. The model by Di Lazzaro *et al.* (2012) suggests that the effects of TMS cTBS are localised to the pyramidal cells in layer II and III, and then indirectly activates the pyramidal cells in layer V and local interneurons. As the beta power in MI LV after cTBS in MI LIII is not increased, it questions if the model is telling the complete story, or parts of it. cTBS is suggested to affect $GABA_A$-transmission (Tanaka *et al.*, 1997; Frerking *et al.*, 1998; Stagg *et al.*, 2009); this would affect the ongoing beta oscillations in MI LV which depend on this type of transmission (Yamawaki *et al.*, 2008). However, cTBS is also reported to have effects on NMDA-transmission and plasticity (Pattwell *et al.*, 2012) and Pell *et al.* (2011) has emphasised that effects of cTBS may well incorporate other neurotransmitter systems.

None of the studies reviewed have focused on changes in frequency after cTBS. We speculate that this is predominantly due to the differences in analysis approach. Oscillatory frequency features is particularly interesting here since it can be considered representative of the underlying network size and behaviour. We were not able to determine the frequency changes in the MEG recordings due to software differences. However, *in vitro* $cTBS_{MI LV}$ significantly decreased the ongoing mean peak frequency and $cTBS_{SI LIV}$ resulted in a significant decrease in oscillatory mean peak frequency in SI LIV. The absence of this effect in MI LIII after $cTBS_{MI LIII}$ could be due to the wider preference of natural resonance frequencies in MI LIII, and/or low experimental numbers.

The exception from the finding of local effects of cTBS, was the significantly increase in mean downstate power in SI LIV after cTBS$_{MI\ LIII}$; a similar increase was not seen after cTBS$_{MI\ LV}$ or cTBS$_{SI\ LIV}$. This implies effective connectivity between MI LIII and SI LIV. It is unclear if the effects seen at a more distant network, in relation to cTBS location, are direct results of the cTBS itself, or delayed and indirect results from changes of activity in one location. In addition, the modulation of the power of the oscillatory activity in MI LIII after cTBS$_{SI\ LIV}$, although non-significant and temporary, further indicates a complex connectivity between these areas.

7.4.4. Effects of cTBS on oscillatory power in both MEG and *in vitro*

Neuroimaging studies using TMS-based cTBS have reported a decrease in the excitability of MI and the responsiveness of excitatory neurons (Di Lazzaro *et al.*, 2005), as well as an increase in GABA concentration in MI (Stagg *et al.*, 2009). Although beta power increased in the stimulated hemisphere in the MEG experiments, there was no significant increase in peak power in these *in vitro* experiments. However, the *in vitro* experiments showed significant increases in mean upstate power in MI LIII and SI LIV. A change in bursting patterns could increase the variance which renders the peak power change less obvious. The primary suggested effects of cTBS are on the pyramidal cells in layer II/III, which then indirectly excite the pyramidal cells in layer V and local interneurons (Di Lazzaro *et al.*, 2012). Thus, the effects of cTBS applied in MI LIII *in vitro* should be similar to the effects seen after TMS-cTBS. This holds true in our experiments to some degree. The effects are seen on the mean power in the oscillatory state rather than on the peak power. The relevance of this difference is unclear since the available network is smaller and the ongoing oscillations are induced by continuous application of drugs *in vitro*.

7.5. Conclusion

We have showed that there is a beta power increase in the stimulated hemisphere in humans. We then went on to characterise the mechanisms of this increase *in vitro* and showed that the mean peak frequency of the local networks to which cTBS was applied decreased. Although there were no significant differences in mean peak power *in vitro*, the oscillatory state power was significantly increased in both MI LIII and SI LIV after cTBS in MI LIII, and in SI LIV after cTBS in SI LIV. These results indicate that cTBS particularly affect the *patterns* of oscillatory activity *in vitro*, indirectly through excitability and inhibition level in the local sensorimotor neuronal networks. From this we conclude that cTBS applied in the sensorimotor cortex affects the local oscillatory power and frequency, *in vitro* and in MEG. The effects of cTBS depend on modulation of neurotransmitter systems including GABA$_A$-transmission. In this study, we have confirmed that results from these two modalities are comparable with regards to oscillatory power and we have started to elucidate which mechanisms underlie effects on sensorimotor oscillations.

Chapter 8. Sensorimotor beta oscillations in Parkinson's disease and their GABAergic modulation

8.1 Background

8.1.1. Introduction

In previous chapters we discussed the features of spontaneous oscillatory activity in the sensorimotor cortex both in healthy humans and *in vitro* preparations. Additionally, we have revealed effects on the sensorimotor beta oscillatory activity from GABAergic and frequency stimulation modulation. Here we consider beta oscillations in MI in human subjects with Parkinson's disease. In addition, we investigate the effects of GABAergic modulation with zolpidem on these oscillations and the PD motor symptomatology.

Cortical oscillations and motor cortex excitability have been found to be altered in PD patients (Ridding *et al.*, 1995; Lefaucheur, 2005; Pollock *et al.*, 2012) as well as facilitation and inhibition in the intracortical pathways (MacKinnon *et al.* 2005). The oscillatory beta dynamics surrounding movement and stimulation in the sensorimotor cortex also appear different in PD patients compared to healthy subjects (Labyt *et al.*, 2005; Brown, 2007); suggesting an undetermined role of the cerebral cortex in generating and/or maintaining the abnormal rhythm. The PMBR frequency amplitude in the motor cortex has been found to be decreased in PD subjects, compared to control subjects (Degardin *et al.*, 2009). This implies changed somatosensory processing and somaesthetics in PD (Tamburin *et al.*, 2003), since beta ERS is believed to reflect the motor offset command, as well as re-afference from the somatosensory areas (Cassim *et al.*, 2001; Pfurtscheller *et al.*, 2005). Overall, the motor excitability after sensory input is conclusively altered in PD patients, compared to control subjects (Sailer *et al.,* 2003; 2007). To date the cortical activity alterations in PD patients and the central role of cortex in functional connectivity are implicit, but poorly understood.

The abnormal appearance of beta oscillations in the motor system in PD subjects is accompanied by motor deficits. Cortico-cortical coherence in the upper and lower beta band correlate with the severity of the Parkinsonian symptoms (Silberstein *et al.* 2005). Some of the symptoms of PD can initially be reduced with dopaminergic drugs such as L-Dopa (Cotzias *et al.*, 1969; Eskow-Jaunarajs *et al.*, 2011) or deep-brain stimulation to the basal ganglia (Brown *et al.*, 2001; Benabid 2003; Silberstein *et al.*, 2005; Brown 2007; Bronstein *et al.*, 2011). Symptom relief provided by these methods is supportive of the importance of basal ganglia in the motor system as, at least partly, responsible for modulation of the abnormal beta oscillations. The importance of dopaminergic neurons in the basal ganglia is further supported by animal models, such as the 6-hydroxy-dopamine (6-OHDA) and 1-methyl-4-phenyl-1,2,3,6 tetrahydropyridine (MPTP) models. Studies

using animal models of PD often report that the beta oscillatory activity in the motor system is abnormal in the power domain (Sharott *et al.*, 2005; Mallet *et al.*, 2008a; 200b). However, this is not reported to the same extent in human PD subjects. Here the reported effects concern the frequency domain with a reported slowing of cortical oscillatory activity and altered functional connectivity.

Previous research have shown that GABAergic substances affects the beta oscillatory activity and dynamics in healthy and stroke patients (Baker & Baker 2003; Jensen *et al.*, 2005; Hall *et al.*, 2009; 2010; 2011) and beta oscillations have been found to also be modulated by dopaminergic substances (Litvak et al, 2010; Jenkinson & Brown 2011). However, the altered motor patterns and diminished inhibition with increasing MPTP levels (Leblois *et al.*, 2007) is not just evidence that dopaminergic connections are essential and their destruction underlies PD, it also indicates the importance of the GABAergic inhibitory system in PD and relevant motor symptoms. Another important substance in PD with regards to the GABAergic system is BDNF, which is synthesised and used in the nigrostriatal system. Decreased production of this substance leads to loss of the dopaminergic cells typically seen in PD (Porritt *et al.*, 2005), while up-regulation of BDNF is also suggested as a potential mechanism for the long-lasting symptomatic improvement seen in PD after deep-brain stimulation of STN (Spieles-Engemann *et al.*, 2011). As was briefly discussed in the chapter on TBS, BDNF has been reported to modulate $GABA_A$-R mediated transmission (Tanaka *et al.*, 1997).

The significance of the GABAergic system in modulating abnormal beta oscillations and movements has been shown in case studies involving administration of zolpidem to stroke patients with lesions over their sensorimotor cortex and subsequent impaired movement (Clauss *et al.* 2000; Hall *et al.* 2010). Zolpidem is also known to improve symptom severity in PD (Daniele *et al.*, 1997). Modulating either or both of the dopaminergic and GABAergic systems, would indistinctly and inevitably affect the other and in the wider perspective all other activity in the brain, including oscillations in the cortex. The disease state and medication status are important when considering the effects of zolpidem administration on beta oscillatory activity (Silberstein *et al.*, 2005; Stoffers *et al.* 2007; Pollok *et al.,* 2012). In normal subjects, oscillatory beta activity in the contralateral hemisphere is suppressed during movement. The findings by Pollok *et al.* indicated increased and equal beta activation in both hemispheres during motor activity in PD patients, in contrast to medicated patients where the opposite was seen. Here we have studied unilateral and early state PD-patients who are not on medication.

8.1.2. Aims and research objectives

The information on the effects sensorimotor beta oscillations in PD patients are limited by the investigation of medicated, later stage patients. This was addressed here by studying sensorimotor oscillations in non-medicated, unilaterally impaired early-stage PD patients. The GABAergic modulator zolpidem has been found to decrease severity of sensorimotor symptoms in PD patients (Daniele *et al.*, 1997). There is limited research available on the effects of zolpidem administration on the abnormal cortical beta oscillations seen in PD patients. However, recent studies in stroke, suggests that zolpidem acts as a desynchronising agent, which reduces the power of pathologically elevated beta oscillations. Here, sub-sedative doses were administered to PD patients and sensorimotor beta oscillations, before and after administration, were studied with MEG. We aimed to understand the effects of PD in our specific PD population before and after zolpidem. We address the following questions:

- o What are the oscillatory differences between affected compared to unaffected MI hemispheres in PD?
- o What are the effects of zolpidem on neuronal network activity in PD?
- o What is the relationship between neuronal network changes and functional improvement following zolpidem in PD?

8.2 Methods

This study was done in collaboration with the neurlogist consultant Dr Adrian C Williams at Queen Elizabeth Hospital in Birmingham. The participants were diagnosed by and recruited through Dr Williams, and he also performed the Unified Parkinson's Disease Rating Scale (UPDRS) assessments. UPDRS measures the longitudinal symptomatic course of PD through self-evaluation, interview and clinical observation. It consists of several sections where different aspects of the symptoms: mentation, behaviour and mood, daily life activities and motor skills, are scored independently. We used the motor assessment in this study. Nine subjects (3F), age range 56-68 years, were seated in an upright position in the 275-channel MEG scanner (CTF, Canada). The study was performed in accordance with the Declaration of Helsinki, and approved by the Ethics Committee of the School of Life and Health Sciences at Aston University. Written informed consent was obtained from all participants. The same pharmaco-MEG protocol used for healthy subjects, see chapter 5, was used for uni-lateral PD participants without prior medication history. They received visual instructions from a monitor positioned outside the shielded room, which was visible through a small window. This informed the subjects about when to perform self-paced finger movements, when they would receive electrical stimulation to their index finger (Digitimer Ltd, UK) and when they should remain seated and rest. The visual instruction and stimulation events were delivered through the software Presentation (Neurobehavioural Systems Inc., US).

Immediately prior to the first MEG experiment the patients were evaluated using the UPDRS. After the first MEG experiment the patients were given a sub-sedative dose of zolpidem (0.05 mg/kg) orally. The UPDRS evaluation of their symptoms was then repeated 50 minutes after the ZPD administration, immediately before the second MEG assessment. Both the contralateral (to symptoms) and the ipsilateral hemisphere were investigated and compared to controls. MI was localized by SAM using the PMBR, as described in chapter 2 and 3. Recorded trials with too much head movement and/or artefacts were discarded. One participant was discarded due to this. The recorded data was analysed in the time-frequency domain by calculating group average Morelet-Wavelet spectrograms for periods of interest: rest, surrounding movement and stimulation events. These were then further analysed by custom-made MatLab scripts (Mathworks Inc., US). As previously discussed, temporal averaging prohibits investigation of frequency variability; therefore the frequency variability was investigated on 30s of resting data by using a slide PSD window approach, as described in the analysis section in the chapter 2.

8.3 Results

8.3.1. Spontaneous sensorimotor oscillatory beta activity in PD patients

In PD patients the hemisphere contralateral to symptoms exhibited beta oscillations with higher peak amplitude compared to the ipsilateral hemisphere; 9.2±4.6 nAm, compared to 3.32±2.12 nAm. The beta frequency observed in the contralateral hemisphere was 18.2±5.73 Hz, compared to 22.1±5.44 Hz in the ipsilateral. The difference in peak frequency was non-significant. Although considerable subject variability in MI beta power in the pre-zolpidem condition, the beta power in the contralateral hemispheres was consistently and significantly higher than the ipsilateral side before zolpidem administration ($t_{[7]}$=3.28, p=0.014) (figure 8.1a-b).
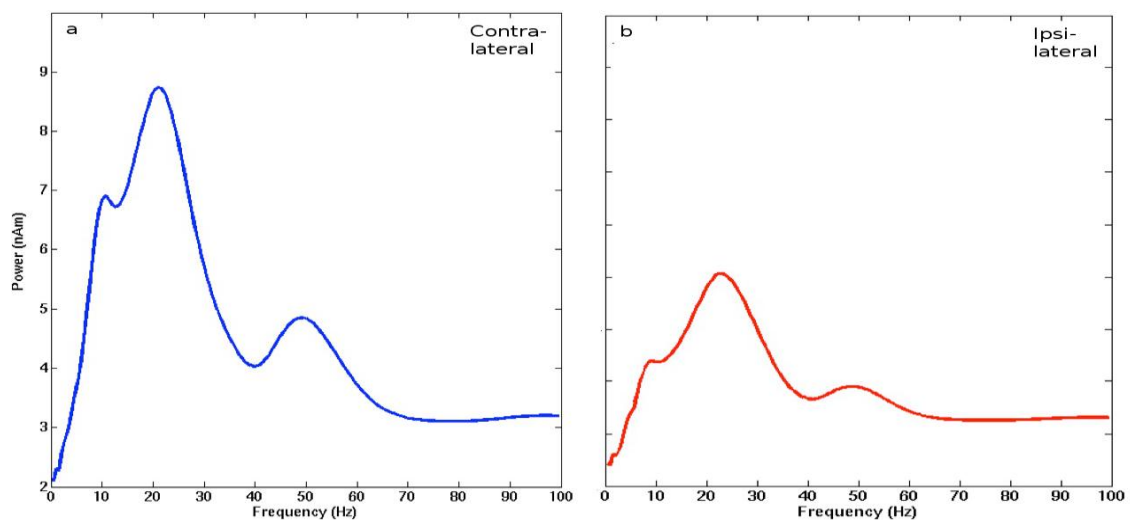
Figure 8. 1a-b. Group and time average PSD plots showing oscillatory activity in the (to symptoms) contralateral, seen in a (left), and ipsilateral, seen in b (right), MI in PD patients. The difference in peak power was significant, p<0.05.

8.3.2. Effects of sub-sedative doses of zolpidem administration on UPDRS in PD patients

The PD patients were assessed with UPDRS. This confirmed their unilateral and individual level of symptom severity, mean UPDRS 14.25±5.0. Given the previously discussed relationship between cortical beta power and symptom severity in PD, we tested this prior to zolpidem administration. There was no correlation between cortical beta power and UPDRS symptom severity (r^2=0.0005, p=0.58). The administration of zolpidem significantly improved overall severity of symptoms, mean UPDRS improved with 7.5 score points, p=0.006. Individual categories all improved significantly, with the exception of the speech category, see figure 8.2.
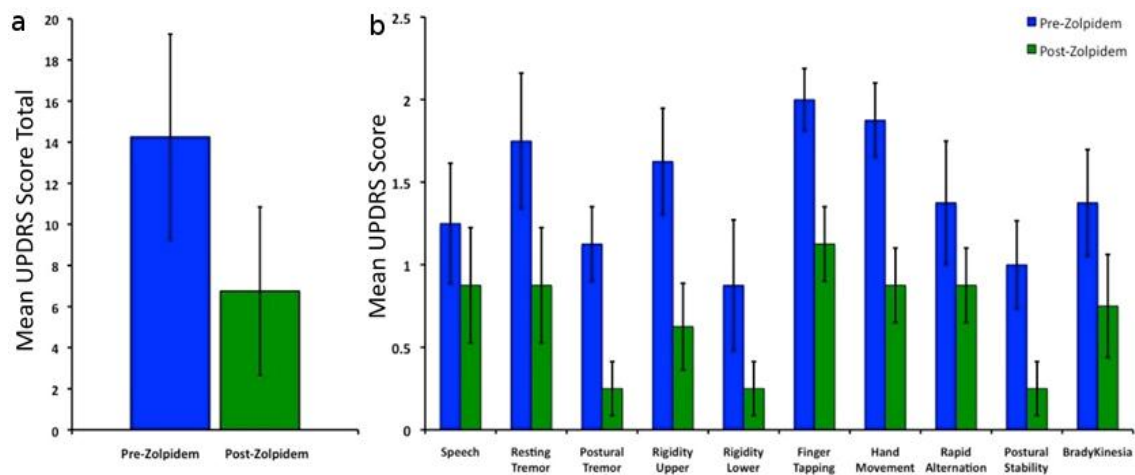
Figure 8. 2a-b. Significant improvements were seen in the total mean UPDRS score, as well as all individual categories, p<0.05, except speech where there was a non-significant effect.

8.3.3. Effects of zolpidem administration on oscillatory sensorimotor beta activity

Administration of zolpidem significantly decreased the oscillatory beta power in the contralateral hemisphere with 2.7±2.9 nAm, $t_{[7]}$=2.62, p=0.034. The frequency after zolpidem changed from 18.1 to 21.8Hz, which was non-significant. In the ipsilateral hemisphere the beta power increased significantly with 1.7±1.1 nAm, which was significant, $t_{[7]}$=4.26, p=0.004. See figure 8.3a-b for the changes in ongoing oscillatory power. The frequency after zolpidem administration in the ipsilateral hemisphere increased from 22.1 to 24.2 Hz, which was non-significant.
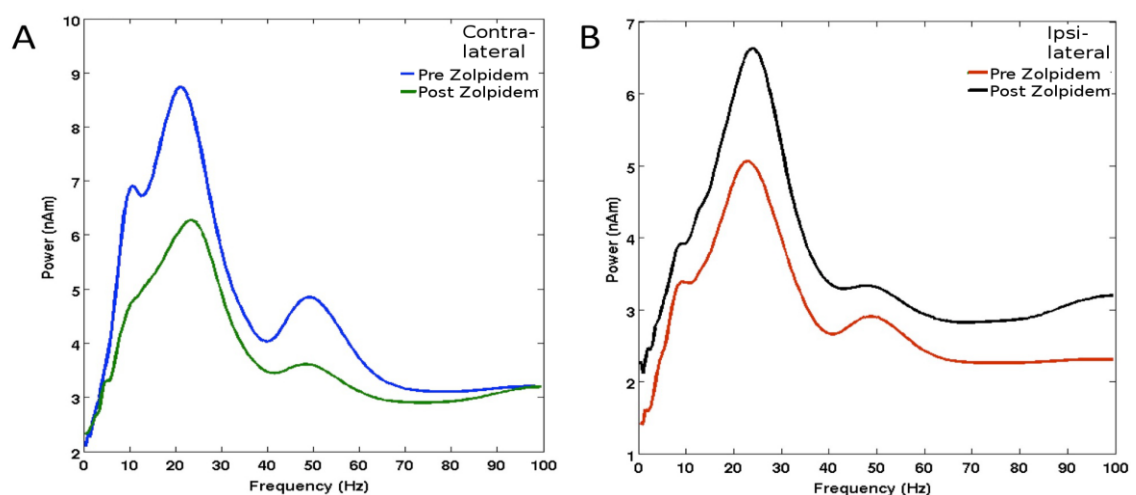
Figure 8. 3a-b. Administration of sub-sedative doses of zolpidem significantly decreased the ongoing beta activity in the contralateral, a (left), and increased in the ipsilateral, b (right), hemisphere.

There was no significant relationship between the UPDRS improvement and decrease in beta power in either the contralateral or ipsilateral hemispheres. However, we noted that after zolpidem administration the beta power decreased in the contralateral hemisphere and beta power increased in the ipsilateral hemisphere. We theorised that the ratio of hemispheric beta power was important with regards to the symptom severity. The beta power ratio between hemispheres indicated an increase in the mean MI inter-hemispheric ratio from 0.59 to 1.1. Pearson correlation calculations revealed a significant correlation between the MI inter-hemispheric ratio and UPDRS scores, r^2=0.40, p=0.009. In addition, there was also significant correlation between some of the UPDRS individual categories and prediction of improvement (fig 8.4). Specifically upper limb rigidity: r^2=0.60, p=0.024; finger tapping: r^2=0.58, p=0.027 and rapid alternating hand movement r^2=0.55, p=0.034, respectively (not corrected for multiple comparisons).
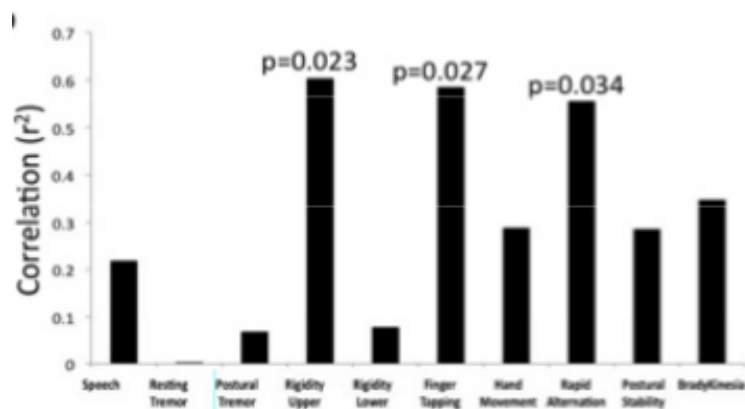
Figure 8. 4. Plot showing the correlation between ratio change and the improvement in individual UPDRS categories. The p-values of the three significant (p<0.05) correlations are displayed above respective bar: upper limb rigidity, finger tapping and rapid alterating hand movement.

Beta activity in MI before zolpidem administration shows greater stationarity at peaks around 10 and 20 Hz. After zolpidem administration, the frequency distribution has shifted to lower and higher frequencies. Computation of t-statistics for each frequency bin indicated a significant reduction in the stationarity of the samples at peak frequency between 15 and 21 Hz. In addition, there were significant increases in peak frequency samples in 30 and 42 Hz (figure 8.5a-b). There was a significant correlation between the change in peak frequency distribution in the low-beta frequency range, e.g. 15 to 21 Hz, and overall UPDRS improvement, r^2=0.75, p=0.0053. Furthermore there was also a significant correlation between the change in peak frequency distribution in the high beta/low gamma frequency range, e.g. 30 to 42 Hz, and UPDRS improvement, r^2=0.66, p=0.014.
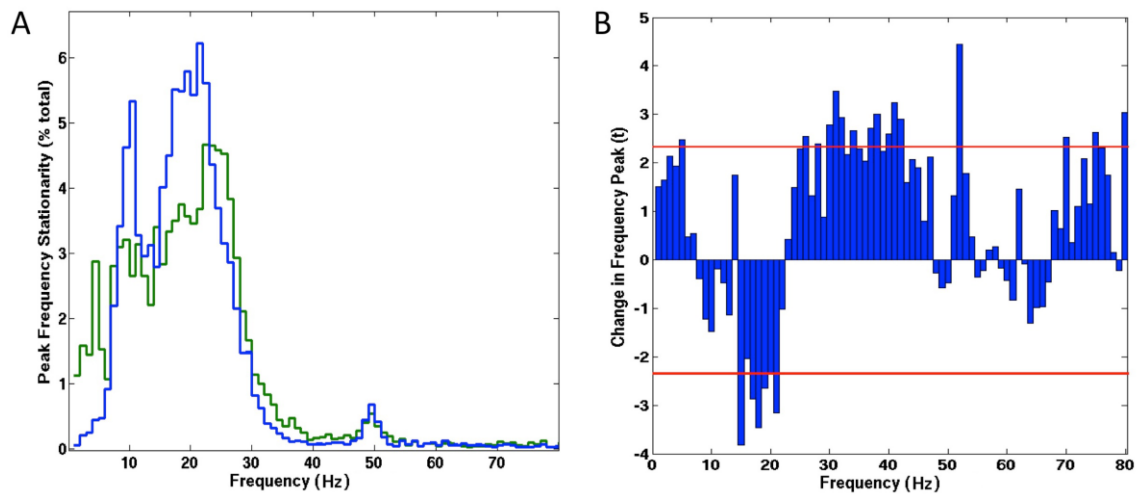
Figure 8. 5a-b. The peak frequency variability is significantly changed in the contralateral hemisphere after zolpidem administration, as shown in the 1 Hz binned frequency distribution histogram seen in A. The peak frequency distribution before zolpidem administration is illustrated by the blue outline, and post-zolpidem is illustrated by the green outline. In particular activity seen in the low beta and high beta/low gamma frequency range as affected by zolpidem administration, seen in the t-distribution plot in B. The red lines indicate the threshold for statistical significance at p<0.05.

8.4 Discussion

8.4.1. Summary

We found that administration of sub-sedative doses of zolpidem significantly improves the symptomatic severity in unilateral early-stage PD patients. Zolpidem administration significantly decreased the power of the ongoing beta oscillations in the contralateral MI, while significantly increasing the beta power in the ipsilateral MI. The improvement in overall UPDRS score was significantly correlated to the increase in hemispheric ratio of beta power, rather than the beta power in the individual hemispheres. Furthermore, we found that PD patients have a less dynamic peak frequency distribution with preference for lower beta frequencies. This peak distribution is significantly changed after zolpidem administration in the low beta and low gamma frequency ranges. The change in the frequency distribution at these ranges was significantly correlated with UPDRS improvement.

8.4.2. The "pathological" beta oscillations observed in PD patients

Although the beta oscillations in the motor network is a topic widely debated within PD research, the "pathological" versions of beta oscillations have been primarily located to the sub-cortical parts of the motor network (Brown 2001; 2007; Crowell *et al.*, 2012; Stein & Bar-Gad 2012). The term, "pathological" oscillations, is ambiguous as it is unclear which features of these oscillations are correlated to the PD symptoms. In terms of effects on power, previously cited articles report augmented beta power in the sub-cortical motor network, in combination with increased coherence (Sharott *et al.*, 2005). Additionally, applying transcranial beta stimulation, e.g. 20 Hz, has been coupled to impaired movement ability (Pogosyan *et al.*, 2009; Joundi *et al.*, 2012). Recently, early-stage PD subjects have been reported to display increased beta synchronisation in the contralateral MI (Pollok *et al.*, 2012). In our PD patients the ongoing beta oscillatory activity in the contralateral MI showed significantly stronger beta power compared to the ipsilateral MI, supportive of previous findings by Pollok *et al.* (2012). However, we found no correlation between contralateral, or ipsilateral, MI beta power to symptom severity. Therefore, we argue that the differences in contralateral MI beta power seen in unilateral and early stage PD patients is not enough to explain the PD motor symptomatology.

Previous reports have reported that PD patients show a lower peak frequency of the ongoing activity in MI, e.g. the peak power was found at lower beta frequencies (Bosboom *et al.,* 2006; Moazami *et al.,* 2008), with links to disease severity and UPDRS symptom

severity (Vardy *et al.*, 2011). We found no significant differences in the peak frequency between contralateral and ipsilateral MI in our non-medicated, unilateral and early-stage PD patients. However, the patients in the study by Vardy *et al.* had the average disease duration of 5 years and were on medication at the time of the experiment. We speculate that those factors contribute to the difference seen between our results.

Although there were no significant differences in frequency between opposite hemispheres, we did find that the peak frequency distribution in the contralateral hemisphere appeared shifted towards lower frequencies and displayed less dynamicity. The ongoing activity in the contralateral MI showed preference to remain at lower beta frequencies. A similar observation of beta frequency peak variability was correlated to clinical state by Little *et al.* (2012). Our results suggest that our measure of peak frequency distribution is representative of the underlying neuronal network responsible for the observed oscillations. In addition, our results indicate that reduced dynamicity and preference of low frequency activity are features of, and related to, PD motor symptoms as determined by UPDRS.

8.4.3. GABAergic modulation of beta oscillations in PD patients with zolpidem

The GABAergic modulator zolpidem has previously shown to reduce abnormal sensorimotor beta oscillations in stroke patients (Hall *et al.*, 2010), and benzodiazepines are known to increase beta power in healthy subjects (Domino *et al.* 1989; Baker & Baker 2003; Jensen *et al.*, 2005; Hall *et al.,* 2009; 2011). We showed in chapter 5 that the non-benzodiazepine imidazopyridine zolpidem also increased MI beta power in healthy subjects. In this study we have showed that, similar to patients with a sensorimotor stroke lesion (Hall *et al.*, 2010), administration of a subsedative dose of zolpidem significantly decreased the power of the "pathological" beta oscillations in the contralateral MI. In contrast, zolpidem significantly increased the power of the beta oscillations in the ipsilateral MI.

Initially, our working hypothesis was a speculated correlation between contralateral beta power in MI and symptom severity, since this has been implicitly discussed in previously cited research. However, we found no significant relationship between these. There is substantial abnormal sensorimotor processing and event-related beta oscillatory activity in PD patients, compared to healthy subjects (Sailer *et al.*, 2003; Tamburin *et al.*, 2003; Degardin *et al.*, 2009). We observed strong inter-subject variability in beta power,

especially between the two hemispheres and therefore we speculated that movement symptomatology was correlated to beta power ratio between the hemispheres, since the atypical sensorimotor processing is related to the sensorimotor beta power. We found that zolpidem increased the hemispheric beta power ratio, and that this increase showed a strong linear relationship to improvement of UPDRS motor scores. Additionally, we also found that the differences in contralateral MI beta peak frequency variability were significantly changed in the low beta and gamma frequency ranges after zolpidem administration. These changes also showed strong correlation to the UPDRS improvement.

In vitro studies have elucidated some of the mechanisms underlying the effects of zolpidem on beta oscillatory activity. Zolpidem affects the $GABA_A$ transmission, and thus play an important role in the generation and sustenance of beta oscillations in motor cortex, e.g. MI LV (Yamawaki *et al.*, 2008; Prokic *et al.*, under review). We showed in chapter 5 that the beta peak power of sensorimotor, e.g. MI LV, MI LIII and SI LIV, oscillatory activity is increased by zolpidem application. Furthermore, there is *in vitro* evidence suggesting a dose-dependent response of zolpidem, with regards to tonic and phasic GABAergic transmission in MI (Prokic *et al.*, under review). This complicates the suggested mechanisms underlying the effects of zolpidem on MI beta oscillations in PD subjects. The mechanisms of zolpidem on GABAergic transmission in PD subjects are further obscured by the suggested genetic and biological differences in relation to PD pathophysiology (Olanow & Tatton 1999, Davie 2008; Zuccato & Cattaneo 2009). An example of this is the down-regulated BDNF expression in the dopaminergic nigrostriatal system in PD (Porritt *et al.*, 2005), and correlation of serum-levels of BDNF with PD motor impairment (Zuccato & Cattaneo 2009; Scalzo *et al.*, 2010). BDNF modulates the $GABA_A$ mediated transmission (Tanaka *et al.*, 1997); as BDNF levels are reportedly perturbed in PD this would also contribute to differences in the effects of zolpidem on GABAergic transmission, and inevitably on beta oscillations in MI.

8.4.4. Symptomatic improvement through GABAergic modulation with zolpidem

Previous studies over the last decades have found that the GABAergic modulation provided by the hypnotic zolpidem improves symptoms, measured with UPDRS, in PD patients (Daniele *et al.,* 1997). Our results supported this established finding. We wanted to investigate the link between the previously reported elevated beta power in the contralateral motor network and symptoms (Brown 2001; 2007; Crowell *et al.*, 2012;

Pollok *et al.*, 2012; Stein & Bar-Gad 2012). We tested the relationship of the beta power in the contralateral MI to UPDRS score and found no significant correlation. We therefore concluded that beta power in the contralateral, or ipsilateral, MI is not representative as a biological marker of PD.

During the course of analysis we observed that zolpidem had opposite effects on the MI beta power in either hemisphere. The beta power in the contralateral hemisphere decreased after zolpidem administration, while the ipsilateral MI beta power increased in power. This led us to consider the ratio of beta power between the contralateral and ipsilateral MI as a potential cause of symptoms in PD. The ratio of beta power between the hemispheres showed a strong linear relationship with UPDRS score; in particular finger tapping and the movement sub-set of the UPDRS in our patients. This is particularly interesting when the reported differences in sensorimotor processing and motor cortex excitability (Ridding *et al.*, 1995; Sailer *et al.*, 2003; Lefaucheur, 2005) in PD patients are taken into account. PD patients have altered sensorimotor network connectivity and processing (Tamburin *et al.*, 2003), with differences predominantly seen in event-related changes surrounding movement and stimulation (Labyt *et al.*, 2005; Brown, 2007; Degardin *et al.*, 2009). The beta ERD is bilateral just prior to movement (Pfurtscheller & Lopes da Silva 1999), and an imbalance in the ratio of beta power between MI in the opposite hemispheres would potentially confound this pattern. However, while the difference in beta power ratio between the opposite MI in the two hemispheres is a neat explanation of these results, our study only includes early-stage patients which present with unilateral symptoms. Later-stage patients often present with symptoms on both sides, which cannot be explained by the change in hemispheric ratio of beta power. The sensorimotor system and associated processing in these patients have most likely developed further plasticity and network modification and it is therefore not possible to extrapolate these results onto those patients.

The concept of PD-induced altered cortical excitability and activity fits well with the suggestions of transformed network activity and layout, followed by changes in synchrony found in PD as well as other neuropathies (Uhlhaas & Singer 2006; Brown 2007; Hammond *et al.*, 2007). The findings from this study confirm the idea of abnormal ongoing beta activity in the sensorimotor beta network, which subsequently result in beta oscillatory functional discrepancies in PD, compared to controls. Alterations to this network would most likely depend on how far the disease has progressed and medication status. This agrees with the hypothesis that diseases arise when there is a disturbance in the synchronised activity of areas (Hammond *et al.* 2007; Crowell *et al.* 2012). In PD there is wide-spread imbalance in sensorimotor network and its oscillatory features (Uhlhaas &

Singer 2006; Brown 2007; Hammond *et al.*, 2007; Lalo *et al.*, 2008; Stam 2010; Timmermann & Fink 2011). In this study we have revealed some of the characteristic oscillatory features in MI of PD patients, their correlation to motor symptomatology, and how this can be modulated by the GABAergic modulator zolpidem. Essentially, this will contribute to better diagnosis and treatment of PD patients.

8.5. Conclusion

Our results supports the idea of impaired sensorimotor processing in early-stage unilateral PD patients, represented by the differences in hemispheric MI ratio in beta power and changes in the peak frequency distribution. We conclude that GABAergic modulation with zolpidem temporarily readdresses this balance. This is based on the significant correlation between symptomatic UPDRS improvement and the return of the hemispheric ratio to approximately 1. In addition, we also base this on the significant linear relationship between UPDRS improvement and the changes in peak frequency variability seen after zolpidem administration. These findings could be used for further studies of relevant biological markers of early stage, unilateral, PD.

Chapter 9. General discussion and future perspectives

9.1. Introduction

This project aimed to investigate oscillatory activity in the sensorimotor cortex using two different recording methods. Our results are interpreted in a translational manner, in which we explore the extent to which non-invasive data from living humans are comparable with invasive *in vitro* data from brain slices. In this chapter we will discuss the main research highlights from the individual studies with a view to the translational perspective that has imbued our presented work.

9.2. Methodological considerations

MEG and LFP recordings are not novel technologies. Both are straight-forward methods, well-established and reliable from a replication point of view. However, one of the primary difficulties in assessing the comparability between *in vitro* and MEG oscillations was coming to terms with the differences in conventional analysis approaches. There are several limitations to conventional approaches; mostly based on the attenuation of variability with averaging and the use of pre-set frequency bands. Variability in the oscillatory signal is important since it features not just between individuals and/or recordings, but also within the recordings over time. We observed early on that there appeared to be more variability in frequency in the MEG signals, which showed up as frequency-wise broad activity in PSD graphs. In contrast, the *in vitro* oscillations appeared as a reliable and persistent sharp peak in the PSDs. Additionally, in Morelet-wavelet spectrograms we saw differences in the frequency and power over time, between recordings and areas, more so in MEG recordings. Although few studies have approached the concept of variability in oscillatory activity, we wanted to compare results from interventions using these two modalities, therefore it was pertinent that we characterised the underlying cause for the distinction of appearances.

In approaching this research question additional insight into the neuronal substrates and networks which underlie the oscillatory signals recorded *in vitro* and in MEG would also be gained. We designed MatLab scripts that would help us characterise the variability and distribution in oscillatory frequency and power, as well as reliable peak information, which was not skewed from acceptable, but extreme, values. The chapter on Parkinson's disease emphasised the importance of frequency variability. Likewise, as was shown in the incision experiments, in chapter 4, disrupting sensorimotor connectivity affect the frequency variability. These results provide evidence for the frequency variability as a further indicator of the neuronal network activity. In terms of developing and expanding this analysis approach there is an abundance of possibilities and options.

9.3. The rhythm *en arceau* and the sensorimotor cortex

The first task in this project was to investigate the spontaneous and ongoing oscillatory activity found in the sensorimotor cortex of humans and in rats. We expected to, and indeed did, find mu and beta oscillations in the human MEG recordings. However, we were surprised to see that there was no significant difference in the mean peak frequency between these areas, although the amplitude differed significantly. Our measure of network distribution, mean FWHM, also indicated that there were no significant differences between MI and SI. Most previous research investigating human sensorimotor oscillations have focused on changes in the oscillatory activity after task performance or stimulus application (Pfurtscheller & Lopes Da Silva 1999; Neuper & Pfurtscheller 2001; Cheyne, 2012). Spontaneous ongoing oscillations and their features are relatively uncharacterised. In addition, analysis approaches which focus on changes in a pre-determined oscillatory frequency range, specific for an area, would not necessarily pick up on similarities between areas. Given the strong inter-individual differences in cortical anatomical layout, it is plausible that the localisation of spontaneous beta and mu oscillations in MI and SI is highly individual to both the recording and the subject. This is an important topic of investigation and should be pursued further along with additional characterisation of the ongoing oscillatory activity in the sensorimotor cortex in humans.

Studying ongoing oscillatory activity in MI *in vitro* confirmed previous findings of beta oscillations in the deeper and superficial layers (Yamawaki *et al.*, 2008). However, we also found mu co-existing with the beta activity in the superficial layers of MI, as well as in middle layers of SI. Mu oscillations have previously been reported *in vitro* to some extent from other sensory areas, although specific locations are less lucid. However, we have not found any previous reports on mu oscillatory activity originating in superficial layers of MI.

Investigating the network and peak frequency distribution in the different sensorimotor laminae *in vitro* highlighted significant differences between areas. Peak frequency distribution was significantly different between all recorded laminae and the mean FWHM was significantly smaller in MI LV, compared to SI LIV. The difference in mean FWHM between MI LV and MI LIII did not show significance, which is intriguing since previous research has shown that oscillatory beta activity in MI LIII depends on MI LV (Yamawaki *et al.*, 2008). These findings indicate that there are sub-areas of the neuronal networks in MI and SI which display slightly different frequencies. MI LIII, MI LV and SI LIV could be considered to be one large sensorimotor network as shown in connectivity functional studies and causality modelling (Brovelli *et al.*, 2004), but we theorize that there also exists smaller sub-networks within areas. We will discuss the relevance of connectivity in

neuronal network activity further in the next section below (9.4). The finding of mu oscillatory activity in sagittal sensorimotor slices is thus in some respects novel. This finding provides an opportunity to study underlying mechanisms and effects of interventions on the mu rhythm in greater detail, as well as its relation to other frequency bands in the sensorimotor cortex.

Sensorimotor mu oscillations and changes to these have been linked cognition, attention, mirror neurons and many other higher order functions (Cochin *et al.*, 1998; Pineda, 2005; Moore *et al.*, 2008; van Dijk *et al.*, 2008; Jones *et al.*, 2010; Anderson & Ding 2011; Francuz & Zapala 2011; van Ede *et al.*, 2011; Freyer *et al.*, 2012). The lack of findings of sensorimotor mu oscillations *in vitro* have in some respects indirectly and anecdotally contributed to the idea of mu as a higher order rhythm. We do not dispute the assignment of mu oscillatory activity to any of the above. However, we have shown that mu can exist in isolation from higher order functioning, e.g. *in vitro*. Additionally, the finding of mu oscillations *in vitro* indicated that the sensorimotor oscillatory activity in LFP recordings *in vitro* was more similar to the oscillatory activity seen in sensorimotor MEG recordings than we had first believed. Given that MEG is recorded from outside the scalp, while *in vitro* recordings are performed closer to the oscillating neuronal substrate in the slice, we decided to integrate the recordings from MI LIII and MI LV to see how far this would resemble the MEG MI oscillatory signal. We found that integration provided a frequency-wise broader PSD and spectrogram representation of the ongoing activity, similar to the MEG MI. Furthermore, since the MEG sensors are further away from the deeper layer than the superficial layers of MI, weighting provided an additional factor in our integration process. This created an aggregate oscillatory signal with a PSD further resembling the MEG recordings, but based on the less complex *in vitro* signals. The integration was done at the last stages of this project and we believe that this would be particularly useful in the future for comparative studies between interventions *in vitro* and in MEG and thus provide the empirical evidence for the validation of comparison.

9.4. Connectivity and networks; consequences on oscillatory activity

We established that the differences in the oscillatory signals seen in MEG and *in vitro* were due to contributing number networks and their inherent frequency variability. We went on to determine how the connectivity of oscillatory neuronal networks affected the

recorded activity. Necessarily this was done *in vitro*, as this method allows for invasive probing of network activity. We compared oscillatory activity in different laminae between intact slices where the connectivity between MI and SI was untouched, to microslices, where MI and SI were physically separated prior to recording. There were significant differences in the mean peak frequencies in MI LV and SI LIV. In addition we found that placing an incision between MI and SI while recording significantly decreased the peak frequency variability in SI LIV. We concluded that while the two areas display activity which is generated locally, the activity in both areas is also affected by the other. This is particularly obvious in the case of SI LIV where the oscillatory profile changes dramatically and the peak frequency variability is affected by the acute incision. We showed that both mu and beta rhythms can exist in physically isolated MI and SI, but most importantly, these experiments established the importance of connectivity in the features of ongoing oscillatory network activity in the sensorimotor cortex. Appropriate future directions for these findings would be to probe the ongoing oscillatory activity with pharmacological modulation to see if responses are similar or different in the connected areas, compared to isolated areas. Our focus has been on the ongoing oscillatory activity rather than evoked potentials, as well as effects from frequency tuning; we did not find any significant or consistent effects on the ongoing oscillatory activity from preliminary single pulse experiments. Nevertheless, single pulse stimulation experiments would offer an understanding about the direct connectivity between the laminae in MI and SI areas in the *in vitro* preparation.

Additionally, although research employing physical separation of cortical laminae has already been performed (Flint & Connors 1996; Roopun *et al.*, 2006; Yamawaki *et al.*, 2008), the pharmacological blocking and physical separation of areas and laminae specifically in the sensorimotor cortex, including association areas, would provide further relevance of connectivity on ongoing sensorimotor oscillatory activity. It would also be of interest to adapt *in silico* methods with causality approaches to determine if the directionality in different sizes of physical networks, e.g. microslices, intact slices, intact sensorimotor areas/brain, is similar or if directionality changes with decreasing network size.

9.5. Modulating sensorimotor oscillations with stimulation and drugs

9.5.1. GABAergic modulation with zolpidem

Once we had established the profiles of ongoing oscillations in the two modalities we wanted to determine if interventions of these oscillations would be comparable as well. As GABAergic modulation is one of the main research interests, and there is much expertise, in our group we chose to start with a GABAergic modulation, specifically the hypnotic imizadozepyridine zolpidem.

Zolpidem is a $GABA_A$-R α-1 agonist and thus modulates GABAergic transmission. Prior research has established that the beta oscillations in MI LV are $GABA_A$-dependent and MI oscillations in the beta range increase in power after addition of zolpidem, although there is also concentration-dependency (Yamawaki *et al.*, 2008; Prokic *et al.*, under review). *In vitro*, we used 100 nM, previously reported to increase beta oscillations. As it is difficult to calculate an equivalent dose for humans, although attempts have been made, and because we wanted to study effects on awake subjects with no other medication, we gave our participants sub-sedative doses of zolpidem. We found that zolpidem significantly increases the power of ongoing oscillations in all locations *in vitro* as well as in MI and SI in humans. In particular, the power in the beta frequency range increased, while the mu was less affected (data not shown). The frequency decreased in MI *in vitro*, significant in MI LV, in agreement with Yamawaki *et al.* (2008). However, Yamawaki *et al.* used microslices, and we wanted to determine if there were any differences in effects that could be due to the connectivity between MI and SI. Hence, we repeated the zolpidem experiments in both intact and microslices and found similar trends, but less significance. The primary difference was the significant increase in peak frequency variability in MI LV after zolpidem administration. It would be interesting to see if differences between microslices and intact slices are observed for other types of pharmacological modulation; this provides insight into underlying neuronal network arrangement and cellular composition.

We concluded that MEG and *in vitro* responses to zolpidem administration are comparable with respect to oscillatory power; in both modalities the beta power increases after zolpidem administration. This provided us with a framework to discuss and relate to the research we were performing with PD patients. In PD patients the oscillatory beta peak power was enhanced in the affected hemisphere, and zolpidem reduced this increase. The correlation between beta power and symptom severity was not the significant finding. Instead we found that the hemispheric beta power ratio correlated to

symptom severity. This ratio neared 1.0 after zolpidem administration and significantly correlated with the improvement in symptoms. The *in vitro* work performed on sensorimotor slices from healthy rodents assisted in understanding the effects of zolpidem on the beta oscillations, although there are several questions remaining. As an ideal example, the oscillatory activity in MI, as well as application of zolpidem, should be replicated on slices from 6-OHDA lesioned rodents to see the full aspect of comparability. If MI beta oscillations were found to be abnormal in 6-OHDA rodents, then this opens a wide avenue of possibilities to understanding how the cortex mitigates and maintains the pathological oscillatory activity. In vivo work with awake and freely moving rats would provide additional pieces to both the puzzle about comparability between modalities, but also in understanding the differences in cortical beta oscillations in PD subjects.

9.5.2. Stimulation

The other type of intervention we decided to apply in this project was different types of electromagnetic stimulation. In humans we had results from two types of stimulation; cTBS applied with TMS and different frequencies of electrical stimulation applied through MNS. We compared the results to two stimulation protocols *in vitro*; cTBS applied through electrical stimulation in different sensorimotor laminae, and electrical stimulation in SI LIV, respectively. In addition, most previous research has focused on changes to specific oscillatory frequency bands during stimulation, but we were interested in the long-lasting effects seen after stimulation offset.

Applying different frequencies of stimulation significantly affected the oscillatory activity in MI *in vitro*, but SI in human subjects. We speculated that this was due to peripheral vs. central application of somatosensory stimulation, but this is beyond the scope of testing for these experiments. Nonetheless, we found one particular beta frequency to have a significant effect on the frequency distribution and oscillatory peak frequency values in the sensorimotor cortex. In humans this beta frequency was 36 Hz, and *in vitro* it was 20 Hz. The reason for the distinction is unclear, but we suggest differences in connectivity and network arrangements as likely explanations. Connectivity has previously in this thesis been shown to influence peak frequency distribution and differences in network arrangements display different frequencies of resonance. Interestingly we found that 10 Hz MNS in humans decreased the ongoing oscillatory peak power in SI, contrary to rTMS reports (Veniero *et al.*, 2011). This difference of effects most likely depends on the form of stimulation application. The frequency stimulation experiments showed less similarity between modalities in results. However, we have only briefly touched on the effects on

ongoing oscillations during the stimulation period itself. There is more information in this regarding the information processing in the sensorimotor cortex for different frequencies input. This is the next step of this part of the project and we are currently developing scripts with an independent component analysis approach to further to assist us in this.

The TMS cTBS experiments showed an increase in the beta power in the stimulated MI in human responding subjects, but not in the other hemisphere or at all in non-responding subjects. Our *in vitro* experiments provided evidence that the beta power increase is local to the stimulated area, with the majority of effects on power were seen as increase of the oscillatory mean state power rather than mean peak power. This indicates a change in the oscillatory pattern, with increased power variability, which in turn could contribute to less significance in a mean peak power measure. Whilst cTBS applied to MI LV and SI LIV decreased the ongoing mean peak frequency of oscillatory activity in these same areas, this did not occur in MI LIII. This is particularly interesting as the suggested direct effects of TMS-cTBS are on the pyramidal cells in the superficial layers of MI, which indirectly affects the other laminae and cell populations. This brings into question which parts of the beta network in MI cTBS affects. MI LIII has been shown in previous studies in this thesis to have a wide frequency and network distribution, which could potentially accommodate forced frequency changes further without significant changes in the intrinsic ongoing frequencies. Nonetheless, we did not see any significant increases in mean peak power in MI LV from stimulating in any laminae. If the effects of TMS-cTBS and cTBS in our *in vitro* studies were completely in agreement, then we should have seen an increase in MI LV beta power after cTBS MI LIII. We speculate that this is due to difference in effects of the stimulation protocols and locations; cTBS might very well have further unknown effects.

9.6. Relevance to neurological pathologies

The underlying cause of PD is the disruption to the dopaminergic transmission in the basal ganglia. This disruption affects the neuronal network activities in areas affiliated with the basal ganglia; other parts of the sensorimotor system. Disturbed neuronal network activity in PD is well-established, although details are unclear. We showed that the ratio of beta power between contra- and ipsilateral hemispheres was correlated to the UPDRS score; this was improved by administration of zolpidem. The implications from these findings are that the networks responsible for the altered activity in PD, and the imbalance in hemispheric beta power, are restored to a certain degree with increased GABAergic activity. Since we lack control studies it is difficult to speculate on exactly which features in PD are the most relevant to motor symptomatology. However, based on our findings and previously cited work by Little *et al.*, we suggest that frequency variability is particularly important. Peak frequency distribution is an indication of the network activity and was found altered in PD at low beta and gamma frequencies. This changed with the GABAergic modulation and motor symptomatic improvement. These results provide further evidence for the perturbed network structures and abnormal processing seen in PD patients. Questions remain. Is the abnormal processing an effect of the changed excitatory state of the cortex, or an imbalance of excitation and inhibition, due to changed activity in the basal ganglia and dopaminergic transmission? Do the alterations in activity in the basal ganglia infer the breakdown of small-world cortical network structure and features as suggested by Uhlhaas and Singer (2006), all by itself or as a domino effect? Are the patterns of beta rhythms seen in PD the cause of symptoms or the effect of PD? These questions remain unanswered.

9.7. Concluding remarks

This thesis has confirmed that sensorimotor oscillations span the mu and beta frequency region both *in vitro* and in MEG recordings, with distinct profiles for each recorded laminae *in vitro*, but no significant difference in frequency in humans. We have revealed that there is a mu rhythm co-existing with beta oscillations in MI LIII and established that less complex signals with oscillatory activity from MI laminae can be integrated *in silico* to resemble aggregate MEG MI oscillatory signals. This highlights the usefulness of combining these two methods when elucidating neuronal network oscillations in the sensorimotor cortex and manipulations thereof. Furthermore, the connectivity between MI and SI modulates the ongoing network activity in these areas, as evidenced by connectivity and stimulation studies. Although the stimulation studies in this project showed limited comparative results, we have presented novel information to the effects of using these paradigms in each modality. Additionally, we have shown that pharmacological modulation with zolpidem changes the neuronal network activity in both healthy and pathological MI, and we can conclude that zolpidem enhances the power of ongoing oscillatory activity in both MI and SI laminae. Finally, our analysis approach has made it possible to reliably compare results between MEG and *in vitro*.

In conclusion, this translational neuroscience project has contributed to the understanding of the characteristics of ongoing sensorimotor oscillations and evidenced the effects of two common forms of interventions in two recording modalities analysed with the same approach.

References

Abbruzzese, G. & Berardelli, A. 2003. Sensorimotor integration in movement disorders. *Movement Disorders,* 18(3), pp. 231-40.

Adesnik, H. & Scanziani, M., 2010. Lateral competition for cortical space by layer-specific horizontal circuits. *Nature*, 464(7292), pp. 1155–1160.

Adrian, E.D. & Yamagiwa, K. 1935. The Origin of the Berger Rhythm. *Brain*, 58(3), pp. 323-351.

Alegre, M., Alvarez-Gerriko, I., Valencia, M., Iriarte, J. & Artieda, J. 2008. Oscillatory changes related to the forced termination of a movement. *Clinical Neurophysiology,* 119, pp. 290-300.

Alegre, M., Garcia de Burtubay, I., Labarga, A., Iriarte, J., Malanda, A. & Artieda, J. 2004. Alpha and beta oscillatory activity during a sequence of two movements. *Clinical Neurophysiology*, 115, pp. 124-130.

Alegre, M., Labarga, A., Gurtubay, I. G., Iriarte, J., Malanda, A. & Artieda, J. 2002. Beta electroencephalograph changes during passive movements: sensory afferences contribute to beta event-related desynchronization in humans. *Neuroscience Letters*, 331, pp. 29–32.

Andersen, P., Bland, B., Skrede, K., Sveen, O. & Westgaard, R. 1972. Single unit discharge in brain slices maintained *in vitro. Acta Physiologica Scandinavia* 84(1-2), abstract.

Anderson, C.T., Sheets, P.L., Kiritani, T. & Sheperd, G.M. 2010. Sublayer-specific microcircuits of cortico-spinal and corticostriatal neurons in motor cortex. *Nature Neuroscience*, 13(6), pp. 739-744.

Anderson, K. L., & Ding, M. 2011. Attentional modulation of the somatosensory mu rhythm. *Neuroscience,* 180, pp. 165-80.

Ascoli, G.A., Alonso-Nanclares, L., Anderson, S.A., Barrionuevo, G., Benavides-Piccione, R., Burkhalter, A., Buzsáki, G., Cauli, B., DeFelipe, J., Fairén, A., Feldmeyer, D., Fishell, G., Fregnac, Y., Freund, T.F., Gardner, D., Gardner, E.P., Goldberg, J.H., Helmstaedter, M., Hestrin, S., Karube, F., Kisvárday, Z.F., Lambolez, B., Lewis, D.A., Marin, O., Markram, H., Muñoz, A., Packer, A., Petersen, C.C.H, Rockland, K.S., Rossier, J., Rudy, B., Somogyi, P., Staiger, J.F., Tamas, G., Thomson, A.M., Toledo-Rodriguez, M., Wang, Y., West, D.C. & Yuste, R. 2008. Petilla terminology: nomenclature of features of GABAergic interneurons of the cerebral cortex. *Nature Reviews Neuroscience*, 9(7), pp. 557-568.

Avanzini, P., Fabbri-Destro, M., Dalla Volta, R., Daprati, E., Rizzolatti, G. & Cantalupo, G. 2012. The Dynamics of Sensorimotor Cortical Oscillations during the Observation of Hand Movements: An EEG Study. *PLoS One*, 7(5), pp. e37534-e37543.

Azevedo, F. A.C., Carvalho, L. R. B. Grinberg, L. T., Farfel, J. M., Ferretti, R. E. L., Leite, R. E. P., Filho, W. J., Lent, R. & Herculano-Houzel, S. 2009. Equal Numbers of Neuronal and Nonneuronal Cells Make the Human Brain an Isometrically Scaled-Up Primate Brain. *Journal of Comparative Neurology*, 513, pp. 532–541.

Bacci, A., Rudolph, U., Huguenard, J.R. & Prince, D.A. 2003. Major Differences in Inhibitory Sunpatic Transmission onto Two Neocortical Interneuron Subclasses. *Journal of Neuroscience*, 23(29), pp. 9664-9674.

Baker, M. R. & Baker, S. N. 2003. The effect of diazepam on motor cortical oscillations and corticomuscular coherence studied in man. *Journal of Physiology*, 546.3, pp. 931-942.

Baker, S. N., Kilner, J. M., Pinches, E. M. & Lemon, R. N. 1999, The role of synchrony and oscillations in the motor output. *Experimental Brain Research*, 128, pp. 109–117.

Baker, S. N., Olivier, E. & Lemon, R. N. 1997. Coherent oscillations in monkey motor cortex and hand muscle EMG show task-dependent modulation. *Journal of Physiology*, 501.1, pp. 225-241.

Başar, E., Başar-Eroglu, C., Karakaş, S. & Shürmann, M. 2001. Gamma, alpha, delta and theta oscillations govern cognitive processes. *International Journal of Psychophysiology,* 39, pp. 241-248.

Belelli, D. & Lambert, J.J. Neurosteroids: endogenous regulators of the GABAA-receptor. *Nature Reviews Neuroscience*, 6, pp. 565-575.

Benabid, A. L. 2003. Deep brain stimulation for Parkinson's disease. *Current Opinion in Neurobiology*, 13, pp. 696-706.

Benali, A., Trippe, J., Weiler, E., Mix, A., Petrasch-Parwez, E., Girzalsky, W., Eysel, U. T. Erdmann, R. & Funke, K. 2011. Theta-Burst Transcranial Magnetic Stimulation Alters Cortical Inhibition. *Journal of Neuroscience*, 31 (4), pp. 1193–1203.

Bennett, M.R. 1999. The early history of the synapse: from Plato to Sherrington. *Brain Research Bulletin,* 50(2), pp. 95-118.

Biswal, B., Yetkin, F. Z., Haughton, V. M. & Hyde, J. S. 1995. Functional Connectivity in the Motor Cortex of Resting Human Brain Using Echo-Planar MRI. *Magnetic Resonance in Medicine*, 34, pp. 537-541.

Bonnet M. Decety J., Jeannerod M. & Requin, J. 1997. Mental simulation of an action modulates the excitability of spinal reflex pathways in man. *Cognitive Brain Research*, 5, pp. 221–228.

Bosboom, J. L. W., Stoffers, D., Stam, C. J., van Dijk, B. W., Verbun, J., Berendse, H. W. & Wolters, E.C. 2006. Resting state oscillatory brain dynamics in Parkinson's disease: An MEG study. *Clinical Neurophysiology,* 117, pp. 2521-2531.

Bosboom, J. L. W., Stoffers, D., Wolters, E. C., Stam, C. J. & Berendse, H. W. 2009. MEG resting state functional connectivity in Parkinson's disease related dementia. *Journal of Neural Transmission*, 116, pp. 193-202.

Bouyer, J.J., Montaron, M.F., Vahnee, J.M., Albert, M.P. & Rogeul, A. 1987. Anatomical Localization of Cortical Beta Rhythms in Cat. *Neuroscience*, 22(3), pp. 863-869.

Bronstein, J.M., Tagliati, M., Alterman, R.L., Lozano, A.M., Volkmann, J., Stefani, A., Horak, F.B., Okun, M.S., Foote, K.D., Krack, P., Pahwa, R., Henderson, J.M., Hariz, M.I., Bakay, R.A., Rezai, A., Marks, W.J., Moro, E., Vitek, J.L., Weaver, F.M., Gross, R.E. & DeLong, M.R. 2011. Deep Brain Stimulation for Parkinson Disease. *Archives of Neurology*, 68(2), pp. 165-171.

Brovelli, A., Ding, M., Ledberg, A., Chen, Y., Nakamura, R. & Bressler, S.L. 2004. Beta oscillations in a large-scale sensorimotor cortical network: Directional influences revealed by Granger causality. *PNAS*, 101(26), pp. 9849-9854.

Brown, P. 2006. Bad oscillations in Parkinson's disease. *Journal of Neural Transmission*, 70, pp. 27-30.

Brown, P. 2007. Abnormal oscillatory synchronisation in the motor system leads to impaired movement. *Current Opinion in Neurobiology*, 17, pp. 656-664.

Brown, P., Marsden, J., Defebvre, L., Cassim, F., Mazzone, P., Oliviero, A., Altibrandi, M. G., Lazzaro, V., Limousin-Dowsey, P., Fraix, V., Odin, P. & Pollak, P. 2001. Intermuscular coherence in Parkinson's disease: relationship to bradykinesia. *NeuroReport*, 12 (11), pp. 2577-2581.

Brown, S.P. & Hestrin, S. 2009. Intracortical circuits of pyramidal neurons reflect their long-range axonal targets. *Nature*, 457(7233), pp. 1133-1136.

Buhl, E.H., Tamas, G. & Fisahn, A. 1998. Cholinergic activation and tonic excitation induce persistent gamma oscillations in mouse somatosensory cortex *in vitro*. *Journal of Physiology,* 513(1), pp. 117-126.

Buzsáki, G. & Draugh, A. 2004. Neuronal Oscillations in Cortical Networks. *Science*, 304, pp. 1926-1929.

Buzsaki, G. & Wang, X.J. 2012. Mechanisms of Gamma Oscillations. *Annual Reviews Neuroscience*, 35, pp. 203-225.

Buzsáki, G. 2006. *Rhythms of the Brain*. Oxford University Press, New York, U.S.A.

Cachalane, D.J., Charvet, C.J. & Finlay, B.L. 2012. Systematic, balancing gradients in neuron density and number across the primate isocortex. *Frontiers in Neuroanatomy,* 6 (28), pp. 1-12.

Cantello, R., Tarletti, R. & Civardi, C. 2002. Transcranial magnetic stimulation and Parkinson's disease. *Brain Research Reviews*, 38, pp. 309–327.

Capaday, C. 2004. The Integrated Nature of Motor Cortical Function. *The Neuroscientist*, 10 (3), pp. 207-220.

Capaday, C., Ethier, C., Brizzi, L., Sik, A., van Vreeswijk, C. & Gingras, D. 2009. On the Nature of the Intrinsic Connectivity of the Cat Motor Cortex: Evidence for a Recurrent Neural Network Topology. *Journal of Neurophysiology,* 102, pp. 2131-2141.

Capocchi, G., Zampolini, M. & Larson, J. 1992. Theta burst stimulation is optimal for induction of LTP at both apical and basal dendritic synapses on hippocampal CA1 neurons. *Brain Research*. 591(2), pp. 332-6.

Cardin, J.A., Carlen, M., Meletis, K., Knoblich, U., Zhang, F., Deisseroth, K., Tsai, L.H. & Moore, C.I. 2009. Driving fast-spiking cells induces gamma rhythm and controls sensory responses. *Nature*, 459, pp.663-670.

Cassim, F., Monaca, C., Szurhaj, W., Bourriez, J. L., Defebvre, L., Derambure, P. & Guieu, J. D. 2001. Does post-movement beta synchronization reflect an idling motor cortex? *NeuroReport*, 12 (17), pp. 3859-3864.

Castro-Alamancos, M. A., Donoghue, J. P. & Connors, B. W. 1995. Different Forms of Synaptic Plasticity in Somatosensory and Motor Areas of the Neocortex. *Journal of Neuroscience*, 15 (7), pp. 5324-5333.

Chagnac-Amitai, Y. & Connors, B.W. 1989. Synchronized Excitation and Inhibition Driven by Intrinsically Bursting Neurons in Neocortex. *Journal of Neurophysiology*, 62(5), pp. 1149-1162.

Cheeran,B., Talelli, P., Mori, F., Koch, G., Suppa, A., Edwards, M., Houlden, H., Bhatia, K., Greenwood, R., & Rothwell, J. C. 2008. A common polymorphism in the brain-derived neurotrophic factor gene (BDNF) modulates human cortical plasticity and the response to rTMS. *Journal of Physiology,* 586, pp. 5717-25.

Chen, C. C., Hsieh, J. C., Wu, Y.Z., Lee, P. L., Chen, S. S., Niddam, D. M., Yeh, T. C. & Wu, Y. T. 2008. Mutual-information-based approach for neural connectivity during self-paced finger lifting task. *Human Brain Mapping*. 29 (3), pp. 265-80.

Chen, R., Classen, J., Gerloff, C., Celnik, P., Wasserman, E.M., Hallett, M. & Cohen, L.G. 1997. Depression of motor cortex excitability by low-frequency transcranial magnetic stimulation. *Neurology,* 48(5), pp. 1398-1402.

Chen, R., Corwell, B. & Hallett, M. 1999. Modulation of motor cortex excitability by median nerve and digit stimulation. *Experimental Brain Research*, 129, pp. 77–86.

Chen, R., Yaseen, Z., Cohen, L. G. & Hallett, M. 1998. Time Course of Cortico-spinal Excitability in Reaction Time and Self-Paced Movements. *Annals of Neurology*, 44(3), pp. 317-325.

Cheyne, D. O. 2012. MEG studies of sensorimotor rhythms: A review. *Experimental Neurology*. 2012 Sep 7, Epub ahead of print, pp. 1-13.

Cheyne, D., Bells, S., Ferrari, P., Gaetz, W. & Bostan, A. C. 2008. Self-paced movements induce high-frequency gamma oscillations in primary motor cortex. *NeuroImage*, 42, pp. 332–342.

Cheyne, D., Gaetz, W., Garnero, L., Lachaux, J.P., Ducorps, A., Schwartz, D. & Varela, F.J. 2003. Neuromagnetic imaging of cortical oscillations accompanying tactile stimulation. *Cognitive Brain Research*, 17, pp. 599–611.

Chrobak. J. J. & Buzsaki, G. 1998. Gamma Oscillations in the Entorhinal Cortex of the Freely Behaving Rat. *Journal of Neuroscience*, 18 (1), pp. 388–398.

Chu, Z., Galarreta, M. & Hestrin, S. 2003. Synaptic Interactions of Late-Spiking Neocortical Neurons in Layer I. *Journal of Neuroscience*, 23(1), pp. 96-102.

Clauss, R.P. & Nel, H.W. 2005. Evidence for Zolpidem efficacy in brain damage. *South African Family Practice*, 47(3), pp. 49-50.

Clauss, R.P., Güldenpfennig, W.M., Nel, W.H., Sathekge, M.M. & Venkannagari, R.R. 2000. Extraordinary arousal from semi-comatose state on zolpidem: A case report. *South African Medical Journal*, 90 (68), pp. 68-73.

Clauss, R.P., van der Merwe, C.E. & Nel, H.W. 2001. Arousal from a semi-comatose state on zolpidem. *South African Medical Journal*, 91(10), pp. 788-789.

Cobb, S.R., Buhl, E.H., Halasy, K., Paulsen, O. & Somogyi, P. 1995. Synchronization of neuronal activity in hippocampus by individual GABAergic interneurons. *Nature*, 378, pp. 75-78.

Cochin,S., Barthelemy, C., Lejeune, B., Roux, S. & Martineau, J. 1998. Perception of motion and qEEG activity in human adults. *Electroencephalography and Clinical Neurophysiology,* 107(4), pp. 287-295.

Cooper, J.A., Sagar, H.J., Tidswell, P. & Jordan, N. 1994. Slowed central processing in simple and go/no-go reaction time tasks in Parkinson's disease. *Brain*, 117, pp. 517-529.

Cope, D. W., Halbsguth, C., Karayannis, T., Wulff, P., Ferraguti, F., Hoeger, H., Leppa, E., Linden, A. M., Oberto, A., Ogris, W., Korpi, E. R., Sieghart, W., Somogyi, P., Wisden, W. & Capogna, M. 2005 Loss of zolpidem efficacy in the hippocampus of mice with the GABAA receptor ɣ2 F77I point mutation. *European Journal of Neuroscience*, 21, pp. 3002–3016.

Cope, D. W., Wulff, P., Oberto, A., Aller, M. I., Capogna, M., Ferraguti, F., Halbsguth, C., Hoeger, H., Jolin, H. E., Jones, A., Mckenzie, A. N. J., Ogris, W., Poeltl, A., Sinkkonen, S.T., Vekovischeva, O. Y., Korpi, E. R., Sieghart, W., Sigel, E., Somogyi, P. & Wisden, W. 2004. Abolition of zolpidem sensitivity in mice with a point mutation in the GABAA receptor ɣ2 subunit. *Neuropharmacology* 47, pp. 17–34.

Cotzias, G.C., Papavasilious, P.S. & Gellene, R. 1969. Modification of Parkinsonism – Chronic Treatment with L-Dopa. *New England Journal of Medicine*, 280, pp. 337-345.

Crestani, F., Martin, J. R., Mohler H. & Rudolph, U. 2000. Mechanism of action of the hypnotic zolpidem in vivo. *British Journal of Pharmacology*, 131, pp. 1251-1254.

Crone, N.E., Miglioretti, D.L., Gordon, B., Sieracki, J.M., Wilson, M.T., Uematsu, S. & Lesser, R.P. 1998. Functional mapping of human sensorimotor cortex with electrocorticographic spectral analysis I. Alpha and beta event-related desynchronization. *Brain*, 121, pp. 2271-2299.

Crowell, A. L., Ryapolova-Webb, E. S., Ostrem, J. L., Galifianakis, N. B., Shimamoto, S., Lim, D. A. & Starr, P. A. 2012. Oscillations in sensorimotor cortex in movement disorders: an electrocorticography study. *Brain*, 135(2), pp. 615-30.

Csicsvari, J., Jamieson, B., Wise, K.D. & Buzsaki, G. 2003. Mechanisms of Gamma Oscillations in the Hippocampus of the Behaving Rat. *Neuron,* 37, pp. 311-322.

Cunningham, M.O., Davies, C.H., Buhl, E.H., Kopell, N. & Whittington, M.A. 2003. Gamma Oscillations Induced by Kainate Receptor Activation in the Entorhinal Cortex *In vitro*. *Journal of Neuroscience*, 23(30), pp. 9761-9769.

Cunningham, M.O., Whittington, M.A., Bibbig, A., Roopun, A., LeBeau, F.E.N. Vogt, A., Monyer, H., Buhl, E.H. & Traub, R.D. 2004. A role for fast rhythmic bursting neurons in cortical gamma oscillations *in vitro*. *PNAS,* 101(18), pp. 7152-7157.

D'Avella, A., Portone, A., Fernandez, L. & Lacquaniti, F. 2006. Control of Fast-Reaching Movements by Muscle Synergy Combinations. *Journal of Neuroscience*, 26(30), pp. 7791–7810.

Damoiseaux, J. S., Rombouts, S. A. R. B., Barkhof, F., Scheltens, P., Stam, C. J., Smith, S. M. & Beckmann, C. F. 2006. Consistent resting-state networks across healthy subjects. *PNAS*, 103 (37), pp. 13848–13853.

Daniele, A., Albanese, A., Gainotti, G., Gregori, B. & Bartolomeo, P. 1997. Zolpidem in Parkinson's disease. *The Lancet*, 349, pp. 1222-1223.

Davie, C.A. 2008. A review of Parkinson's disease. *British Medical Bulletin,* 86, pp. 109-127.

Deacon, T.W. Rethinking Mammalian Brain Evolution. 1990. *American Zoologist,* 30(3), pp. 629-705.

Deco, G. Jirsa, V. K. & McIntosh, A. R. 2011. Emerging concepts for the dynamical organization of resting-state activity in the brain. *Nature Reviews Neuroscience,* 12, pp. 43-56.

Defebvre, L., Bourriez, J.L., Destee, A. & Guieu, J.D. 1996. Movement related desynchronisation pattern preceeding voluntary movement in untreated Parkinson's disease. *Journal of Neurology, Neurosurgery, and Psychiatry*, 60, pp. 307-312.

DeFelipe, J., Alonso-Nanclares, L. & Arellano, J.I. 2002. Microstructure of the neocortex: comparative aspects. *Journal of Neurocytology,* 31 (3-5), pp. 299-216.

Degardin, A., Houdayer, E., Bourriez, J.-L., Destée, Defebvre, L., Derambure, P. & Devos, D. 2009. Deficient "sensory" beta synchronization in Parkinson's disease. *Clinical Neurophysiology,* 120, pp. 636-642.

Destexhe, A. 2000. Modelling corticothalamic feedback and the gating of the thalamus by the cerebral cortex. *Journal of Physiology*, 94, pp. 391-410.

Devanne, H., Cohen, L. G., Nezha Kouchtir-Devanne, N. & Capaday, C. 2002. Integrated Motor Cortical Control of Task-Related Muscles During Pointing in Humans. *Journal of Neurophysiology,* 87, pp. 3006-3017.

Diazepam @ PubChem Compound, National Center for Biotechnology Information 2012: http://pubchem.ncbi.nlm.nih.gov/summary/summary.cgi?cid=3016. [Accessed 11/12/2012].

Di Lazzaro, V., Pilato, F., Dileone, M., Profice, P., Oliviero, A., Mazzone, P., Insola, A., Ranieri, F., Meglio, M., Tonali, P. A. & Rothwell J. C. 2008. The physiological basis of the effects of intermittent theta burst stimulation of the human motor cortex. *Journal of Physiology*, 586.16, pp. 3871–3879.

Di Lazzaro, V., Pilato, F., Saturno, E., Oliviero, A., Dileone, M., Mazzone, P., Insola, A., Tonali, P. A., Ranieri, F., Huang Y. Z. & Rothwell J. C. 2005. Theta-burst repetitive transcranial magnetic stimulation suppresses specific excitatory circuits in the human motor cortex. *Journal of Physiology*, 565.3, pp. 945–950

Di Lazzaro, V., Profice, P., Ranieri, F., Capone, F., Dileone, M., Oliviero, A., & Pilato, F. 2012. I-wave origin and modulation. *Brain Stimulation*, 5, pp. 512–25.

Diamond, D. M., Dunwiddie, T. V. & Rose G. M. 1988. Characteristics of Hippocampal Primed Burst Potentiation *in vitro* and in the Awake Rat. *Journal of Neuroscience*, 8 (11), pp. 4079-4088.

Disbrow, E., Litinas, E., Recanzone, G. H., Padberg, J. & Krubitzer, L. 2003. Cortical Connections of the Second Somatosensory Area and the Parietal Ventral Area in Macaque Monkeys. *Journal of Comparative Neurology*, 462, pp. 382-399.

Domino, E.F., French, J., Pohorecki, R., Galus, C.F. & Pandit, S.K. 1989. Further observations on the effects of subhypnotic doses of midazolam in normal volunteers. *Psychopharmacology Bullentin*, 25(3), pp. 460-465.

Donoghue, J.P. & Wise, S.P. 1982. The motor cortex of the rat: cytoarchitecture and microstimulation mapping. *Journal of Comparative Neurology,* 212(1), pp. 76-88.

Douglas, R.J. & Martin, K.C. 2004. Neuronal Circuits of the Neocortex. *Annual Reviews of Neuroscience,* 27, pp. 419-451.

Douglas, R.J. & Martin, K.C. 2007a. Mapping the matrix: The Ways of Neocortex. *Neuron,* 56, pp. 226-238.

Douglas, R.J. & Martin, K.C. 2007b. Recurrent neuronal circuits in the neocortex. *Current Biology,* 17(13), pp. R496-500.

Drachman, D. A. 2005. Do we have a brain to spare? *Neurology,* 64 (12), pp. 2004-2005

Drouot, X., Oshino, S., Jarraya, B., Besret, L., Kishima, H., Remy, P., Dauguet, J., Lefaucheur, J. P., Dolle, F., Conde, F., Bottlaender, M., Peschanski, M., Keravel, Y., Hantraye, P. & Palfi, S. 2004. Functional Recovery in a Primate Model of Parkinson's Disease following Motor Cortex Stimulation. *Neuron*, Vol. 44, pp. 769–778.

Eggers, C., Fink, G. R. & Nowak, D. A. 2010. Theta burst stimulation over the primary motor cortex does not induce cortical plasticity in Parkinson's disease. *Journal of the Neurological Sciences*, 257, pp. 1669–1674.

Engel, A.K., Fries, P. & Singer, W. 2001. Dynamic predictions: oscillations and synchrony in top-down processing. *Nature Reviews Neuroscience,* 2(10), pp. 704-16.

Eskow-Jaunarajs, K.L., Angoa-Perez, M., Kuhn, D.M. & Bishop, C. 2011. Potential mechanisms underlying anxiety and depression in Parkinson's disease: consequences of L-Dopa treatment. *Neuroscience and Biobehavioural Reviews*, 35(3), pp. 556-564.

Eusebio, A. & Brown, P. 2009. Synchronisation in the beta frequency-band - The bad boy of parkinsonism or an innocent bystander? *Experimental Neurology*, 217, pp. 1–3.

Eusebio, A., Chu Chen, C., Song Lu, C., Tseng Lee, S., Haw Tsai, C., Limousin, P., Hariz, M. & Brown, P. 2008. Effects of low-frequency stimulation of the subthalamic nucleus on movement in Parkinson's disease. *Experimental Neurology,* 209, pp. 125–130.

Evarts, E.V., Teräväinen, H. & D.B. Calne. 1981. Reaction Time in Parkinson's Disease. *Brain*, 104, pp. 167-186.

Farrant, M. & Nusser, Z. 2005. Variations on an inhibitory theme: phasic and tonic activation of GABAA-receptors. *Nature Reviews Neuroscience*, 6, pp. 215-230.

Felleman, D. J. & Van Essen, D.C. 1991. Distributed Hierarchical Processing in the Primate Cerebral Cortex. *Cerebral Cortex,* 1 (1), pp. 1-47.

Feurra, M., Bianco, G., Santarnecchi, E., Del Testa, M., Rossi, A. & Rossi, S. 2011a. Frequency-Dependent Tuning of the Human Motor System Induced by Transcranial Oscillatory Potentials. *Journal of Neuroscience*, 31 (34), pp. 12165–12170.

Feurra, M., Paulus, W., Walsh, V. & Kanai, R. 2011b. Frequency specific modulation of human somatosensory cortex. *Frontiers in Perception Science*, 2 (13), pp. 1-6.

Filipović, S. R., Rothwell, J. C. & Bhatia, K. 2010. Low-frequency repetitive transcranial magnetic stimulation and off-phase motor symptoms in Parkinson's disease. *Journal of the Neurological Sciences*, 291, pp. 1–4.

Fingelkurtz, A.A., Fingelkurtz, A.A., Kivisaari, R., Pekkonen, E., Ilmoniemi, R.J. & Kähkönen. 2004. The interplay of lorazepam-induced brain oscillations: microstructural electromagnetic study. *Clinical Neurophysiology*, 115, pp. 674-690.

Fisahn, A., Pike, F. G., Buhl, E. H. & Paulsen, O. 1998. Cholinergic induction of network oscillations at 40Hz in the hippocampus *in vitro*. *Nature,* 394, pp. 186-189.

Fitzgerald, P. B., Fountain, S. & Daskalakis, Z. J. 2006. A comprehensive review of the effects of rTMS on motor cortical excitability and inhibition. *Clinical Neurophysiology,* 117, pp. 2584–2596.

Flint, A. C. & Connors, B. W. 1996. Two Types of Network Oscillations in Neocortex Mediated By Distinct Glutamate Receptor Subtypes and Neuronal Populations. *Journal of Neurophysiology,* 75 (2), pp. 951-956.

Forss, N., Salmelin, R. & Hari, R. 1994a. Comparison of somatosensory evoked fields to airpuff and electric stimuli. *Electroencephalography and clinical Neurophysiology ,* 92, pp. 510-517.

Forss, N., Hari, R., Salmelin, R., Ahonen, A., Himiliinen, M., Kajola, M., Knuutila, J. & Simola, J. 1994b. Activation of the human posterior parietal cortex by median nerve stimulation. *Experimental Brain Research,* 99, pp. 309-315.

Francuz, P. & Zapala, D. 2011. The suppression of the μ rhythm during the creation of imagery representation of movement. *Neuroscience Letters,* 495(1), pp. 39-43.

Franschetti, S., Guatteo, E., Panzica, F., Sancini, G., Wanke, E. & Avanzini, G. 1995. Ionic mechanisms underlying burst firing in pyramidal neurons: intracellular study in rat sensorimotor cortex. *Brain Research*, 696, pp. 127-139.

Frerking, M., Malenka, R. C. & Nicoll, R. A. 1998. Inhibitory, But Not Excitatory, Transmission in the CA1 Brain-Derived Neurotrophic Factor (BDNF) Modulates Region of the Hippocampus. *Journal of Neurophysiology,* 80, pp. 3383-3386.

Freyer, F., Reinacher, M., Nolte, G., Dinse, H.R. & Ritter, P. 2012. Repetitive tactile stimulation changes resting-state functional connectivity-implications for treatment of sensorimotor decline. *Frontiers in Human Neuroscience*, 6, pp. 1-11.

Fries, P. 2005. A mechanism for cognitive dynamics: neuronal communication through neuronal coherence. *Trends in Cognitive Sciences,* 9 (10), pp. 474-480.

Fries, P. 2009. Neuronal Gamma-Band Synchronization as a Fundamental Process in Cortical Computation. *Annual Reviews Neuroscience*, 32, pp. 209–24.

Fuggetta, G., Fiaschi, A. & Manganotti, P. 2005. Modulation of cortical oscillatory activities induced by varying single-pulse transcranial magnetic stimulation intensity over the left primary motor area: A combined EEG and TMS study. *NeuroImage,* 27, pp. 896 – 908.

Fukuda, T. & Kosaka, T. 2000. Gap Junctions Linking the Dendritic Network of GABAergic Interneurons in the Hippocampus. *Journal of Neuroscience*, 20(4), pp.1519-1528.

Funke, K. & Benali, A. 2011. Modulation of cortical inhibition by rTMS – findings obtained from animal models. *The Journal of Physiology*, 589.18, pp. 4423–4435.

Gaetz, W. & Cheyne, D. 2006. Localization of sensorimotor cortical rhythms induced by tactile stimulation using spatially filtered MEG. *NeuroImage*, 30, pp. 899-908.

Gaetz, W., Edgar, J. C., Wang, D. J. & Roberts, T. P. L. 2011. Relating MEG measured motor cortical oscillations to resting γ-Aminobutyric acid (GABA) concentration. *NeuroImage*, 55, pp. 616–621.

Gaetz, W., MacDonald, M., Cheyne, D. & Snead, O.C. 2010. Neuromagnetic imaging of movement-related cortical oscillations in children and adults: Age predicts post-movement beta rebound. *NeuroImage*, 51, pp. 792-807.

Gangitanoa, M., Valero-Cabre, A., Tormos, J. M., Mottaghy, F. M., Romero, J. R. & Pascual-Leone, A. 2002. Modulation of input–output curves by low and high frequency repetitive transcranial magnetic stimulation of the motor cortex. *Clinical Neurophysiology,* 113, pp. 1249–1257.

Gastaut, H.J. & Bert, J.B. 1954. EEG Changes During Cinematographic Presentation. *Electroencephalograpy and Clinical Neurophysiology,* 6, pp. 433-444.

Gauggel, S., Rieger, M. & Feghoff, T.A. 2004. Inhibition of ongoing responses in patients with Parkinson's disease. *Journal of Neurology, Neurosurgery and Psychiatry,* 75(4), pp. 539-544.

Gentner, R., Wankerl, K., Reinsberger, C., Zeller, D. & Classen J. 2007. Depression of Human Cortico-spinal Excitability Induced by Magnetic Theta-burst Stimulation: Evidence of Rapid Polarity-Reversing Metaplasticity. *Cerebral Cortex,* 18, pp. 2046-2053.

Gerloff, C., Richard, J., Hadley, J., Schulman, A. E., Honda, M. & Mark Hallett, M. 1998. Functional coupling and regional activation of human cortical motor areas during simple, internally paced and externally paced finger movements. *Brain*, 121, pp. 1513–1531.

Geyer, S., Matelli, M., Luppino, G. & Zilles, K. 2000. Functional neuroanatomy of the primate isocortical motor system. *Anatomy and Embryology*, 202(6), pp. 443-447.

Ghosh, S., Brinkman, C. & Porter, R. 1987. A quantitative study of the distribution of neurons projecting to the precentral motor cortex in the monkey (M. fascicularis). *Journal of Comparative Neurology*, 259 (3), pp. 424-444.

Gilbert, C.D. & Wiesel, T.N. 1989. Columnar Specificity of Intrinsic Horizontal and Corticocortical Connections in Cat Visual Cortex. *Journal of Neuroscience*, 9 (7), pp. 2432-2442.

Goldsworthy, M. R., Pitcher, J. B. & Ridding, M. C. 2012. A comparison of two different continuous theta burst stimulation paradigms applied to the human primary motor cortex. *Clinical Neurophysiology*, 123, pp. 2256–2263.

Gotti, C., Moretti, M., Gaimarri, A., Zanardi, A., Clementi, F. & Zoli, M. 2007. Heterogeneity and complexity of native brain nicotinic receptors. *Biochemical Pharmacology*, 74 (8), pp. 1102-1111.

Gradinaru, V., Mogri, M., Thompson, K.R., Henderson, J.M. & Deisseroth, K. 2009. Optical Deconstruction of Parkinsonian Neural Circuitry. *Science*, 324, pp. 354-359.

Granger, A.J., Gray, J.A., Lu, W. & Nicoll, R.A. 2011. Genetic analysis of neuronal ionotropic glutamate receptor subunits. *Journal of Physiology*, 589(17), pp. 4095-4101.

Gray, C. M. 1994. Synchronous Oscillations in Neuronal Systems: Mechanisms and Functions. *Journal of Computational Neuroscience*, 1, pp. 11-38.

Gray, C.M. & McCormick, D.A. 1996. Chattering Cells: superficial pyramidal neurons contribution to the generation of synchronous oscillations in the visual cortex. *Science*, 274, pp. 109-114.

Guatteo, E., Franceschetti, S., Bacci, A., Avanzini, G. & Wanke, E. 1996. A TTX-sensitive conductance underlying burst firing in isolated pyramidal nerons from rat neocortex. *Brain Research,* 741, pp. 1-12.

Gupta, A., Wang, Y. & Markram, H. 2000. Organizing principles for a diversity of GABAergic interneurons and synapses in the neocortex. *Science*, 287, pp. 273-279.

Haas, L.F. 2003. Hans Berger (1873-1941), Richard Caton (1842-1926), and electroencephalography. *Journal of Neurology, Neurosurgery and Psychiatry,* 74(1), p. 9.

Haegens, S., Handel, B.F. & Jensen, O. 2011b. Top-Down Controlled Alpha Band Activity in Somatosensory Areas Determines Behavioural Performance in a Discrimination Task. *Journal of Neuroscience¸*31(14), pp. 5197-5204.

Haegens, S., Nacher, V., Hernandez, A., Luna, R., Jensen, O. & Romo, R. 2011a. Beta oscillations in the monkey sensorimotor network reflect somatosensory decision making. *PNAS*, 108(26), pp. 10708-10713.

Haegens, S., Nacher, V., Luna, R., Romo, R. & Jensen, O. 2011c. α-Oscillations in the monkey sensorimotor network influence discrimination performance by rhythmical inhibition of neuronal spiking. *PNAS*, 108(48), pp. 19377-19382.

Hall, S. D. Barnes, G. R. Furlong, P. L. Seri, S. & Hillebrand A. 2009. Neuronal Network Pharmacodynamics of GABAergic Modulation in the Human Cortex Determined Using Pharmaco-Magnetoencephalography. *Human Brain Mapping*, 31, pp. 581–594.

Hall, S. D., Yamawaki, N., Fisher, A. E., Clauss, R. P., Woodhall G. L. & Stanford I. M. 2010. GABA(A) alpha-1 subunit mediated desynchronization of elevated low frequency oscillations alleviates specific dysfunction in stroke – A case report. *Clinical Neurophysiology*, 121, pp. 549–555.

Hall, S.D., McAllister, C.J., Ronnqvist, K.C., Williams, A.C., Yamawaki, N., Prokic, E.J., Woodhall, G.L. & Stanford, I.M. 2012. Neuronal Network Changes Underlying GABA Mediated Symptomatic Improvement in Early Stage Parkinson's Disease. *Brain*, UNDER REVIEW.

Hall, S.D., Stanford, I.M., Yamawaki, N., McAllister, C.J. Ronnqvist,, K.C., Woodhall, G.L. & Furlong, P.L. 2011. The role of GABAergic modulation in motor function related neuronal network activity. *NeuroImage*, 56, pp. 1506-1510.

Hämäläinen, M., Hari, R., Ilmoniemi, R. J., Knuutila, J. & Lounasmaa, O. V. 1993. Magnetoencephalography - theory, instrumentation, and applications to noninvasive studies of the working human brain. *Reviews of Modern Physics*, 65 (2), pp. 413-497.

Hammond, C., Bergman, H. & Brown, P. 2007. Pathological synchronization in Parkinson's disease: networks, models and treatments. *Trends in Neurosciences,* 30(7), pp. 357-364.

Hari, R. & Kaukoranta, E. 1985. Neuromagnetic Studies of Somatosensory System: Principles and Examples. *Progress in Neurobiology,* 24, pp. 233-256.

Hari, R. 2006. Action-perception connection and the cortical mu rhythm. *Progress in Brain Research*, 159, pp. 253-260.

Hari, R., Antervo, A., Katila, T., Poutanen, T., M, Seppanen, M., Tuomisto, T. & Varpula, T. 1983. Cerebral Magnetic Fields Associated with Voluntary Limb Movements in Man. *Il Nuovo Cimento D,* Marzo-Aprile 1983, 2(2), pp. 484-494.

Hari, R., Reinikainen, K., Kaukoranta, E., Hämäläinen, M., Ilmoniemi, R., Penttinen, A., Salminen, J. & Teszner, D. 1984. Somatosensory evoked cerebral magnetic fields from SI and SII in man. *Electroencephalography Clinical Neurophysiology*, 57(3), pp. 254-63.

Hasenstaub, A., Shu, Y., Haider, B., Kraushaar, U., Duque, A. & McCormick, D.A. 2005. Inhibitory Postsynaptic Potentials Carry Synchronized Frequency Information in Active Cortical Networks. *Neuron*, 47, pp. 423-435.

Helmich, R. C., Siebner, H. R., Bakker, M., Munchau, A. & Bloem, B. R. 2006. Repetitive transcranial magnetic stimulation to improve mood and motor function in Parkinson's disease. *Journal of the Neurological Sciences*, 248, pp. 84-96.

Herculano-Houzel, S., Collins, C. E., Wong, P., Kaas, J.H. & Lent, R. (2007) The basic nonuniformity of the cerebral cortex. *PNAS*, 105 (34), pp. 12593–12598**.**

Hess, G. & Donoghue, J. P. 1996. Long-term Depression of Horizontal Connections in Rat Motor Cortex. *European Journal of Neuroscience*, 8, pp. 658-665.

Hess, G. & Donoghue, J. P. 1999. Facilitation of long-term potentiation in layer II/III horizontal connections of rat motor cortex following layer I stimulation: route of effect and cholinergic contributions. *Experimental Brain Research*, 127, pp. 279–290.

Hess, G., Jacobs, K. M. & Donoghue, J. P. 1994. N-methyl-D-aspartate receptor mediated component of field potentials evoked in horizontal pathways of rat motor cortex. *Neuroscience,* 61(2), pp. 225-35.

Hillebrand, A. & Barnes, G.R. 2002. A Quantitative Assessment of the Sensitivity of Whole-Head MEG to Activity in the Adult Human Cortex. *NeuroImage*, 16, pp. 638-650.

Hillebrand, A. & Barnes, G.R. 2003. The use of anatomical constraints with MEG beamformers. *NeuroImage*, 20, pp. 2302-2313.

Hillebrand, A. & Barnes, G.R. 2011. Practical constraints on estimation of source extent with MEG beamformers. *NeuroImage*, 54, pp. 2732-2740.

Hillebrand, A., Singh, K. D., Holliday, I. E., Furlong, P. L. & Barnes, G. R. 2005. A New Approach to Neuroimaging With Magnetoencephalography. *Human Brain Mapping,* 25, pp. 199 –211.

Hirsch, J.A., Gallagher, C.A., Alonso, J.M. & Martinez, L.M., 1998. Ascending projections of simple and complex cells in layer 6 of the cat striate cortex. *Journal of Neuroscience,* 18(19), pp. 8086-8094.

Hluštík, P., Solodkin, A., Gullapalli, R. P., Noll, D. C. & Small, S. L. 2001. Somototopy in Human Primary Motor Somoatosensory Hand Representations Revisited. *Cerebral Cortex*, 11, pp. 312-312.

Hoogendam, J. M., Ramakers, G. M. J. & Di Lazzaro, V. 2010. Physiology of repetitive transcranial magnetic stimulation of the human brain. *Brain Stimulation*, 3, 95–118.

Hooks, B. M., Hires, S. A., Zhang, Y., Huber, D., Petreanu, L., Svoboda, K. & Shepherd, G. M. G. 2011. Laminar Analysis of Excitatory Local Circuits in Vibrissal Motor and Sensory Cortical Areas. *PLoS Biology*, 9(1), pp. e1000572.

Hopkins, W.D. & Rilling, J.K., 2000. A comparative MRI study of the relationship between neuroanatomical asymmetry and interhemispheric connectivity in primates: Implication for the evolution of functional asymmetries. *Behavioral Neuroscience*, 114(4), pp. 739–748.

Hsu, W.Y. & Chiu, N.Y. 2012. Intravenous Zolpidem Injection in a Zolpidem Abuser. *Pharmacopsychiatry*, October 2012: EPub ahead of print.

Huang, Y., Chen, R., Rothwell, J. C. & Wen, H. 2007a. The after-effect of human theta burst stimulation is NMDA receptor dependent. *Clinical Neurophysiology*, 118, pp. 1028–1032.

Huang, Y., Edwards, M. J., Rounis, E., Bhatia, K. P. & Rothwell, J. C. 2005. Theta Burst Stimulation Report of the Human Motor Cortex. *Neuron*, 45, pp. 201–206.

Huffman, K.J. & Krubitzer, L. 2001. Area 3a: topographic organization and cortical connections in marmoset monkeys. *Cerebral Cortex*, 11(9), pp. 849-867.

Jackson, A.C. & Nicoll, R.A. 2011. The Expanding Social Network of Ionotropic Glutamate Receptors: TARPS and Other Transmembrane Auxiliary Subunits. *Neuron*, 70(2), pp. 178-199.

Jasper, H. & Penfield, W. 1949. Zur Deutung des normalen Elektrencephalogramms und selner Veriinderungen. *Archiv für Psychiatrie und Zeitsehrift Neurologie*, 183, pp. 163-174.

Jenkinson, N. & Brown, P. 2011. New insights into the relationship between dopamine, beta oscillations and motor function. *Trends in Neurosciences*, 34 (12), pp. 611-618.

Jensen, O., Goel, P., Kopell, N., Pohja, M., Hari, R. & Ermentrout, B. 2005. On the human sensorimotor-cortex beta rhythm: Sources and Modelling. *NeuroImage*, 26, pp. 347–355.

Johnston, G.A.R. 1996. GABA$_A$ receptor pharmacology. *Pharmacology & Therapeutics,* 69(3), pp. 173-198.

Jones, E. G. & Powell, T. P. S. 1968. The commissural connexions of the somatic sensory cortex in the cat. *Journal of Anatomy*, 103 (3), pp. 433-455.

Jones, E.G. & Wise, S.P. 1979. Size, laminar and columnar distribution of efferent cells in the sensory-motor cortex of monkeys. *Journal of Comparative Neurology*, 175(4), pp. 391-438.

Jones, S.R., Kerr, C.E., Wan, Q., Pritchett, D.L., Hämäläinen, M. & Moore, C.I. 2010. Cued Spatial Attention Drives Functionally-Relevant Modulation of The Mu Rhythm in Primary Somatosensory Cortex. *Journal of Neuroscience*, 30(41), pp. 13760-13765.

Jones, S.R., Pritchett, D.L., Sikora, M.A., Stufflebeam, S.M., Hämäläinen, M. & Moore, C.I. 2009. Quantitative Analysis and Biophysically Realistic Neural Modeling of the MEG Mu Rhythm: Rhythmogenesis and Modulation of Sensory-Evoked Responses. *Journal of Neurophysiology*, 102, pp. 3554-3572.

Joundi, R.A., Jenkinson, N., Brittain, J.-S., Aziz, T.Z. & Brown, P. 2012. Driving Oscillatory Activity in the Human Cortex Enhances Motor Performance. *Current Biology*, 6(22), pp. 403-407.

Juergens, E., Guettler, A. & Eckhorn, R. 1999. Visual stimulation elicits locked and induced gamma oscillations in monkey intracortical- and EEG-potentials, but not in human EEG. *Experimental Brain Research,* 129(2), pp. 247-259.

Jung, S. H., Shin, J. E., Jeong, Y. & Shin ,H. 2008. Changes in motor cortical excitability induced by high-frequency repetitive transcranial magnetic stimulation of different stimulation durations. *Clinical Neurophysiology,* 119, pp. 71–79.

Jurkiewicz, M. T., Gaetz, W. C., Bostan, A. C. & Cheyne, D. 2006. Post-movement beta rebound is generated in motor cortex: Evidence from neuromagnetic recordings. *NeuroImage,* 32, pp. 1281–1289.

Kaas, J.H., 2007. The evolution of sensory and motor systems in primates. *Evolution of Nervous Systems*, 4, pp. 35–57.

Kaas, J.H., 2008. The evolution of the complex sensory and motor systems of the human brain. *Brain Research Bulletin*, 75(2-4), pp. 384–390.

Kanwisher, N. Functional specificity in the human brain: A window into the functional architecture of the mind. *PNAS*, 107(25), pp. 111630-11170.

Kaplan, B.J. 1979. Morphological evidence that feline SMR and human mu are analogue rhythms. *Brain Research Bullentin,* 4(3), pp. 431-3.

Katz, L.C., 1987. Local circuitry of identified projection neurons in cat visual cortex brain slices. *Journal of Neuroscience*, 7(4), pp. 1223-1249.

Kawaguchi, Y. & Kubota, Y. 1997. GABAergic Cell Subtypes and their Synaptic Connections in Rat Frontal Cortex. *Cerebral Cortex*, 7, pp. 476-486.

Kawaguchi, Y. 1993. Groupings of nonpyramidal and pyramidal cells with specific phyiological and morphological characteristics in rat frontal cortex. *Journal of Neurophysiology*, 69, pp. 416-431.

Kawaguchi, Y. 1995. Physiological Subgroups of Nonpyramidal Cells with Specific Morphological Characteristics in Layer II/III of Rat Frontal Cortex. *Journal of Neuroscience,* 15(4), pp. 2638-2655.

Keller, A. 1993. Intrinsic synaptic organization of the motor cortex. *Cerebral Cortex,* 3, pp. 430-441.

Kirkwood, A., Dudek, S. R., Gold, J. T., Aizenman, C. D. & Bear, M. F. 1993. Common Forms of Synaptic Plasticity in the Hippocampus and Neocortex *in vitro*. *Science*s 260 (5113), pp. 1518-1521.

Klausberger, T., Magill, P.J., Márton, L.F., Roberts, J.D.B., Cobden, P.M., Buzsáki, G. & Somogyi, P. 2003. Brain-state- and cell-type-specific firing of hippocampal interneurons *in vivo*. *Nature*, 421, pp. 844-848.

Koelewijn, T., van Schie, H.T., Bekkering, H., Oostenveld, R. & Jensen, O. 2008. Motor-cortical beta oscillations are modulated by correctness of observed action. *NeuroImage*, 40, pp. 767-775.

Kopell, N. & Ermentrout, B. 2004. Chemical and electrical synapses perform complementary roles in the synchronization of interneuronal networks. *PNAS*, 101 (43), pp. 15482–15487.

Kopell, N., Ermentrout, G. B., Whittington, M. A., & Traub R. D. 2000. Gamma rhythms and beta rhythms have different synchronization properties, PNAS, 97 (4), pp. 1867–1872.

Kopell, N., Kramer, M.A., Malerba, P. & Whittington, M.A. 2010. Are different rhythms good for different functions? *Frontiers in Human Neuroscience*, 4(187), pp. 1-9.

Krubitzer, L.A. & Kaas, J.H., 1990. The organization and connections of somatosensory cortex in marmosets. *Journal of Neuroscience*, 10(3), pp. 952-974.

Kühn, A.A., Tsui, A., Aziz, T., Ray, N., Brücke, C., Kupsch, A., Schneider, G.-H. & Brown, P. 2009. Pathological synchronisation in the subthalamic nucleus of patients with Parkinson's disease relates to both bradykinesia and rigidity. *Experimental Neurology,* 215, pp. 380-387.

Kuncel, A.M., Cooper, S. E., Wolgamuth, B. R., Clyde, M. A., Snyder, S. A., Montgomery, E. B. Jr, Rezai, A. R. & Grill, W. M. 2006. Clinical response to varying the stimulus parameters in deep brain stimulation for essential tremor. *Movement Disorders*. 21(11), pp. 1920-8.

Labyt, E., Cassim, F., Devos, D., Bourriez, J.L., Destée, A., Guieu J.D., Defebvre, L. & Derambure, P. 2005. Abnormal cortical mechanisms in voluntary muscle relaxation in de novo parkinsonian patients. *Journal of Clinical Neurophysiology,* 22(3), pp. 192-203.

Lalo, E., Gilbertson, T., Doyle, L., Di Lazzaro, V., Cioni, B. & Brown, P. 2008. Phasic increases in cortical beta activity are associated with alterations in sensory processing in the human. *Experimental Brain Research*, 177, pp. 137-145.

Larsen, D.D. & Krubitzer, L., 2008. Genetic and epigenetic contributions to the cortical phenotype in mammals. *Brain Research Bulletin*, 75(2-4), pp. 391-397.

Larson, J. & Lynch, G. 1988. Role of N-methyl-D-aspartate receptors in the induction of synaptic potentiation by burst stimulation patterned after the hippocampal theta-rhythm. *Brain Research*, 16 441(1-2), pp. 111-118.

Leblois, A., Meissner, W., Bioulac, B., Gross, C. E., Hansel, D. & Boraud, T. 2007. Late emergence of synchronized oscillatory activity in the pallidum during progressive parkinsonism. *European Journal of Neuroscience*, 26, pp. 1701-1713.

Lefaucheur, J.P. 2005. Motor cortex dysfunction revealed by cortical excitability studies in Parkinson's disease: influence of antiparkinsonian treatment and cortical stimulation. *Clinical Neurophysiology,* 116, pp. 244-253.

Leocani, L., Toro, C., Zhuang, P. Gerloff, C. & Hallett, M. 1997. Event-related coherence and event-related desynchronization/synchronization in the 10 Hz and 20 Hz EEG during self-paced movements. *Electroencephalograpy and Clinical Neurophysiology,* 104(3), pp. 199-206.

Leocani, L., Toro, C., Zhuang, P. Gerloff, C. & Hallett, M. 2001. Event-related desynchronization in reaction time paradigms: a comparison with even-related potentials and cortico-spinal excitability. *Clinical Neurophysiology,* 112, pp. 923-930.

Lewis, J. W. & Van Essen, D. C. 2000. Corticocortical Connections of Visual, Sensorimotor, and Multimodal Processing Areas in the Parietal Lobe of the Macaque Monkey. *Journal of Comparative Neurology*, 428, pp. 112–137.

Linkenkaer-Hansen, K., Nikouline, V. V., Palva, J. M. & Ilmoniemi, R. J. 2001. Long-Range Temporal Correlations and Scaling Behavior in Human Brain Oscillations. *Journal of Neuroscience*, 21 (4), pp. 1370-1377.

Linkenkaer-Hansen, K., Nikulin, V.V., Palva, S., Ilmoniemi, R.J. & Palva, J.M. 2004. Prestimulus Oscillations Enhance Psychophysical Performance in Humans. *Journal of Neuroscience*, 24(45), pp. 10186-10190.

Little, S., Pogosyan, A., Kuhn, A. A. & Brown, P. 2012. Beta band stability over time correlates with Parkinsonian rigidity and bradykinesia. *Experimental Neurology,* 236, pp. 383–388.

Litvak, V. Jha, A. Eusebio, A. Oostenveld, R. Foltynie, T. Limousin, P. Zrinzo, L. Hariz, M. I. Friston K. & Brown, P. 2010. Resting oscillatory cortico-subthalamic connectivity in patients with Parkinson's disease. *Brain*, 134, pp. 359-374.

Llinas, R.R., Grace, A.A. & Yarom, Y. 1991. *In vitro* neurons in mammalian cortical layer 4 exhibit intrinsic oscillatory activity in the 10-to-50 Hz frequency range. *PNAS*, 88, pp. 897-901.

Logothetis, N., Pauls, J., Augath, M., Trinath, T. & Oeltermann, A. 2001. Neurophysiological investigation of the basis of the fMRI signal. *Nature*, 412, pp. 150-157.

Lømo, T. 2003. The discovery of long-term potentiation. *Philosophical Transactions of the Royal Society*, 358, pp. 617–620

Lopes da Silva, F.H., Vos, J.E., Mooibroek, J. & Van Rotterdam, A. 1980. Relative Contributions of Intracortical and Thalamo-Cortical Processes in the Generation of Alpha Rhythms, Revealed by Partial Coherence Analysis. *Electroencephalography and Clinical Neurophysiology,* 50, pp. 449-456.

Lukasiewicz, P.D. & Wong, R.O. 1997. GABAC receptors on ferret retinal bipolar cell: a diversity of subtypes in mammals? *Visual neuroscience,* 14(5), pp. 989-994.

Lund, J.S., Henry, G.H., MacQueen, C.L & Harvey, A.R., 1979. Anatomical organization of the primary visual cortex (area 17) of the cat. A comparison with area 17 of the macaque monkey. *Journal of Comparative Neurology*, 184(4), pp. 599–618.

Lytton, W.W. & Sejnowski, T.J. 1991. Simulations of cortical Pyramidal Neurons Synchronized by Inhibitory Interneurons. *Journal of Neurophysiology*, 66(3), pp. 1059-1079.

MacKinnon, C.D., Gilley, E.A., Weis-McNulty, A. & Simuni, T. 2005. Pathways Mediating Abnormal Intracortical Inhibition in Parkinson's Disease. *Annals of Neurology,* 58(4), pp. 516-524.

Mäki, H. & Ilmoniemi, R. J. 2010. EEG oscillations and magnetically evoked motor potentials reflect motor system excitability in overlapping neuronal populations. *Clinical Neurophysiology*, 121, pp. 492–501.

Malenka, R. C. & Bear, M. F. 2004. LTP and LTD: An Embarrassment of Riches. *Neuron*, 44, pp. 5-21.

Mallet, N., Pogosyan, A., Marton, L. F., Bolam, J. P., Brown, P. & Magill, P. J. 2008b. Parkinsonian Beta Oscillations in the External Globus Pallidus and Their Relationship with Subthalamic Nucleus Activity. *Journal of Neuroscience*, 28 (52), pp. 14245–14258.

Mallet, N., Pogosyan, A., Sharott, A., Csicsvari, J., Bolam, J. P., Brown, P. & Magill, P. J. 2008a. Disrupted Dopamine Transmission and the Emergence of Exaggerated Beta Oscillations in Subthalamic Nucleus and Cerebral Cortex. *Journal of Neuroscience*, 28 (18), pp. 4795– 4806.

Mantini, D., Marzetti, L., Corbetta, M., Romani, G.L. & Del Gratta, C. 2010. Multimodal Integration of fMRI and EEG Data for High Spatial and Teporal Resolution Analysis of Brain Networks. *Brain Topography*, 23, pp. 150-158.

Mantini, D., Perrucci, M.G., Del Gratta, C., Romani, G.L. & Corbetta, M. 2007. Electrophysiological signatures of resting state networks in the human brain. *PNAS*, 104(32), pp. 13170-13175.

Marini, G., Ceccarelli, P. & Mancia, M. 2008. Characterization of the 7-12 Hz EEG oscillations during immobile waking and REM sleep in behaving rats. *Clinical Neurophysiology,* 119, pp. 315-320.

Markram, H., Toledo-Rodriguez, M., Wang, Y., Gupta, A., Silberberg, G. & Wu, C. 2004. Interneurons of the neocortical inhibitory system. *Nature Reviews Neuroscience,* 5, pp. 793-809.

Martin, I.L. & Dunn, S.M. GABA Receptors. *Tocris Reviews*, 20, pp. 1-8.

Martin, K.A. & Whitteridge, D., 1984. Form, function and intracortical projections of spiny neurones in the striate visual cortex of the cat. *Journal of Physiology*, 353(1), pp. 463-504.

McAllister, S. M., Rothwell, J. C. & Ridding, M. C. 2011. Cortical oscillatory activity and the induction of plasticity in the human motor cortex. *European Journal of Neuroscience*, 33, pp. 1916-1924.

McFarland, D.J., Miner, L.A., Vaughan, T.M. & Wolpaw, J.R. 2000. Mu and Beta Rhythm Topographies During Motor Imagery and Actual Movements. *Brain Topography*, 12(3), pp. 177-186.

McKernan, R. M. & Whiting, P.J. 1996. Which GABAA-receptor subtypes really occur in the brain? *Trends in Neurosciences*, 19(4), pp. 139-144.

Meldrum, B.S. 2000. Glutamate as a neurotransmitter in the brain: review of physiology and pathology. *Journal of Nutrition*, 130(4S), pp. 107S-1015S.

Meyer, H.S., Schwarz, D., Wimmer, V.C., Schmitt, A.C., Kerr, J.N.D., Sakmann, B. & Helmstaedter, M. 2011. Inhibitory interneurons in a cortical column form hot zones of inhibition in layers 2 and 5A. *PNAS*, 108(40), pp. 16807-16812.

Millet, D. 2002. The origins of EEG. *Seventh annual meeting of the International Society for the History of the Neurosciences*, abstract 24.

Mitzdorf, U. 1987. Properties of the Evoked Potential Generators: Current Source-Density Analysis of Visually Evoked Potentials in the Cat Cortex. *International Journal of Neuroscience,* 33, pp. 33-59.

Moazami-Goudarzi, M. Sarnthein, J., Michels, L., Moukhtieva, R. & Jeanmonod, D. 2008. Enhanced frontal low and high frequency power and synchronization in the resting EEG of parkinsonian patients. *NeuroImage*, 41, pp. 985-997.

Moca, V.V., Nikolic, D., Singer, W. & Muresan, R.C. 2012. Memrane resonance enables stable and robust gamma oscillations. *Cerebral Cortex,* October 2012: Epub ahead of print.

Möhler, H. 2006. GABA$_A$ receptors in central nervous system disease: anxiety, epilepsy, and insomnia. *Journal of Receptors and Signal Transduction*, 26(5-6), pp. 731-740.

Möhler, H. 2007. Molecular regulation of cognitive functions and developmental plasticity: impact of GABA$_A$ receptors. *Journal of Neurochemistry*, 102, pp. 1-12.

Moore, R.A., Gale, A., Morris, P.H. & Forrester, D. 2008. Alpha power and coherence primarily reflect neural activity related to stages of motor response during a continuous monitoring task. *International Journal of Psychophysiology,* 69(2), pp. 79-89.

Moran, A. & Bar-Gad, I. 2010. Revealing neuronal functional organization through the relation between multi-scale oscillatory extracellular signals. *Journal of Neuroscience Methods*, 186, pp. 116-129.

Moro, E., Esselink, R. J., Xie, J., Hommel, M., Benabid, A. L. & Pollak, P. 2002. The impact on Parkinson's disease of electrical parameter settings in STN stimulation. *Neurology*, 59 (5), pp. 706-13.

Mountcastle, V.B. 1997. The columnar organization of the neocortex. *Brain*, 120, pp. 701-722.

Muellbacher, W., Ziemann, U., Boroojerdi, B. & Hallett, M. 2000. Effects of low-frequency transcranial magnetic stimulation on motor excitability and basic motor behaviour. *Clinical Neurophysiology,* 111, pp. 1002-1007.

Murakami, S. and Yoshio Okada, Y. 2006. Contributions of principal neocortical neurons to magnetoencephalography and electroencephalography signals. *Journal of Physiology*, 575 (3), pp. 925–936.

Murthy, V. & Fetz, E.B. 1992. Coherent 25- to 35-Hz oscillations in the sensorimotor cortex of awake behaving monkeys. *PNAS*, 89, pp. 5670-5674.

Murthy, V. & Fetz, E.B. 1996. Oscillatory Activity in Sensorimotor Cortex of Awake Monkeys. Synchronization of Local Field Potentials and Relation to Behavior. *Journal of Neurophysiology*, 76(6), pp. 3949-3967.

Muthukumaraswamy, S. D. 2010. Functional Properties of Human Primary Motor Cortex Gamma Oscillations. *Journal of Neurophysiology,* 104, pp. 2873-2885.

Nagamine, T., Kajola, M., Salmelin, R., Shibasaki, H. & Hari, R. 1996. Movement-related slow cortical magnetic fields and changes of spontaneous MEG- and EEG-brain rhythms. *Electroencephalography and Clinical Neurophysiology,* 99(3), pp. 274-286.

Neuper, C. & Pfurtscheller, G. 2001a. Event-related dynamics of cortical rhythms: frequency-specific features and functional correlates. *International Journal of Psychophysiology*, 43, pp. 41-58.

Neuper, C. & Pfurtscheller, G. 2001b. Evidence for distinct beta resonance frequencies in human EEG related to specific sensorimotor cortical areas. *Clinical Neurophysiology*, 112, pp. 2084–2097.

Neuper, C., Wortz, M. & Pfurtscheller, G. 2006. ERD/ERS patterns reflecting sensorimotor activation and deactivation. *Progress in Brain Research,* 159, pp. 211-222.

Nguyen, P. V., & Kandel, E. R. 1997. Brief theta-burst stimulation induces a transcription-dependent late phase of LTP requiring cAMP in area CA1 of the mouse hippocampus. *Learning & Memory*, 4 (2), pp. 230-43.

Nicholson, A.N. & Pascoe, P.A. 1986. Hypnotic activity of an imidazo-pyridine (zolpidem). *British Journal of Clinical Pharmacology*, 21, pp. 205-211.

Nikouline, V. V., Linkenkaer-Hansen, K., Wikstrom, H., Kesaniemi, M., Antonova, E. V., Ilmoniemi, R. J. & Huttunen, J. 2000. Dynamics of mu-rhythm suppression caused by median nerve stimulation: a magnetoencephalographic study in human subjects. *Neuroscience Letters*, 294, pp. 163-166.

Niswender, C.M. & Conn, J.P. 2010. Metabotropic Glutamate Receptors: Physiology, Pharmacology and Disease. *Annual Reviews Pharmacology and Toxicology,* 50, pp. 295-322.

Noh, N. A., Fuggetta, G., Manganotti, P. & Fiaschi, A. 2012. Long Lasting Modulation of Cortical Oscillations after Continuous Theta Burst Transcranial Magnetic Stimulation. *PLoS ONE*, 7 (4), pp. 1-12.

Nyakale, N. E., Clauss, R. P., Nel, W. & Sathekge, M. 2010. Clinical and brain SPECT scan response to zolpidem in patients after brain damage. *Arzneimittelforschung*, 60 (4), pp. 177-81.

Olanow, C.W. & Tatton, W.G. 1999. Etiology and Pathogenesis of Parkinson's Disease. *Annual Reviews Neuroscience*, 22, pp. 123-144.

Olman, C.A. & Yacoub, E. 2011. High-Field fMRI for Human Applications: An Overview of Spatial Resolution and Signal Specificity. *The Open Neuroimaging Journal*, 5, pp. 74-89.

Palva, S. & Palva, J.M. 2007. New vistas for a-frequency band oscillations. *Trends in Neurosciences*, 30(4), pp. 150-158.

Papadelis, C., Poghosyan, V., Fenwick, P. B. C. & Loannides, A. A. 2009. MEG's ability to localise accurately weak transient neural sources. *Clinical Neurophysiology*, 120, pp. 1958-1970.

Pascual-Leone, A., Valls-Solé, J., Wassermann, E. M. & Hallett, M. 1994. Responses to rapid-rate transcranial magnetic stimulation of the human motor cortex. *Brain*. 117 (4), pp. 847-58.

Pascual-Leone, A., Walsh, V. & Rothwell, J. 2000. Transcranial magnetic stimulation in cognitive neuroscience – virtual lesion, chronometry, and functional connectivity. *Current Opinion in Neurobiology*, 10, pp. 232–237.

Pattwell, S. S., Bath, K. G., Perez-Castro, R., Lee, F. S., Chao, M. V. & Ninan I. 2012. The BDNF Val66Met Polymorphism Impairs Synaptic Transmission and Plasticity in the Infralimbic Medial Prefrontal Cortex. *Journal of Neuroscience*, 32 (7), pp. 2410 –2421.

Paus, T., Sipila, P. K. & Strafella, A. P. 2001. Synchronization of Neuronal Activity in the Human Primary Motor Cortex by Transcranial Magnetic Stimulation: An EEG Study. *Journal of Neurophysiology,* 86, pp. 1983-1990.

Pell, G. S., Roth, Y. & Zangen, A. 2011. Modulation of cortical excitability induced by repetitive transcranial magnetic stimulation: Influence of timing and geometrical parameters and underlying mechanisms. *Progress in Neurobiology*, 93, pp. 59–98.

Penttonen, M. & Buzsaki, G. 2003. Natural logarithmic relationship between brain oscillators. *Thalamus & Related Systems,* 2, pp. 145-152.

Pfurtscheller, G. 1981. Central beta rhythm during sensorimotor activities in man. *Electroencephalography and Clinical Neurophysiology,* 51, pp. 253-264.

Pfurtscheller, G. 1992. Event-related synchronization (ERS): an electrophysiological correlate of cortical areas at rest. *Electroencephalography and Clinical Neurophysiology,* 83, pp. 62-69.

Pfurtscheller, G. & Aranibar, A. 1977. Event-related cortical desynchronisation detected by power measurements of scalp EEG. *Electroencephalography and Clinical Neurophysiology,* 42(6), pp. 817-826.

Pfurtscheller, G. & Lopes da Silva, F. H. 1999. Event-related EEG/MEG synchronization and desynchronization: basic principles. *Clinical Neurophysiology,* 110, pp. 1842-1857.

Pfurtscheller, G. & Neuper, C. 1997. Motor imagery activates primary sensorimotor area in humans. *Neuroscience Letters*, 239(2-3), pp. 65-68.

Pfurtscheller, G. & Solis-Escalante, T. 2009. Could the beta rebound in the EEG be suitable to realize a "brain switch"? *Clinical Neurophysiology,* 120, pp. 24-29.

Pfurtscheller, G., Stancák, A., Jr. & Edlinger, G. 1997. On the existence of different types of central beta rhythms below 30 Hz. *Electroencephalography and Clinical Neurophysiology,* 102, pp. 316-325.

Pfurtscheller, G., Zalaudek, K. & Neuper, C. 1998. Event-related beta synchronization after wrist, finger and thumb movement. *Electroencephalography and Clinical Neurophysiology*, 109, pp. 154-160.

Pfurtscheller, G., Woerz, M., Müller, G., Wriessnegger, S. & Pfurtscheller, K. 2002. Contrasting behaviour of beta event-related synchronization and somatosensory evoked potential after median nerve stimulation during finger manipulation in man. *Neuroscience Letters,* 323, pp. 113-116.

Pfurtscheller, G., Neuper, C., Brunner, C. & Lopes da Silva, F. 2005. Beta rebound after different types of motor imagery in man. *Neuroscience letters*, 378, pp. 156-159.

Pfurtscheller, G., Brunner, C., Schlogl, A. and Lopes da Silva, F.H. 2006. Mu rhythm (de)synchronization and EEG single-trial classification of different motor imagery tasks. *NeuroImage,* 31, pp. 153–159.

Picciotto, M.R., Higley, M.J. & Mineur, Y.S. 2012. Acetylcholine as a neuromodulator: cholinergic signalling shapes nervoussystem function and behaviour. *Neuron*, 76(1), pp. 116-29.

Piccolino, M. 1997. Luigi Galvani and animal electricity: two centuries after the foundation of electrophysiology. *Trends in Neurosciences,* 20(10), pp.443-448.

Pineda, J.A. 2005. The functional significance of mu rhythms: Translating "seeing" and "hearing" into "doing". *Brain Research Reviews*, 50, pp. 57-68.

Pinto, D.J., Jones, S.R. Kaper, T.J. & Kopell, N. 2003. Analysis of State-Dependent Transitions in Frequency and Long-Distance Coordination in a Model Oscillatory Cortical Circuit. *Journal of Computational Neuroscience*, 15, pp. 283-298.

Pogosyan, A., Gaynor, L.D., Eusebio, A. & Brown, P. Boosting cortical activity at Beta-band frequencies slows movement in humans. *Current Biology,* 19(19), pp. 1637-1641.

Pollok, B. Krause, V. Martsch, W. Wach, C. Schnitzler, A. & Sudmeyer, M. 2012. Motor-cortical oscillations in early stages of Parkinson's disease. *Journal of Physiology,* 590.13, pp. 3203-3212.

Pons, T.P., Garraghty, P.E. & Mishkin, M., 1992. Serial and parallel processing of tactual information in somatosensory cortex of rhesus monkeys. *Journal of Neurophysiology,* 68(2), pp. 518.

Porritt, M.J., Batchelor, P.E. & Howells, D.W. 2005. Inhibiting BDNF expression by antisense oligonucleotide infusion causes loss of nigral dopaminergic neurons. *Experimental Neurology*, 192, pp. 226-234.

Preuss, T.M. 2000. Taking the measure of diversity: comparative alternatives to the model-animal paradigm in cortical neuroscience. *Brain, Behavior and Evolution,* 55(6), pp. 287-299.

Priker, S., Schwarzer, D., Wieselthaler, A., Sieghart, W. & Sperk, G. 2000. GABA(A) receptors: immunocytochemical distribution of 13 subunits in the adult rat brain. *Neuroscience*, 101(4), pp. 815-50.

Prinz, A.A., Bucher, D. & Marder, E., 2004. Similar network activity from disparate circuit parameters. *Nature Neuroscience,* 7(12), pp. 1345–1352.

Priori*, A., Ardolino, G., Marceglia, S., Mrakic-Sposta, S., Locatelli, M., Tamma, F., Rossi, L. & Foffani G. 2006. Low-frequency subthalamic oscillations increase after deep brain stimulation in Parkinson's disease. *Brain Research Bulletin*, 71, pp. 149–154.

Prokic, E.J., Stanford, I.M., Yamawaki, N., Hall, S.D. & Woodhall, G.L. 2012. Benzodiazepine-site modulation of tonic inhibition in fast spiking interneurons alters cortical oscillatory dynamics. *Neuropharmacology,* UNDER REVIEW.

Qi, H.X., Lyon, D.C. & Kaas, J.H. 2002. Cortical and thalamic connections of the parietal ventral somatosensory area in marmoset monkeys (Callithrix jacchus). *Journal of Comparative Neurology*, 443(2), pp. 168-82.

Raichle, M. E., MacLeod, A. M., Snyder, A. Z., Powers, W, J., Gusnard, D. A. & Shulman, G. L. 2001. A default mode of brain function. *PNAS*, 98 (2), pp. 676–682.

Raichle, M.E. 2010. The brain's dark energy. *Scientific American*, 302(3), pp. 44-49.

Richter, L., de Graaf, C. Sieghart, W., Varagic, Z., Mörzinger, M., de Esch, I.J.P., Ecker, G.F. & Ernst, M. 2012. Diazepam-bound GABAA receptor models identify new benzodiazepine binding-site ligands. *Nature Chemical Biology*, 8(5), pp. 455-464.

Ridding, M.C., Inzelberg, R. & Rothwell, J.C. 1995. Changes in excitability of motor cortical circuitry in patients with Parkinson's disease. *Annals of Neurology*, 37(2), pp. 181-188.

Rivara, C.B., Sherwood, C.C., Bouras, C. & Hof, P.R. 2003. Stereologic Characterization and Spatial Distribution Patterns of Betz Cells in the Human Primary Motor Cortex. *The Anatomical Record Part A,* 270A, pp. 137-151.

Rivlin-Etzion, M., Marmor, O., Heimer, G., Raz, A., Nini, A. & Bergman, H. 2006. Basal ganglia oscillations and pathophysiology of movement disorders. *Current Opinion in Neurobiology,* 16, pp. 629-637.

Romero, J. R., Anschel., D., Sparing, R., Gangitano, M. & Pascual-Leone, A. 2002 Subthreshold low frequency repetitive transcranial magnetic stimulation selectively decreases facilitation in the motor cortex. *Clinical Neurophysiology,* 113, pp. 101–107.

Roopun, A. K., Middleton, S. J., Cunningham, M. O., LeBeau, F. E. N., Bibbig, A., Whittington, M. A. & Traub, R. D. 2006. A beta2-frequency (20–30 Hz) oscillation in nonsynaptic networks of somatosensory cortex. *PNAS*, 103 (42), pp. 15646–15650.

Roopun, A.K., Kramer, M.A., Carracedo, L.M., Kaiser, M., Davies, C.H., Traub, R.D., Kopell, N.J. & Whittington, M.A. 2008a. *Frontiers in Cellular Neuroscience,* 2(1), pp. 1-8.

Roopun, A.K., Kramer, M.A., Carracedo, L.M., Kaiser, M., Davies, C.H., Traub, R.D., Kopell, N.J. & Whittington, M.A. 2008b. Temporal interactions between cortical rhythms. *Frontiers in Neuroscience*, 2(2), pp. 145-154.

Roopun, A.K. LeBeau, F.E.N., Rammell, J., Cunningham, M.O., Traub, R.D. & Whittington, M.A. 2010. Cholinergic neuromodulation controls directed temporal communication in neocortex *in vitro. Frontiers in Neural Circuits,* 4(8), pp. 1-10.

Rosanova, M., Casali, A., Bellina, V., Resta F., Mariotti, M. & Massimini M. 2009. Natural Frequencies of Human Corticothalamic Circuits. *Journal of Neuroscience*, 29 (24), pp. 7679 –7685.

Rosenberg, R.P. 2006. Sleep maintenance insomnia: strengths and weaknesses of current pharmacologic therapies. *Annual Clinical Psychiatry*, 18(1), pp. 49-56.

Rothwell, J. C. 1991. Physiological studies of electric and magnetic stimulation of the human brain. *Electroencephalography and Clinical Neurophysiology Supplement,* 43, pp. 29-35.

Rougeul, A., Bouyer, J.J., Dedet, L. & Debray, O. 1979. Fast somato-parietal rhythms during combined focal attention and immobility in baboon and squirrel monkey. *Electroencephalography and Clinical Neurophysiology*, 46, pp. 310-319.

Rowe, T.B., Macrini, T.E. & Luo, Z.X. 2011. Fossil evidence on origin of the mammalian brain. *Science*, 332, pp. 885-957.

Rudolph, U. & Knophlach, F. 2012. Beyond classical benzodiazepines: Novel therapeutic potential of GABA$_A$ receptor subtypes. *Nature Reviews Drug Discovery*, 10(9), pp. 685-697.

Rudolph, U. Crestani, F. Benke, D. Brunig, I. Benson, J. A. Fritschy, J. Martin, J. R. Bluethmann, H. & Möhler, H. 1999. Benzodiazepine actions mediated by specific gamma-aminobutyric acid-A receptor subtypes. *Nature*, 401, pp. 796-800.

Sailer, A., Molnar, G.F., Paradiso, G., Gunraj, C.A., Lang, A.E. & Chen, R. 2003. Short and long latency afferent inhibition in Parkinson's disease. *Brain*, 126, pp. 1883-1894.

Sailer, A., Cunic, D.I., Paradiso, G.O., Gunraj, C.A., Wagle-Shukla, A., Moro, E., Lozano, A.M., Lang, A.E. & Chen R. 2007. Subthalamic nucleus stimulation modulates afferent inhibition in Parkinson disease. *Neurology*, 68(5), pp. 356-363.

Salenius, S. & Hari, R. 2003. Synchronous cortical oscillatory activity during motor action. *Current Opinion in Neurobiology*, 13, pp. 678–684.

Salenius, S., Schnitzler, A., Salmelin, R., Jousmaki, V. & Hari, R. 1997. Modulation of Human Cortical Rolandic Rhythms during Natural Sensorimotor Tasks. *NeuroImage*, 5, pp. 221–228.

Salmelin, R. & Hari, R. 1994. Spatiotemporal characteristics of sensorimotor neuromagnetic rhythms related to thumb movement. *Neuroscience,* 60 (2), pp. 537-550.

Salmelin, R., Hämäläinen, M., Kajola, M & Hari, R. 1995. Functional Segregation of Movement-Related Rhythmic Activity in the Human Brain. *NeuroImage*, 2, pp. 237-243.

Sancar, F., Ericksen, S.S., Kucken, A.M., Teissere, J.A. & Czajkowski, C. 2007. Structural Determinants for High-Affinity Zolpidem Binding to GABA-A receptors. *Molecular Pharmacology,* 71(1), pp. 38-46.

Sanes, J.N. & Donoghue, J.P. 1993. Oscillations in local field potentials of the primate motor cortex during voluntary movement. *PNAS*, 90, pp. 4470-4474.

Sanes, J. N. & Donoghue, J. P. 2000. Plasticity and primary motor cortex. *Annual Reviews of Neuroscience*. 23, pp. 393-415.

Sarto-Jackson, I. & Sieghart, W. 2008. Assembly of GABA(A) receptors. *Molecular Membrane Biology,* 25(4), pp. 302-10.

Scalzo, P., Kummer, A., Bretas, T.L., Cardoso, F. & Teixeira, A.L. 2010. Serum levels of brain-derived neurotrophic factor correlate with motor impairment in Parkinson's disease. *Journal of Neurology*, 257(4), pp. 540-545.

Scheiber, M. H. 2001. Constraints on Somatotopic Organization in the Primary Motor Cortex. *Journal of Neurophysiology,* 86, pp. 2125-2143.

Schnitzler, A. & Gross, J. 2005. Normal and pathological oscillatory communication in the brain. *Nature Reviews Neuroscience,* 6, pp. 285-296.

Schnitzler, A., Salenius, S., Salmelin, R., Jousmaki, V. & Hari, R. 1997. Involvement of Primary Motor Cortex in Motor Imagery: A Neuromagnetic Study. *NeuroImage*, 6, pp. 201–208.

Selverston, A.I. & Moulins, M., 1985. Oscillatory neural networks. *Annual Review of Physiology,* 47(1), pp. 29–48.

Sharott, A., Magill, P.J., Harnack, D., Kupsch, A., Meissner, W. & Brown P. 2005. Dopamine depletion increases the power and coherence of beta-oscillations in the cerebral cortex and subthalamic nucleus of the awake rat. *European Journal of Neuroscience,* 21(5), pp. 1413-1422.

Shepherd, G. M. G. 2009. Intracortical cartography in an agranular area. *Frontiers in Neuroscience,* 3 (3), pp. 337-343.

Shipp, S. 2005. The importance of being agranular: a comparative account of visual and motor cortex. *Philosophical Transactions of The Royal Society Biology*, 360, pp. 797-814.

Shipp, S. 2007. Structure and function of the cerebral cortex. *Current Biology*, 17(12), pp. R443-450.

Sieghart, W. & Sperk, G. 2002. Subunit composition, distribution and function of GABA(A) receptor subtypes. *Current Topics in Medicinal Chemistry,* 2(8), pp. 795-816.

Sieghart, W., Ramerstorfer, J., Sarto-Jackson, I. Varagic, Z. & Ernst, M. 2012. A novel GABA(A) receptor pharmacology: drugs interacting with the α(+) β(-) interface. *British Journal of Pharmacology,* 166(2), pp. 476-485.

Silberstein, P., Pogosyan, A., Kühn, A. A. Hotton, G., Tisch, S., Kupsch, A., Dowsey-Limousin, P., Hariz, M.I. & Brown, P. 2005. Cortico-cortical coupling in Parkinson's disease and its modulation by therapy. *Brain*, 128, pp. 1277-1291.

Singer, W. & Gray, C.M. 1995. Visual feature integration and the temporal correlation hypothesis. *Annual Reviews Neuroscience*, 18, pp. 555-586.

Sirota, A., Csicsvari, J., Buhl, D. & Buzsaki, G. 2003. Communication between neocortex and hippocampus during sleep in rodents. *PNAS*, 100(4), pp. 2065-2069.

Sobolewski, A., Swiejkowski, D.A., Wrobel, A. & Kubklik, E. 2011. The 5-12 Hz oscillations in the barrel cortex of awake rats – Sustained attention during behavioural idling? *Clinical Neurophysiology,* 122(3), pp. 483-489.

Somogyi P. & Klausberger, T. 2005. Defined types of cortical interneuron structure space and spike timing in the hippocampus. *Journal of Physiology*, 562(1), pp. 9-26.

Spiegel, J., Tintera, J., Gawehn, J., Stoeter, P. & Treede, R. D. 2000. Functional MRI of human primary somatosensory and motor cortex during median nerve stimulation. *Clinical Neurophysiology*, 110, pp. 47-52.

Spieles-Engemann, A.L., Steece-Colloer, K., Behbehani, M.M., Collier, T.J., Wohlgenant, S.L., Kemp, C.J., Cole-Strauss, A., Levine, N.D., Gombash, S.E., Thompson, V.B., Lipton, J.W. & Sortwell, C.E. 2011. Subthalamic Nucleus Stimulation Increases Brain Derived Neurotrophic Factor in the Nigrostriatal System and Primary Motor Cortex. *Journal of Parkinsons Disease*, 1(1), pp. 123-126.

Stagg, C.J., Wylezinska, M., Matthews, P.M., Johansen-Berg, H., Jezzard, P., Rothwell, J.C. & Bestmann, S. 2009. Neurochemical Effects of Theta Burst Stimulation as Assessed by Magnetic Resonance Spectroscopy. *Journal of Neurophysiology,* 101, pp. 2872-2877.

Stam, C.J. 2010. Use of magnetoencephalography (MEG) to study functional brain networks in neurodegenerative disorders. *Journal of the Neurological Sciences,* 289, pp. 128-134.

Stancák, A. Jr. & Pfurtscheller, G. 1995. Desynchronization and recovery of beta rhythms during brisk and slow self-paced finger movements in man. *Neuroscience Letters*, 196, pp. 21-24.

Stancák, A. Jr. & Pfurtscheller, G. 1996. Event-related desynchronisation of central beta-rhythms during brisk and slow self-paced finger movement of dominant and nondominant hand. *Cognitive Brain Research*, 4, pp. 171-183.

Stefan, K., Kunesch, E., Cohen, L. G., Benecke, R. & Classen, J. 2000. Induction of plasticity in the human motor cortex by pairing associative stimulation. *Brain*, 123, pp. 572-584.

Stein, E. & Bar-Gad, I. 2012. Beta oscillations in the cortico-basal ganglia loop during parkinsonism. *Experimental Neurology*, e-pub ahead of print, August 23 2012.

Stepniewska, I., Preuss, T.M. & Kaas, J.H. 1993. Architectonics, somatotopic organization, and ipsilateral cortical connections of the primary motor area (M1) of owl monkeys. *Journal of Comparative Neurology,* 330(2), pp. 238-271.

Steriade, M. 2001. Impact of Network Activities on Neuronal Properties in Corticohalamic Systems. *Journal of Neurophysiology,* 86(1), pp. 1-39.

Steriade, M. 2006. Grouping of Brain Rhythms in Corticohalamic Systems. *Neuroscience,* 137, pp. 1087–1106.

Stoffers, D., Bosboom, J.L.W., Deijen, J.B., Wolters, E.Ch., Berendse, H.W., & Stam, C.J. 2007. Slowing of oscillatory brain activity is a stable characteristic of Parkinson's disease without dementia. *Brain*, 130, pp. 1847-1860.

Stoffers, D., Bosboom, J.L.W., Deijen, J.B., Wolters, E.Ch., Stam, C.J. & Berendse, H.W. 2008. Increased cortico-cortical functional connectivity in early-stage Parkinson's disease: An MEG study. *NeuroImage*, 41, pp. 212-222.

Suffczynski, P., Kalitzin, S., Pfurtscheller, G. & Lopers da Silva, F.H. 2001. Computational model of thalamo-cortical networks: dynamical control of alpha rhythms in relation to focal attention. *International Journal of Psychophysiology,* 43, pp. 25-40.

Suppa, A., Ortu, E., Zafar, N., Deriu, F., Paulus, W., Berardelli , A. & Rothwell, J. C. 2008. Theta burst stimulation induces after-effects on contralateral primary motor cortex excitability in humans. *Journal Physiology,* 586.18, pp. 4489-4500.

Suppa, A., Marsili, L., Belvisi, D., Conte, A., Iezzi, E., Modugno, N., Gabbrini, G. & Berardelli, A. 2011. Lack of LTP-like plasticity in primary motor cortex in Parkinson's disease. *Experimental Neurology,* 227, pp. 296-301.

Swartz, B.E. & Goldensohn, E.S. 1998. Timeline of the history of EEG and associated fields. *Electroencephalography and Clinical Neurophysiology,* 106, pp. 173-176.

Szabadics, J., Lorincz, A. & Tamás, G. 2001. Beta and Gamma Frequency Synchronization by Dendritic GABAergic Synapses and Gap Junctions in a Network of Cortical Interneurons. *Journal of Neuroscience,* 21(15), pp. 5824-5831.

Szurhaj, W., Derambure, P., Labyt E., Cassim, F., Bourriez, J.L. Isnard, J. Guieu, J.D. & Mauguiere, F. 2003. Basic mechanisms of central rhythms reactivity to preparation and execution of a voluntary movement: a stereoelectroencephalographic study. *Clinical Neurophysiology*, 114(1), pp. 107-119.

Tallon-Baudry, C. & Bertrand, O. 1999. Oscillatory gamma activity in humans and its role in object representation. *Trends in Cognitive Sciences*, 3(4), pp. 151-163.

Tamás, G., Buhl, E. H., Lörincz, A. & Somogyi P. 2000. Proximally targeted GABAergic synapses and gap junctions synchronize cortical interneurons. *Nature Neuroscience,* 3 (4), pp. 366-371.

Tamburin, S., Fiaschi, A., Andreoli, A., Marani, S. & Zanette, G. 2003. Sensorimotor integration to cutaneous afferents in humans: the effect of the size of the receptive field. *Experimental Brain Research*, 167, pp. 362-369.

Tan, K.R., Rudolph, U. & Lüscher, C. 2011. Hooked on benzodiazepines: GABA$_A$ receptor subtypes and addiction. *Trends in Neurosciences,* 34(4), pp. 188-197.

Tanaka, T., Saito, H. & Matsukim, N. 1997. Inhibition of GABAA Synaptic Responses by Brain-Derived Neurotrophic Factor (BDNF) in Rat Hippocampus. *Journal of Neuroscience*, *17* (9), pp. 2959–2966.

Thomson, A.M. & Lamy, C. 2007. Functional maps of neocortical local circuitry. *Frontiers in Neuroscience,* 1(1), pp. 19-42.

Thut, G. & Miniussi, C. 2011. New insights into rhythmic brain activity from TMS–EEG studies. *Trends in Cognitive Sciences*, 13 (4), pp.182-9.

Thut, G., Schyns, P. G. & Gross, J. 2011b. Entrainment of perceptually relevant brain oscillations by non-invasive rhythmic stimulation of the human brain. *Frontiers in Psychology*, 2, pp. 1-10.

Thut, G., Veniero, D., Romei, V., Miniussi, C., Schyns, P. & Gross, J. 2011a. Rhythmic TMS Causes Local Entrainment of Natural Oscillatory Signatures. *Current Biology*, 21, pp. 1176–1185.

Tiesinga, P. & Sejnowski, T.J. 2009. Cortical Enlightenment: Are Attentional Gamma Oscillations Driven by ING or PING? *Neuron*, 63(6), pp. 727-732.

Tiihonen, J., Kajola, M. & Hari, R. 1989. Magnetic mu rhythm in man. *Neuroscience,* 32(3), pp. 793-800.

Timmermann, L. & Fink, G. R. 2011. Pathological network activity in Parkinson's disease: from neural activity and connectivity to causality? *Brain,* 134 (2), pp. 332-334.

Ting, L. H. & McKay, J. L. (2007) Neuromechanics of muscle synergies for posture and movement. *Current Opinion in Neurobiology*, 17, pp. 622–628.

Tokimura, H., Di Lazzaro, V., Tokimura, Y., Oliviero, A., Profice, P., Insola, A., Mazzone, P., Tonali, P. & Rothwell, J. C. 2000. Short latency inhibition of human hand motor cortex by somatosensory input from the hand. *Journal of Physiology,* 523.2, pp. 503-513.

Tort, A.B.L., Fontanini, A., Kramer, M.A., Jones-Lush, L.M., Kopell, N.J. & Katz, D.B. 2010. Cortical networks produce three distinct 7-12 Hz rhythms during single sensory responses in the awake rat. *Journal of Neuroscience*, 30(12), pp. 4315-4324.

Traub, R. D. & Bibbig, A. 2000. A Model of High-Frequency Ripples in the Hippocampus Based on Synaptic Coupling Plus Axon–Axon Gap Junctions between Pyramidal Neurons. *Journal of Neuroscience*, *20*(6) pp. 2086–2093.

Traub, R. D., Spruston, N., Soltesz, I., Konnerthk, A., Whittington, M. A. & Jefferys, J. G. R. 1998. Gamma-frequency oscillations: a neuronal population phenomenon, regulated by synaptic and intrinsic cellular processes, and inducing synaptic plasticity. *Progress in Neurobiology*, 55, pp. 563-575.

Traub, R.D., Whittington, M.A., Colling, S.B., Buzsáki, G. & Jefferys, G.R. 1996a. Analysis of gamma rhythms in the rat hippocampus *in vitro* and in vivo. *Journal of Physiology*, 493(2), pp. 471-484.

Traub, R.D., Whittington, M.A., Stanford, I.M. & Jefferys, G.R. 1996b. A mechanism for generation of long-range synchronous fast oscillations in the cortex. *Nature*, 383, pp. 621-624.

Tsujimoto, T., Mima, T., Shimazu, H. & Isomura, Y. 2009. Directional organization of sensorimotor oscillatory activity related to the electromyogram in the monkey. *Clinical Neurophysiology*, 120, pp. 1168–1173.

Uhlhaas, P. J. & Singer. W. 2006. Neural Synchrony in Brain Disorders: Relevance for Cognitive Dysfunctions and Pathophysiology. *Neuron*, 52, pp. 155–168.

Van Der Werf, Y. D. & Paus, T. 2006. The neural response to transcranial magnetic stimulation of the human motor cortex. I. Intracortical and cortico-cortical contributions. *Experimental Brain Research*, 175, pp. 231–245.

van Dijk, H., Schoffelen, J.M. Oostenveld, R. & Jensen, O. 2008. Prestimulus Oscillatory Activity in the Alpha Band Predicts Visual Discrimination Ability. *Journal of Neuroscience,* 28(8), pp. 1816-1823.

van Ede, F., de Lange, F., Jensen, O. & Maris, E. 2011. Orienting Attention to an Upcomping Tactile Event Involves a Spatially and Temporally Specific Modulation of Sensorimotor Alpha- and Beta-Band Oscillations. *Journal of Neuroscience*, 31(6), pp. 2016-2024.

VanRullen, R. & Dubios, J. 2011. The psychophysics of brain rhythms. *Frontiers in Psychology,* 2(203), pp. 1-10.

Vardy, A.N., van Wegen, E.E.H., Kwakkel, G., Berendse, H.W., Beek, P.J. & Daffertshofer, A. 2011. Slowing of M1 activity in Parkinson's disease during rest and movement – An MEG study. *Clinical Neurophysiology,* 122, pp. 789-795.

Varela, F., Lachaux, J.P. Rodriguez, E. & Martinerie, J. 2001. The Brainweb: Phase synchronization and large-scale integration. *Nature Reviews Neuroscience*, 2, pp. 229-240.

Veniero, D., Brignani, D., Thut, G. & Miniussi, C. 2011. Alpha-generation as basic response-signature to transcranial magnetic stimulation (TMS) targeting the human resting motor cortex: A TMS/EEG co-registration study. *Psychophysiology*, 48 (10), pp. 1381-9.

Vogt, B.A. & Pandya, D.N. 1978. Cortico-cortical connections of somatic sensory cortex (areas 3, 1 and 2) in the rhesus monkey. *Journal of Comparative Neurology,* 177(2), pp. 179-191.

Vrba, J. & Robinson, S. E. 2001. Signal processing in magnetoencephalography. *Methods*, 25(2), pp. 249-271.

Wang, X.J. & Buszaki, G. 1996. Gamma Oscillation by Synaptic Inhibition in a Hippocampal Interneuronal Network Model. *Journal of Neuroscience*, 16(20), pp. 6402-6413.

Wang, X.J. 1999. Fast burst firing and short-term synaptic plasticity: a model of neocortical chattering neurons. *Neuroscience*, 89(2), pp. 347-362.

Wang, X.J. 2010. Neurophysiological and Computational Principles of Cortical Rhythms in Cognition. *Physiological Reviews,* 90(3), pp. 1195-1268.

Ward, L.M. 2003. Synchronous neural oscillations and cognitive processes. *Trends in Cognitive Sciences*, 7(12), pp. 553-560.

Wassermann, E. M. & Zimmermann, T. 2012. Transcranial magnetic brain stimulation: Therapeutic promises. *Pharmacology & Therapeutics*, 133, pp. 98-107.

Weiler, N., Wood, L., Yu, J., Solla, S. A. & Shepherd, G. M. G. (2008) Top-down laminar organization of the excitatory network in motor cortex. *Nature Neuroscience*, 11(3), pp. 360–366.

Whittington, M.A. & Traub R.D. 2003. Interneuron Diversity series: Inhibitory interneurons and network oscillations *in vitro. Trends in Neurosciences,* 26(12), pp. 676-682.

Whittington, M.A., Traub, R.D. & Jeffrys, J.G.R. 1995. Synchronized oscillations in interneuron networks driven by metabotropic glutamate receptor activation. *Nature*, 373, pp. 612-615.

Whittington, M.A., Traub, R.D., Kopell, N., Ermentrout, B. & Buhl, E.H. 2000. Inhibition-based rhythms: experimental and mathematical observations on network dynamics. *International Journal of Psychophysiology,* 38, pp. 315-336.

Witham, C. L., Wang, M., & Baker, S. N. 2010. Corticomuscular coherence between motor cortex, somatosensory areas and forearm muscles in the monkey. *Frontiers in Systems Neuroscience*, 4, pp. 1-14.

Womelsdorf, T., Fries, P., Mitra, P.P. & Desimone, R. 2006. Gamma-band synchronization n visual cortex predicts speed of change detection. *Nature*, 439, pp. 733-736.

Wong, C.G.-T. & Snead, O.C. 2001. The $GABA_A$ Receptor: Subunit-Dependent Functions and Absence Seizures. *Epilepsy Currents,* 1(1), pp. 1-5.

Wu, T., Wang, L., Chen, Y., Zhao, C., Li, K. & Chan, P. 2009. Changes of functional connectivity of the motor network in the resting state in Parkinson's disease. *Neuroscience Letters,* 460, pp. 6-10.

Yamamoto, C. & McIlwain, H. 1966. Electrical activities in thin sections from the mammalian brain maintained in chemically-defined media *in vitro. Journal of Neurochemistry,* 13, pp. 1333-1343.

Yamawaki, N. 2008. Beta frequency neuronal network activity in the primary motor cortex. *PhD Thesis, Aston University*, UK.

Yamawaki, N., Magill, P. J., Woodhall, G. L., Hall, S. D. & Stanford, I. M. 2012. Frequency selectivity and dopamine-dependence of plasticity at glutamatergic synapses in the subthalamic nucleus. *Neuroscience,* 203, pp. 1-11.

Yamawaki, N., Stanford, I. M., Hall, S. D. & Woodhall, G. L. 2008. Pharmacologically Induced and Stimulus Evoked Rhythmic Neuronal Oscillatory Activity in the Primary Motor Cortex *In vitro. Neuroscience,* 151, pp. 386–395.

Yang, D.G. & Guo, Y. 2011. Entrainment of a thalamocortical neuron to periodic sensorimotor signals. *BMC Neuroscience Poster Presentation: Stockholm 2011*, 12(S1): P135.

Yazdan-Shahmorad, A., Kipke, D.R. & Lehmkuhle, M.J. 2011. Polarity of cortical electrical stimulation differentially affects neuronal activity of deep and superficial layers of rat motor cortex. *Brain Stimulation*, 4, pp. 228-242.

Zaehle, T., Rach, S. & Herrmann, C. S. 2010. Transcranial Alternating Current Stimulation Enhances Individual Alpha Activity in Human EEG. *PLoS ONE*, 5 (11), pp. 1-7.

Zarkowski, P., Shin, C. J., Dang, T., Russo, J. & Avery, D. 2006. EEG and the Variance of Motor Evoking Potential Amplitude. *Clinical EEG and Neuroscience*, 37 (3), pp. 247-251.

Zhang, Y. & Ding, M. 2010. Detection of a wak somatosensory stimulus: role of the presimulus mu rhythm and its top-down modulation. *Journal of Cognitive Neuroscience*, 22(2), pp. 307-322.

Zhang, Y., Chen, Y., Bressler, S.L. & Ding, M. 2007. Response preparation and inhibition: The role of the cortical sensorimotor beta rhythm. *Neuroscience,* 156(1), pp. 238-246.

Zhang, Z.W. & Deschenes, M., 1997. Intracortical axonal projections of lamina VI cells of the primary somatosensory cortex in the rat: a single-cell labelling study. *Journal of Neuroscience*, 17(16), pp. 6365-6379

Zhu, J., Jiang, M., Yang, M., Hou, H. & Shu, Y. 2011. Membrane Potential-Dependent Modulation of Recurrent Inhibition in Rat Neocortex. *PLoS Biology*, 9(3), e1001032, pp. 1-13.

Ziemann, U., Hallett, M. & Cohen, L. G. 1998. Mechanisms of Deafferentation-Induced Plasticity in Human Motor Cortex. *Journal of Neuroscience*, 18 (17), pp. 7000-7007.

Zolpidem @ PubChem Compound, National Center for Biotechnology Information 2012: http://pubchem.ncbi.nlm.nih.gov/summary/summary.cgi?cid=5732/. [Accessed: 11/12/2012].

Zuccato, C. & Cattaneo, E. 2009. Brain-derived neurotrophic factor in neurodegenerative diseases. *Nature Reviews Neurology*, 5(6), pp. 311-322.